

Chemistry and Physiology of Selected Food Colorants

ACS SYMPOSIUM SERIES **775**

Chemistry and Physiology of Selected Food Colorants

Jennifer M. Ames, EDITOR
University of Reading

Thomas Hofmann, EDITOR
Deutsche Forschungsanstalt für Lebensmittelchemie

Downloaded by 77.122.45.2 on October 24, 2009 | <http://pubs.acs.org>
Publication Date: January 4, 2001 | doi: 10.1021/bk-2001-0775.fw001



American Chemical Society, Washington, DC



Library of Congress Cataloging-in-Publication Data

Chemistry and physiology of selected food colorants / Jennifer M. Ames, editor, Thomas F. Hofmann, editor.

p. cm.—(ACS symposium series ISSN 0097-6156; 775)

Includes bibliographical references and index.

ISBN 0-8412-3705-0

1. Coloring matter in food—Congresses.

I. Ames, Jennifer M., 1957-. II. Hofmann, Thomas F., 1968-. III. American Chemical Society. Division of Agricultural and Food Chemistry. IV. Series.

TP456.C65 C48 2000
664'.06—dc21

00-63964

The paper used in this publication meets the minimum requirements of American National Standard for Information Sciences—Permanence of Paper for Printed Library Materials, ANSI Z39.48-1984.

Copyright © 2001 American Chemical Society

Distributed by Oxford University Press

All Rights Reserved. Reprographic copying beyond that permitted by Sections 107 or 108 of the U.S. Copyright Act is allowed for internal use only, provided that a per-chapter fee of \$20.00 plus \$0.50 per page is paid to the Copyright Clearance Center, Inc., 222 Rosewood Drive, Danvers, MA 01923, USA. Republication or reproduction for sale of pages in this book is permitted only under license from ACS. Direct these and other permission requests to ACS Copyright Office, Publications Division, 1155 16th St., N.W., Washington, DC 20036.

The citation of trade names and/or names of manufacturers in this publication is not to be construed as an endorsement or as approval by ACS of the commercial products or services referenced herein; nor should the mere reference herein to any drawing, specification, chemical process, or other data be regarded as a license or as a conveyance of any right or permission to the holder, reader, or any other person or corporation, to manufacture, reproduce, use, or sell any patented invention or copyrighted work that may in any way be related thereto. Registered names, trademarks, etc., used in this publication, even without specific indication thereof, are not to be considered unprotected by law.

PRINTED IN THE UNITED STATES OF AMERICA

Foreword

The ACS Symposium Series was first published in 1974 to provide a mechanism for publishing symposia quickly in book form. The purpose of the series is to publish timely, comprehensive books developed from ACS sponsored symposia based on current scientific research. Occasionally, books are developed from symposia sponsored by other organizations when the topic is of keen interest to the chemistry audience.

Before agreeing to publish a book, the proposed table of contents is reviewed for appropriate and comprehensive coverage and for interest to the audience. Some papers may be excluded in order to better focus the book; others may be added to provide comprehensiveness. When appropriate, overview or introductory chapters are added. Drafts of chapters are peer-reviewed prior to final acceptance or rejection, and manuscripts are prepared in camera-ready format.

As a rule, only original research papers and original review papers are included in the volumes. Verbatim reproductions of previously published papers are not accepted.

ACS Books Department

Preface

Attractive appearance, including color, is crucial to the selection of foods and beverages. Therefore, the food industry is interested in how to maximize color retention in colorful items, such as fruits, and how to optimize color in processed commodities, for example, breakfast cereals and beer. The consumer is very concerned about artificial colorants and wishes to avoid them, thus creating a need for natural alternatives. During the past few years, attention has turned to the non-nutritive physiological effects of certain food components, including those with antioxidant properties, for example, β -carotene. Thus research in the field has grown and there were many reasons for holding a symposium focusing on food colorants.

The symposium brought together leading scientists from around the world: the United Kingdom, Germany, Switzerland, Brazil, Japan, Spain, and the United States. This book is based on the presentations.

The book is unique because of its specific focus: the chemical and physiological properties of selected food colorants, that is, carotenoids, anthocyanins, the products of enzymatic browning, and components formed by non-enzymatic browning.

Following an overview chapter, sections cover analytical aspects, anthocyanins, other plant-derived colorants (including carotenoids and those formed by enzymatic browning), and non-enzymatic browning.

This book is intended for food scientists, food technologists, and sensory analysts in both academia and the food industry.

JENNIFER M. AMES

Department of Food Science & Technology
The University of Reading
Whiteknights
Reading RG6 6AP, United Kingdom

THOMAS HOFMANN

German Centre for Food Chemistry
Lichtenbergstrasse 4
D-85748 Garching, Germany

Chapter 1

Selected Natural Colorants in Foods and Beverages

Jennifer M. Ames¹ and Thomas Hofmann²

¹Department of Food Science and Technology, The University of Reading, Whiteknights, Reading RG6 6AP, United Kingdom

²German Research Centre for Food Chemistry, Lichtenbergstrasse 4, D-85748 Garching, Germany

Four major categories of food colorants are reviewed, i.e., carotenoids, anthocyanins, the products of enzymatic browning and substances formed by non-enzymatic browning. Topics covered within each class are structure, biosynthesis, occurrence, stability, effects of food processing and physiological properties. Much is known concerning the structures and formation of carotenoids, anthocyanins and theaflavins while the structures of thearubigins and products of non-enzymatic browning largely remain to be elucidated. There is a lack of knowledge concerning the uptake, distribution, bioavailability and bioactivity of food colorants in the human body.

A wide range of materials gives color to the food we eat. They include various pigments, such as naturally occurring cell constituents, e.g., carotenoids and anthocyanins. Other colorants are formed on food processing and include the products of enzymatic browning and the materials produced on non-enzymatic (including Maillard) browning. Enzymatic browning is central to the formation of color in black tea and includes the formation of theaflavins and thearubigins. The Maillard reaction is responsible for the development of yellow-brown colors in most thermally processed foods, e.g., bread, malt, breakfast cereals. In this case, the colored components are structures of low molecular mass and macromolecular materials (the melanoidins).

Dietary components, including food colorants, can have five types of physiological effect. They can act as a source of nutrients, the provitamin A carotenoids, such as β -carotene, being the most obvious example. In addition, they can have beneficial but non-nutritive effects and a good example is the antioxidant activity of, e.g., lycopene. Thirdly, they may complex with nutrients, such as metals, thereby possibly reducing their absorption. Fourthly, it is possible

that food colorants may have undesirable, or even toxic, physiological effects in some situations and this has been discussed for β -carotene and some colored phenolic compounds by Diplock et al. (1). Finally, they may affect the activities of digestive enzymes or the growth of gut bacteria.

The non-nutritive effects of food colorants are perhaps the ones that have been studied the most and so it is worth considering them in more depth. Antioxidant activity is the non-nutritive effect that has been studied in most detail and this has implications for the etiology of various human degenerative diseases, e.g., coronary heart disease (CHD) and cancer (1). For example, epidemiological studies suggest that preventative effects towards atherogenic lesions are associated with increased uptake of lipophilic antioxidants, e.g., carotenoids (2). Also, the idea that antioxidants prevent carcinogenesis by scavenging free radicals is supported by epidemiological studies (3).

It is by no means certain that, because a food component, e.g., β -carotene, has a particular effect, e.g., an antioxidant effect, in a food or in an *in vitro* system, that the same component will behave as an antioxidant in the human body (1). In order for any physiological effect of a dietary component to be realized in the human body, various hurdles have to be overcome. First, the component must survive food processing and storage. Next, it must be absorbed in the gut (unless the effect is on the gut bacteria). Then, it must be transported to the active site. Finally, it must be bioactive at this site. The absorption and bioavailability of dietary components is affected by genetic factors, lifestyle and the nutrient status of the host, as well as by the consumption of other dietary components, e.g., lipid.

This review focuses on four selected categories of food colorants, i.e., carotenoids, anthocyanins and the colored products formed by enzymatic as well as non-enzymatic browning. Chemical aspects, such as colorant formation, occurrence, stability, effects of food processing and physiological aspects of these natural food colorants are discussed.

Carotenoids

Structure and biosynthesis

The carotenoids can be divided into the carotenes, which are hydrocarbons, and their oxygenated derivatives, the xanthophylls (4). In addition, there are the apocarotenoids, a degraded form. In this chapter, the commonly used, trivial names of carotenoids are used. Lists of carotenoids, their structures and all their names (trivial, obsolete and semi-systematic) are available, e.g., (5). Carotenoids are synthesized *de novo* from isoprene units by higher plants, spore bearing vascular plants, algae and photosynthetic bacteria (6). Initial observations indicated that these isoprenoid monomers are biosynthetically derived from mevalonate in animal cells and yeast (7). However, very recent investigations using site-specific labeled precursors elucidated the existence of an alternative non-mevalonate pathway for the formation of the isoprenoid monomers, isopentenyl pyrophosphate 4 and dimethylallyl pyrophosphate 5, in higher plants and microorganisms involving 1-deoxy-D-xylulose-5-phosphate 3 as the key

intermediate (8,9). As outlined in Figure 1, 1-deoxy-D-xylulose-5-phosphate is formed from pyruvate 1 and glyceraldehyde phosphate 2 in a thiamine pyrophosphate-dependent reaction. *In vivo* experiments documented unequivocally that the linear carbohydrate is then converted to the branched isoprenoid precursors involving an intramolecular rearrangement.

It is estimated that over one hundred million tons of carotenoids are produced annually in nature (10), most of which is due to fucoxanthin in various algae, and to lutein, violaxanthin and neoxanthin in green leaves. Carotenoids that are more commonly associated with food materials include β -carotene, which is widely distributed in nature, and lycopene, which gives red tomatoes their color. Structures of some carotenoids are given in Figure 2. Carotenoids are present in food plant materials in various concentration levels (Table I). Where carotenoids are present in animal tissues, e.g., egg yolk, and salmon flesh, their origin is carotenoid-containing plant tissue that has been consumed by the animal and deposited in the tissue concerned. Levels of selected carotenoids, quoted as a percentage of the total level, in some fruits and vegetables are given in Table II. The information in Tables I and II illustrates the range of levels of total carotenoids, e.g., from 12 mg/kg in oranges to 1756 mg/kg in paprika, as well as the variation in the profile of carotenoids in different commodities and the distribution of selected carotenoids among certain foods.

Table I Concentrations of Total Carotenoids in Selected Foods (4)

<i>Food</i>	<i>Conc. (mg/kg)</i>
Carrots	94
Tomatoes	950
Apricots	35
Apple peel	13
Oranges	12
Paprika	1756
Red pepper	281

Table II Levels of Selected Individual Carotenoids as a % of Total Carotenoids in some Foods (4)

<i>Material</i>	α - <i>Caro-</i> <i>tene</i>	β - <i>Caro-</i> <i>tene</i>	<i>Crypto-</i> <i>xanthin</i>	<i>Zea-</i> <i>xanthin</i>	<i>Neox-</i> <i>anthin</i>	<i>Lycopene</i>	<i>Caps-</i> <i>an-</i> <i>thin</i>
Carrots	34.0	55.3	-	-	-	-	-
Tomatoes	2.30	-	-	-	-	66.7	-
Apricots	-	54.0	3.1	0.7	-	1.0	-
Apple peel	-	7.9	2.4	3.1	19.4	-	-
Oranges	1.0	2.0	10.6	10.2	2.5	-	-
Paprika	-	15.4	12.3	3.1	2.0	-	33.3
Red bell peppers	-	11.0	-	-	-	-	60.0

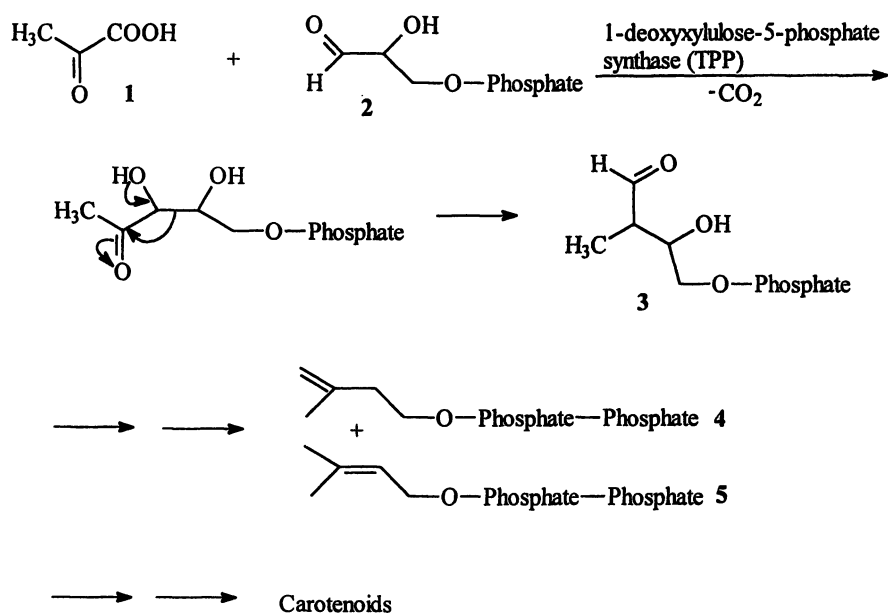


Figure 1. Biosynthesis of carotenoids via the deoxy-D-xylulose 5-phosphate pathway (8,9).

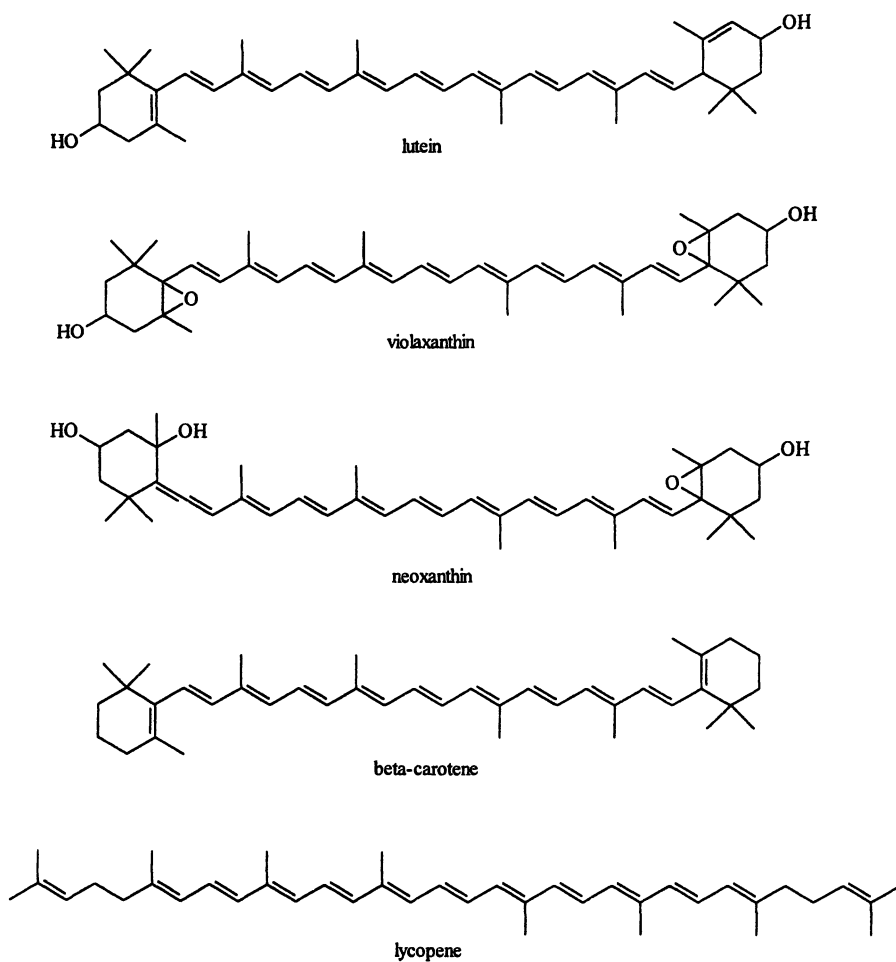


Figure 2. Structures of selected carotenoids.

Stability and Effects of Food Processing

The relative stability of carotenoids and their solubility in lipids has led to their use as coloring agents in, e.g., margarine, cheese, ice cream, baked goods, non-dairy creamers and confectionery. The development of water-dispersable formulations and concern expressed by the consumer regarding artificial colorants, such as tartrazine, has extended their application to soft drinks and other water-based foods, e.g., soups, sauces.

Nevertheless, carotenoids are degraded under certain conditions upon food processing as summarised in Figure 3 (11). In the absence of oxygen, thermal transformations occur, e.g., during canning. At more elevated temperatures, β -carotene can undergo fragmentation to give aromatic hydrocarbons, e.g., ionone (11). Extensive loss of carotenoids occurs when the food materials are processed in the presence of oxygen. Stimulated by light, enzymes or fatty acid hydroperoxides, carotenoids are degraded to form a wide range of compounds (11).

Physiological Properties

A wide range of carotenoids, including extracts from various plant and algal sources are approved world-wide for use as food colorants. Carotenoids possess pronounced antioxidant activity *in vitro* (12,13) due to their ability to scavenge singlet oxygen ($^1\text{O}_2$) and/or peroxy radicals. Carotenoids are the most effective natural quenchers of $^1\text{O}_2$ while peroxy radicals are scavenged by chemical interactions. The most consistent body of epidemiological evidence for a protective effect of an antioxidant nutrient on cancer is for β -carotene, especially for lung cancer, where twenty-four out of twenty-five studies have shown a protective effect (14). β -Carotene also seems to protect against stomach cancer but no consistent associations have been established for colorectal, prostate or breast cancers (1). Also, preventative effects towards atherogenic lesions are associated with increased uptake of carotenoids (2). A possible association between consumption of lycopene intake *via* tomato products and prostate cancer was recently reported (15). It was shown that a significant reduction in prostate cancer occurred with increased consumption of tomatoes cooked in oil, tomato sauce and pizza. However, no correlation was observed between the incidence of prostate cancer and consumption of tomato juice. These results illustrate the importance of other dietary components, such as, e.g., oil, that can affect the bioavailability of compounds with possible protective effects.

Sufficient studies have been performed to draw the conclusion that supplementation of normal individuals with moderate amounts of β -carotene can be undertaken safely (1). However, extrapolation of this conclusion to heavy smokers is not warranted since two studies have been conducted showing an association between β -carotene supplementation and the incidence of lung cancer (1).

Table III. Substituents on the Flavylum Cation Structure in Different Anthocyanidins

<i>Anthocyanidin</i>	<i>Substituent on Carbon^a</i>		
	3'	4'	5'
Cyanidin	OH	OH	H
Delphinidin	OH	OH	OH
Malvidin	OCH ₃	OH	OCH ₃
Pelargonidin	H	OH	H
Peonidin	OCH ₃	OH	H
Petunidin	OCH ₃	OH	OH

^a See Figure 4 for substitution.

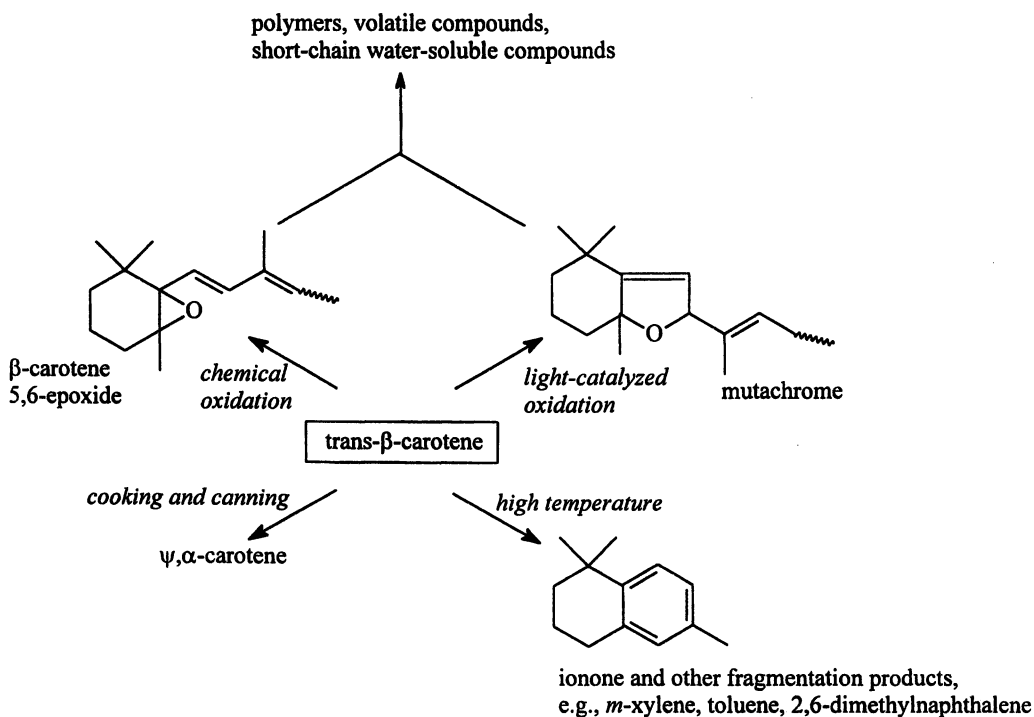


Figure 3. Possible degradation pathways for β -carotene. (Adapted with permission from reference 11.)

A number of epidemiological studies also indicate a protective effect of carotenoids against cardiovascular disease (16). For example, a high β -carotene intake or serum level of β -carotene is correlated with a decreased risk of CHD.

Some non-nutritive effects of food colorants are unrelated to any antioxidant activity, for example, some carotenoids inhibit growth of transformed fibroblasts (17), possibly because they have a role in inter-cellular signaling involved in growth control. Also, β -carotene and lycopene are reported to have inhibitory effects on cell proliferation for several human cancer cell lines (18).

Anthocyanins

Structure and Biosynthesis

Anthocyanins, belonging to the class of flavonoids, are responsible for the color of many fruits, e.g., strawberries, cherries, and grapes, as well as some vegetables, e.g., radish, and many flowers (4). The anthocyanins consist of an anthocyanidin glycosidically linked to several carbohydrate moieties (19). The biosynthesis of the aglycone is displayed in Figure 4. An activated hydroxyl cinnamic acid molecule reacts with three molecules of activated malonic acid, to give a chalcone. This rearranges to a flavanone skeleton which undergoes a series of transformations to yield the flavanol. Finally, the flavanol loses a molecule of water to give the anthocyanidin. The structures of selected anthocyanins are given in Table III, which shows that the actual anthocyanidin is determined by the substitution at positions 3' and 5'. Levels of anthocyanins in plant tissues can vary considerably, as shown in Tables IV and V.

Table IV Occurrence of Total Anthocyanins in Selected Fruits (4)

<i>Fruit</i>	<i>Conc. (mg/kg)</i>
Strawberries	127
Red grape	80-3880
Cranberry	460-1720
Sweet cherry	3500-4500
Blackcurrant	2500

Stability and Effects of Food Processing

Anthocyanins are inherently unstable and are affected by pH, temperature, light, oxygen, sulfite and ascorbic acid (19,20). E.g., Anthocyanins change color dramatically when the pH is modified and the chemical changes concerned are summarized in Figure 5, using malvidin-3-glucoside as an example. The blue quinoidal base becomes protonated, as the pH is lowered, to give the red

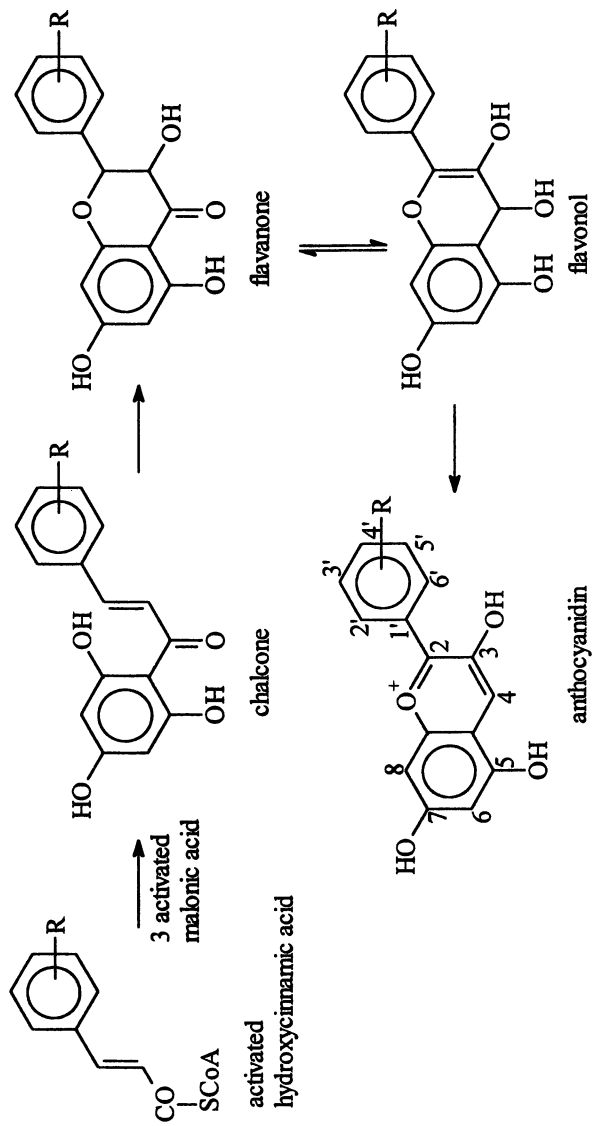


Figure 4. Biosynthesis of anthocyanidins (19).

Table V Levels of Selected Individual Anthocyanins as a % of Total Anthocyanins in some Fruits (4)

<i>Fruit</i>	<i>Cy 3gl</i>	<i>cy 3ga</i>	<i>cy 3rt</i>	<i>dp 3gl</i>	<i>Mv 3gl</i>
Strawberry	0 – 50				
Grape	1 – 6			5 – 17	36 – 43
Cranberry		16 – 25			
Tart cherry	3 – 19		11 – 27		
Blackcurrant	17		35	13	

cy, cyanidin; dp, delphinidin; mv, malvidin; gl, glucoside; ga, galactoside; rt, rutoside.

flavylium cation. This is able to hydrate to form the colorless carbinol pseudobase which exists in equilibrium with the colorless chalcone (20). Therefore, the relative proportions of the different forms of anthocyanins vary with pH. However, the flavylium cation and the carbinol pseudobase are the dominant forms, the quinoidal base and the chalcone each accounting for less than ten per cent of the total amount up to pH 5 (20). For malvidin-3-glucoside, the flavylium cation and the carbinol pseudobase exist in approximately equal amounts at pH 2.5. As the pH increases above this value, progressive bleaching occurs. Also, sulfite bleaches anthocyanins (19). In this case, sulfite is attached to the anthocyanidin ring structure at position 2 or 4, giving the carbinol base (Figure 6). The color is, however, restored on acidification to pH 1 (19).

Physiological Properties

Anthocyanins (and other flavonoids) are reported to scavenge peroxy, hydroxyl and superoxide anion radicals *in vitro*, thereby forming a phenoxy radical (21,22). There is little information concerning the antioxidant activities of flavonoids *in vivo* (12). Gut bacteria are able to hydrolyse the glycosides and metabolise most of the aglycone (23), resulting in very low levels of free flavonoids in human plasma. In addition, their bioavailability is poor and they are rapidly conjugated in phase II detoxification reactions (1). No human studies appear to have been performed on the absorption and metabolism of anthocyanins (1).

Anthocyanin extracts prepared from vegetables and edible fruits are approved for use as food colors world-wide (1). Various studies have indicated that the toxicity of these materials is negligible. An average daily intake of 2.5 mg/kg body weight/day has been allocated by the World Health Organisation (1982) for anthocyanin color from grape skin extracts.

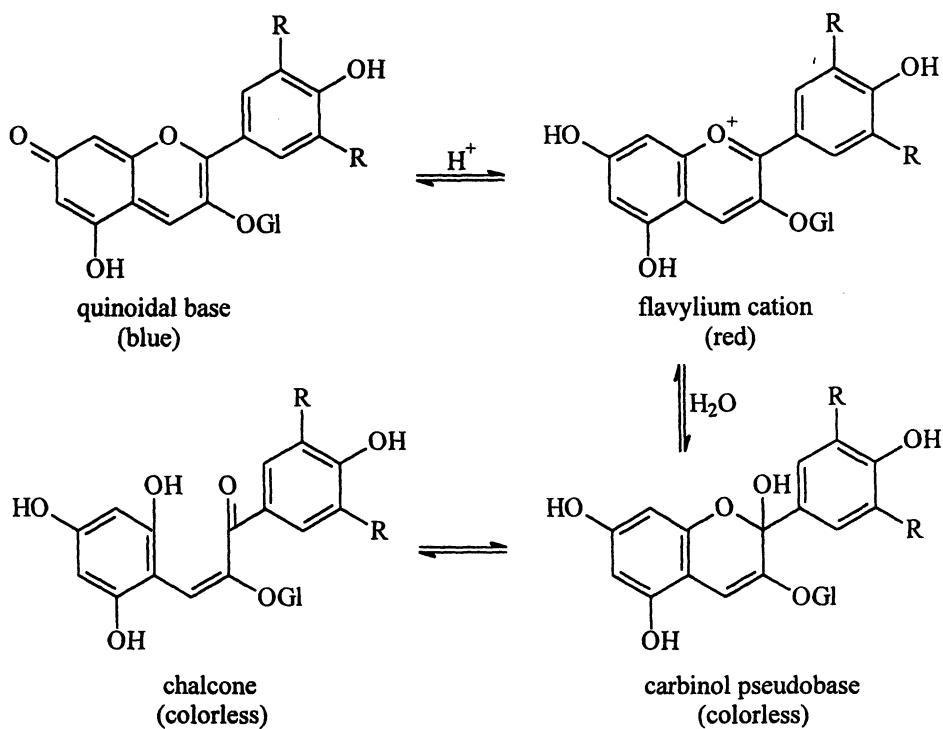


Figure 5. Effect of pH on the structure and color of anthocyanidins. (Adapted with permission from reference 11.)

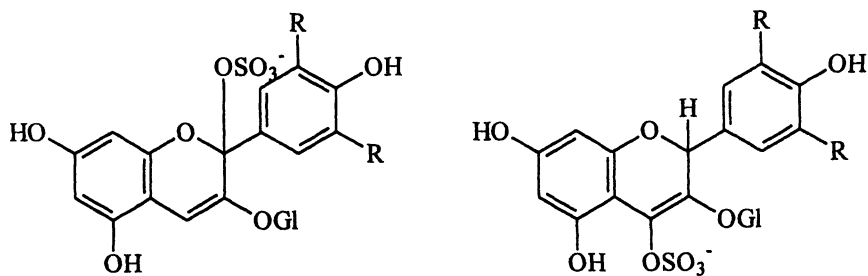


Figure 6. Structures of anthocyanidin-sulfite reaction products.

Products of Enzymatic Browning

Enzymatic browning is of most significance in a food context when fruits and vegetables become damaged, or for black tea processing. Since, after water, tea is probably the most consumed beverage in the world (24) this makes enzymatic browning of particular interest to the food scientist.

Biosynthesis and Structure

Enzymatic browning is mediated by phenolase enzymes. These have two different activities, namely cresolase and catecholase. The most important substrates for enzymatic browning are tyrosine (which is also the only substrate for enzymatic browning in animal tissue) and chlorogenic acid, which is widely distributed in plant tissue, including apples, pears and potatoes (25). The sequence of events resulting in color development is shown in Figure 7. A monophenol is converted to an *o*-diphenol in the presence of oxygen by the cresolase activity of phenolase enzymes. The *o*-diphenol is subsequently oxidized to its *o*-quinone by the catecholase activity of the same enzymes. *o*-Quinones spontaneously convert to hydroxyquinones, which in turn form colored polymers (25).

In black tea manufacturing, important substrates for enzymatic browning are colorless flavanols such as (-)-epicatechin-3-gallate (19). These become oxidized to *o*-quinones, by the action of phenolase enzymes (19). These oxidized flavanols are converted to theaflavins and, by loss of gallic acid, to epitheaflavic acids (Figure 8). The oxidized flavanols, theaflavins and epitheaflavic acids are able to undergo further reactions, resulting in thearubigins, the structures of which are, as yet, not completely characterized. Further detail of the chemistry of the two main classes of colored components in black tea, the theaflavins and thearubigins, is given by Robertson (26). The theaflavins, which account for 0.3-2% of black tea, are bright red in color and contribute to the brightness of tea (27). The thearubigins are reddish/yellow or brown in color and account for most of the red/yellow of black tea. They account for 10-20% of the dry weight of black tea and 30-60%, of a hot water extract. In addition, thearubigins contribute to astringency and to the typical taste of black tea. Only *ca.* 10% of the catechins lost during black tea manufacture are accounted for by theaflavins and theaflavic acids. The remainder are converted to thearubigins (27).

Effects of food processing

Processing conditions can be chosen in order to minimize discoloration caused by enzymatic browning in fruits and vegetables or to optimize controlled pigment formation, e.g., in black tea.

In fruits and vegetables, a substrate, the phenolase enzyme in the active form, and oxygen are all required for enzymatic browning. Various strategies can be

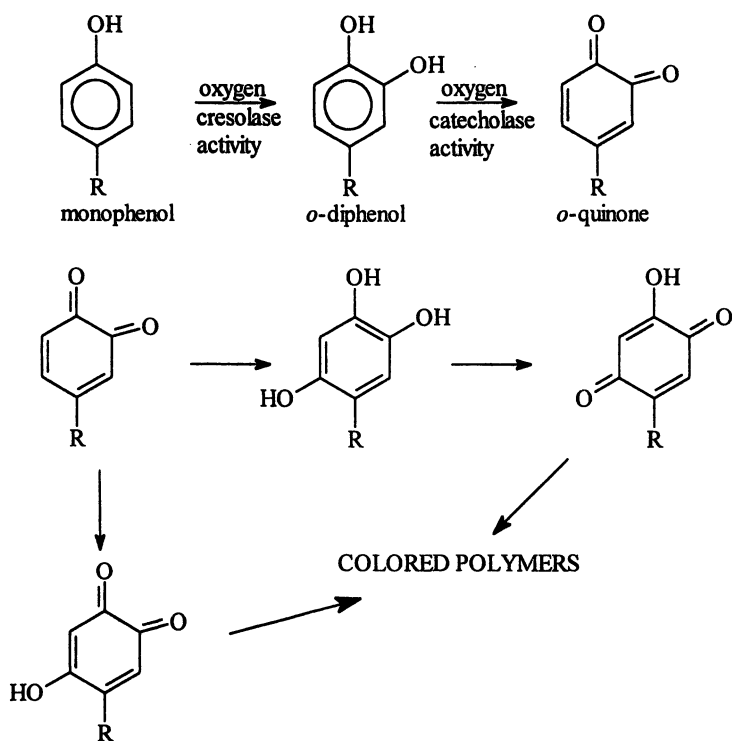


Figure 7. Outline of the biochemical steps involved in enzymatic browning (25).

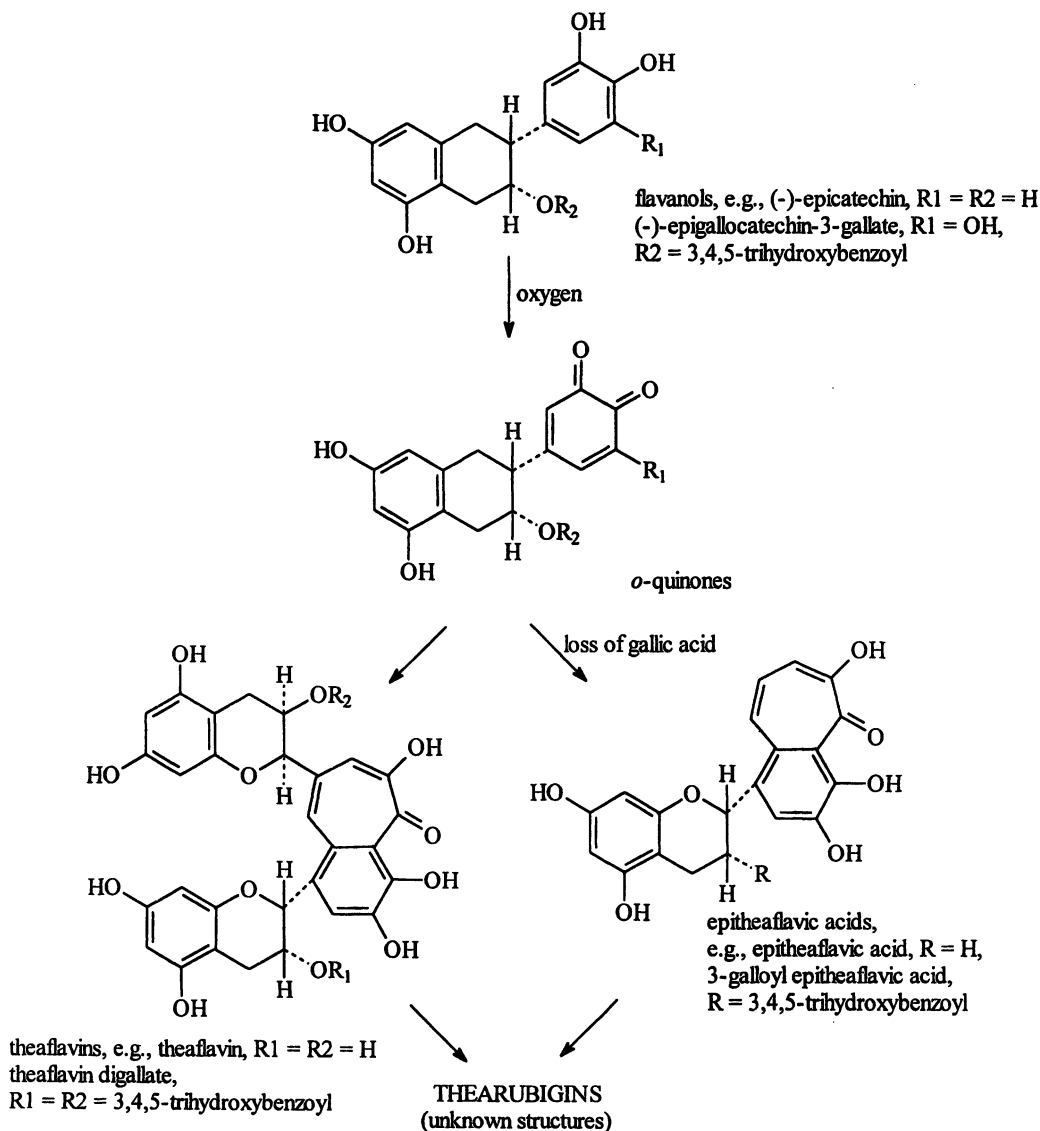


Figure 8. Outline of the conversion of flavanols to epitheafavic acids, theaflavins and thearubigins during black tea manufacture. (Adapted with permission from reference 19.)

adopted to avoid enzymatic browning. Eliminating tissue damage, e.g., by bruising or insect attack will avoid the substrate and enzyme coming into contact, but, if physical damage of plant tissue is unavoidable, e.g., in potato slicing, the cut material can be immersed in water, in order to minimize contact with air (19). Immersion in water of a pH below the optimum for phenolase, or in water containing sulfite, will further reduce enzymatic browning. Another strategy is to inactivate phenolase by blanching. Finally, ascorbic acid is a powerful inhibitor of enzymatic browning by operating in a number of ways. It is able to chelate copper, which is a component of the active site of phenolase, it can act as an antioxidant and it reacts directly with *o*-quinones by reducing them back to *o*-diphenols.

The three main stages of black tea manufacture are withering, fermentation and firing (19). During withering, a reduction in green color occurs due to chlorophyll degradation. Fermentation is the main stage for the formation from catechins of theaflavins and thearubigins, the main colored components of black tea. Other colorants isolated from black tea include theacitrins (28). The oxygen level, pH, temperature and time of fermentation can all be modified and such modifications will affect theaflavin and thearubigin formation. Oxidation of carotenoids also occurs during fermentation and, at the end of this processing step, the tea is copper red in color. The final step of black tea processing is firing. Temperatures of up to 75°C are used. About 10-15% of the total theaflavins are formed during firing and thearubigins, which account for most of the color of black tea, are also formed here. In addition, firing causes conversion of chlorophyll degradation products (formed during withering) to phaeophytins and these give black tea its characteristic color (19).

Physiological Properties of Theaflavins and Thearubigins

There is a large body of literature concerned with the possible protective effects of tea, or its individual components, such as catechins, against age-related diseases (primarily CHD and cancer). However, most of the reports deal with *in vitro* or animal (rather than human) studies. When selected fractions of tea are investigated, effort has usually focused on the colorless or pale yellow polyphenols, such as the catechins, rather than on the strongly colored theaflavins and thearubigins.

While catechins and other flavonoids from tea have strong antioxidant activity *in vitro*, the effects *in vivo* depend on the concentrations of the compounds concerned in tea and the amount of tea consumed (29). The *in vitro* antioxidant capacities (measured as Trolox Equivalents, TE) of green tea, containing no theaflavins or thearubigins, and black tea appear to be very similar, with values for black teas being slightly higher (29). Levels of total polyphenols in black teas also appear to be slightly higher than those in green teas (see Table VI). However, the observed differences between the two categories could be due to variations in growing conditions and processing methods, since the teas came from different sources.

Table VI Range of Antioxidant Capacity and Phenolic Content of Commercial Green and Black Teas (29)

<i>Tea</i>	$\mu\text{mol TE/g}$	<i>Total phenolics mg/g</i>
Black	478-1526	109-147
Green	236-1197	32-133

In experiments concerned with maintaining the effects of tea compounds on growth of human cancer cell lines, theaflavin-3,3'-digallate has been shown to strongly inhibit the growth of, or to cause cytotoxic effects on, lung (H661) and Ha-ras transformed bronchial epithelial (21 BES) cells (30). In a separate study (31), various fractions were prepared from black tea and tested for their abilities to inhibit DNA synthesis in HTC rat hepatoma cells and DS19 mouse erythroleukemia cells. The fraction containing mainly catechins and theaflavins was more effective than those containing either mainly thearubigins or components not extracted from tea by ethyl acetate or *n*-butanol.

From their studies on cancer cells lines Yang *et al.* (32) concluded that the growth inhibition activity of theaflavin-3,3'-digallate was similar to that of epigallocatechin-3-gallate (EGCG) and higher than that of theaflavin-3(3')-gallate, which in turn was higher than that of theaflavin. They suggest that the combined activities of the theaflavins, together with EGCG, and three further catechins, i.e., (-)-epigallocatechin, (-)-epicatechin-3-gallate and (-)-epicatechin, may account for most of the cell growth inhibition activity of black tea extracts. Although thearubigins are the major components of black tea, their activity is probably weaker, but requires further study.

In animal studies, theaflavins have been shown to inhibit lung (33) and esophageal (34) carcinogenesis in mice but the bioactivities of thearubigins are unknown (30).

Products of Non-Enzymatic Browning

Effects of Food Processing

During thermal processing of foods, e.g., baking of bread, roasting of coffee, kilning of malt or manufacturing of breakfast cereals, cookies and toffees, Maillard reactions between reducing carbohydrates and amino acids, peptides as well as proteins lead to intense browning (35). A brief outline of the chemical processes leading to the low molecular mass and the macromolecular materials is given in Figure 9. Also, in the absence of amino compounds, reducing carbohydrates can undergo degradation to form colored material, so called

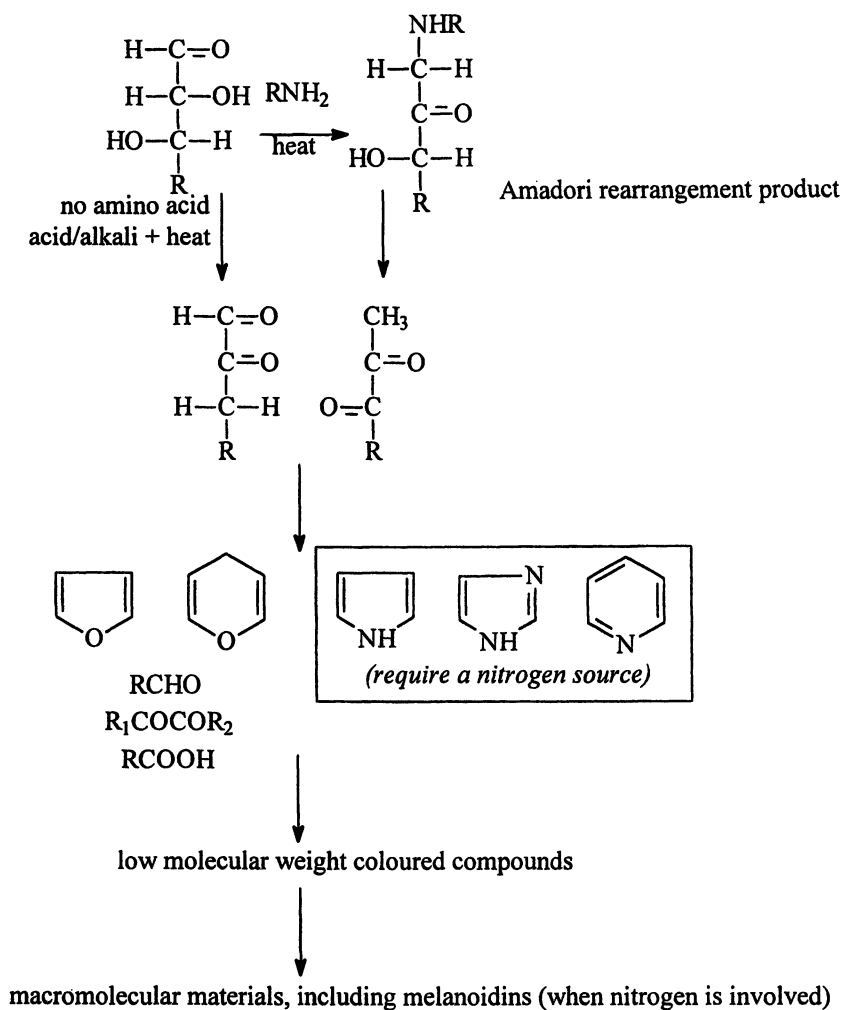


Figure 9. Outline of the formation of colored compounds formed during caramelization and the Maillard reaction.

caramelization. The chemistry of these reactions is as yet only partly understood (36).

The Maillard reaction is strongly affected by the pH value, the water activity and the temperature and time of processing (37). The reaction increases with temperature and time of heating and with pH (within the range encountered in foods). Intermediate levels of water activity favor the reaction over higher or lower values (37,38).

Physiological Properties

Since the Maillard reaction involves ascorbic acid or essential amino acids such as lysine as precursors, the nutritional value of the food may be compromised (39), especially for those on restricted diets, e.g., babies, and those being fed intravenously.

Melanoidins are reported to possess antioxidant activity in food systems (40) due to their ability to scavenge free radicals (41) and to complex metals, such as copper, which promote oxidation reactions (42). When metals of nutritional significance are complexed, again, the nutritional value of the food may be reduced. Whether colored Maillard reaction and caramelization products have additional physiological effects is as yet not clear. The above mentioned effects of Maillard reaction and caramelization products operating *in vivo* depend on their absorption and fate in the body. Finot (43) states that premelanoidins, presumably including low-molecular weight colored compounds and low molecular mass melanoidins, are partly absorbed and not completely excreted in the urine, a fraction being retained by the body. Therefore, it would seem that at least it is possible that these materials could exert physiological effects *in vivo*.

In contrast, non-dialyzable and insoluble melanoidins are not absorbed (43) and, therefore, any physiological effects they may possess must operate in the gut. This includes the possible inhibition of intestinal enzymes, promotion or suppression of the growth of gut bacteria and retardation of the absorption of other dietary components. These components may be beneficial, e.g., nutritionally important minerals such as copper or undesirable components, e.g., pesticide residues.

Various physiological effects have been observed in rats and humans as a result of feeding foods that have undergone the Maillard reaction (43). However, in most cases, no attempt was made to identify the specific Maillard products causing the effect.

Conclusion

A considerable amount of information is available concerning the structures and effects of food processing for carotenoids, anthocyanins and theaflavins. In contrast, very little is known about the low molecular mass colored Maillard products and almost no information is available concerning the structures of

thearubigins and melanoidins. Key questions remain to be answered about the uptake and distribution in tissues of all food colorants in the human body, as well as their bioavailabilities and bioactivities. In addition, with the exception of β -carotene, there is a need for more work on the physiological properties in humans for all four classes of food colorant discussed.

Literature Cited

1. Diplock, A.T.; Charleux, J.-L.; Crozier-Willi, G.; Kok, F.J.; Rice-Evans, C.; Roberfroid, M.; Stahl, W.; Vifa-Ribes, J. *British Journal of Nutrition* 1998, 80, suppl. 1, S77-S112.
2. Rimm, E.B.; Stampfer, M.J.; Ascherio, A.; Giovannucci, E.; Colditz, G.A.; Willett, W.C. *New England Journal of Medicine* 1993, 328, 1450-1456.
3. Flagg, E.W.; Coates, R.J.; Greenberg, R.S. *Journal of the American College of Nutrition* 1995, 14, 419-426.
4. Eder, R. In *Handbook of Food Analysis*; Nollet, L.M.L. Ed.; Dekker: New York, 1996, Vol. 1, Physical Characterization and Nutrient Analysis. pp 937-1014.
5. *Key to Carotenoids by Otto Straub*; Pfander, H.; Gerspacher, M.; Rychener, M.; Schwabe, R., Eds.; 2nd edn.; Birkhäuser: Basel, Switzerland, 1987.
6. Goodwin, T.W. *The Biochemistry of Carotenoids*; Goodwin, T.W., Ed.; Chapman and Hall: London, UK, 1980.
7. Folkers K.; Wolf, D.E. *J. Am. Chem. Soc.* 1956, 78, 5273-5275.
8. Arigoni, D.; Sagner, S.; Latzel, Ch.; Eisenreich, W.; Bacher, A.; Zenk, M.H. *Proc. Natl. Acad. Sci. USA* 1997, 94, 10600-10650.
9. Eisenreich, W.; Schwarz, M.; Cartayrade, A.; Arigoni, D.; Zenk, M.H.; Bacher, A. *Chem. & Biol.* 1998, 5, R221-R233.
10. Isler, O. *Carotenoids*; Birkhäuser: Basel, Switzerland, 1971.
11. Tannenbaum, S.R.; Young, V.R.; Archer, M.C. In *Food Chemistry*; Fennema, O.R. Ed.; 2nd ed.; Dekker: New York, 1985, pp 477-544.
12. Stahl, W.; Sies, H. *Annals of the New York Academy of Sciences* 1993, 691, 10-19.
13. Olson, J.A.; Krinsky, N.I. *FEBS Letters* 1995, 9, 1547-1550.
14. van Poppel, G.; Goldbohm, R.A. *American Journal of Clinical Nutrition* 1995, 62, Suppl., 1393S-1402S.
15. Giovannucci, E.; Ascherio, A.; Rimm, E.B.; Stampfer, M.J.; Colditz, G.A.; Willett, W.C. *Journal of the National Cancer Institute* 1995, 87, 1767-1776.
16. Kohlmeier, L.; Hastings, S.B. *American Journal of Clinical Nutrition* 1995, 62, 1370S-1376S.
17. Bertram, J.S.; Bortkiewicz, H. *American Journal of Clinical Nutrition* 1995, 62, 1322S-1326S.
18. Sharoni, Y.; Levi, J. In *Natural Antioxidants and Food Quality in Atherosclerosis and Cancer Prevention*; Kumpulainen, J.T.; Salonen, J., Eds.; Royal Society of Chemistry: Cambridge, UK, 1996, pp 378-385.

- 19 Belitz, H.-D.; Grosch, W. *Food Chemistry*; Springer-Verlag: Berlin, Germany, 1987.
20. Francis, F.J. In *Food Chemistry*; Fennema, O.R. Ed.; 2nd ed.; Dekker: New York, 1985, 545-584.
21. Rice-Evans, C.; Miller, N.J.; Bolwell, P.G.; Bramley, P.M.; Pridham, J.B. *Free Radical Research* 1995, 22, 375-383.
22. Rice-Evans, C.; Miller, N.J. *Biochemical Society Transactions* 1996, 24, 790-795.
23. Hackett, A.M. In *Progress in Clinical and Biological Research*; Cody, V.E.; Middleton, J.R.; Harborne, H.B., Eds.; A R Liss: New York, 1986, vol. 213, pp 177-194.
24. Marks, V. In *Tea Cultivation to Consumption*; Willson, K.C.; Clifford, M.N., Eds.; Chapman and Hall: London, UK; 1992; pp 707-739.
25. Coultate, T.P. *Food Chemistry*; Royal Society of Chemistry: Cambridge, UK, 1989; pp 126-158.
26. Robertson, A. In *Tea Cultivation to Consumption*; Willson, K.C.; Clifford, M.N., Eds.; Chapman and Hall: London, UK; 1992; pp 555-601.
27. Balentine, D.A.; Wiseman, S.A.; Bouwens, L.C.M. *Crit. Revs. Food Sci. Nutr.* 1997, 37, 693-704.
28. Davis, A.L.; Lewis, J.R.; Cai, Y.; Powell, C.; Davis, A.P.; Wilkins, J.P.G.; Pudney, P.; Clifford, M.N. *Phytochem.* 1997, 46, 1397-1402.
29. Prior, R.L.; Cao, G. *Proceedings of the Society for Experimental Biology and Medicine*, 1999, 220, 255-261.
30. Yang, C.S.; Kim, S.; Yang, G.-Y.; Lee, M.-J.; Liao, J.; Chung, J.Y.; Ho, C.-T. *Proceedings of the Society for Experimental Biology and Medicine* 1999, 220, 213-217.
31. Lea, M.A.; Xiao, Q.; Sathukhan, A.K.; Cottle, S.; Wang, Z.-Y.; Yang, C.S. *Cancer Lett.* 1993, 68, 231-236.
32. Yang, G.-Y.; Liao, J.; Kim, K.; Yurkow, E.J.; Yang, C.S. *Carcinogenesis* 1998, 19, 611-616.
33. Yang, G.-Y.; Liu, Z.; Seril, D.N.; Liao, J.; Ding, W.; Kim, S.; Bondoc, F.; Yang, C.S. *Carcinogenesis* 1997, 18, 2361-2365.
34. Morse, M.A.; Kresty, L.A.; Steele, V.E.; Kelloff, G.J.; Boone, C.W.; Balentine, D.A.; Harbowy, M.E.; Stoner, G.D. *Nutr. Cancer* 1997, 29, 7-12.
35. Ames, J.M. *Food Chem.* 1998, 62, 431-439.
36. Ledl, F.; Schleicher, E. *Angew. Chem. Int. Ed. Engl.* 1990, 29, 565-706.
37. Ames, J.M. *Trends in Food Science and Technology* 1990, 1, 150-154.
38. Reineccius, G.A. In *The Maillard Reaction in Food Processing, Human Nutrition and Physiology*; Finot, P.A.; Aeschbacher, H.U.; Hurrell, R.F.; Liardon, R. Eds; Birkhäuser: Basel, Switzerland, 1990, pp157-170.
39. Freidman, M. *J. Agric. Food Chem.* 1996, 44, 631-653.
40. Wijewickreme, A.N.; Kitts, D.D. *J. Food Sci.* 1998, 63, 466-471.
41. Hayase, F. In *The Maillard Reaction. Consequences for the Chemical and Life Sciences*; Ikan, R. Ed.; Wiley: Chichester, UK; 1996; pp 89-104.
42. O'Brien, J.; Morrissey, P.A. *Food Chem.* 1997, 58, 17-27.
43. Finot, P.A. In *The Maillard Reaction in Food Processing, Human Nutrition and Physiology*; Finot, P.A.; Aeschbacher, H.U.; Hurrell, R.F.; Liardon, R. Eds; Birkhäuser: Basel, Switzerland, 1990, pp 259-272.

Chapter 2

Separation of Natural Food Colorants by High-Speed Countercurrent Chromatography

Andreas Degenhardt, Holger Knapp, and Peter Winterhalter

Institute of Food Chemistry, Technical University of Braunschweig,
Schleinitzstrasse 20, DE-38106 Braunschweig, Germany
(e-mail: P.Winterhalter@tu-bs.de)

High Speed Countercurrent Chromatography (HSCCC) was applied to the separation of water-soluble carotenoids from saffron and *Gardenia jasminoides*, flavonol glycosides from black tea and anthocyanins from a wide range of foodstuffs. In this chapter we describe the isolation, clean-up and subsequent separation of these compounds on a preparative scale. Peak purity and identity of compounds were made by ¹H-NMR, ESI-MS/MS and HPLC-DAD. Furthermore, biological activities of the food colorants under investigation are summarized.

Purification of compounds by distribution between two immiscible liquids is a long established practice in the chemical laboratory. However, it is a long way from liquid-liquid extraction using a separatory funnel (or a series of them, e.g., in the '*Craig countercurrent distribution apparatus*') to the development of the highly efficient separation technique of countercurrent chromatography (CCC).

The modern era of CCC began in the early 1980's with the development by Ito (1,2) of the coil planet centrifuge, a technique which was marketed as multilayer coil countercurrent chromatography (MLCCC) or as high speed countercurrent chromatography (HSCCC). Since these techniques have been applied in the present study, the working principle will be briefly outlined. More detailed descriptions can be found in the monographs on countercurrent chromatography (3-5).

In multilayer, as well as in high speed, CCC the separating column consists of a PTFE tubing that is wrapped around a holder in several layers (multilayer coil). The radius, r , of the coiled column depends on the number of layers. In essence, the coil undergoes a synchronous planetary motion while the column holder revolves around the central axis of the apparatus. The revolution radius is

R, and the ratio of r/R is defined as the β -value, which may vary from 0.25 to 0.8. The apparatus is designed with an anti-twist mechanism that ensures continuous solvent flow without requiring a rotating seal. During rotation, an Archimedean screw force is achieved causing the migration of the stationary phase towards one end of the column. The mobile phase is now introduced in the opposite direction. During operation, the interfacial frictional force and the Archimedean screw force counteract and create a *hydrodynamic equilibrium* depending on the rotation speed, flow rate, β -value and viscosity of the solvent. Ideally, the mobile phase can be pumped through the system with the stationary phase being almost completely (*ca.* 80 %) retained.

The mixing of the two immiscible phases is automatically achieved. When the β -value exceeds 0.5, the trajectory forms a loop in which the force field is much lower compared with the opposite part of the loop. This difference leads to the following behavior of a two phase system in the coil. When the force field is strong, the phases are separated (settling step), when the force field is weak (in the loop), mixing of the two phases occurs (mixing step). Injection of a sample can result in 50 000 liquid-liquid partitions per hour as it successively passes through alternate settling and mixing zones of the coiled column, thus enabling efficient separation of the solutes.

CCC is an all-liquid technique and has no solid stationary phase. Therefore, artifact formation as a result of irreversible adsorption effects on stationary phases is minimised. The separations are performed within short separation times. Although the number of theoretical plates is seldom higher than 1000 (3), CCC offers good separations due to its high volume of stationary phase. Elution times can be easily predicted by measuring partition coefficients. Separations can be improved by changing solvent polarity and/or solvent selectivity through selective interactions between solutes and solvents. A great number of solvent systems is available for HSCCC separations. Therefore, CCC is an extremely versatile technique. Moreover, separations can be run using "normal" phase or, by reversing the head to tail connections, in the "reversed" phase mode (3-5).

Countercurrent chromatography is emerging as a superior technique for preparative separations, especially in the field of natural products where often mixtures of tremendous complexity are encountered. As a support-free technique, CCC appears to be the method of choice for separations of labile plant-derived pigments. Results of the application of CCC to the separation of different classes of natural food colorants will be reported here.

Experimental

Materials

Saffron (dried red stigmata of *Crocus sativus* L.) was purchased from a local supplier. A methanolic extract from fruits of *Gardenia jasminoides* was supplied by Professor N. Watanabe, Shizuoka University, Japan. Black tea was a low grown Ceylon type, purchased from a local supplier. Calyces from roselle (*Hibiscus sabdariffa* L.) were supplied by Martin Bauer GmbH & Co KG (Vestenbergsgreuth, Germany). Concentrated liquid extracts of red cabbage

(*Brassica oleracea* L.) and black currant (*Ribes nigrum* L.) were donated by Plantextrakt (Vestenbergsgreuth, Germany). Californian red wine was purchased in a local supermarket. *Tradescantia pallida* was grown in a greenhouse in the local botanical garden.

Extraction of Water-soluble Carotenoids from Saffron

Dried stigmata of *Crocus sativus* (4 g) were extracted with diethyl ether in order to remove the less polar constituents. The residue was then extracted with methanol by stirring for 1 hour in the dark. The methanolic extract was used for HSCCC without further purification.

Extraction of Flavonol Glycosides from Black Tea

The flavonol glycosides were extracted from black tea following a procedure by Engelhardt *et al.* (6) and cleaned-up on a polyamide column. The eluate was freeze-dried prior to HSCCC separation.

Isolation of Anthocyanins from Red Wine

After evaporation of ethanol *in vacuo*, the dealcoholised red wine (0.7 L) was applied to an Amberlite XAD-7 column (50 cm × 4 cm, Fluka Chemie, Buchs, Switzerland). The column was washed with 1 L of water, to remove sugars and organic acids. The anthocyanins were eluted with 500 mL of a mixture of methanol/acetic acid (19/1, v/v). The solvent was evaporated and the residue was twice partitioned against 300 mL of ethyl acetate. The aqueous phase was concentrated *in vacuo* and freeze-dried to yield 1.1 g of a violet powder which was used for HSCCC.

Extraction of Pigments from Roselle

Calyces from roselle (15 g) were extracted with 100 mL of 0.1 % HCl in methanol over 48 hours in the dark. The slurry was filtered and the solvent was evaporated at 30 °C using a rotary evaporator. The residue was separated by HSCCC without further purification or enrichment.

Clean-up of Pigments from Black Currant and Red Cabbage

15 g of each of the extracts were acidified with 10 % aqueous formic acid (5 mL), diluted with 50 mL of water and extracted 2 times with 150 mL of ethyl acetate. The pooled aqueous phase was applied to an Amberlite XAD-7 column (50 cm × 4 cm, Fluka Chemie, Buchs, Switzerland). The column was washed with

1 L of water and elution of anthocyanins was carried out with 500 mL of a mixture of methanol/acetic acid (19:1, v/v). The eluate was concentrated *in vacuo*, water (30 mL) was added and the aqueous solution was freeze-dried.

Isolation of Anthocyanins from *Tradescantia pallida*

Leaves of *Tradescantia pallida* were collected in the local botanical garden, cut into fine pieces and extracted at room temperature overnight with methanol/acetic acid (19:1, v/v). The extract was filtered and partitioned twice against 400 mL of pentane. The pentane phase was discarded. The methanolic phase was evaporated *in vacuo*. After partitioning twice against 300 mL of ethyl acetate, the aqueous phase was cleaned-up on an Amberlite XAD-7 column as described for the isolates from black currant and red cabbage. The eluate was evaporated *in vacuo* and freeze-dried.

Countercurrent Chromatography (CCC)

a) A high speed Model CCC-1000 (I) manufactured by Pharma-Tech Research Corporation (Baltimore, Maryland, USA) was equipped with 3 preparative coils, connected in series (total volume: 850 mL). The separations were run at a revolution speed of 1000 rpm and at flow rates from 2.5 to 5 mL/min. A Biotronik HPLC pump BT 3020 was used to pump the liquids. All samples were dissolved in an 1:1 mixture of light and heavy phase and injected into the system by loop injection. The amount of sample injected varied from 100 mg to 2 g. Stationary phase retention was in the range of 53-80 %. 10 mL fractions were collected with a Pharmacia LKB Super Frac fraction collector. Elution was monitored with a Knauer UV-Vis detector and chromatograms were recorded on a Knauer L 250 E plotter. Chromatograms were digitalised using a scanner.

b) Second CCC system was a Multi-Layer Coil Countercurrent Chromatograph (II) by P.C. Inc. (Potomac, Maryland, USA) equipped with a single coil (volume: 360 mL). Revolution speed was set at 800 rpm, the flow rate was 2.5 mL/min.

General procedure for CCC separations:

1. Selection of suitable solvent system, measurement of partition coefficients (7).
2. Selection of elution mode ("normal" or "reversed-phase" mode) by changing the head to tail connections.
3. Loading of coils with stationary phase, i.e., one phase of a biphasic solvent system, which was carefully equilibrated in a separatory funnel (time required for HSCCC apparatus: *ca.* 90 minutes).
4. Injection of sample via loop.
5. Start of rotation.
6. Loading of mobile phase.

7. Equilibration of the system until no more stationary phase is displaced from the system (time required: 40 to 120 minutes, depending on solvent system).
8. Elution of compounds according to their partition coefficients (time required: 10 to 240 minutes).

HPLC with Diode Array Detection (HPLC-DAD)

A Jasco ternary gradient unit LG-980-02, with degasser and MD-910 multiwavelength detector driven by BORWIN chromatography software was used. A second HPLC system was a System Gold Solvent Module 126 from Beckman Instruments with Diode Array Detector 168 and Beckman 502 Autosampler.

Anthocyanins

The chromatographic separation was performed on a Superspher RP18 column 5 μm (250 mm \times 4 mm) from Merck (Darmstadt, Germany) at ambient temperature. The mobile phase was a linear gradient of 10 % aqueous formic acid (solvent A) and acetonitrile/10 % aqueous formic acid (9:1, v/v; solvent B). Conditions: initial, 95 % A, 5 % B; linear gradient over 45 minutes to 75 % A, 25 % B; linear gradient over 15 minutes to 50 % A, 50 % B; returned to the initial conditions; detection at 520 and 320 nm, flow rate: 0.8 mL/min.

Flavonol glycosides

Nucleosil RP18 column 5 μm (250 mm \times 4.6 mm) from Teclab (Erkerode, Germany); 2 % aqueous acetic acid (solvent A), acetonitrile (solvent B). Conditions: initial, 94 % A, 6 % B; linear gradient over 28 minutes to 83 % A, 17 % B; linear gradient over 25 minutes to 80 % A, 20 % B; 12 minutes isocratic at 80 % A, 20 % B; flushing with 100 % B for 20 minutes to condition the column; detection at 354 nm, flow rate: 1 mL/min.

Water-soluble carotenoids

LUNA RP18 column 5 μm (150 \times 4.6 mm) from Phenomenex (Aschaffenburg, Germany), water (solvent A), acetonitrile (solvent B). Conditions: initial, 95 % A, 5 % B; linear gradient over 30 minutes to 50 % A, 50 % B; detection at 450 nm, flow rate: 0.5 mL/min.

Proton Magnetic Resonance Spectroscopy ($^1\text{H-NMR}$)

All experiments were performed on a Bruker AMX 300 spectrometer (300 MHz). Spectra of anthocyanins were recorded in $\text{CD}_3\text{OD-CF}_3\text{COOD}$ (19:1, v/v). Assignments were made on the basis of spectral data published by Pedersen *et al.* (8).

Electrospray Ionization Ion Trap Multiple Mass Spectrometry (ESI-MS/MS)

Flow injection on a Bruker Esquire-LC-MS/MS with electrospray ionization in the positive or negative mode was used. Dry gas was nitrogen with a gas flow of 4 L/min (350 °C); the nebulizer was set at 10 psi. For analysis of anthocyanins the parameters were: positive mode, capillary: -2500 V, end plate: -2000 V, capillary exit: 110 V, skim 1: 35 V, skim 2: 8 V. MS/MS-experiments were performed with different fragmentation amplitudes. The set of parameters was optimised for each application.

Results and Discussion

Of the three major quality factors in food, namely color, flavor and texture, color can be considered as the most important one. Any deviation in the expected color can lead to rejection of the food by the consumer. Thus, the stability of colorants is an important issue for food manufacturers. In the past, color stability was often guaranteed by using synthetic colorants. More recently problems have arisen as a result of the consumer trend towards 'natural' colorants. Many of the widely used natural food colorants, such as carotenoids and anthocyanins, are to some extent unstable on storage, susceptible to pH changes, and difficult to characterize because of their polymeric nature.

With regard to the analysis of colorants, HPLC is often the method of choice. However, for an accurate quantitative determination of compounds in a mixture, as well as for the screening of physiological properties, authentic reference compounds are required. The potential of CCC with regard to the rapid isolation of standard compounds was tested in the present study. Furthermore, CCC was used in order to assist us in the search for stable pigments from alternative natural sources.

Non-polar (Apo-) Carotenoids

Various CCC separations of carotenoids have been published (9-11). Retinals (9) can be separated using the solvent system of cyclohexane-pentane-acetonitrile-methanol (50/20/50/1.1). Apocarotenoids from *Cochlospermum tinctorium* (10) have been successfully separated with a solvent system consisting of carbon tetrachloride-methanol-water (5/4/1). Another publication describes the separation of carotenoids from parsley (11) with petroleum ether-acetonitrile-methanol (50/10/40).

Our work focused on the separation of polar carotenoid derivatives from saffron and *Gardenia jasminoides*.

Water-soluble Carotenoids

Saffron (Crocus sativus L.)

A methanolic extract from saffron was separated by HSCCC. The solvent system was TBME-*n*-butanol-acetonitrile-water (2/2/1/5), the flow rate 5.0

mL/min, with the less dense layer acting as stationary phase (Figure 1). The elution was monitored at 435 nm. The first eluting peak could be identified as *trans*-crocin (**1**) by HPLC-DAD and ESI-MS/MS. The absorption maxima of **1** in the visible region were determined by HPLC-DAD to be at 439 and 467 nm. The observed shift of 5 nm compared to data published by Straubinger (12) is most likely due to the different solvents used in the present study. The UV-Vis spectrum of the second eluting peak showed, besides maxima at 435 and 459 nm, an additional maximum at 327 nm which is characteristic for carotenoids with a *cis*-configured double bond between carbons 12 and 13. **2** was therefore assigned to 13-*cis* crocin (Figure 2). The molecular weight for both compounds, as determined by ESI-MS, was 976 daltons (pseudomolecular ion at m/z 999: $[M(976)+Na]^+$). ESI-MS/MS fragments at m/z 907, 675, 583, 347 were identical for both compounds.

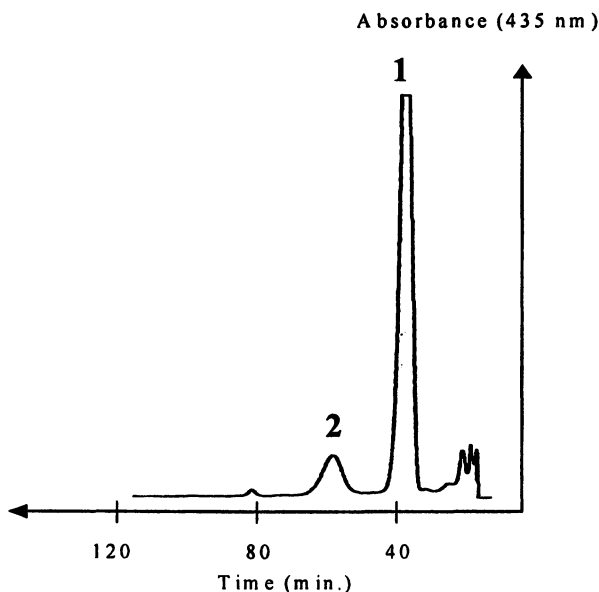


Figure 1. HSCCC separation of water-soluble carotenoids from saffron. **1** *trans*-crocin, **2** *cis*-crocin (HSCCC conditions see text).

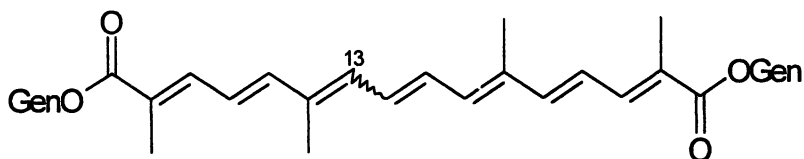


Figure 2. Structures of isolated carotenoids from saffron (see Figure 1):
1 *trans*-crocin,
2 *cis*-crocin (Gen=gentiobiosyl).

Gardenia jasminoides

Fruits of *Gardenia jasminoides* are known to contain the same type of water-soluble carotenoids as saffron (13). Extracts from *Gardenia jasminoides* (gardenia yellow) are widely used as natural food additives for coloring Japanese food. Due to the high price of saffron, gardenia yellow may serve as a cheaper substitute for saffron. The HSCCC separation (solvent system TBME-*n*-butanol-acetonitrile-water 2/2/1/5, less dense layer acting as stationary phase, flow rate 5 mL/min) of a methanolic *Gardenia* extract confirmed the presence of *trans*- and *cis*-crocin (Figure 3). *cis*-Crocin coeluted with an unknown compound, which was tentatively identified as an iridoid glycoside on the basis of its ESI-MS spectrum (13). From 0 to 120 minutes, the mobile phase was the more dense lower phase, from 120 to 140 minutes the elution mode was reversed, which led to the elution of a less polar component, i.e., crocetin-monogentiobiosyl ester 3. UV-Vis absorption maxima and ESI-MS/MS data of 1 and 2 were identical with the respective compounds from saffron. The molecular weight of 3 was determined to be 652 daltons (pseudomolecular ion at m/z 675: $[M(652)+Na]^+$). It should be noted that a successful HSCCC separation of gardenia yellow has been previously reported by Oka *et al.* (13) employing ethyl acetate-*n*-butanol-water (2/3/5) as solvent mixture.

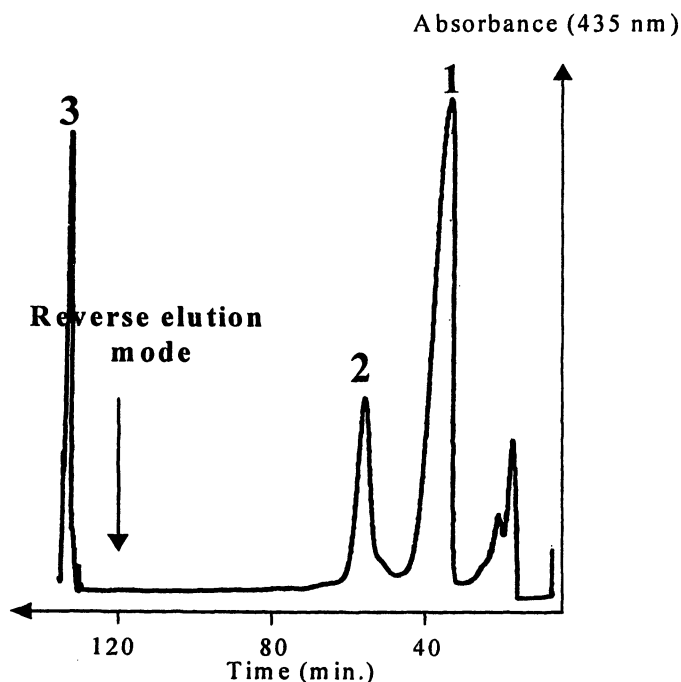


Figure 3. HSCCC separation of methanolic extract from *Gardenia jasminoides* (1 *trans*-crocin, 2 *cis*-crocin, 3 crocetin-monogentiobiosyl ester; HSCCC conditions see text).

Separation of flavonol glycosides from tea leaves (*Camellia sinensis* L.)

Flavonol glycosides are yellow compounds, which are considered to be responsible for the color of green tea. Apart from their coloring properties, flavonol glycosides have attracted enormous interest due to their antioxidative capacities (14). Various health benefits of tea, fruit and vegetables consumption are related to their flavonoid content (15). Investigation of the composition of flavonol glycosides from tea has shown that tea leaves contain a variety of different flavonol-*O*-glycosides. The aglycones myricetin, quercetin and kaempferol are glycosylated with one, two or three sugar residues (6). About 14 different flavonol glycosides are known to be present in tea. The complexity is further enhanced by the presence of a number of flavone-*C*-glycosides. They represent another 8 compounds of similar polarity (14). By using HSCCC, we managed to purify 2 flavonol glycosides in a single run on a preparative scale. Peaks were assigned by means of HPLC-DAD and ESI-MS/MS through comparison with reference compounds on the basis of work carried out previously at our institute (6).

The polarity of the solvent system was adjusted stepwise to ideally resolve the compounds in a single run. Starting with an apolar solvent system (Figure 4), where no separation was achieved and all components eluted in one peak, the polarity of the solvent system was steadily increased (Figure 5). It is apparent that, with a higher polarity of the solvent system, a better resolution of flavonol glycosides can be obtained. Two compounds, i.e., quercetin-rutinoside and kaempferol-rutinoside (Figure 6) were successfully purified with a mixture of ethyl acetate-water (1/1) (Figure 7). Sample loads in the gram range could be applied. Therefore, HSCCC is capable of purifying gram quantities of the above mentioned flavonol glycosides within two hours. In order to separate the mixture of compounds that co-eluted under peak A (Figure 7), the polarity of the solvent system was further increased by addition of *n*-butanol (Figure 8). The presence of *n*-butanol in the solvent system dramatically increased retention of the solutes through enhanced partitioning into the organic phase. However, due to the complexity of the mixture, only partial separation was achieved under these conditions.

Anthocyanins

Anthocyanins, part of the flavonoid family, are responsible for red, blue and purple colors in many fruits and vegetables. The color of anthocyanins is pH dependent and the coloring properties of anthocyanins also depend on various

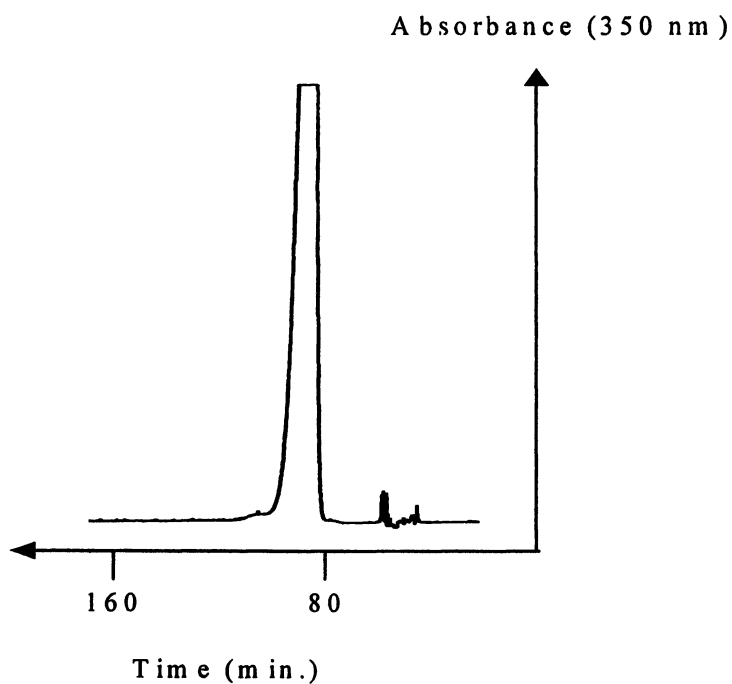


Figure 4. Analysis of flavonol glycosides from black tea by HSCCC; solvent system: hexane-ethyl acetate-methanol-water (3.5/5/3.5/5); upper phase = stationary phase, flow rate: 2.8 mL/min.

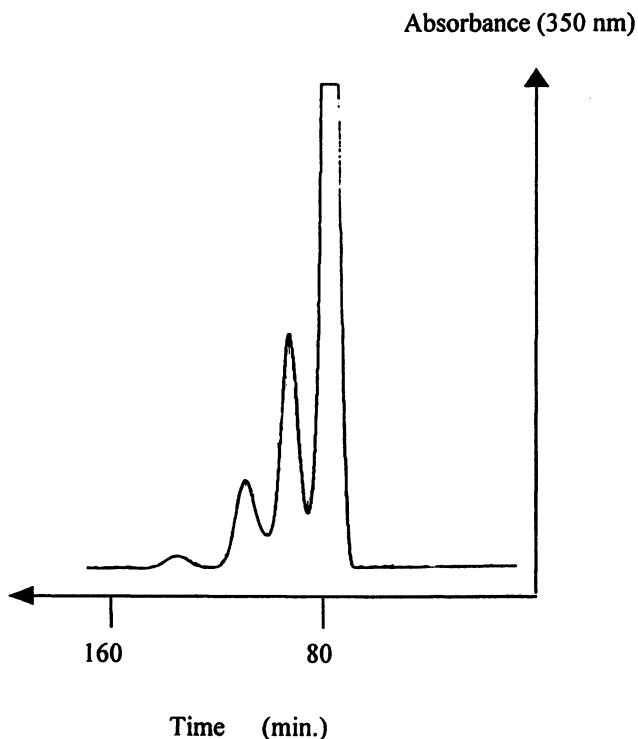


Figure 5. Separation of flavonol glycosides from black tea by HSCCC; solvent system: hexane-ethyl acetate-methanol-water (2/5/2/5); upper phase=stationary phase; flow rate: 2.8 mL/min.

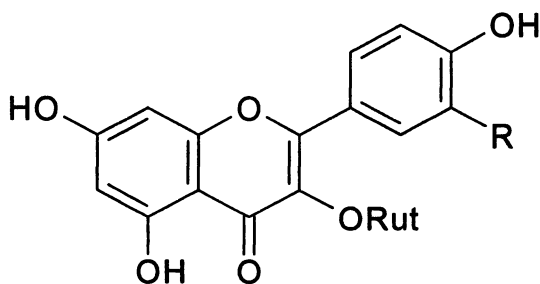


Figure 6. Structures of isolated compounds (see HSCCC trace in Figure 7): C: kaempferol 3-O-rutinoside: R=H (UV-maxima by HPLC-DAD: 265, 346 nm; ESI-MS negativ mode: m/z 593 $[M-H]^-$, ESI-MS/MS of 593: m/z 285). B: quercetin 3-O-rutinoside: R=OH (UV-maxima by HPLC-DAD: 256, 353 nm; ESI-MS negative mode: m/z 609 $[M-H]^-$, ESI-MS/MS of 609: m/z 301).

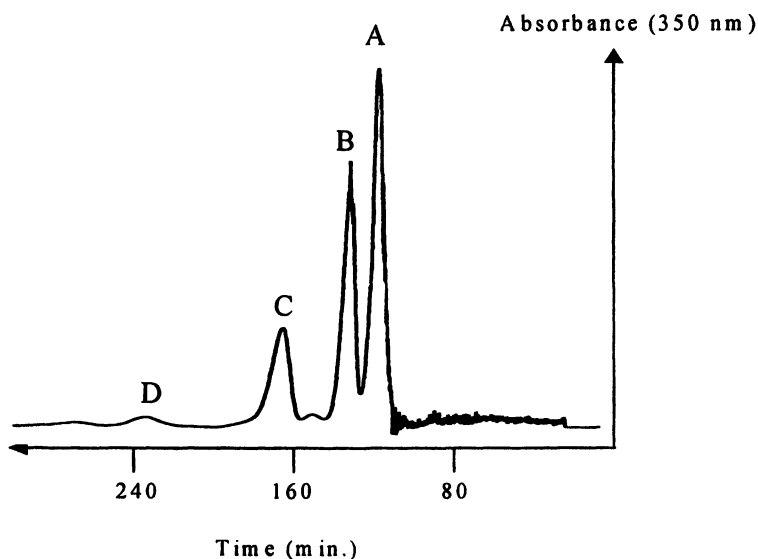


Figure 7. Separation of flavonol glycosides from black tea by HSCCC; solvent system: ethyl acetate-water (1/1); upper phase=stationary phase; flow rate: 2.8 mL/min; peak A: mixture of flavone-C-glycosides and flavonol-O-trisaccharides, peak B: quercetin 3-O-rutinoside; peak C: kaempferol 3-O-rutinoside; peak D: unknown.

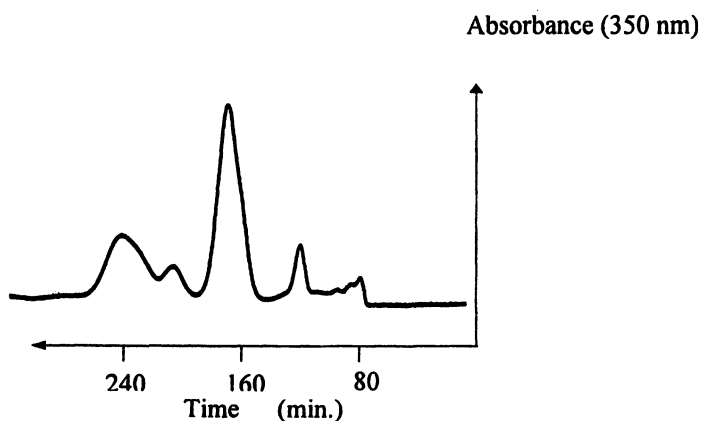


Figure 8. Attempted HSCCC separation of peak A (see Figure 7) with ethyl acetate-n-butanol-water (3.5/1.5/5). Only partial purification of the flavonoid mixture could be achieved in this run.

other factors like, e.g., copigmentation with plant flavonoids (16). The prevalent form of anthocyanins at pH values of below pH 2.0 is the red flavylium cation, which undergoes various structural transformations with increasing pH values (17). Sensitivity to bleaching by sulphur dioxide (18) and chemical conversions at pH values of above pH 4.0 (19) are limiting factors in the use of anthocyanins as food colorants. Reports of anthocyanins which are stable in food systems over a wide pH range revived the interest in their use as natural colorants (18,20-22). Among other modifications, acylation of the anthocyanin molecule was found to be one factor leading to an increased color stability (23).

CCC was chosen as a gentle preparative separation technique in order to assist us in the search for novel stable anthocyanins. By using known anthocyanin mixtures, e.g., from black currant, the separation power of CCC, with regard to this class of polar colorants, was tested. For anthocyanin separation, two commercial CCC systems have been applied: a high-speed countercurrent chromatograph (HSCCC) and a multilayer coil countercurrent chromatograph (MLCCC). The MLCCC apparatus is equipped with one coil at a total volume of 360 mL. In contrast, HSCCC uses three coils, which are connected in series (total volume: 850 mL). As can be seen from equation I, the volume of stationary phase is a factor, which is important for peak resolution. A rule of thumb is as follows: the higher the volume of stationary phase, the better the peak resolution.

$$R_s = \frac{1}{4} (\alpha - 1) \sqrt{N} \left[\frac{K}{K + \frac{V_m}{V_s}} \right]$$

Equation I: R_s =Resolution; α =selectivity factor; N =number of theoretical plates; K =partition coefficient; V_s , V_m =volume of stationary and mobile phase, respectively. The equation is based on the fundamental equation describing peak resolution in chromatography, but is more applicable to CCC. For a more detailed description see reference 3.

*Anthocyanins from Black Currant (*Ribes nigrum* L.)*

In the case of black currant anthocyanins, the influence of stationary phase volume was investigated. Figure 9 shows the separation of the natural anthocyanin mixture on the preparative MLCCC (360 mL single coil) versus the separation on the 850 mL preparative HSCCC (3 coils connected in series). It is apparent that in the case of MLCCC the first eluting rutinoides could not be resolved, whereas almost baseline separation was achieved with HSCCC. This clearly demonstrates the importance of large volumes of stationary phase for a successful separation of anthocyanins.

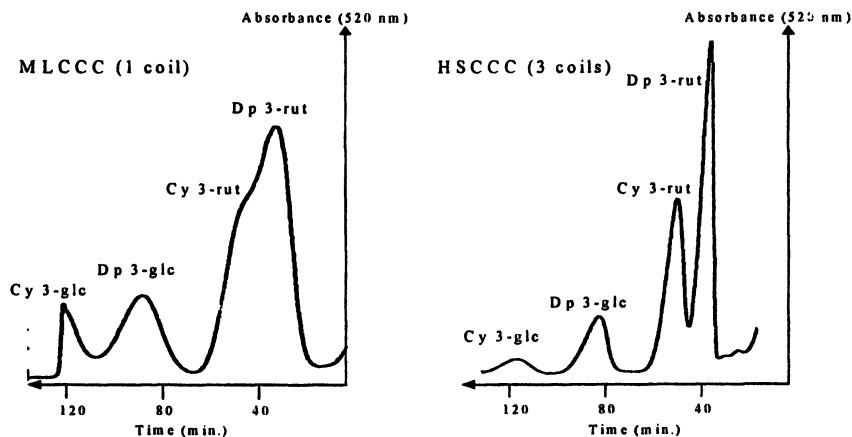


Figure 9. Comparison of separations of black currant anthocyanins using CCC: (left) MLCCC with 1 coil and 360 mL of volume; (right) HSCCC with 3 coils connected in series and 850 mL of volume. Solvent system: TBME-*n*-butanol-acetonitrile-water (2/2/1/5, acidified with 0.1 % trifluoroacetic acid); flow rate 2.5 mL/min for MLCCC and 5 mL/min for HSCCC; less dense layer as stationary phase; abbreviations: Dp 3-rut=Delphinidin 3-rutinoside; Cy 3-rut=Cyanidin 3-rutinoside; Dp 3-glc=Delphinidin 3-glucoside; Cy 3-glc=Cyanidin 3-glucoside. Separation of 430 mg of an XAD-7 isolate by HSCCC yielded 16 mg of pure Dp 3-rut, 11 mg of Cy 3-rut, 5 mg of Dp 3-glc and 3 mg of Cy 3-glc, respectively.

The next question was the reproducibility of the separation. In order to avoid reloading the CCC-system, the possibility of multiple injections was examined. Multiple injections save time and also reduce the consumption of solvents. The result is shown in Figure 10. After complete elution of the sample, the mixture was twice reinjected into the same system. Although some peak broadening was observed, the four major peaks could still be obtained with satisfactory purity (checked by NMR). Therefore, three separations, using multiple injection, of an anthocyanin sample can be carried out during a working day.

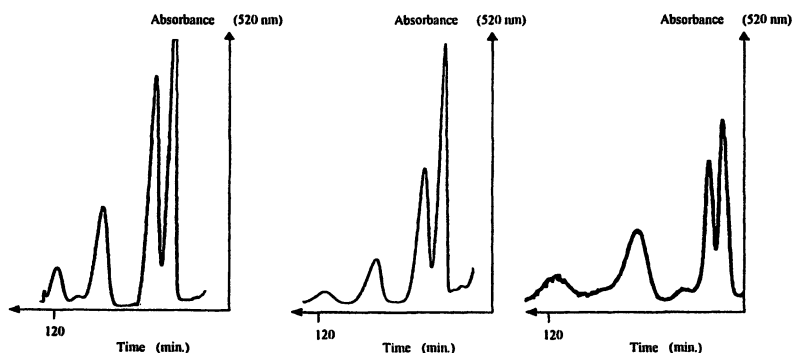


Figure 10. Three consecutive injections of an anthocyanin sample from black currant using HSCCC (Conditions same as in Figure 9); first injection on left side.

Anthocyanins from Red Wine

Also in the case of wine, HPLC is routinely used for the analysis of the anthocyanin fraction. Identification of the separated peaks is often difficult since authentic reference compounds are either missing or are only offered at a high price. We have examined the possibility of applying CCC to the isolation of pure standards.

HSCCC enabled *inter alia* a rapid isolation of malvidin 3-glucoside from red grapes or red wine. Prior to HSCCC separation, anthocyanins from one bottle (0.75 L) of red wine were cleaned-up by adsorption on Amberlite XAD-7 followed by partitioning against ethyl acetate to remove other phenolics. Figure 11 shows the separation of 1.1 g of XAD-7 isolate to yield 43 mg of pure malvidin 3-glucoside in one run. Peak purity and identity was checked by HPLC-DAD (UV-Vis-maxima: 279, 347, 527 nm), ESI-MS/MS (molecular peak at m/z 493 $[M]^+$, ESI-MS/MS of 493: m/z 331) and $^1\text{H-NMR}$.

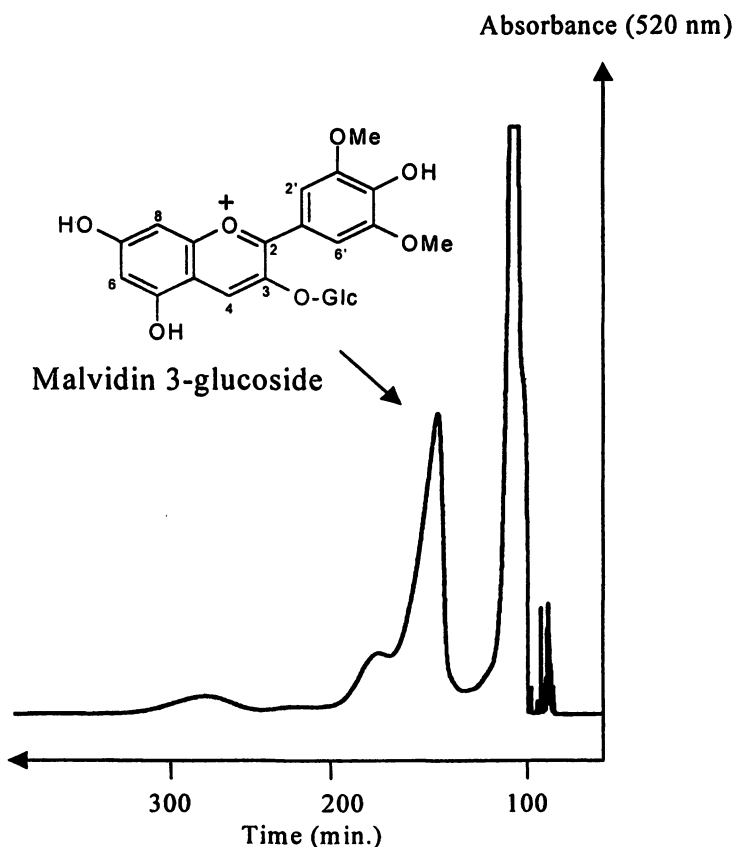


Figure 11. Separation of anthocyanins from red wine by HSCCC. Solvent system: TBME-n-butanol-acetonitrile-water (2/2/1/5, acidified with 0.1 % TFA); less dense layer as stationary phase; flow rate: 5 mL/min.

Anthocyanins from Roselle (Hibiscus sabdariffa L.)

Anthocyanins from this tropical plant are suitable for coloring jams, jellies and fruit beverages with a brilliant red colour (17). Dry calyces, which are used to make tea ("Karkade"), contain about 1.5 g of anthocyanins/100 g dry weight (16). The HSCCC separation of a crude methanolic extract from roselle yielded two major compounds. Peak purity was checked by HPLC-DAD. Through comparison with literature data, the isolated compounds were tentatively identified by ESI-MS/MS as delphinidin 3-sambubioside and cyanidin 3-sambubioside (Figure 12).

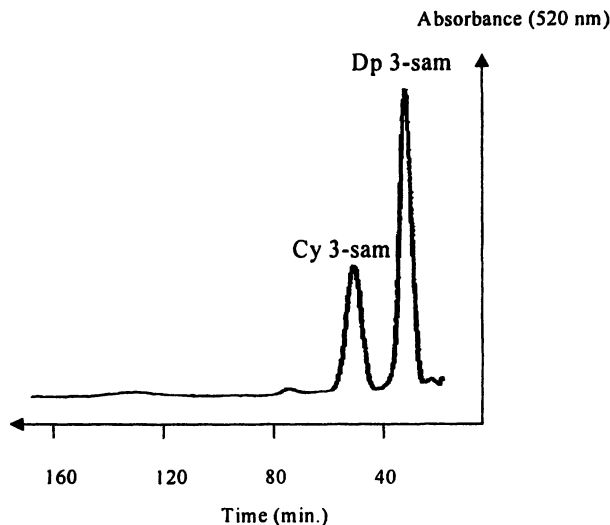


Figure 12. HSCCC separation of anthocyanins from roselle. Solvent system: TBME-n-butanol-acetonitrile-water (2/2/1/5, acidified with 0.1 % TFA); less dense layer as stationary phase; flow rate: 5 mL/min. Dp 3-sam=Delphinidin 3-sambubioside (UV-Vis maximum by HPLC-DAD: 527 nm; ESI-MS positive mode: m/z 597 $[M]^+$, ESI-MS/MS of 597: m/z 303); Cy 3-sam=Cyanidin 3-sambubioside (UV-Vis maximum by HPLC-DAD: 519 nm; ESI-MS positive mode: m/z 581 $[M]^+$, ESI-MS/MS of 581: m/z 287). Sambubioside= β -D-xylopyranosyl-(1 \rightarrow 2)-D-glucopyranoside.

Anthocyanins from Red Cabbage (Brassica oleracea L.)

Red cabbage anthocyanins have gained growing importance as coloring agents. Due to the acylation of the anthocyanins, colorants manufactured from red cabbage possess greater heat and storage stability compared to colorants obtained from grapes, red beets or cranberries (17). It is known that red cabbage can contain up to 15 different anthocyanins (17). Their common basic structural feature is a cyanidin-3-glucoside backbone. Red cabbage anthocyanins differ by varying degrees of acylation with substituted cinnamic acids.

HSCCC allowed the purification of four major pigments from red cabbage (Figure 13). According to ESI-MS, $^1\text{H-NMR}$ and HPLC-DAD data, the fractions

were of good purity, except for the first fraction which was a mixture of isomeric anthocyanins 1 and 2. Through comparison with literature data (17,24), the isolated anthocyanins were tentatively identified as outlined in Figure 13 and Table I.

Further 2D-NMR, as well as NOE experiments, are necessary in order to confirm the exact structures of the isolated pigments. Separation of 300 mg of the XAD-7 extract yielded 30 mg of compounds 1/2, 32 mg of 3, 5 mg of 4 and 4 mg of pure compound 5, respectively.

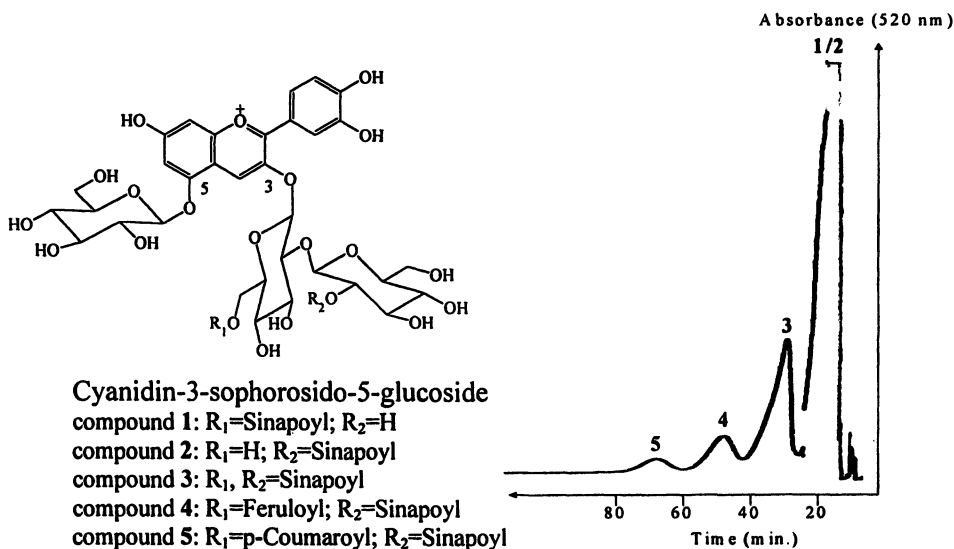


Figure 13. HSCCC separation of anthocyanins from red cabbage (for experimental conditions see Figure 12).

Anthocyanins from *Tradescantia pallida*

Leaves of *Tradescantia pallida* are also known to contain stable anthocyanins which may have potential in coloring different foods (20). Separation of anthocyanins from *Tradescantia pallida* was achieved by HSCCC with the solvent system TBME-*n*-butanol-acetonitrile-water (2/2/1/5, acidified with 0.1 % TFA, flow rate: 5 mL/min) and the less dense layer as the stationary phase (Figure 14). The major anthocyanin pigment isolated from *Tradescantia pallida* was 3-*O*-[6-*O*-[2,5-di-*O*-(*E*)-feruloyl- α -L-arabinofuranosyl]- β -D-glucopyranosyl]-7,3'-di-*O*-[6-*O*-(*E*)-feruloyl- β -D-glucopyranosyl]cyanidin (20).

Table I. ESI-MS/MS data of Red Cabbage Anthocyanins (see Figure 13)

<i>Compound No.</i>	<i>Elution Time HSCCC (min)</i>	<i>ESI-MS/MS Prominent Ions</i>
1/2	18	979 [M] ⁺ , daughter ions of [M] ⁺ : 817 [Cy+2Glc+Sinapoyl] ⁺ , 449 [Cy+Glc] ⁺ , 287 [Cy] ⁺
3	30	1185 [M] ⁺ , daughter ions of [M] ⁺ : 1023 [Cy+2Glc+2Sinapoyl] ⁺ , 449 [Cy+Glc] ⁺ , 287 [Cy] ⁺
4	50	1155 [M] ⁺ , daughter ions of [M] ⁺ : 993 [Cy+2Glc+Sinapoyl+Feruloyl] ⁺ , 449 [Cy+Glc] ⁺ , 287 [Cy] ⁺
5	72	1125 [M] ⁺ , daughter ions of [M] ⁺ : 963 [Cy+2Glc+Coumaroyl+Sinapoyl] ⁺ , 449 [Cy+Glc] ⁺ , 287 [Cy] ⁺

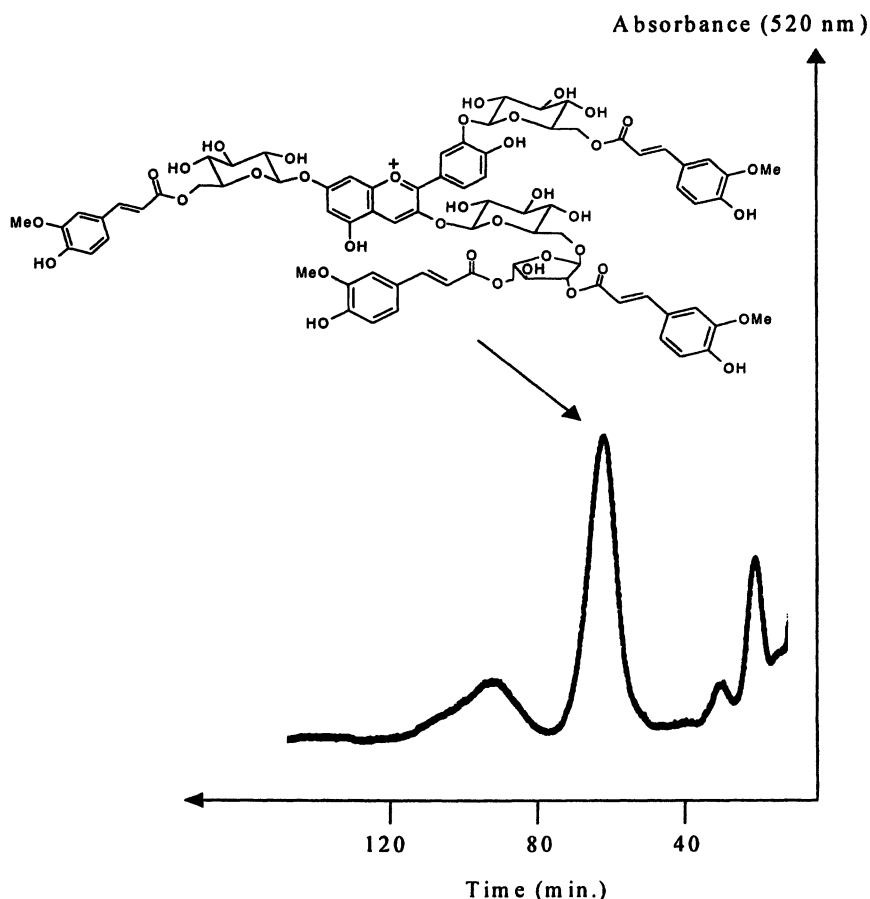


Figure 14. HSCCC separation of anthocyanins from *Tradescantia pallida* (for experimental conditions see text).

Biological Activity of Plant-derived Food Colorants

The biological activities of food colorants are diverse. Therefore, only a brief summary on reported physiological activities of the colorants under investigation can be presented.

It is well documented that the role of carotenoids in the human diet is not restricted to the provitamin A function of β -carotene. This wide-spread polyene pigment is also known to protect the human skin from excessive UV-irradiation. The xanthophylls lutein and zeaxanthin have been found to prevent the development of macular degeneration and cataracts, both leading causes of blindness (25). Lycopene, a tomato-derived carotenoid, has mainly attracted attention due to its potent antioxidant activity. Lycopene is transported in the blood by lipoproteins where antioxidant protection of LDL-cholesterol may slow down the progression of atherosclerosis (25).

Also, for the water-soluble carotenoids from saffron and *Gardenia jasminoides*, biological activity has been reported. Importantly, crocin derivatives as well as the dicarboxylic acid crocetin and its methylester, dimethyl crocetin, were found to be highly effective in inhibiting the proliferation of a leukemic cell line. Concentrations that induced 50 % inhibitions of cell growth were only slightly higher as observed for all-*trans* retinoic acid. Thus, saffron carotenoids have been suggested as alternative antitumor agents which, alone, or in combination with other chemical substances, may have potential for the treatment of certain forms of cancer in the future (26-29).

In the case of flavonoids, multiple activities have been reported, including antibacterial, antiviral, anti-inflammatory, antiallergenic, anticancerogenic and antioxidative activity (30,31). The potential role of flavonoids in coronary heart disease (CHD) prevention was underpinned by epidemiological studies which showed that the consumption of a flavonoid-rich diet is inversely associated with mortality from coronary heart disease (15).

The "French Paradox" (high intake of fat but low incidence of CHD) is potentially related to the high consumption of red wine in certain areas of France. The potential health effects of red wine have been linked to its flavonoid content (32). Anthocyanins are known to be very active in scavenging free radicals under physiological conditions (33-35). Using the TEAC test (36) the antioxidative capacities of some of the isolated anthocyanins have been determined. It was found that the antioxidative power is comparable to known antioxidants, such as catechin and rutin (Table II).

Conclusions

CCC has been successfully applied to the separation of water-soluble carotenoids from saffron and *Gardenia jasminoides*, flavonol glycosides from black tea and anthocyanins from black currant, red wine, roselle, red cabbage and *Tradescantia pallida*.

CCC is an extremely useful technique that enables the isolation of pure natural food colorants on a preparative scale. CCC is suitable for the separation of

Table II. Trolox Equivalent Antioxidant Capacity (TEAC) Values for Some of the Isolated Anthocyanins and Other Known Antioxidants (37)

<i>Compound</i>	<i>Molecular Weight (daltons)</i>	<i>TEAC value (mmol Trolox/mmol)</i>
Delphinidin 3-rutinoside	611	2.3
Anthocyanin from red cabbage 3 (Figure 13 and Table I)	1185	3.6
Rutin	610	2.8
Catechin	290	2.8

non-polar, as well as polar, food colorants. The gentle operation conditions (inert system, room temperature) even allow the isolation of labile compounds. Cost factors also play a role: in CCC cheap solvent systems instead of expensive solid phases can be used; isolation of compounds by HSCCC can be less time-consuming compared to preparative HPLC analysis, and gram quantities can be separated in one HSCCC run within a few hours.

Acknowledgments

Dr. D. Pierzina is thanked for his assistance in flavonol glycoside analysis. Mrs B. Baderschneider's skillful assistance in performing antioxidant testing is gratefully acknowledged. Prof. U. Engelhardt from our institute is thanked for helpful discussions.

Literature Cited

1. Ito, Y. *J. Chromatogr.* **1981**, *214*, 122-125.
2. Ito, Y. *CRC Crit. Rev. Anal. Chem.* **1986**, *17*, 65-143.
3. Conway, W. D. *Countercurrent Chromatography: Apparatus, Theory, and Application*; VCH publishers, Inc.: New York, NY, 1990.
4. Mandava, N.B.; Ito, Y. *Countercurrent Chromatography: Theory and Practice*; Marcel Dekker: New York, NY, 1988.
5. *Modern Countercurrent Chromatography*; Conway, W.D.; Petroski, R.J.; Eds.; ACS Symp. Ser. 593; American Chemical Society: Washington, DC, 1995.
6. Engelhardt, U.H.; Finger, A.; Herzig, B.; Kuhr, S. *Deutsche Lebensmittel-Rundschau* **1992**, *3*, 69-73.
7. Oka, F.; Oka, H.; Ito, Y. *J. Chromatogr.* **1991**, *538*, 99-108.
8. Pedersen, A.T.; Andersen, Ø.M.; Aksnes, D.W.; Nerdal, W. *Magn. Reson. Chem.* **1993**, *31*, 972-976.
9. Bruening, R. C.; Derguini, F.; Nakanishi, K. *J. Chromatogr.* **1986**, *357*, 340-343.
10. Marston, A.; Slacanin, I.; Hostettmann, K. *Phytochemical Analysis* **1990**, *1*, 3-17.

11. Francis, G.W.; Isaksen, M. *Chromatographia* **1989**, *27*, 549-551.
12. Straubinger, M. Ph.D. thesis, Friedrich-Alexander-Universitaet, Erlangen-Nuernberg, Germany, 1998.
13. Oka, H.; Ikai, Y.; Yamada, S.; Hayakawa, J.; Harada, K.-I.; Suzuki, M.; Nakazawa, H.; Ito, Y. In *Modern Countercurrent Chromatography*; Conway, W. D.; Petroski, R. J., Eds.; ACS Symposium Series 593; American Chemical Society: Washington, DC, 1995; pp. 92-106.
14. Engelhardt, U.H.; Galensa, R. In *Analytiker Taschenbuch*; Vol. 15; Guenzler, H; Bahadir, A.M.; Borsdorf, R.; Danzer, K.; Fresenius, W.; Galensa, R.; Huber, W.; Linscheid, M.; Luederwald, I.; Schwedt, G.; Toelg, G.; Wissler, H., Eds.; Springer-Verlag: Berlin, Heidelberg, Germany, 1997, pp. 147-178.
15. Hertog, M.G.L.; Feskens, E.J.M.; Hollman, P.C.H.; Katan, M.B.; Kromhout, D. *Lancet* **1993**, *342*, 1007-1011.
16. Bridle, P.; Timberlake C.F. *Food Chem.* **1997**, *58*, 103-109.
17. Mazza, G.; Miniati, E. *Anthocyanins in Fruits, Vegetables, and Grains*; CRC Press: Boca Raton, FL, 1993.
18. Bakker, J.; Timberlake, C.F. *J. Agric. Food Chem.* **1997**, *45*, 35-43.
19. Marcus, F.-K. *Zucker- Suesswaren. Wirtsch.* **1992**, *45*, 313-317.
20. Baublis, A.J.; Berber-Jiménez, M.D. *J. Agric. Food Chem.* **1995**, *43*, 640-646.
21. Shi, Z.; Francis, F.J.; Daun, H. *J. Food Sci.* **1992a**, *57*, 768-770.
22. Shi, Z.; Lin, M.; Francis, F.J. *J. Food Sci.* **1992b**, *57*, 761-765.
23. Saito, N.; Tatsuzawa, F.; Yoda, K.; Yokoi, M.; Kasahara, K.; Iida, S.; Shigihara, A.; Honda, T. *Phytochemistry* **1995**, *40*, 1283-1289.
24. Shimizu, T.; Muroi, T.; Ichi, T.; Nakamura, M.; Yoshihira, K. *J. Food Hyg. Soc. Japan* **1996**, *38*, 34-38.
25. Schweitzer, C.M. *Ingredients, Health & Nutrition* **1998**, *spring issue*, 32-33.
26. Tarantilis, P.A.; Morjani, H.; Polissiou, M.; Manfait, M. *Anticancer Res.* **1994**, *14*, 1913-1918.
27. Nair, S.C.; Panikkar, B.; Panikkar, K.R. *Cancer Lett.* **1990**, *57*, 109-114.
28. Morjani, H.; Tarantilis, P.; Polissiou, M.; Manfait, M. *Anticancer Res.* **1990**, *10*, 1398.
29. Tarantilis, P.A.; Polissiou, M.; Morjani, H.; Beljebbar, A.; Manfait, M. *Anticancer Res.* **1990**, *12*, 1398.
30. Cook, N.C.; Samman, S. *Nutr. Biochem.* **1996**, *7*, 66-76.
31. Rice-Evans, C.A.; Miller, N.J.; Paganga, G. *Free Radical Biol. Med.* **1996**, *20*, 933-956.
32. Waterhouse, A.L. *Chem. Ind.* **1995**, 338-341.
33. Frankel, E.N.; Waterhouse, A.L.; Teissedre, P.L. *J. Agric. Food Chem.* **1995**, *43*, 890-894.
34. Lapidot, T.; Harel, S.; Akiri, B.; Granit, R.; Kanner, J. *J. Agric. Food Chem.* **1999**, *47*, 67-70.
35. Tamura, H.; Yamagami, A. *J. Agric. Food Chem.* **1994**, *42*, 1612-1615.
36. Miller, N.J.; Rice-Evans, C.; Davies, M.J.; Gopinathan, V.; Milner, A. *Clinical Science*, **1993**, *84*, 407-412.
37. Degenhardt, A.; Knapp, H.; Winterhalter, P. *J. Agric. Food Chem.* **2000**, *48*, 338-343.

Chapter 3

Physical Aspects of Color in Foods

P. Joshi

Department of Food Science and Process Research, Nestlé Research
Center, Lausanne, Switzerland

The influence of color and appearance on our perceptions of freshness and taste are both well known and well documented. For the food industry, gaining an in-depth understanding of color generation, stabilization and in some cases, suppression, is an invaluable tool for the enhancement of overall product quality. Color is most commonly generated by the addition of chemical colorants or the production of biological chromophores within the food system. To obtain the complete picture, however, physical aspects of color must also be detailed. Colorant location and migration, light-scattering and crystal size will all influence the final appearance of a product. Furthermore, the science of color physics enables quantification – so important in quality-control and the correlation with sensory data. This paper will discuss the above issues; looking at color from a physical standpoint and highlighting its importance in an industry where, ultimately, the human eye is the final arbiter.

Visual aspects of food can act as many different kinds of markers – to indicate freshness, ripeness, completion of cooking and even composition. Appearance, and most predominantly color, may also provide sensory cues to stimulate the appetite and trigger perceptions of sweetness, bitterness or acidity. It is long acknowledged, therefore, that the color of the products we consume, be it natural or artificial, is the first step in the acceptance of the food (*1*).

The journey made by food from its source to the consumer's plate may involve numerous processing steps. Many of these involve harsh conditions of temperature, pressure and frictional forces. Natural colors are not always able to withstand such effects resulting in the loss of their visual effectiveness. With the addition of synthetic colorants becoming increasingly unfavorable as a result of increased legislative control, it is becoming more important to optimize the use of those colors already present in our foods. This means gaining an in-depth understanding of how colorant

molecules behave within their immediate environment and how they interact with the light incident upon them to induce that visual sensation we know as color.

How We See Color

There are three components essential for color vision. A light source, an object and an observer. See Figure 1.

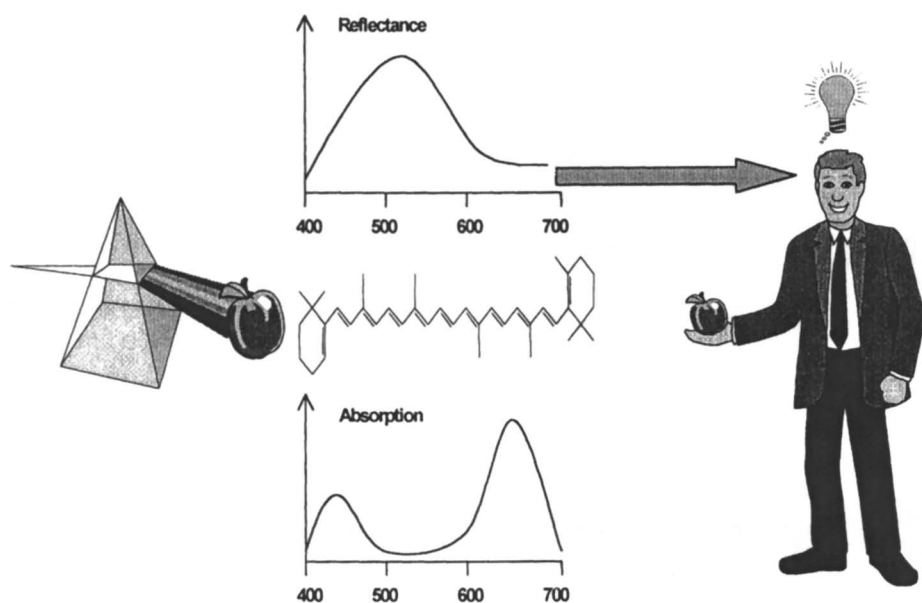


Figure 1. How we see color – from light source to object, to observer

The source of light provides the incident electromagnetic energy with which an object generates its color. Of course, our most common light source is the sun which provides so called “white light” – a combination of energies from across the whole range of the visible spectrum *ca.* 400nm – 700nm. However, having real daylight as a source is not always possible and so there are many artificial light sources used in different situations. The nature of the light source, or its Spectral Power Distribution (SPD) is all important in determining the final color of the object. An object may only interact with the energy given to it. As an extreme example, shining red light onto an object will not allow that object to be seen as anything other than red or black. Such extremes are often used in sensory analysis where it is the food flavor or mouthfeel that are under investigation and so must not be influenced by visual appearance.

The object itself may generate color by several means; absorption, reflection and scattering being the most commonly encountered. Most natural products, such as fruit

and vegetables, contain chromophoric groups, which, by virtue of their conjugated double-bond structure have the propensity to absorb light from within the visible area of the electromagnetic spectrum. Absorption of certain wavelengths leaves the remainder to be reflected to the observer; thus it is this reflected light which is responsible for the visual color we see. Details of chromophoric systems will not be discussed here but there are excellent references dealing with their characterization and application (2).

A very useful tool is the color circle, see Figure 2.

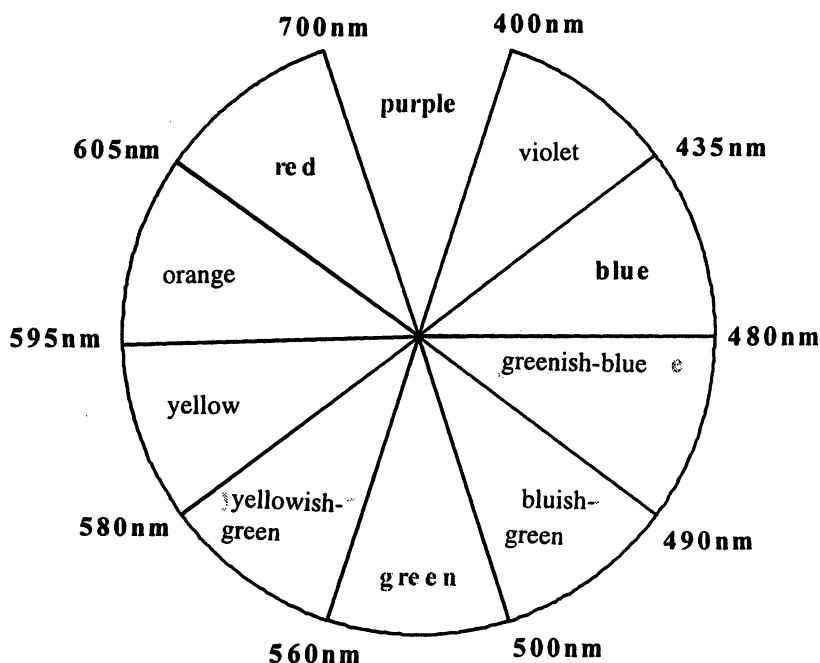


Figure 2. The color circle

This illustrates the continuity of colors absorbed when progressing through the visible spectrum – from the short wavelength violet and blues through to the longer wavelengths oranges and reds. When a colored species absorbs in a certain region, the color observed is given by its complementary, i.e., the color in the opposite segment of the circle. For example, the dye quinoline yellow absorbs blue light between 435nm and 480nm and is, therefore, perceived to be yellow. Of note is the position of purple in the circle. Purple is known as a non-spectral color as it is produced by reflection alone; it can only be seen when its complementary, green, is absorbed.

The final essential component of color perception is the observer. Any light reaching us must be converted by our brain into meaningful information. This is achieved by receptors in the retina known as rods and cones. Rods are responsible for

our night vision being best able to perform in low levels of luminosity. Cones, which give us color vision, are divided into three groups each being stimulated by roughly red, green and blue wavelengths of light. A deficiency in one or more type of cone cell will lead to problems in color vision and in the most extreme cases color blindness. The presence of three retinal pigments was established following the early nineteenth century work of Maxwell, Young and Helmholtz (3).

Modern day colorimeters use trichromatic vision as the basis for their design, although the leap from nerve reception to image formation in the brain still remains much of a mystery.

Physical Aspects of Appearance

As mentioned above, objects can generate color by means of absorption and then reflectance depending upon their chromophoric content. But it is not simply these electronic transitions that determine the nature of light that reaches the observer. Physical considerations must also be taken into account. The arrangement or packing of the object, the refractive indices of the component parts and the surface texture will all influence what we see.

Color cannot merely be attributed to the concentration of colorants. Take the simple example of sugar crystals colored with a blue food dye. As the crystal size is decreased, by grinding or some other mechanical activity, the relative blueness of the crystals also decreases. That is, the number of scattering species increases causing the incident white light to be more dominant. Research has shown that crystal form and habit will affect the optical properties of the system (4). As shown in Figure 3, colored crystals many thick layers below an illuminated surface might not receive any incident light due to a low transmission efficiency. Conversely, thin plate-like crystals may have a high transmission efficiency allowing even multiple layers to permit the passage of the incident light.

Thus, physical environment can, in some cases, be just as, or even more influential than, the colorant itself. Light must reach the colorant in order to interact with it, so the surrounding medium is all important. Perceived aspects such as translucency or turbidity depend upon the scattering and transmission of light.

Another phenomenon is that of color generation in the absence of colorants. The color of milk is a good example. The presence of riboflavin gives rise to the absorption of short-wavelength light and, thus, the predominantly creamy yellow colour of milk. Other components, however, can also influence its appearance. Skimmed milk is often perceived as thinner and bluer than full fat milk. This can be illustrated by the spectrophotometric reflectance curves shown in Figure 4 (5).

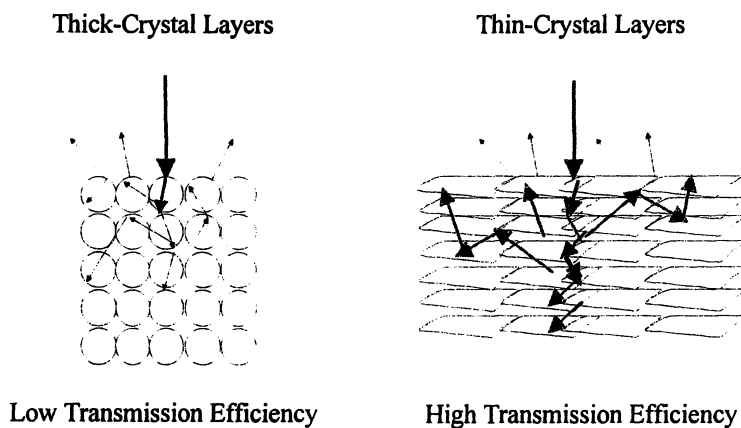


Figure 3. Influence of shape in absorption efficiency.

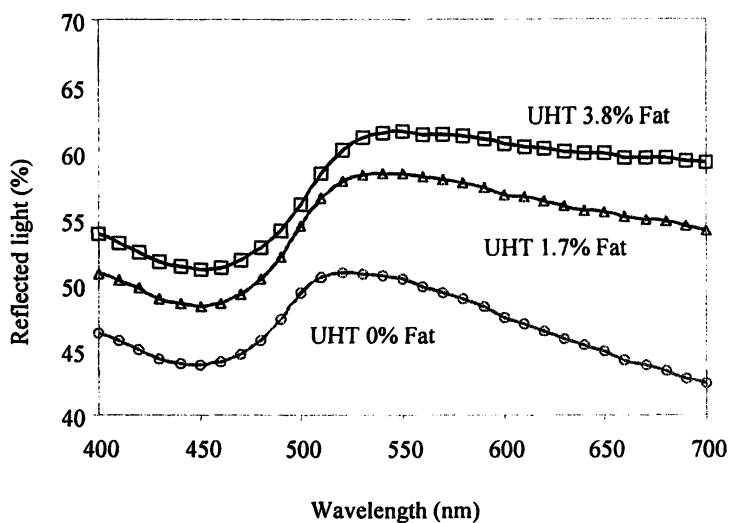


Figure 4. Reflectance spectra for milks of varying fat content.

The presence of fat in the milk acts to scatter the incident light. The fat droplet size and the wavelength of the incident light determine this scattering efficiency. The whole milk (3.8% fat) has a greater reflectance across the whole visible range, with a flatter long-wavelength region indicating high lightness and whiteness. In skimmed milk, the nature and population of scattering species is much different resulting in decreased scattering in the long-wavelength region that corresponds to a visual perception of blueness

Another aspect of appearance is that of gloss. Gloss is the property of a surface that involves specular reflectance and is responsible for a mirror-like or lustrous appearance (6). Although high natural gloss is uncommon in most foods its presence does influence observed color both visually and instrumentally. This point must be addressed when using color measurement as part of quality control. Different extents of glossiness are shown in Figure 5.

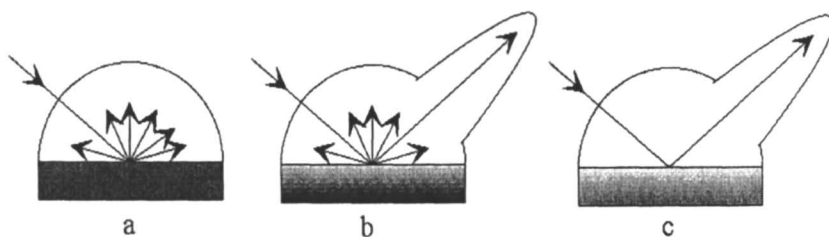


Figure 5. Light reflected from a) matt b) semi-matt and c) high gloss surfaces.

If light is specularly reflected, it does not penetrate the object's bulk to interact with colorants but instead reflects directly off the surface at an angle equal to that of incidence. In this respect gloss has no color other than that of the incident light. If a semi-matt surface is observed, gloss can be the more dominant aspect of appearance and thus make the role of internal colorants less influential.

Every-day Color Physics

In such complicated systems as food and beverages it can be seen that the properties detailed above can have a great bearing on how the consumer would view the product. In many instances our first visual impression can provide us with cause to accept or reject that product. Consider the case of espresso coffee. It is not uncommon for an unsuitably colored coffee-foam to lead to product rejection even before any tasting has been done. The foam is a network of bubbles on the surface of the bulk coffee liquid. Bubbles themselves have no intrinsic color but merely reflect the color of their surrounding environment in a manner dictated by their physical nature, i.e., shape, size, wall-thickness, packing density. To create the right foam, with respect to appearance, therefore, involves bringing together many color physics concepts as well as producing the right liquid coffee color, see Figure 6.

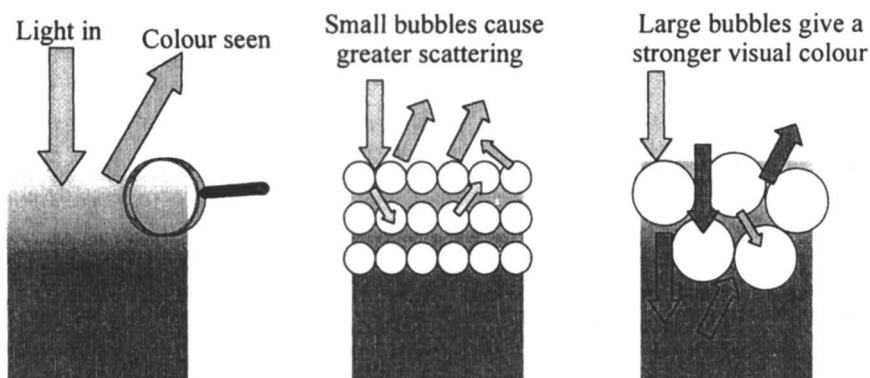


Figure 6. Influence of bubble-size on the color of espresso coffee foam.

Color physics also plays an important role in the daily preparation of a cup of tea or coffee. The consumer's perception of taste, strength and bitterness is influenced by the amount of added milk or creamer, that is, the addition of a highly scattering component to a highly absorbing one. There are, thus, numerous optical events occurring simultaneously. These require instrumental methods to measure them discretely and theoretical means by which to combine them into meaningful results. One theory for assessing the contributions of both scattering and absorbing components was proposed by Paul Kubelka and Franz Munk in the 1930s (7). They related measured reflectance, $R\%$, to the ratio between the absorption coefficient (K)

and the scattering coefficient (S) in the form $\frac{K}{S} = \frac{(1 - R)^2}{2R}$. This is a two-flux theory

which considers the quantities of light travelling in two directions (up and down) and how these fluxes are affected by the components in the sample. One of the major advantages of the Kubelka-Munk theory is its additivity, which allows multi-component mixtures to be characterized. This analysis is most commonly used in the paint and textile industries but it can equally be applied to food products and in fact may prove a very important means of characterizing very heterogeneous products. Despite the stated importance of appearance in foods, it is in other more traditional color-using industries where the real optical theory advances have been made. Models exist to study all manner of heterogeneous systems from powders through to emulsions (8,9) and it is possible to effectively adapt these to use with many food products.

Quantifying Color

In order to control and understand color as scientists, we require some means of quantifying it. Colored solutions have long been measured by techniques using visible

spectrometry with the Beer-Bouger-Lambert law dating back to the eighteenth century (10):

$$T = \frac{I}{I_0} = e^{-kbc}$$

where T is the transmittance, I_0 is the incident intensity (%), I is the transmitted intensity (%), k is a constant, b is the path-length (usually in cm) and c the concentration of absorbing species (usually gL^{-1}).

This approach works well for true solutions, i.e., those with no scattering effects and samples which do not undergo any color change that might require analysis at a different wavelength. Unfortunately, actual food products are rarely so accommodating, with samples often absorbing/transmitting and scattering/reflecting incident light, not to mention being composed of several colorants. The problems are further compounded by the need to correlate physical measurements with sensory observations, since our eyes see all these effects simultaneously, as shown in Figure 7.

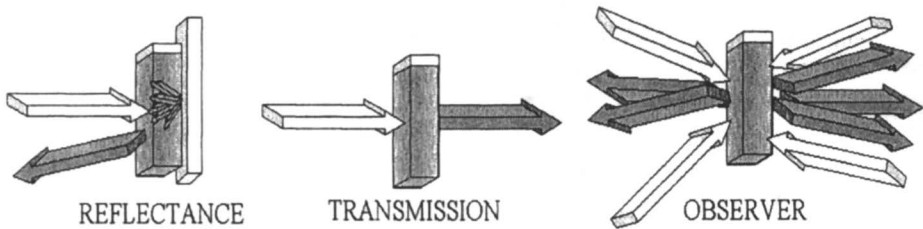


Figure 7. How light interacts with colored samples.

Color measurement instruments have been developed to try and replicate what the human eye might see. Two common devices in many laboratories today are the colorimeter and the spectrophotometer. Both of these work on the principle of illuminating a sample with a well defined source of light and then collecting light reflected from it, as shown in Figure 8. The simpler colorimeter passes the reflected light through three filters designated R, G, B which act as the human eye's receptor cones in sending only either red, green or blue light through to the processing diodes. More advanced spectrophotometers collect the reflected light via a diffraction grating which allows a whole "fingerprint" to be obtained across the visible spectrum.

Once again, the nature of the light source plays an important role as does the "observer" or data collection port. Reflected light is usually only collected at one angle, commonly 8° from normal to the sample surface and so the nature of the sample surface can have a great bearing on the light coming off it, i.e., the gloss effect discussed earlier. Many modern instruments overcome these surface effects by using a sphere optics arrangement, as shown in Figure 8a. In these cases, there is a specular port located at 8° on the other side of the normal from the collection port. If this port is closed, gloss, or specular reflection, remains within the sphere. So, in the specular component included mode (SCI) measured results will represent color only, regardless of texture. If this specular port is opened, however, there can be no incident light at 8°

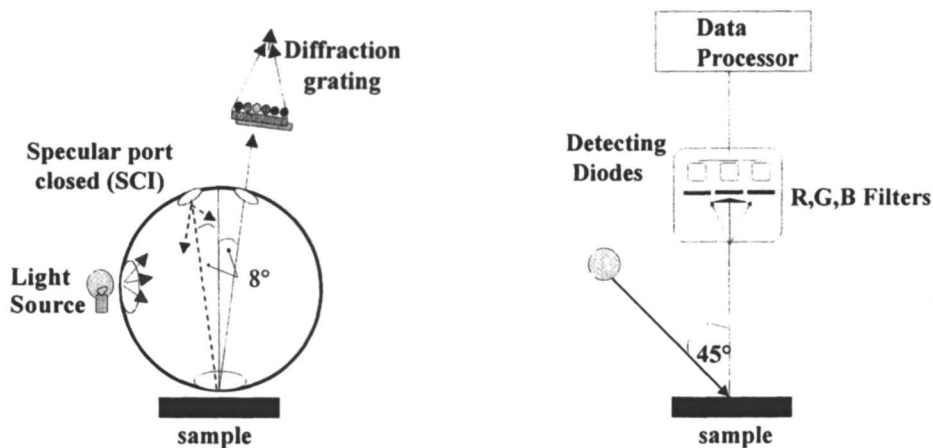


Figure 8. Schematic representations of a) Spectrophotometer in Specular Component Included (SCI) mode and b) Tristimulus Colorimeter.

and thus no measurable specular component. That is, in specular component excluded mode (SCE) the nature of the surface is influential such that a highly glossy sample will show significantly lower reflectance than a matt one. Taking measurements in both modes provides a means for the quantification of gloss effects.

Despite the advances in spectrophotometry, foods present separate challenges to the color physicist. They are usually neither opaque nor transparent and can be infinite shapes, sizes and structures. Conventional bench-top spectrophotometers are often unsuitable and impractical. Nowadays, many portable hand-held machines are available with numerous attachments to measure powders, to vary the measurement aperture and even with fiber-optic probes, which may be dipped into liquids and gels, providing efficient in-line analysis. All these advances are helping to take color measurement beyond a simple concentration determination and towards being a tool for quality control and new product development. Generating data, therefore, is no longer a problem, but how we deal with it and communicate its meaning still provides a challenge.

CIE parameters

Visualizing a color from a set of numerical data is no simple task and, for many years, the concept of a color space has been used. The Commission Internationale de l'Eclairage (CIE) began its work in 1931 with the aim of defining a uniform color space so that the distance between two colors in three-dimensional space would correlate to their visual color difference (4). Progressing via trichromatic theory and many numerical models, the CIE $L^*a^*b^*$ system was established in 1976. Today, numerous color specification systems exist, providing ample reason for confusion and highlighting the importance for full definition of measurement parameters when presenting or publishing any color data.

CIEL*a*b* is probably the most internationally recognized system and is based upon a set of rectangular coordinates, as shown in Figure 9.

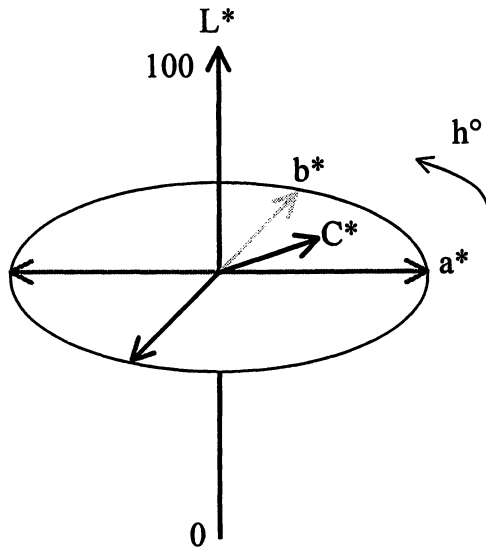


Figure 9. 1976 CIE L*a*b* space where L^* represents lightness, a^* redness-greenness and b^* yellowness-blueness.

The distance that a point is away from the central L^* axis represents its saturation or chroma, C^* . Furthermore, the distance around the circle from the a^* axis is an indication of the dominant hue. Using color space coordinates proves very valuable in the description of colors. Most colorimeters can express their three component data in terms of $L^*a^*b^*$ whilst spectrophotometers provide these figures as well as full reflectance curves.

The Full Picture

Despite the important role of color physics, this subject alone will not allow us to understand fully our colored food systems. To complete the picture we must include other chemical, biological and sensorial information. Color changes are often governed by chemical reactions, which we may monitor by observing our reflectance curves, but will not understand without essential chemical analyses.

Most important to the food manufacturer is acceptance by the consumer, our customer. Sensory studies combined with physical color measurement can allow the definition of color tolerance areas for a particular product to mark the boundaries of acceptability in new product development and factory quality control.

In conclusion, color appearance depends not only upon the type and concentration of colorants used but also on the optical environment of our product. Gaining a greater understanding of color physics can help us to increase the whole optical quality of the foods we consume. Using color science as a tool can aid in our process development and quality control, whilst when applied in combination with chemical analyses and sensory evaluation, it can put us well on the way to achieving the full picture.

Literature Cited

1. Hutchings, J.B. *Food Color and Appearance*; Blackie Academic & Professional: Glasgow, Scotland, 1994; pp 14-17.
2. Fessenden, R.J.; Fessenden, J.S. *Organic Chemistry*, 4th edition; Brooks/Cole Publishing Company: Pacific Grove, CA, 1990; pp 853-867.
3. *Instrumentation and Sensors for the Food Industry*; Kress-Rogers, E., Ed; Butterworth-Heinemann Ltd.: Oxford, England, 1993; pp 39-59.
4. Joshi, P. Ph.D. thesis, Dept. of Color Chemistry and Dyeing, University of Leeds, Leeds, England, 1998.
5. Joshi, P. *unpublished data*; Nestlé Research Center, Dept. of Food Science and Process Research, Lausanne, Switzerland, 1998.
6. Hunter, R.S.; Harold, R.W. *The Measurement of Appearance*, 2nd edition; Wiley-Interscience: New York, 1987; p399.
7. *Color Physics for Industry*, 2nd edition; McDonald, R., Ed.; Society of Dyers and Colorists: Bradford, England, 1997; pp 294-309.
8. Shah, H.S.; Desai, P.R.; Roy, M.S. *Applied Optics* 1997, 36, 3538-3546.
9. McClements, D.J.; Chantrapornchai, W.; Clydesdale, F. *J. Food Sci.* 1998, 63, 935-939.
10. Owen, A. *Fundamentals of Modern UV-visible Spectroscopy – A Primer*; Hewlett-Packard: Germany, 1996; pp 24-28.

Chapter 4

Changes in Anthocyanins during Food Processing: Influence on Color

Cristina García-Viguera and Pilar Zafrilla

Lab. Fitoquímica, Dept. Ciencia y Tecnología de los Alimentos, CEBAS-CS1C, Murcia, Spain (phone: +34-968-215717, fax: +34-968-266613; email: cgviguera@natura.cebas.csic.es)

The influence of different factors has been studied in order to determine their effects on anthocyanin concentration and color in several products, i.e., raspberry and strawberry jam and pomegranate juice and jelly. The factors investigated here were fruit variety, freezing prior to processing and storage, the use of additives (ascorbic acid or benzoate) and pH. Results showed that freezing the fruit prior to jam manufacture, or addition of benzoate did not produce significant differences in concentrations of anthocyanins or color changes. However, other factors, such as variety or addition of ascorbic acid, did give products with differences in anthocyanins and/or color. Nevertheless, these differences in anthocyanin concentrations were not directly related to color changes. pH variations must also be considered if a more red hue is required. However, one of the main factors that has to be considered is the processing and storage time and temperature. Long storage periods at temperatures over 25°C or processing at boiling temperature for long times cause anthocyanin degradation resulting in unacceptable colors. Furthermore, the relationship between anthocyanin degradation and loss of red hue is more pronounced when juices are analyzed than when jams are studied.

One of the main problems that the food industry encounters is the stability of color in red fruit products. Loss of red color and increased browning during production and storage of raspberry or strawberry products are influenced by many factors. These include temperature and time of processing (1,2) and storage (3,4), pH, acidity, phenolic compounds, sugar, fruit maturity, thawing time (e.g., 5-8), and fruit cultivar (9).

One of the objectives of our research is to determine the influence of some of these parameters on strawberry or raspberry jams, as well as on novel pomegranate-derived products, such as juices, jams and jellies. Here we shall summarize some of the results obtained with these manufactured products. Specifically, we shall focus on the influence of variety, processing and storage time and temperature on raspberry and strawberry jams (10-12) and also the effect of pH, addition of ascorbic acid and benzoate on some pomegranate products (13-16).

Materials and Methods

Raspberry and strawberry fruit were harvested, stored and jam was prepared as previously reported (10-12). Pomegranates were harvested in September 1996 and juices and jellies were manufactured as previously described (13,15).

Anthocyanin extraction, HPLC analyses, identification and quantification have also been described (10-13,15).

CIEL*a*b* color measurements of jams and jellies were performed by reflectance on a color spectrophotometer model CM-508i (Osaka, Japan) with a granular cover set CM-A40 (17). Juices were measured in glass cells of 2 cm path length (CT-A22), using the same apparatus coupled with transmittance adaptator model CM-A760 (15). Color differences were expressed as $\Delta E^*_{ab} = [(\Delta L^*)^2 + (\Delta a^*)^2 + (\Delta b^*)^2]^{1/2}$. $\Delta E^*_{ab} \leq 5$ were not perceptible to the human eye. Therefore, no differences in color could be detected.

Results and Discussion

Influence of Variety.

It is well known that the first factor that should be taken into consideration when preparing a manufactured fruit-derived product is the variety of the fruit. Different varieties may possess different concentrations of flavonoids and/or behave differently during processing. As an example, in a previous study (11) we analyzed three different strawberry cultivars (Chandler, Tudla and Oso Grande) which possessed different anthocyanin concentrations (Figure 1). This resulted in distinct jams prepared from them (Figure 1). Strawberry jams prepared from fruit possessing the lowest anthocyanin concentration also showed the lowest concentration of anthocyanins. However, this was not well correlated with color where it was seen that those products prepared with 'Chandler' and 'Tudla' possessed red hues (Chandler $a^* = 42.71$; Tudla $a^* = 42.12$), even if differences in anthocyanin concentrations were detected (Figure 1). On the other hand, pigment concentration was related to the red hue when data for Oso Grande cultivar ($a^* = 35.37$) were considered. It could even be said that there was no perceptible difference in the color of the jams prepared with Tudla or Chandler varieties ($\Delta E^* = 0.59$), but there was a slight visual difference when we compared them with those prepared with Oso Grande ($\Delta E^* = 7.34$). These results were confirmed by the sensory panel (11).

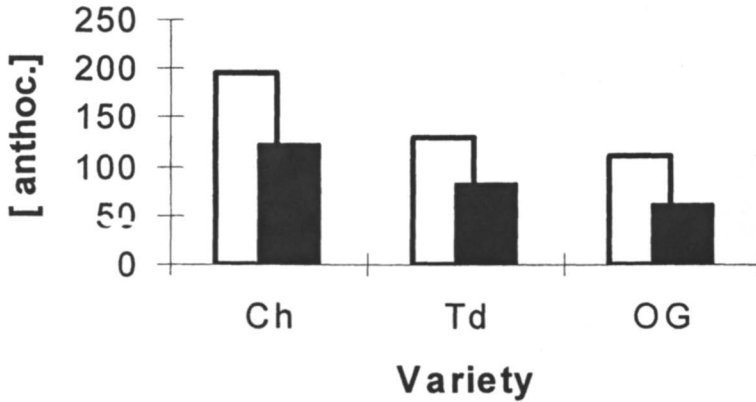


Figure 1. Anthocyanin concentration ($\mu\text{g/g jam}$) of Chandler (Ch), Tudla (Td) and Oso Grande (OG) strawberries. Fresh fruit (white bars) and jams (black bars).

Results obtained in another study (10), where jams prepared with two red raspberry varieties (Zeva and Heritage) were compared, demonstrated that differences in anthocyanin concentration of the fruit (Figure 2) did not result in significant differences in the concentration of these pigments in the processed product (Figure 2). Nevertheless, in this case, when the color measurements of the jams, prepared with the two varieties, were obtained, slight variations in color were observed ($\Delta E^* = 7.52$), due to differences in all CIEL*a*b* parameters (10).

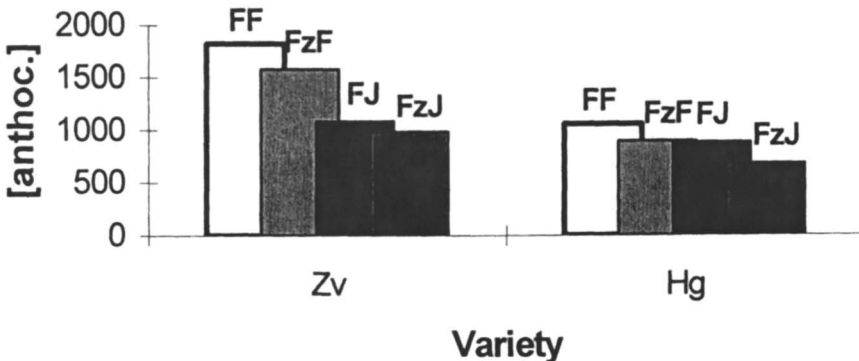


Figure 2. Anthocyanin concentration ($\mu\text{g/g jam}$) of fresh raspberry fruit (FF), frozen (FzF) and jams prepared with fresh (FJ) or frozen (FzJ) fruit. Zv= Zeva cv; Hg= Heritage cv.

Influence of Freezing the Fruit.

The influence of freezing the fruit (-20°C) for short periods (24 hours), prior to jam preparation, was also determined for raspberry jams (10). Frozen fruit possessed

lower anthocyanin concentrations than fresh fruit ($\pm 15\%$), for both varieties (Figure 2) and this was also perceptible when analyzing the colored flavonoid concentrations of the jams (Figure 2). Nevertheless, similar color was obtained for those jams prepared with fresh or frozen Zeva fruit ($\Delta E^* = 1.81$), or Heritage fruit ($\Delta E^* = 1.57$).

Other analyses performed with strawberries (12) showed that, with longer periods of storage (1 year) at -20°C , a great loss of anthocyanins (over 77%) occurred (Figure 3), although, only 20% loss of anthocyanins occurred after 6 months storage at the same temperature (Figure 3). In fact, a significant percentage of the loss occurs on thawing, as it has been pointed out previously (6).

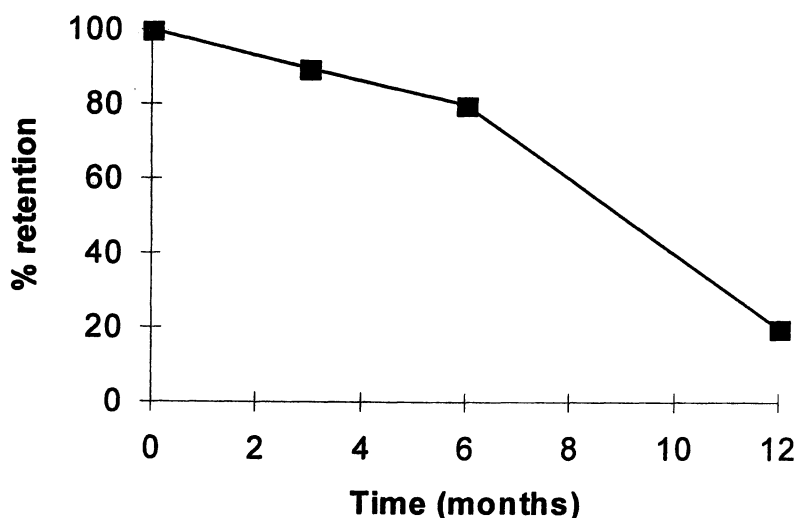


Figure 3. Percentage of anthocyanin retention in strawberries after 1 year storage at -20°C

Influence of Processing Conditions

Previous studies have demonstrated that during processing a great amount of anthocyanin is lost. This percentage of loss is similar (40%) for all the strawberry varieties analyzed (11), but it was quite different when raspberry products were considered (10). The anthocyanin concentration was reduced by 20% and 40%, respectively, when fruits of Heritage and Zeva were made into jams using the same processing conditions (Figure 2).

Other analyses performed with Oso Grande strawberries indicated that variations in the processing method could result in changes to the anthocyanin concentration and

this could be related to color changes (12). For example, when jams were processed under industrial conditions (15 min. at 78°C under vacuum), *ca.* 40% of the anthocyanins were degraded (Figure 4). In contrast, when jams were prepared in the laboratory following traditional procedures (boiling at atmospheric pressure for 15 min) the percentage of the anthocyanins degradation increased by *ca.* 50%.

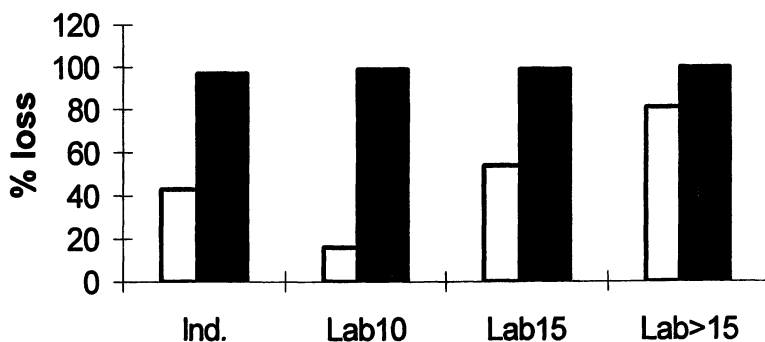


Figure 4. Percentage of strawberry anthocyanin loss during jam preparation under different conditions (Ind= Industry conditions, Lab10=jams prepared in the laboratory, 10 min. boiling, Lab15= 15 min. boiling and Lab>15= boiled over 15 minutes). Fruit anthocyanin concentration (white bars), Jam anthocyanin concentration (black bars)

When the boiling time was reduced to 10 min in the laboratory, the degradation was reduced to *ca.* 16%, and when it was longer that 15 min the degradation increased drastically to *ca.* 80%, rendering a product with an unacceptable appearance. These differences in anthocyanin concentrations were also detected when color analyses were done. Jams prepared under industrial conditions or in the laboratory, by boiling for 10 minutes, possessed similar color ($\Delta E^* = 5.27$). Any variance was due to a higher CIEL* value for jams manufactured using the industrial process, rendering a lighter product, but with the same red hue. Moreover, for those jams prepared using traditional conditions in the laboratory (15 min boiling), the color became more purple ($\Delta E^* = 15.17$), due to lower CIEa* and CIEb* values. Again, those that were boiled for longer than 15 min (*ca.* 80% anthocyanin loss), possessed an unacceptable brownish color, very different from those manufactured under industrial conditions ($\Delta E^* = 23.75$). Consequently, we can deduce that there is a relationship between anthocyanin concentration and color, since when the free anthocyanin loss is very high the color is unacceptable. Due to this, processing factors (time and temperature) should be

considered when producing this foodstuff, in order to minimize anthocyanin degradation.

Influence of Storage Conditions

The previous sections have discussed the influence of certain parameters that affect the color of processed products, such as jams, and the relationship between the anthocyanin concentration and degradation. In this section, discussion focuses on one of the most decisive factors that modify pigment concentration and its relationship with color, i.e., storage. Previous studies with raspberry jams (10) have demonstrated that storage temperature has a decisive effect on color when these products are kept at 30°C for 6 months, independent of the variety or if the fruit was previously frozen or not. The resulting products have a brown hue, with no detectable free anthocyanins.

Similar results were obtained when strawberry jams were analyzed (11) indicating that when the product was stored at 37°C, anthocyanin degradation was more than 98% after 3 months (Figure 5), while the same level of degradation occurred after 6 months storage at 20°C for all three varieties used (Chandler, Tudla and Oso Grande). When comparing, for example, the color of jams prepared from Oso Grande, it was seen that, even if no anthocyanins were detectable at either temperature, those stored at 37°C possessed a more brownish hue. This was due to changes in the CIEL*a*b* parameters during storage at 37°C ($\Delta E^* = 20.04$, when comparing initial jams with those stored for a few months at 37°C), but a smaller color loss occurred if stored for the same time at 20°C, rendering, in this latter case, jams with minor color alterations ($\Delta E^* = 10.17$), even if loss of anthocyanins was more than 98%. Moreover, when the storage temperature was decreased to 5°C (12) the percentage loss of anthocyanins fell to 80% (Figure 5), and an increase in the red hue was observed when compared to the initial value ($\Delta E^* = 8.56$). Also, differences in color were detectable after 6 months between those jams stored at 5°C and 20°C ($\Delta E^* = 10.17$).

Also, the influence of light during storage has been studied, in relation to anthocyanin content and color stability of strawberry jam (12). The obtained results showed that no significant differences were detected between those jams stored under periodical daylight conditions and those stored in the dark for 6 months.

The above mentioned results are in accordance with general findings that anthocyanin concentrations decrease during storage and that anthocyanins are markedly influenced by temperature and storage time (5,18). However, the rate of color loss is slower than the rate of anthocyanin degradation. Therefore, other factors, discussed elsewhere (10,11), may play a significant role in the expression of colour by co-pigmentation, polymerization or some other physicochemical processes. In the same way, the variety of fruit, or method of preparing the jam with fruit frozen for a short time, can influence color or anthocyanin concentration after storage at an elevated temperature (37°C) for 6 months (10,11).

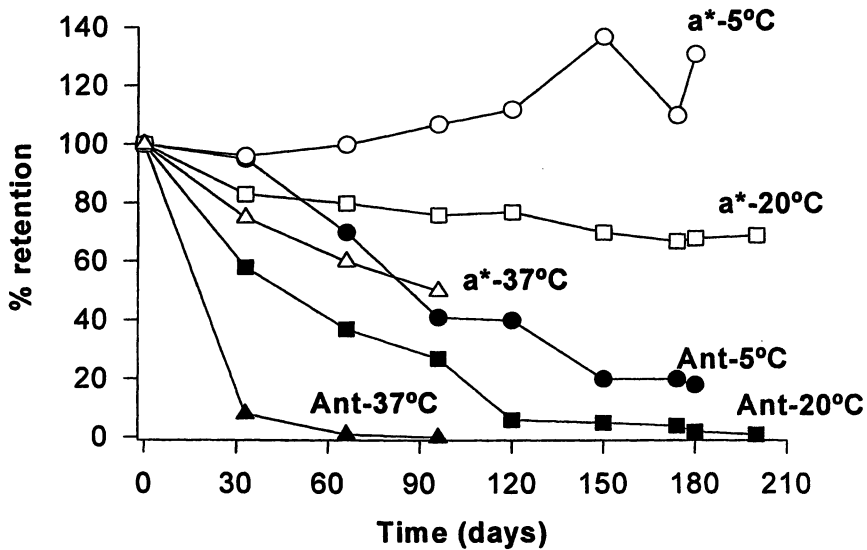
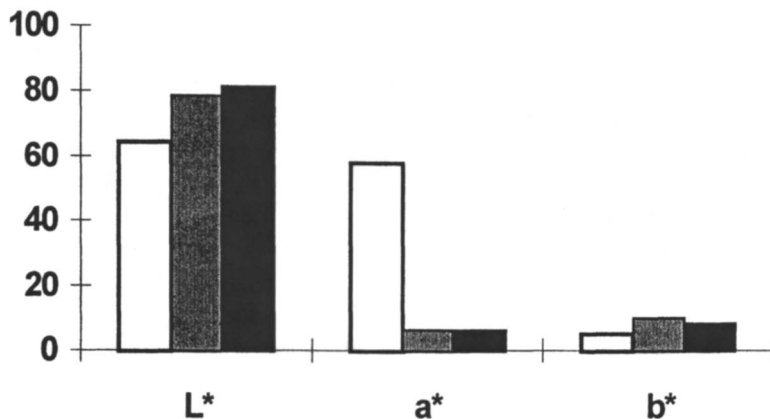


Figure 5. Percentage of anthocyanin and color degradation in strawberry jams, after storage at 5°C (●), 20°C (■) and 37°C (▲). Black symbols= Anthocyanin; white symbols= CIEa* value

Influence of Other Factors

Other factors that could affect certain manufactured products, specifically the addition of ascorbic acid or benzoate and changes in pH, have been studied in relation to novel pomegranate products (juices and jellies).

Benzoate is an additive used by the industry for its antimicrobial properties. When the influence of this additive (0.1% w/v) in a pomegranate juice was studied (16), the results showed that it had no influence on anthocyanin degradation, i.e., after 48 days at 25°C, the percentage loss of these pigments in juices with or without benzoate was the same (ca. 93%) and also the color was very similar at the end of the storage period ($\Delta E^* = 3.03$, Figure 6). Nevertheless, significant color differences were found between the fresh juices and those stored under the above conditions ($\Delta E^* \text{ ca. } 55.15$, Figure 6), mainly because of a great loss in the red hue related to CIEa* value (ca. 82% loss).



*Figure 6. CIEL*a*b* values obtained for pomegranate juice at day 0 (white bars), after storage at 25°C for 48 days control (grey bars) and with benzoate addition (black bars).*

Ascorbic acid (AA) is commonly added to fruit juices to prevent browning as well as an additional source of vitamin C. Nevertheless, the effect of this compound on anthocyanin degradation and its consequent effect on color has been studied previously (19). We also analyzed the effect of ascorbic acid in relation to anthocyanin and color variations in pomegranate juice (15,16). Results showed that the addition of ascorbic acid increased the rate of anthocyanin degradation, stored at 5°C for 160 days (80% and 63% loss with and without ascorbic acid, respectively), besides differences in colors ($\Delta E^*=13.04$) mainly due to lower CIEa* and CIEb* values and a higher CIEL* value for those prepared with ascorbic acid (Figure 7).

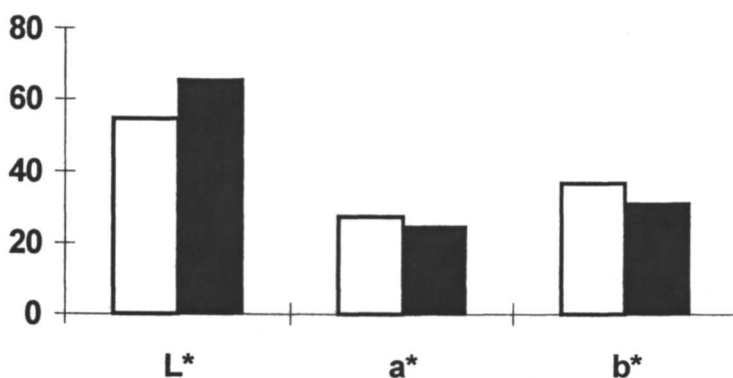


*Figure 7. CIEL*a*b* values obtained for pomegranate juices, with ascorbic acid (black bars) and without ascorbic acid addition (white bars).*

Finally, the consequence of modifying the pH on a novel pomegranate jelly product was determined (13,14). Results demonstrated that acidification of pomegranate juice, cultivar Mollar, with an initial pH of 4, (to pH 3 and pH 3.5), prior to jelly preparation, does affect the final anthocyanin concentration and has a perceptible influence on color. Thus, the anthocyanin concentration was 18% higher when jellies were prepared with juice acidified to pH 3.5 and 43% higher when prepared with pH 3 juice. This was confirmed by color analysis since a brown hue was detected for those products prepared with non-acidified juices (pH 4), while those prepared with pH 3 juice presented a marked red hue ($\Delta E^* = 10.67$). Smaller differences were seen for those prepared with pH 3.5 juice ($\Delta E^* = 6.70$). This was due to a change in the CIEa* value which was much higher for products prepared from juice of lower pH (Figure 8).

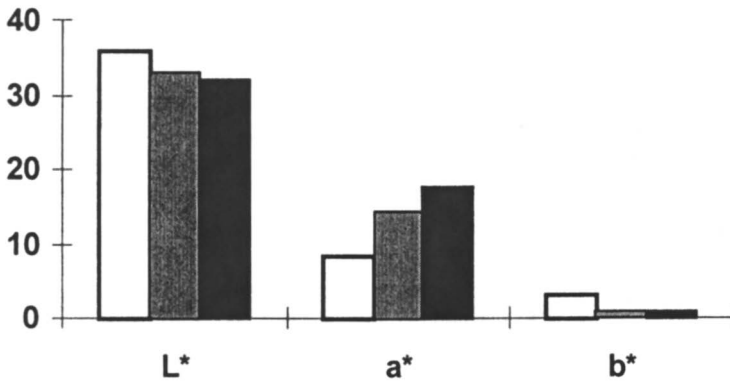


Figure 8. CIEL*a*b* values obtained for jellies prepared with pomegranate juice of pH 4 (white bars), pH 3.5 (grey bars) and pH 3 (black bars).

Conclusion

We can conclude that anthocyanin concentrations decrease during storage and that anthocyanins and color are markedly influenced by temperature and storage time. However, the rate of color loss is slower than the rate of anthocyanin degradation. In the same way, the variety of fruit, method of preparing the jam and freezing the fruit for long periods (over 6 months) have significant effects on colour or anthocyanin concentration. In contrast, using short period frozen fruit (24 hours) has no significant influence on these parameters after stored at high temperature (37°C) for 6 months.

Addition of benzoate has no influence on anthocyanin or color degradation, although pH and ascorbic acid do affect these parameters.

Literature Cited

1. Markakis, P. *Anthocyanins as Food Colours*; Markakis, P. Ed, Academic Press: New York, 1982, pp 163-180.
2. Pilano, L.S.; Wrolstad, R.E.; Heatherbell, D.A. *J. Food Sci.* 1985, 50, 1121-1125.
3. Adams, J.B.; Ongley, M.J. *J. Food Technol.* 1973, 8, 139-145.
4. Irzyniec, Z.; Klimezak, J.; Michalowski, S. *Bioavailability '93- Nutritional, Chemical & Food Processing Implications of Nutrient Availability. Part III*, 1993, pp 398-403.
5. Withy, L.M.; Nguyen, T.T.; Wrolstad, R.E.; Heatherbell, D.A. *J. Food Sci.* 1993, 58, 190-192.
6. Wrolstad, R.E.; Putman, T.P.; Varseveld, G.W. *J. Food Sci.* 1970, 35, 448-452.
7. Abers, J.E.; Wrolstad, R.E. *J. Food Sci.* 1979, 44, 75-78.
8. Rommel, A.; Heatherbell, D.A.; Wrolstad, R.E. *J. Food Sci.* 1990, 55, 1011-1017.
9. Bakker, J.; Bridle, P.; Bellworthy, S.J. *J. Sci. Food Agric.* 1994, 64, 31-37.
10. García-Viguera, C.; Zafrilla, P.; Artés, F.; Romero, F.; Abellán, P.; Tomás-Barberán, F.A. *J. Sci Food Agric.* 1998, 78, 565-573.
11. García-Viguera, C.; Zafrilla, P.; Romero, F.; Abellán, P.; Artés, F.; Tomás-Barberán, F.A. *J. Food Sci.* 1999, 64, 243-247.
12. García-Viguera, C.; Zafrilla, P.; Tomás-Barberán, F.A. *J. Food Sci. Technol.* 1999, 5:6, (in press).
13. Maestre, J.; Senabre, R.; Melgarejo, P.; García-Viguera, C. *I International Symposium on Pomegranate*; Melgarejo, P.; Martínez, J.J.; Martínez, J. Eds; Universidad Miguel Hernández: Orihuela (Alicante, Spain), 1998, 1/7-7/7.
14. Senabre, R.; Ms Thesis; Universidad Miguel Hernández, Orihuela, (Alicante, Spain) 1998.
15. García-Viguera, C.; Martí, N.; Bridle, P.; *Pigments in Food Technology*; Mínguez, M.I. ; Jarén, M.; Hornero, D. Eds.; CSIC; Sevilla, Spain, 1999; 307-310.
16. Martí, N.; Ms Thesis; Universidad Miguel Hernández, Orihuela (Alicante, Spain), 1998.
17. Zafrilla, P.; Valero, A.; García-Viguera, C.; *Food Sci. Technol. Inter.* 1998, 4, 99-105.
18. Jackman, R.L.; Smith, J.L. *Natural Food Colorants*; Hendry, G.A.F., Houghton, J.D. Eds. Blakie Academic & Professional: Glasgow (U.K.), 1996, pp 449-309.
19. García-Viguera, C.; Bridle, P.; *Food Chem.* 1998, 64, 21-26.

Chapter 5

Anthocyanins from Radishes and Red-Fleshed Potatoes

Ronald E. Wrolstad¹, M. Monica Giusti², Luis E. Rodriguez-Saona³,
and Robert W. Durst¹

¹Department of Food Science and Technology, Oregon State University,
Corvallis, OR 97331-6602

²Department of Nutrition and Food Science, University of Maryland,
College Park, MD 20742-7521

³Joint Institute for Food Safety and Applied Nutrition, 200 C Street, SW,
Washington, DC 20204

Maraschino cherries colored with radish anthocyanin extract had an attractive red hue extremely close to those colored with FD&C Red No. 40. The major anthocyanins of radishes are pelargonidin-3-sophoroside-5-glucoside acylated with malonic acid and either ferulic or *p*-coumaric acid, while red-fleshed potatoes contain pelargonidin-3-rutinoside-5-glucoside acylated with *p*-coumaric acid as their major anthocyanin. These identities were confirmed by electrospray mass spectroscopy (ESMS). The site of cinnamic acid acylation for radish anthocyanins was determined to be at position 6 of glucose-1 of the sophorose substituent by 1- and 2-dimensional ¹H- and ¹³C-NMR. Aqueous extracts were prepared from these materials without using organic solvents. The color characteristics of the two materials were similar, radish anthocyanin extract having a hue angle of 37° and potato extract 30° at pH 3.5. FD&C Red No. 40 had a hue angle of 38°. Model beverage solutions colored with radish anthocyanin and potato anthocyanin extracts had half-lives at 25°C of 24 and 11 weeks, respectively.

The maraschino cherry serves as an icon for Oregon State University's Food Science and Technology Department since its founder, Dr. Ernest H. Wiegand, is

credited for its invention. More accurately, Prof. Wiegand, through systematic experimentation, developed the process for preserving cherries in a sulfite and calcium containing brine (1). The firm texture and superior quality of this brined cherry made possible production of the maraschino cherry as we know it today. Prof. Wiegand's invention resulted in the establishment of a brined cherry and maraschino cherry processing industry in Oregon which continues to contribute to Oregon's economy.

The maraschino cherry industry would like a natural colorant which can serve as an alternative to FD&C Red No. 40 (Allura Red) which gives the product its attractive color. This is a challenging assignment since processors want to match the hue of FD&C Red No. 40 colored cherries and have a reasonable shelf-life for a product which can be packed in glass and stored at ambient temperatures.

Radish Anthocyanin Extract

An Effective Colorant for Maraschino Cherries

With support from the cherry industry, we initiated an investigation on the potential of radish anthocyanin extract as a suitable colorant for maraschino cherries. Our inspiration was the chemical structure, pelargonidin-3-sophoroside-5-glucoside acylated with *p*-coumaric, ferulic or caffeic acids, as reported by other investigators (2-5). We predicted that the pelargonidin chromophore should impart a red hue, and that cinnamic acid acylation along with glycosidic substitution should enhance stability. Anthocyanin colorants such as red cabbage and black carrot extracts are cyanidin-based and tend to have a bluish-red hue because of the *ortho* phenolic substituents in the B-ring (6). The anthocyanins in grape-skin extract, mostly malvidin and delphinidin derived, impart a purplish hue.

Radish anthocyanin extract was prepared by acetone extraction of liquid nitrogen powdered radish epidermal tissue (7). The acetone extract was partitioned with chloroform and the aqueous portion further purified on a C-18 column. Water eluted sugars, acids and other water solubles and the anthocyanins were isolated with methanol containing 0.01% HCl. Brined cherries were processed into maraschino cherries using a process typical of commercial operations (7). Residual SO₂ was reduced to less than 500 mg/L by cold water washing and subsequent boiling. The cherries were placed in a 15° brix syrup (pH 3.5) and the syrup concentration increased at 3° increments over a 4 day period to a final sugar concentration of 40° brix. The syrup contained 0.1% potassium sorbate, 0.1% sodium benzoate and 0.25% citric acid. Cherries were colored with two different levels of radish anthocyanin, 600 and 1200 mg/L, and with 200 mg/L FD&C Red No. 40. After pasteurization, the cherries were stored at 25°C both in the dark and with exposure to fluorescent light for 12 months. The following color and pigment measurements were monitored throughout the storage period: total monomeric anthocyanin pigment, polymeric color, and CIE L*a*b* indices, hue angle and chroma (7).

We succeeded in matching the hue angle (40°) of FD&C Red No. 40 colored cherries with radish anthocyanin extract. Figure 1 shows the changes in total monomeric anthocyanin and polymeric color during storage. Anthocyanin degradation followed first order kinetics with half-lives of 28.8 and 33.0 weeks for cherries colored with 600 and 1200 mg anthocyanin pigment/L, respectively. Changes in the CIE $L^*C^*h^*$ indices are shown in Figure 2. Gradual increases in lightness (L^*) and decreases in hue angle and chroma occurred with time in the radish anthocyanin extract colored cherries compared with those colored with FD&C Red No. 40. In our judgement, the color quality was considered acceptable for at least six months storage at 25°C .

The Structure of Radish Anthocyanin Pigments

Figure 3 shows the HPLC separation of radish anthocyanins. Acid hydrolysis of the pigment isolate produced a single anthocyanin aglycon, pelargonidin (8). Saponification of the pigment isolate yielded one major anthocyanin which had an early retention time and uv-vis spectral properties characteristic of pelargonidin-3,5-diglycosides; *p*-coumaric and ferulic acids were generated in nearly equal quantities. This confirmatory information was consistent with previous identifications of pelargonidin-3-sophoroside-5-glucoside acylated with cinnamic acids as radish anthocyanins (2-5). We suspected that geometric isomerization of the acylating cinnamic acids might account for there being two major and two secondary peaks. Electrospray mass spectroscopy (ESMS) of the pigment isolate (Figure 4) revealed 4 distinct mass units in similar proportions to the HPLC peaks. Molecular weights of 902 and 932 daltons for the two smaller molecules corresponded to pelargonidin-3-sophoroside-5-glucoside acylated with *p*-coumaric and ferulic acids, respectively. The two major compounds had a larger mass difference of 86 daltons which is the molecular weight of malonic acid (less water). Saponification experiments were repeated and HPLC organic acid analysis revealed the presence of malonic acid in the hydrolysate. With tandem mass spectrometry (MS-MS), the molecular ion separated in the first quadrupole was bombarded to produce fragmentation (9). The fragmentation pattern consistently showed cleavage at the glycosidic linkages. As illustrated in Figure 5, mass fragments indicated that for peak 4, sophorose was acylated with ferulic acid and that glucose (position 5) was acylated with malonic acid. Similar glycosidic and acylation patterns were shown for the other 3 radish anthocyanins.

Different one- and two-dimensional NMR techniques were used for further elucidation of the structure and conformation of purified radish anthocyanins (10). ^1H NMR showed that all glucose units had the β -configuration. Two-dimensional shift correlation and total correlation analyses (2D NMR COSY and TOCSY) confirmed the 1-2 glycosidic linkage of sophorose. ^1H NMR indicated that the site of acylation was at position six of glucose-1 of sophorose and position 6 for glucose substituted at the 5 position (Figure 6). Acylation of glucose at position 6 with malonic acid and of glucose-1 of sophorose at position 6 with *p*-coumaric or ferulic acid was confirmed by

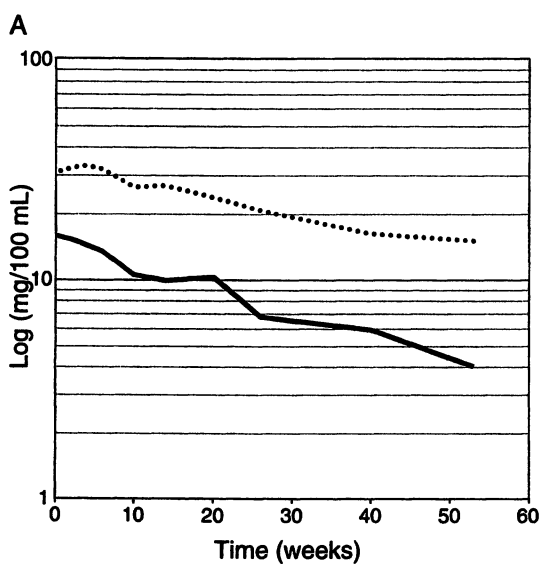


Figure 1. Changes in monomeric anthocyanin content and polymeric color of syrup samples with time. RAE C1 (solid line) and RAE C2 (dotted line). (Reproduced from reference 7. Copyright 1996 Institute of Food Technologists).

Continued on next page.

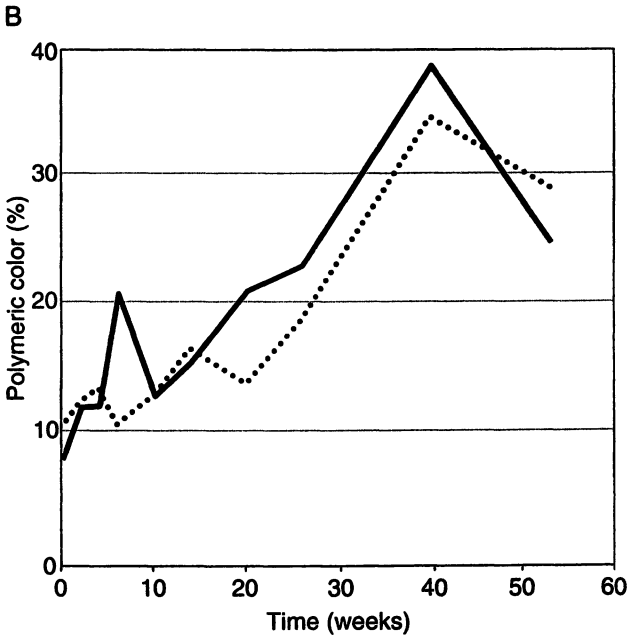


Figure 1. Continued.

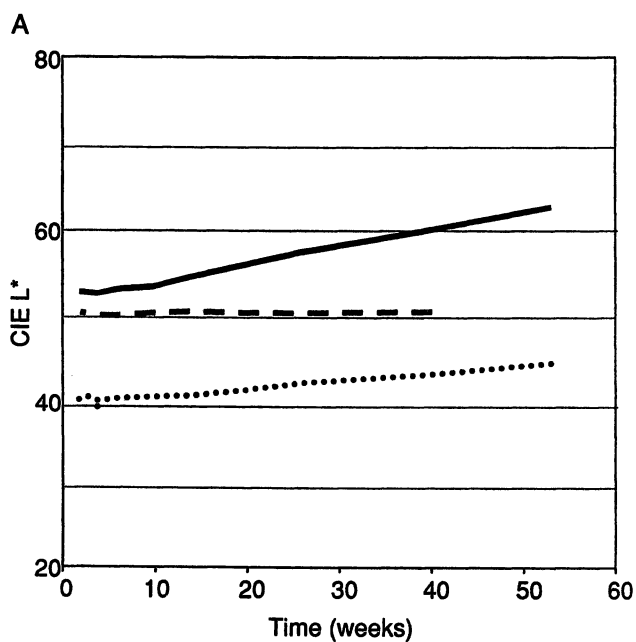


Figure 2. Changes in L, chroma and hue angle of syrup samples with time RAE C1 (solid line) and RAE C2 (dotted line) and FD&C Red No. 40 (dashed line). (Reproduced from reference 7. Copyright 1996 Institute of Food Technologists).*

Continued on next page.

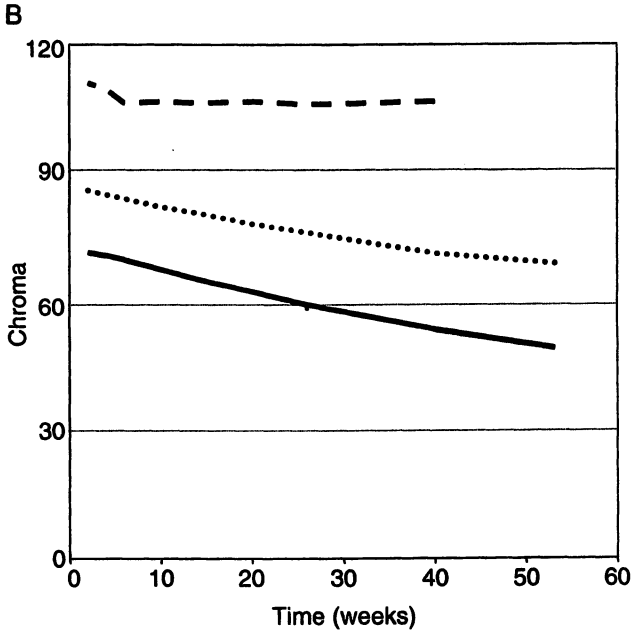


Figure 2. Continued.

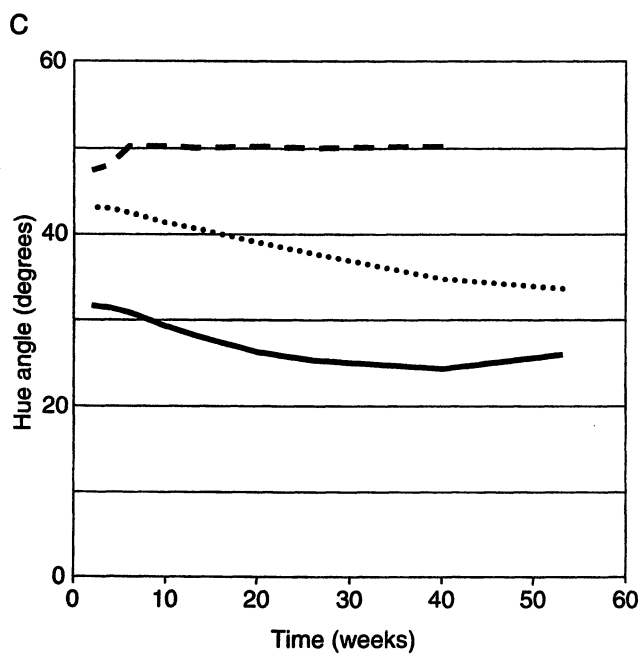


Figure 2. Continued.

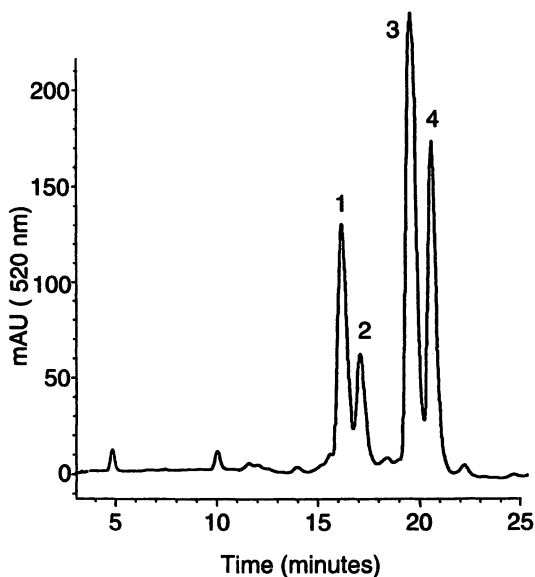


Figure 3. HPLC separation of red radish anthocyanins. Polymer labs PLRP-S, 250 x 4.6 mm i.d. column. Solvent A: 100% acetonitrile; B: 4% phosphoric acid. Linear gradient from 15-20% A over 40 min. Flow rate: 1 mL/min. Injection volume: 50 μ L. Detection at 520 nm. (Reproduced from reference 9. Copyright 1999 American Chemical Society.)

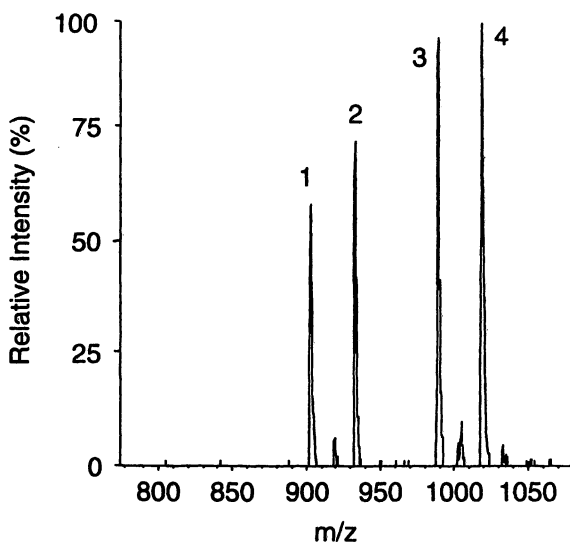


Figure 4. ESMS of radish anthocyanins. The molecular weights correspond to Pg-soph-5-glu acylated with p-coumaric (903.6 daltons), ferulic acid (933.6 daltons), p-coumaric and malonic acids (989.6 daltons) and ferulic and malonic acids (1019.6 daltons). (Reproduced from reference 9. Copyright 1999 American Chemical Society).

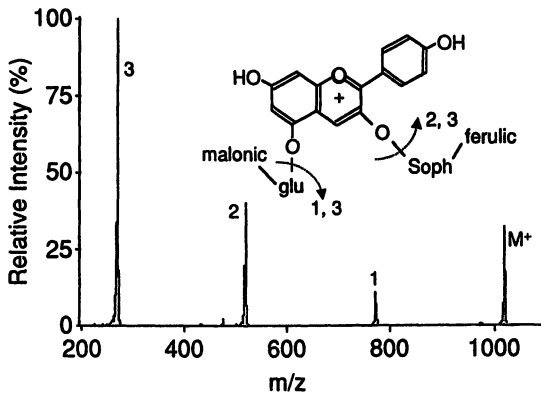


Figure 5. MS-MS fragmentation pattern of radish anthocyanin peak 4 pg-3-(feruloyl-soph)-5-(malonyl-glu). (Reproduced from reference 9. Copyright 1999 American Chemical Society).

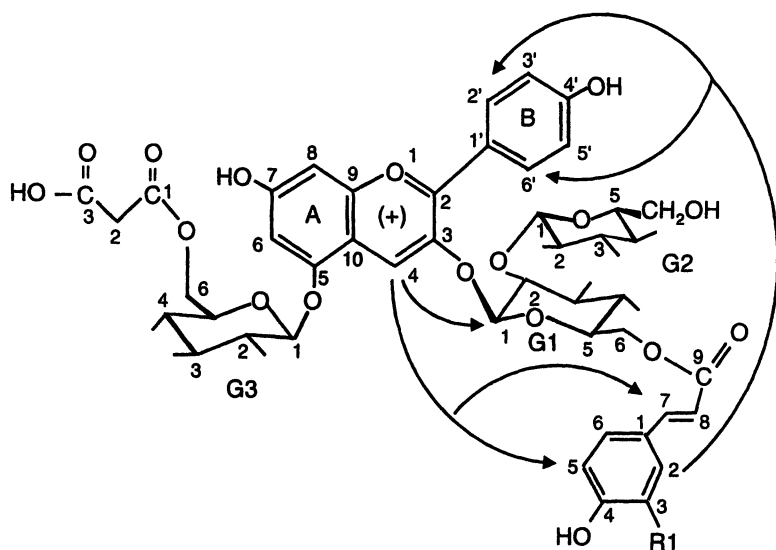


Figure 6. Chemical structure of radish pelargonidin derivatives. Arrows indicate hydrogens in close proximity. R1 = H = p-coumaric acid derivative; R1 = OCH₃ = ferulic acid derivative. (Reproduced from reference 10. Copyright 1998 American Chemical Society).

two-dimensional heteronuclear multiple quantum coherence (HMQC) and heteronuclear multiple bond correlation (HMBC). *J*-coupling constants showed that both cinnamic acids were in the trans configuration. Two-dimensional nuclear overhauser effect spectroscopy (NOESY) showed high correlation between H-4 of the pelargonidin moiety and the hydrogens in positions H-3 and H-5 of *p*-coumaric acid. This goes in agreement with stacking between the aromatic nuclei of the anthocyanin with the planar ring of the cinnamic acid allowing for π - π hydrophobic interactions. Figure 6 shows these structural elements for radish anthocyanins. The zwitterionic characteristic of the malonic acid acylated pigments suggests a likely ionic attraction between the positively charged oxonium anthocyanin moiety and the negatively charged free carboxylic group of malonic acid. Intramolecular copigmentation may account for the enhanced stability and color quality of radish anthocyanin extract described above.

Agronomic Factors

Sources for natural colorants should have high pigment content to receive serious consideration for commercialization. Radishes do have the advantages of being a common agricultural crop which is easily grown and harvested. With the cooperation of Oregon State University horticulturists, we investigated the anthocyanin content and composition of numerous commercially available radish cultivars (11). Radishes were grown at two different locations, Corvallis and Hermiston, OR, over three years. There are two general types of radishes, the conventional spring or salad radish familiar to Western households and the winter or Daikon radish which is popular with several Asian cultures. The spring radishes have their anthocyanin pigment concentrated in the skin while a number of the winter radishes (which are much larger) have pigmentation in the flesh. Five winter cultivars and 22 spring cultivars were included in the investigation. In addition to cultivar, growing location, and seasonal influences, the project examined the effect of maturity.

Total monomeric anthocyanin pigment content ranged from 12.2-53.0 mg/100g root for winter cultivars and from 4.7-38.8 mg/100g root for spring cultivars. For spring cultivars, anthocyanin content calculated on the basis of mg/100g skin, ranged from 39.3 to 185. Since spring cultivars have pigmentation exclusively in the skin, by extracting only the peels one can effectively obtain several orders of pigment concentration. The average value of 185 mg/100g skin for the spring Fuego cultivar compares favorably with such anthocyanin sources as red cabbage (25 mg/100g), grapes (6-600 mg/100g), blackcurrants (130-400 mg/100g), blueberries (25-497 mg/100g), and elderberries (450 mg/100g) (6). In subsequent pilot-plant pigment extraction trials, we found an abrasive peeler to be very efficient for pigment extraction, achieving anthocyanin recoveries of 95% (12). Evidently the turgor

pressure of the radish epidermal cells promotes cell-wall rupture with the anthocyanins being almost completely transferred to the juice and very little present in the filter press-cake residue. The possible anthocyanin pigment yield from radishes was estimated using average values from experimental and published data (11). The spring cultivar Fuego could produce between 9 and 16 kg anthocyanin/ha when grown for 4 or 7 weeks, respectively. Calculations based on data for red cabbage gave an estimate of 14 kg anthocyanin/ha. Thus, anthocyanin production from radishes is of the same order as that for the commercial colorant red cabbage. The yield estimates for radish did not take into consideration the fact that more than one radish harvest can be produced in the same year with growing times of 4-7 weeks for spring and 8-10 weeks for winter cultivars. All of the radish cultivars showed similar qualitative anthocyanin profiles with pigmentation based on pelargonidin-3-sophoroside-5-glucoside acylated with 1 or 2 acids. Differences among cultivars were in the proportions of individual pigments with different acyl substitutions.

Practical Issues and Current Status

The radish anthocyanin extract used in the maraschino cherry coloring experiments (7) was highly purified, being isolated by adsorption on C-18 resin and recovered with acidified methanol. Such a process would not meet regulatory approval. Those anthocyanin-based colorants receiving approval for food use by FDA in recent years have been within the category of fruit or vegetable juice. This classification is extended to include aqueous extracts of dried fruits and vegetables. Examples include red cabbage, black carrot, elderberry, and chokeberry (*Aronia melanocarpa*) juice. Using conventional juice processing unit operations, we succeeded in making radish juice concentrates with anthocyanin content as high as 400 mg/100 mL concentrate (12). While the color quality (attractive hue, minimal anthocyanin degradation) was excellent, these aqueous extracts had undesirable flavors characteristic of glucosinolate and isothiocyanate break-down products. Concentration by conventional thermal evaporation combined with direct osmosis membrane concentration reduced aroma intensity considerably with sensory assessment being of the same order as that of commercial red cabbage colorant. We believe that technologies such as super-critical fluid extraction with CO₂ and nano-filtration should be even more effective for removing undesirable flavor compounds. Presently we know of two Japanese firms and one Taiwanese firm that are manufacturing radish anthocyanin extract for commercial use in their countries. We have analyzed samples of these colorants and have found them to be similar but not identical with respect to the anthocyanin composition and color properties of our extracts. The presence of ethanol in their extracts suggests that they were either alcohol extracted or recovered from resins using ethanol as a solvent.

Red-fleshed Potato Extract

Anthocyanins of Red-fleshed Potatoes

Other investigators have identified acylated derivatives of pelargonidin-3-rutinoside-5-glucoside along with acylated peonidin and malvidin-based anthocyanins in red-fleshed potatoes (13-16). We assumed that the structural similarity to radish anthocyanins (pelargonidin chromophore, glycosidic substitution with a disaccharide at the 3 position and glucose at the 5 position, and cinnamic acid acylation) should yield extracts of comparable stability and color. Crop scientists at Oregon State University and the USDA-ARS laboratory at Prosser, WA, are interested in the commercial potential of red-fleshed potatoes because of consumer and industry interest in colored potatoes for salads and novelty items. With their cooperation we conducted a two-year project on the anthocyanin pigment composition of red-fleshed potatoes (17). Thirty-three cultivars were evaluated for their anthocyanin composition and pigment content. Monomeric anthocyanin content ranged from 2-40 mg/100g tuber fresh weight with two breeding clones, NDOP5847-1 and NDC4069-4, having anthocyanin contents greater than 35 mg/100g tuber fresh weight. Such values are comparable to red cabbage. Higher pigment content has been reported for purple potato cultivars such as Urenika which contained an average of 184 mg petunidin and malvidin-based anthocyanins/100g tuber flesh (16). Through potato breeding it should be possible to develop red-fleshed potato cultivars with higher pigment levels which would make them more suitable for colorant production.

Figure 7 shows the HPLC separation of the anthocyanins from red-fleshed potatoes. Acid hydrolysis generated the aglycon, pelargonidin, with trace amounts of peonidin. Saponification yielded one major peak (87% of total peak area) and three cinnamic acids, *p*-coumaric, ferulic and caffeic acid (Figure 8). More extensive purification of starting material established that caffeic acid was generated from chlorogenic acid and not from the pigments. The UV-visible spectra (Figure 9) were consistent with peaks 4,5, 6 and 7 being mono cinnamic acid acylated pelargonidin-3,5-diglycosides. ESMS of red-fleshed potato anthocyanin isolate (Figure 10) showed four molecular weights corresponding to pelargonidin-3-rutinoside-5-glucoside, its *p*-coumaric and ferulic acylated derivatives, and pelargidin-3-rutinoside. The mass numbers in greatest abundance, however, corresponded to the glycoalkaloids chaconine (852 daltons) and solanine (868 daltons). The positive charge of the alkaloids facilitated their detection of the molecular ion at the low operating voltage effective for anthocyanin detection. Clearly, the process for anthocyanin isolation also recovered the glycoalkaloids. Presence of toxic alkaloids is alarming, and an upper limit of 60-70 mg/kg has been proposed for potato cultivars to be selected for human consumption (18,19). The cultivar from which this pigment extract was isolated were well below this level (10-15 mg/100g). A process which concentrates the toxic alkaloids is of obvious concern. We subsequently developed a process where we precipitated 90% of the glycoalkaloids through adjustment of extracts to pH 8.0 (20). Alkaline conditions are deleterious to anthocyanins, but anthocyanin destruction was limited to 30% under these conditions.

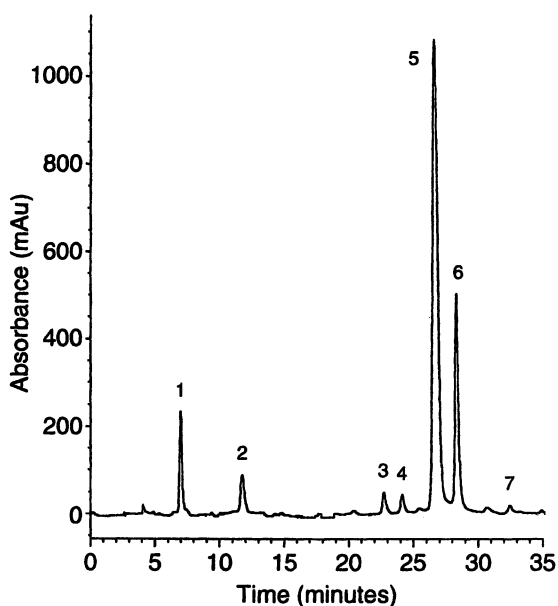


Figure 7. HPLC separation of red-fleshed potato anthocyanins. Polymer Labs PLRP-S, 250 x 4.6 mm i.d. column. Solvent A: 100% acetonitrile, B: 4% phosphoric acid. Linear gradient from 10-20% A over 25 min and isocratic at 20% A for 5 min. Flow rate: 1 mL/min. Injection volume: 50 μ L. Detection at 520 nm. Pigments are: Pg-3-rut-5-glu (1), Pg-3-rut (2), unknown (3), Pg-3-rut-5-glu acylated with p-coumaric acid (4 and 5), Pg-3-rut-5-glu acylated with ferulic acid (6), and Pg-3-rut acylated with p-coumaric acid (7). (Reproduced from reference 17. Copyright 1998 Institute of Food Technologists).

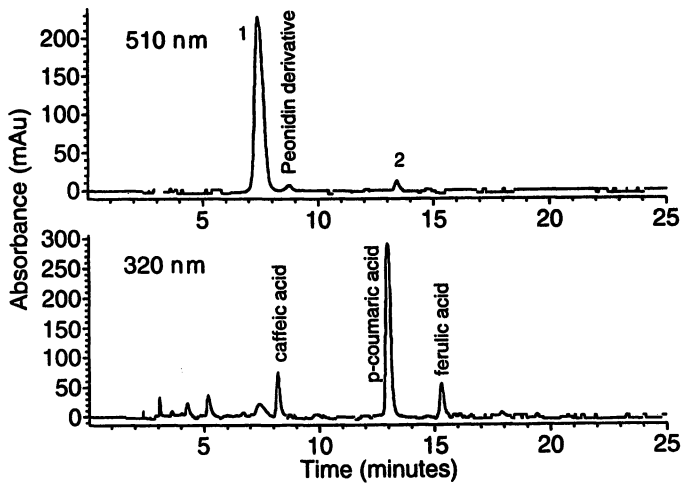


Figure 8. HPLC separation of saponified potato anthocyanins (510 nm) and their acylating groups (320 nm). ODS C-18, 250 x 4.6 mm i.d. column. Solvent A: 100% acetonitrile; B: 1% phosphoric acid, 10% acetic acid, 5% acetonitrile and water. Linear gradient from 0 to 30% A over 30 min. Flow rate: 1 mL / min. Injection volume: 50 μ L. (Reproduced from reference 17. Copyright 1998 Institute of Food Technologists).

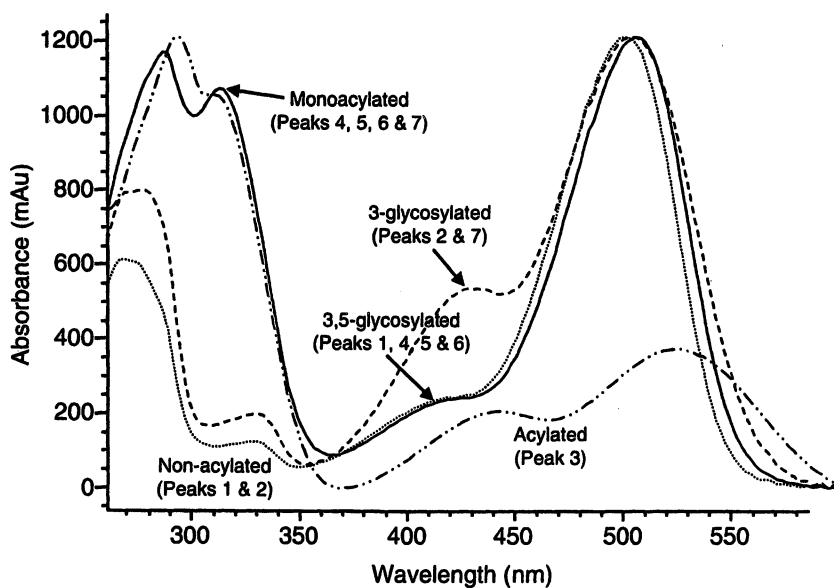


Figure 9. Spectral characteristics of potato anthocyanins indicating glycosylation and acylation patterns. (Reproduced from reference 17. Copyright 1998 Institute of Food Technologists)

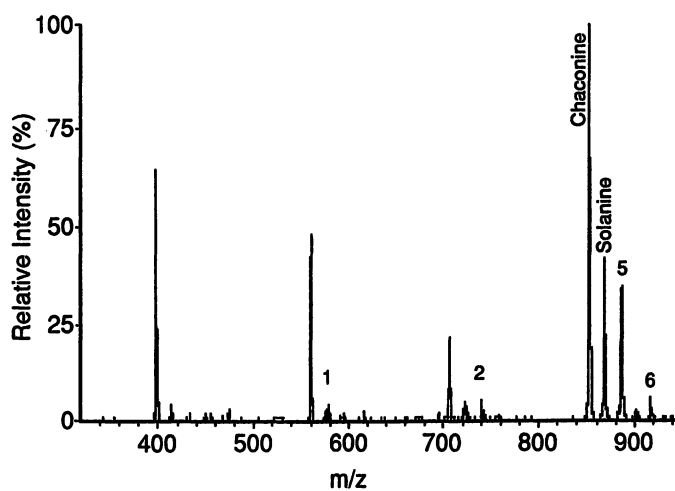


Figure 10. ESMS of potato pigment isolate. Molecular ions correspond to anthocyanin pigments and glycoalkaloids. 1 = Pg-3-rut, 579.2 daltons; 2 = pg-3-rut-5-glu, 741.2 daltons; Chaconine = 852 daltons; Solanine = 868 daltons; 5 = pg-3-rut-5-glu acylated with p-coumaric acid, 886.8 daltons; 6 = pg-3-rut-5-glu acylated with ferulic acid, 917.5 daltons. (Reproduced from reference 17. Copyright 1998 Institute of Food Technologists).

Comparisons of Radish and Red-Fleshed Potato Anthocyanin Extracts

Color Similarities and Differences

The similarity in structure of red-fleshed potato anthocyanins to radish anthocyanins prompted our investigation of potato pigments since we anticipated they would also be similar in color and stability. The hue of pelargonidin pigments has been described as orange-red (21), and the presence of cinnamic acid acylation would be expected to give a bathochromic shift, changing the color to red or reddish-blue depending on the number of acylations (22). Anthocyanin extracts of both materials can come very close to matching the color of FD&C Red No. 40 which exhibits a hue angle of approximately 40°. The major pigments of both extracts have one cinnamic acid acylating group per molecule, but radish anthocyanin has additional acylation with malonic acid giving it zwitterion character. Malonic acid acylation appears not to cause the bathochromic shift that additional cinnamic acid acylation would be expected to provide (23). The two extracts are not identical, however, with respect to their color properties. We measured CIE L*a*b* indices for extracts of the two materials at the same pigment concentration and different pH values. At pH 1 the two extracts were very similar with hue angles of about 40°. At pH 3.0 the hue angles decreased to about 20° and at pH 4.0 to about 15° (bluish-red). While hue angles were similar under these conditions, there were marked differences with respect to chroma. Potato anthocyanins showed a much larger decrease in chroma with increasing pH so that more pigment would be required to achieve similar color intensities.

Pigment and Color Stabilities in Juice Model Systems

The color and pigment stabilities of radish and red-fleshed potato anthocyanins were monitored in juice model systems for one year at both room (25°C) and refrigerated (2°C) temperatures (24). The model juice was composed of corn syrup (10° brix), citric acid (pH 3.5), 0.1% potassium sorbate and 0.1% sodium benzoate. Highly purified radish and red-fleshed potato anthocyanin extracts were prepared by isolation on C-18 resin with subsequent extraction with acidified alcohol. Less purified aqueous extracts were also prepared using juice processing operations that would be amenable to regulatory approval. The process for preparing radish juice has been described earlier. High anthocyanin recoveries were obtained with little anthocyanin degradation. Preparation of red-fleshed potato presented some challenges. Active polyphenol oxidase accelerates anthocyanin destruction and heat treatment gelatinizes starch confounding filtration and concentration. By blending tubers with acidified water (0.5 M citric acid) and blanching at 100°C for 5 min we succeeded in obtaining an extract with minimal pigment destruction that could be clarified and filtered. Glycoalkaloids were precipitated by alkaline pH adjustment as

described earlier. All juice model systems contained anthocyanin levels of 15 mg/100 mL. The visual appearances of all model juices were very close in color to FD&C Red No. 40 (150 ppm solution at pH 3.5) with the color of purified radish extract being the closest (hue angle = 38°, chroma = 66, L* = 67).

Figure 11 shows the changes in total anthocyanin pigment and polymeric color during storage and Figure 12 shows the changes in hue angle, chroma and lightness (L*). Radish extracts showed higher stability during storage than potato extracts, regardless of extraction procedures. At room temperature, purified radish extract had a half-life of 22 weeks while potato juice aqueous extract had a half-life of 10 weeks. We suspect that the diacylation and zwitterion character of radish anthocyanins may account for this enhanced stability. The formation of polymeric color showed the expected inverse relationship to anthocyanin degradation. Refrigerated temperature increased the half-life for all samples to more than one year. Juices colored with potato extracts had higher lightness values and lower chroma after some storage compared to radish extracts which translates to reduced color intensity. Initial hue angle was lower for potato extracts and the rate of change was much greater, resulting in hue angles in the order of 60° and a yellow-orange color characteristic of degraded anthocyanins.

Conclusions

We believe that there is potential for using natural colorants from both radish and red-fleshed potato extracts. Their major advantages are their stability compared to other anthocyanin colorants and their attractive red hue. It is not only manufacturers of maraschino cherries who are seeking colorants with hues similar to FD&C Red No. 40. After all, it has by far the highest *per capita* consumption of the certified colorants (25). Another advantage of radishes and potatoes is that they are common agricultural crops which can be easily grown and harvested. Our estimates show reasonable anthocyanin pigment yields for both crops, but these yields can undoubtedly be increased substantially through classical plant breeding and molecular biology.

Acknowledgments

This work was supported by Grant 94-37500-0808 from the USDA NRI Competitive Grants Program and a grant from Oregon Department of Agriculture's Center for Applied Agricultural Research (CAAR). Matching funds for the CAAR grant were provided by the Oregon Sweet Cherry Commission and the Northwest Cherry Briners Association. We thank James Baggett, Gary L. Reed, James Myers and Alvin Mosley at Oregon State University and Charles Brown from the USDA Research and Extension Center at Prosser, WA, for their cooperation in providing plant materials. We thank Victor Hsu of OSU's Biochemistry and Biophysics Department for his role in NMR experiments and Donald Griffin from OSU's Department of Chemistry for the ESMS analyses.

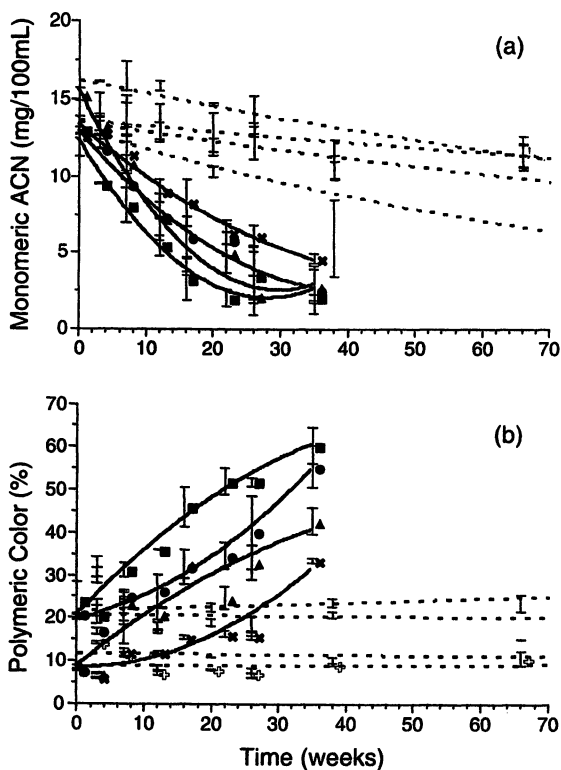


Figure 11. Monomeric anthocyanin degradation (a) and polymeric color formation (b) in model juices colored with radish and potato extracts. ■ Potato Juice concentrate, ▲ Purified Potato Extract, ● Radish Juice Concentrate, ✕ Purified Radish Extract. Filled symbols represent room temperature (25°C) treatments, open symbols represent refrigerated (2°C) treatments. Bars represent the standard deviations, and lines represent the linear or quadratic lines fitted by least squares. (Reproduced from reference 24. Copyright 1999 Institute of Food Technologists.)

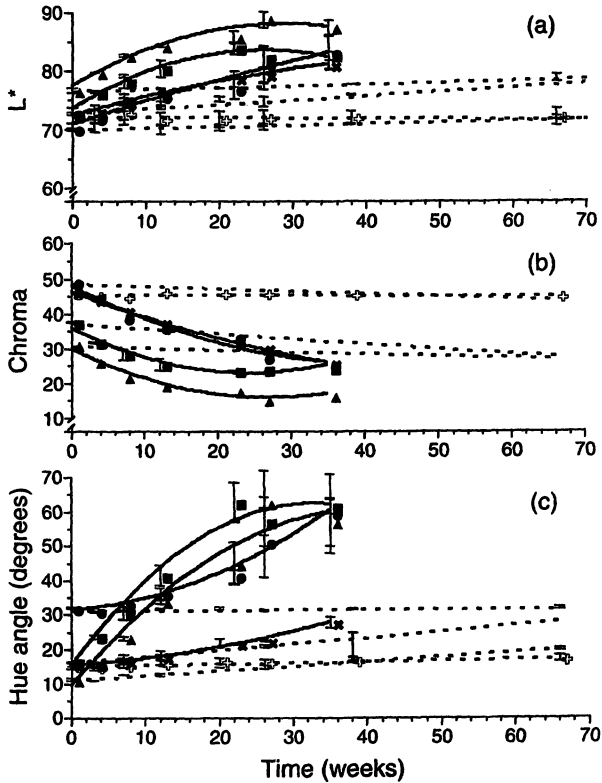


Figure 12. Changes in L^* , chroma, and hue angle of model juices colored with potato and radish anthocyanins during storage. ■ Potato Juice concentrate, ▲ Purified Potato Extract, ● Radish Juice Concentrate, × Purified Radish Extract. Filled symbols represent room temperature (25°C) treatments, open symbols represent refrigerated (2°C) treatments. Bars represent the standard deviations, and lines represent the linear or quadratic lines fitted by least squares. (Reproduced from reference 24. Copyright 1999 Institute of Food Technologists.)

Literature Cited

1. Jolly, J. Christopher. M. A. thesis, Oregon State University, Corvallis, OR, 1999.
2. Harborne, J. B. *Phytochem.* **1963**, *2*, 85-97.
3. Ishikura, N.; Hayashi, K. *Bot. Mag., Tokyo* **1962**, *75*, 23-36.
4. Ishikura, N.; Hayashi, K. *Bot. Mag., Tokyo* **1963**, *76*, 6-13.
5. Fuleki, T. *J. Food Sci.* **1969**, *34*, 365-369.
6. Wrolstad, R. E. In *Natural Colors*; Francis, J. F.; Lauro, G.J., Eds.; Marcel Dekker Inc.: New York, NY, **2000**, *in press*.
7. Giusti, M. M.; Wrolstad, R. E. *J. Food Sci.* **1996**, *61*, 688-694.
8. Giusti, M. M.; Wrolstad, R. E. *J. Food Sci.* **1996**, *61*, 322-326.
9. Giusti, M. M.; Rodriguez-Saona, L. E.; Griffin, D; Wrolstad, R.E. *J. Agric. Food Chem.* **1999**, *47*, 4657-4664.
10. Giusti, M. M.; Ghanadan, H.; Wrolstad, R. E. *J. Agric. Food Chem.* **1998**, *46*, 4858-4863.
11. Giusti, M. M.; Rodriguez-Saona, L. E.; Baggett, J. R.; Reed, G. L.; Durst, R. W.; Wrolstad, R. E. *J. Food Sci.* **1998**, *63*, 219-224.
12. Rodriguez, L. E.; Giusti, M.M.; Durst, R. W.; Wrolstad, R. E. *Unpublished results*.
13. Harborne, J. B. *Biochem. J.* **1960**, *74*, 262-269.
14. Sasche, J. Z. *Lebensm. Unters. Forsch.* **1973**, *153*, 294-300.
15. Anderson, M.; Opheim, S.; Aksnes, D. W.; Froystein, N. A. *Phytochem. Anal.* **1991**, *2*, 230-236.
16. Lewis, C. E. Ph.D. thesis, University of Canterbury, Christchurch, New Zealand, **1996**.
17. Rodriguez-Saona, L. E.; Giusti, M.M.; Wrolstad, R.E. *J. Food Sci.* **1998**, *63*, 458-465.
18. Valkonen, J.; Keskitalo, M.; Vasara, T.; Pietila, L. *Crit. Rev. Plant Sci.* **1996**, *15*, 1-20.
19. Van Gelder, S.M.J. In *Poisonous Plant Contamination of Edible Plants*. Rizk, A-F.M., Ed.; CRC Press: Boca Raton, FL, **1991**, 117-156.
20. Rodriguez-Saona, L.E.; Wrolstad, R.E.; Pereira, C. *J. Food Sci.* **1999**, *64*, 445-450.
21. Mazza, G.; Miniati, E. In *Anthocyanins in Fruits, Vegetables, and Grains*, Mazza, G.; Miniati, E., Eds.; CRC Press: Boca Raton, FL, **1993**; 1-28.
22. Dangles, O.; Saito, N.; Brouillard, R. *Phytochem.* **1993**, *34*, 119-124.
23. Giusti, M.M.; Rodriguez-Saona, L.E.; Wrolstad, R.E. *J. Agric. Food Chem.* **1999**, *47*, 4631-4637.
24. Rodriguez-Saona, L. E.; Giusti, M.M.; Wrolstad, R. E. *J. Food Sci.* **1999**, *64*, 451-456.
25. Newsome, R. L. *Food Technol.*, **1986**, *40*, 49-56.

Chapter 6

Composition of Carotenoids from Annatto

Adriana Zerlotti Mercadante

**Department of Food Science, Faculty of Food Engineering, UN1CAMP,
C.P.: 6121, CEP: 13083-970, Campinas, Brazil
(email: mercadan@obelix.unicamp.br)**

Of the naturally occurring colorants, annatto (*Bixa orellana* L.) ranks first in economic importance in Latin America. The major producers of annatto seeds are Peru, Brazil and Kenya. Commercial annatto preparations are available to impart yellow to red colors to a variety of products such as cheese, butter mixes, sausages and dressings. Approximately 80% of the carotenoid content of annatto seeds is bixin, however, several carotenoids can be found in trace amounts. Recently, fourteen minor carotenoids were isolated and identified by means of spectroscopic data. Eleven of them are newly discovered carotenoids, which may be arranged into two groups: methyl esters of apocarotenoids, and diapocarotenoids with methyl and geranylgeranyl esters, ketone or aldehyde functional groups. Most of them bear the same (9Z)-methyl ester end group of bixin. Therefore, they might be considered as natural metabolites derived from C₄₀ carotenoids by enzymatic oxidative cleavage.

The tree *Bixa orellana* L. (family Bixaceae) was named after Francisco de Orellana, the Conqueror, who explored the Amazon river for the first time in 1541 (1). The plant, known as annatto, is native to tropical America and possesses clusters of brown or crimson capsular fruits covered by flexible thorns. The fruits contain about 10 to 50 small seeds, about the size of grape seeds. The seeds are covered with a thin, highly colored, orange to red resinous layer from where the natural colorant is obtained.

Nowadays, the major producers of annatto seeds are Peru, Brazil and Kenya (2). Commercial production of annatto colorants in Europe and United States (USA) dates back to the 1870's, earlier than any other food color, artificial or natural. Food applications increased in the 1960's when some artificial food dyes were banned. The

USA and Europe are the two largest importers of annatto seeds (3). Japan, where annatto colors were introduced in 1963, doubled the amount imported during the period 1983 to 1990 and became an important market (4). Europe imports approximately 2,500 tons of seeds or seed equivalents per year, with the United Kingdom and the Netherlands being the two principal importers (3), where the main application is in the cheese industry. Annatto has been reported to be the most commonly consumed natural color additive in the United Kingdom (5).

A temporary acceptable daily intake (ADI) of 1.25 mg/kg body weight for annatto extracts was given in the 1970's (6, 7). Further metabolic studies were requested, leading to an expanded monograph and retention of the ADI value (8). However, the ADI decreased to 0.065 mg/kg body weight in 1982 (9).

The earliest recorded case of the use of annatto colorant was for painting faces and bodies among the Carib Indians in northeast South America in the late 15th century. The Yanomami Indians of Amazonia still use annatto to adorn themselves (2). The major application of annatto is in the food industry for coloring cheese and other dairy products, such as ice cream, butter mixes, yoghurt, meat (sausages), fish, margarine, snacks, dressings, sauces and confectionery. Usage varies from country to country because of different food traditions and legislation (3).

Although subject to heavy competition from other colors like β -carotene and paprika, annatto is the only colorant that gives the deep orange hue to Cheddar cheese, "prato" (a typical Brazilian cheese) and cheese wax. This property is a result of the unique characteristic of norbixin which binds with casein molecules and is thereby stabilised and will not leach or bleed colour (3,10). Annatto also shows superior stability compared to β -carotene and paprika in extruded snack products and breakfast cereals (11).

There is general agreement (1,12) that more than 80% of the carotenoid in the *B. orellana* seed coat consists of bixin (methyl hydrogen (9'Z)-6,6'-diapocarotene-6,6'-dioate) (Figure 1), which, to date, has been encountered only in *B. orellana*. Small amounts of norbixin (Figure 1) ((9'Z)-6,6'-diapocarotene-6,6'-dioic acid) are also found in annatto seeds and this becomes the major carotenoid of the aqueous annatto extracts.

Commercial annatto preparations are available to impart yellow to red color to a variety of products. They include oil-soluble colors and annatto powder (which contain bixin as the main pigment), water-dispersible colors (with norbixin as the main colorant), and emulsions, which may contain a combination of both bixin and norbixin or only norbixin. Annatto powder mixed with corn flour, known as "colorífico" in Brazil, is available for domestic use, mainly in the central, north and north-east regions of Brazil. It is very difficult to estimate precisely the market for the different annatto preparations because no official statistics are available.

Many other carotenoids have been isolated in trace amounts from annatto seeds and preparations, but most of them have remained unidentified (13-16). A new carotenoid, methyl (9Z)-8'-oxo-6,8'-diapocarotene-6-oate, and methyl bixin were isolated and identified by means of spectroscopy data by Jondiko and Pattenden (17). Although extensive chromatography was employed, analogs of bixin with a longer skeleton, i.e., C₄₀ or C₃₂, were not found by these authors.

More stringent specifications and knowledge of composition are now required for natural food colors, including annatto. The scope of this work was to report the new

minor carotenoids recently found in annatto seeds, and analyze the annatto preparations available in Brazil.

Experimental

Isolation of New Minor Carotenoids from Annatto Seeds

Carotenoid extraction and isolation by flash column chromatography and thin layer chromatography (TLC) on silica-gel and magnesium oxide were carried out according to Mercadante *et al.* (18–20). The final purification was achieved by semi-preparative high performance liquid chromatography (HPLC) on a reversed-phase column (18–20).

The carotenoids were identified by means of their UV-visible, electron impact mass and nuclear magnetic resonance (NMR) spectra (400 or 500 MHz ^1H , 100 or 125 MHz ^{13}C and DEPT). Two dimensional NMR techniques (correlated spectroscopy, heteronuclear multiple quantum coherence, inverse gradient-selective heteronuclear multiple-bond correlation) were also used, which allowed the assignment of all proton signals for each carotenoid.

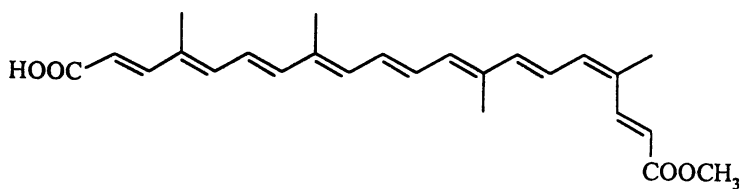
Analysis of Annatto Preparations

Oil-soluble, water-soluble and powder preparations were kindly provided by industries located in Brazil. Seven brands of commercial “colorífico” were bought in Campinas, São Paulo State, Brazil.

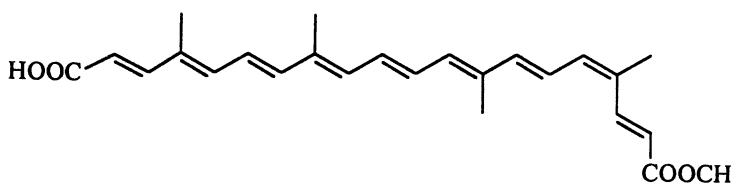
The annatto preparations were weighed and diluted to 25 ml with methanol. Some oil soluble preparations were dissolved first in acetone and afterwards diluted to the same volume with methanol. The “colorífico” powder was exhaustively extracted in an ultrasonic bath five times with acetone and twice with methanol, and the volume made up to 50 ml with methanol. The HPLC separation was carried out with a reversed-phase Spherisorb ODS-2 column, and acetonitrile/2% aqueous acetic acid (65:35) as mobile phase at a flow rate of 1 mL/min, as previously described by Scotter *et al.* (21). The temperature of the column was maintained at 28°C.

Results and Discussion

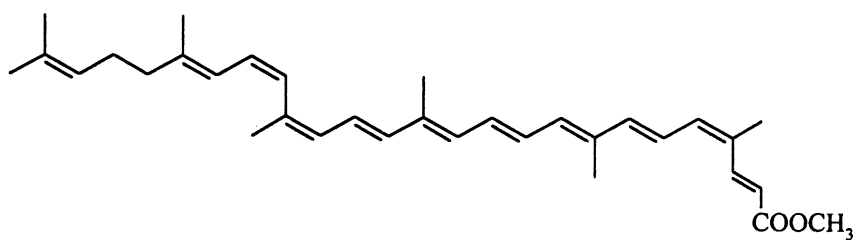
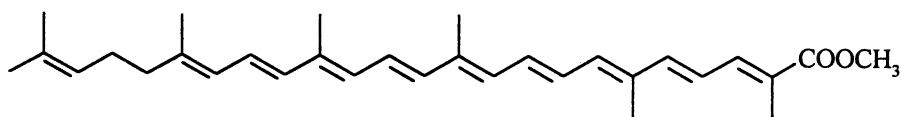
Fourteen minor carotenoids, of which eleven were newly discovered, were identified from annatto seeds. These minor carotenoids were placed into two groups. Methyl esters of apocarotenoids (C_{30} and C_{32}), shown in Figure 2, comprising two new



bixin



norbixin

Figure 1. Chemical structures of bixin and norbixin.*(7Z,9Z,9'Z)-methyl apo-6'-lycopenoate*

methyl apo-8'-lycopenoate

Figure 2. Apocarotenoids isolated from annatto seeds.

geometrical isomers (9'Z)- and (7Z,9Z,9'Z)- along with the (all-E)-methyl apo-6'-lycopenoate, (all-E) and (9Z)-methyl-apo-8'-lycopenoate, and methyl 8'-apo- β -caroten-8'-oate (18, 22). The latter has already been synthesized, on a laboratory scale (23), but this is the first time that this apocarotenoid has been found in nature.

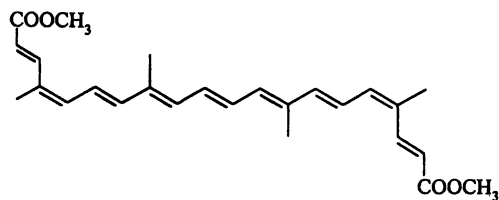
Diapocarotenoids (Figure 3), with ester, ketone or aldehyde groups (C₁₉, C₂₂, C₂₄ and C₂₅), such as dimethyl (9Z,9'Z)-6,6'-diapocarotene-6,6'-dioate, methyl (9Z)-10'-oxo-6,10'-diapocarotene-6-oate, methyl (9Z)-6'-oxo-6,6'-diapocarotene-6-oate and methyl (9Z)-8'-oxo-6,8'-diapocarotene-6-oate were isolated (19). Although no alkali was used during the extraction and isolation procedures, the presence of the new C₂₆ apocarotenoid with a carbonyl group (keto function), methyl (9Z)-6'-oxo-6,5'-diapocarotene-6-oate, is most likely an artifact. It probably arose from an aldol condensation of methyl (9Z)-8'-oxo-6,8'-diapocarotene-6-oate with acetone from the mobile phase used for TLC on magnesium oxide (19). The first reported naturally occurring carotenoid acids esterified with a geranylgeranyl group are found in this second group, which comprises methyl 6-geranylgeranyl 8'-methyl-6,8'-diapocarotene-6,8'-dioate, 6-geranylgeranyl 6'-methyl (9'Z)-6,6'-diapocarotene-6,6'-dioate (Figure 3) and 6-geranylgeranyl 6'-methyl-6,6'-diapocarotene-6,6'-dioate (20).

The presence of C₄₀-carotenes (phytoene, phytofluene, ζ -carotene and neurosporene) was also confirmed (22).

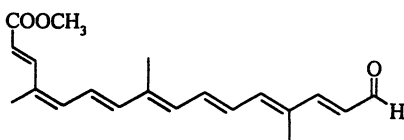
The minor apo and diapocarotenoids may be considered as natural metabolites derived from C₄₀-carotenes by enzymatic oxidative cleavage. It seems that the preferred reaction is a cleavage at the C_{5,6}'-double bond and/or at the C_{5,6}-double bond, yielding structures very similar to bixin. To a smaller extent, cleavage at the C_{7,8}'-double bond and at the C_{5,6}-double bond and at different positions at the other end, such as at the C_{7,8}' and C_{9,10}'-double bonds, also occurred. Cleavage at the C_{5,6}' and C_{13,14}'-double bonds resulted in the new carotenoid derivative, methyl (4Z)-4,8-dimethyl-12-oxo-dodecyl-2,4,6,8,10-pentaenoate (19). Due to the rigid polyene chain in carotenoids, cyclization is limited to the ends of the molecule, where formation of a six-membered ring is common. This must have occurred to produce the carotenoid methyl 8'-apo- β -caroten-8'-oate. It is interesting to point out the presence of diapocarotenoids linked to geranylgeraniol. Geranylgeraniol, in the free form, has already been found in annatto (17,24), and geranylgeranyl diphosphate is well known as an intermediate in the biosynthesis of isoprenoid compounds.

The chromatograms of the annatto preparations are shown in Figures 4, 5 and 6. As expected, all water-soluble samples analyzed showed norbixin as the major carotenoid, with small amounts of its isomers and the absence of bixin (Figure 4). The oil-soluble preparations contained bixin as the major carotenoid with small amounts of norbixin and isomers of bixin (Figure 5). The carotenoid profile of "colorífico" was found to be very similar to that of commercial oil soluble preparations, shown in Figure 5.

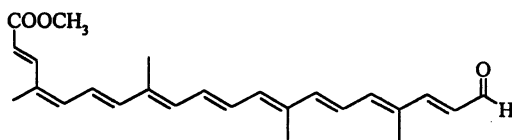
However, the preparation used commercially for coloring cheese, contained as the major pigment, a yellow degradation compound with λ_{\max} at 399 nm (acetonitrile/acetic acid (65:35)) and several bixin isomers, as shown in Figure 6. These compounds might be formed during processing which, according to the manufacturers, employed heat. The yellow product showed very similar characteristics



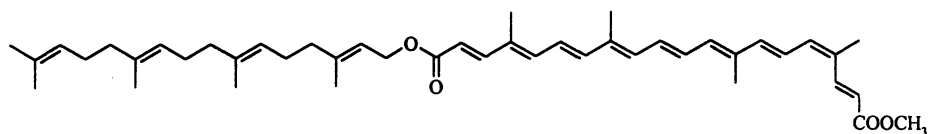
dimethyl (9Z,9'Z)-6,6'-diapocarotene-6,6'-dioate



methyl (9Z)-10'-oxo-6,10'-diapocarotene-6-oate



methyl (9Z)-6'-oxo-6,6'-diapocarotene-6-oate



6-geranylgeranyl 6'-methyl (9Z)-6,6'-diapocarotene-6,6'-dioate

Figure 3. Diapocarotenoids isolated from annatto seeds.

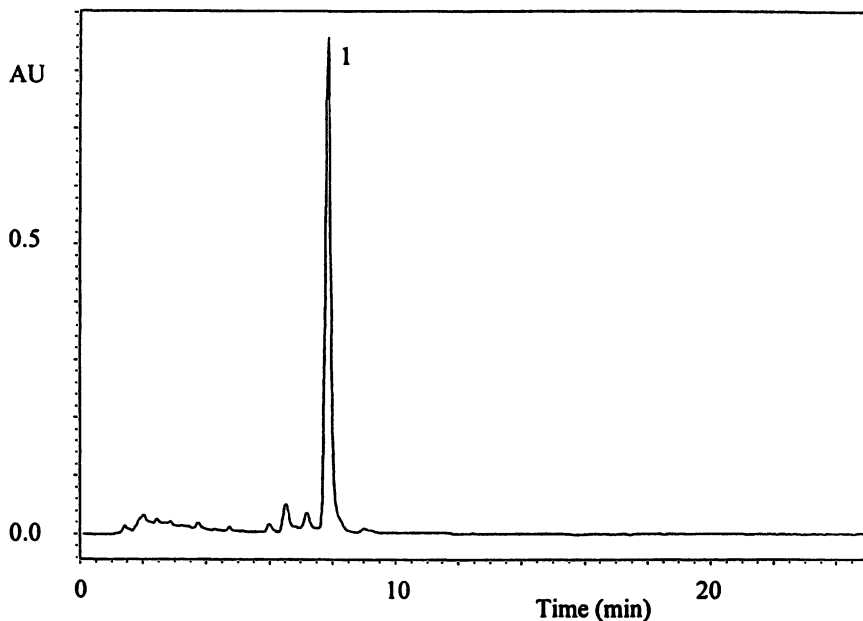


Figure 4. HPLC chromatogram of commercial water soluble annatto preparation. Conditions: C_{18} Spherisorb ($3\ \mu\text{m}$, $4.6 \times 150\ \text{mm}$), acetonitrile/2% aq. acetic acid (65:35) as mobile phase at 1 ml/min. Detection at λ_{max} . Peak 1: norbixin.

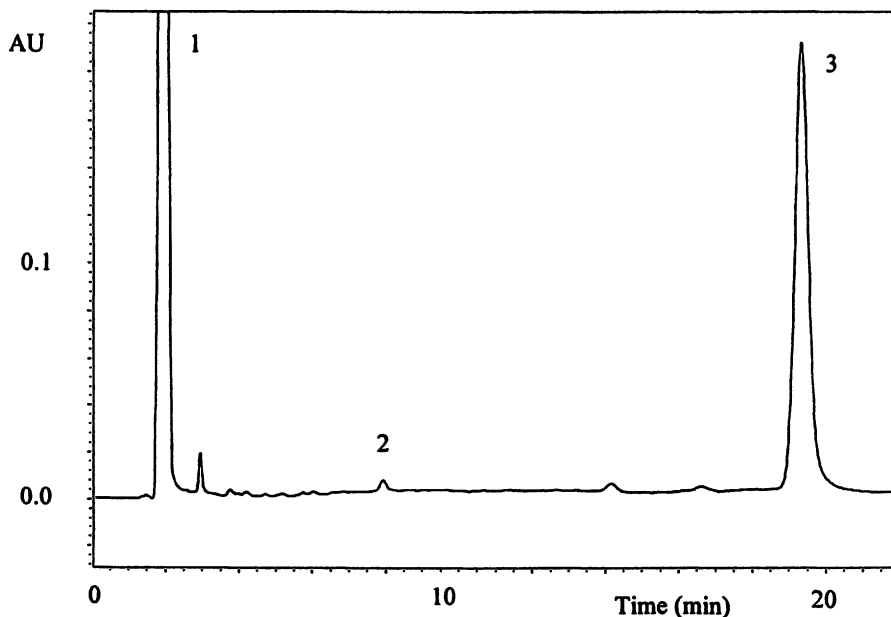


Figure 5. HPLC chromatogram of oil soluble annatto preparation. Conditions: C_{18} Spherisorb ($3\ \mu\text{m}$, $4.6 \times 150\ \text{mm}$), acetonitrile/2% aq. acetic acid (65:35) as mobile phase at 1 ml/min. Detection at λ_{max} . Peak 1: solvent, 2: norbixin, 3: bixin.

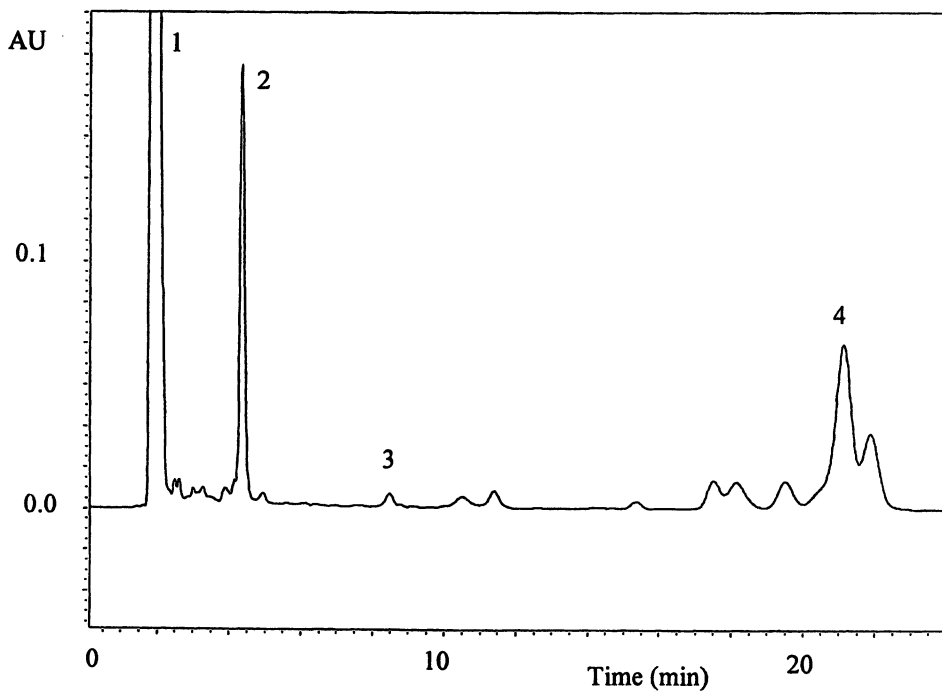


Figure 6. HPLC chromatogram of commercial oil soluble preparation for coloring cheese. Conditions: C_{18} Spherisorb ($3\ \mu\text{m}$, $4.6 \times 150\ \text{mm}$), acetonitrile/2% aq. acetic acid (65:35) as mobile phase at 1 ml/min. Detection at λ_{max} . Peak 1: solvent, 2: yellow compound, 3: norbixin, 4: bixin.

to 4,8-dimethyl-tetradecahexaenedioic acid monomethyl ester, which was previously identified by McKeown (25,26) and Scotter (27).

Conclusions and Future Work

The combined use of different chromatographic systems and modern spectroscopic techniques has allowed the isolation and elucidation of the structures of many new minor carotenoids from annatto seeds. The carotenoid profiles of the annatto preparations, obtained by HPLC, indicated how the colorant was extracted from the seeds.

The development and production of annatto seeds with higher concentrations of bixin is highly desirable, in order to obtain annatto colors that are competitive in price. Alternative formulations of bixin or norbixin should be investigated. Since bixin and related carotenoids are different from the common C₄₀ carotenoids, especially in size and polarity, a more intensive investigation of possible health effects is required.

Because of the recent decrease in the ADI and restrictions for the use of annatto colors, the major producing countries of annatto seeds, mainly developing countries, should make efforts to jointly finance the expensive and long-term toxicological *in vivo* tests required for the reassessment and possible revision of the ADI.

Acknowledgments

The author is grateful to CAPES, FAEP-UNICAMP and FINEP/CNPq/PRONEX for their financial support.

Literature Cited

1. Preston, H. D.; Rickard, M. D. *Food Chem.* **1980**, *5*, 47-56.
2. Lima, L. C. F. *I Simpósio Internacional de Urucum*. Campinas, Brazil, 1991; pp. 199-205.
3. Didriksen, C. *I Simpósio Internacional de Urucum*. Campinas, Brazil, 1991; pp. 209-214.
4. Nakamura, M. *I Simpósio Internacional de Urucum*. Campinas, Brazil, 1991; pp. 217-224.
5. Ministry of Agriculture, Fisheries and Food.. *Food Surveillance Paper 37*; London, 1993.
6. FAO/WHO. *Technical Report Series 445*; Geneve, Switzerland, 1970.
7. FAO/WHO. *Food Additive Series 70.36*; Geneve, Switzerland, 1970.
8. FAO/WHO. *Food Additive Series 7*; Geneve, Switzerland, 1976; 111 pp.
9. FAO/WHO. *Food and Nutrition Paper 25*; Rome, Italy, 1982; pp. 15-22.

10. Freund, P. R.; Washam, C. J.; Maggion, M. *Cereal Foods World* **1988**, *33*, 553-559.
11. Berset, C.; Marty, C. *Lebensm. -Wiss. u. -Technol.* **1986**, *19*, 126-131.
12. Lauro, G. J. *Cereal Foods World* **1991**, *36*, 949-953.
13. McKeown, G. G. *J. Assoc. Off. Agric. Chem.* **1961**, *44*, 347-351.
14. Arima, H. K.; Angelucci, E.; Mattos, S. V. M. *Col. Inst. Tecnol. Alim.* **1980**, *11*, 97-106.
15. Tirimanna, A. S. L. *Mikrochim. Acta* **1981**, *2*, 11-16.
16. Reith, J. F.; Gielen, J. W. *J. Food Sci.* **1971**, *36*, 861-864.
17. Jondiko, I. J. O.; Pattenden, G. *Phytochem.* **1989**, *28*, 3159-3162.
18. Mercadante, A. Z.; Steck, A.; Pfander, H. *J. Agric. Food Chem.* **1997**, *45*, 1050-1054.
19. Mercadante, A. Z.; Steck, A.; Pfander, H. *Phytochem.* **1997**, *46*, 1379-1383.
20. Mercadante, A. Z.; Steck, A.; Pfander, H. *Phytochem.* **1999**, *52*, 135-139.
21. Scotter, M. J.; Thorpe, S. L.; Reynolds, S. L.; Wilson, L. A.; Strutt, P. R. *Food Addit. Contam.* **1994**, *11*, 301-315.
22. Mercadante, A. Z.; Steck, A.; Rodriguez-Amaya, D.; Pfander, H.; Britton, G. *Phytochem.* **1996**, *41*, 1201-1203.
23. Isler, O.; Guex, W.; Rüegg, R.; Ryser, G.; Saucy, G.; Schwieter, U.; Walter, M.; Winterstein, A. *Helv. Chim. Acta* **1959**, *42*, 864-871.
24. Craveiro, A. A.; Oliveira, C. L. A.; Araujo, F. W. L. *Quim. Nova* **1989**, *12*, 297-298.
25. McKeown, G. G. *J. Assoc. Off. Agric. Chem.* **1963**, *46*, 790-796.
26. McKeown, G. G. *J. Assoc. Off. Agric. Chem.* **1965**, *48*, 835-837.
27. Scotter, M. J. *Food Chem.* **1995**, *53*, 177-185.

Chapter 7

Oxidative Transformation of Tea Catechins

Chi-Tang Ho¹, Nanqun Zhu¹, and Tzou-Chi Huang²

¹Department of Food Science, Rutgers University, 65 Dudley Road,
New Brunswick, NJ 08901-8520

²Department of Food Science and Technology, National Pingtung
University of Science and Technology, 912, Pingtung, Taiwan

Tea is one of the most popular beverages consumed worldwide. It is the brew prepared from the leaves of the plant *Camellia sinensis*. Freshly harvested tea leaves require processing to convert them into green, oolong and black teas. The major components in tea are catechins including (-)-epicatechin (EC), (-)-epigallocatechin (EGC), (-)-epicatechin gallate (ECG) and (-)-epigallocatechin gallate (EGCG). During the processing of teas, catechins undergo enzymatic and chemical oxidation leading to oxidized and polymerized polyphenols which contribute to color and taste of tea beverages. The oxidation of catechins is reviewed here. We also reported the novel reaction products isolated from the oxidation of EGCG and EGC with hydrogen peroxide.

Tea refers to the plant *Camellia sinensis*, its leaves, and the extracts and infusions thereof. *Camellia sinensis* was first cultivated in China and then in Japan. With the opening of ocean routes to the East by European traders from the fifteenth to seventeenth centuries, commercial cultivation gradually expanded to Indonesia and then to the Indian subcontinent, including Sri Lanka (1). Tea is now second only to water in worldwide consumption. Annual production of about 1.8 million tons of dried leaf provides world per capita consumption of 40 liters of beverages (2).

Black and green teas are the two main types, defined by their respective manufacturing techniques. Green tea is consumed mostly in Asian countries such as China and Japan, while black tea is more popular in North America and Europe. Oolong tea is an intermediate variant (partially fermented) between green and black tea. Its production is confined to some regions of China including Taiwan.

Major Chemical Changes During Tea Processing

Catechins are the predominate form of flavonoids in fresh tea leaves. Catechins are characterized by di- or trihydroxy group substitution of the B ring and the meta-5,7-dihydroxy substitution of the A ring of the flavonoid structure (Figure 1). The principal catechins presented in fresh tea leaves are (-)-epicatechin (EC), (-)-epigallocatechin (EGC), (-)-epicatechin gallate (ECG) and (-)-epigallocatechin gallate (EGCG) (Figure 2).

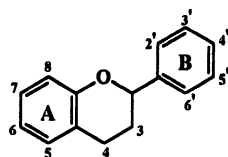
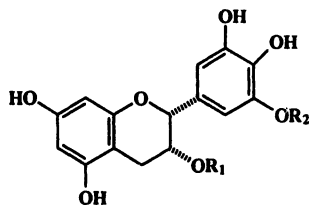


Figure 1. Basic flavonoid structure.



		R ₁	R ₂
(-)-Epicatechin	EC	H	H
(-)-Epicatechin gallate	ECG	Gallate	H
(-)-Epigallocatechin	EGC	H	Gallate
(-)-Epigallocatechin gallate	EGCG	Gallate	Gallate

Figure 2. Major catechins in tea.

The major chemical reaction during tea manufacturing is the oxidative conversion and polymerization of catechins. The oxidative fermentation of catechins in tea results in the development of appropriate flavor and color of oolong and black teas. It will cause a darkening of the leaf and a decrease in astringency. The initial step of fermentation is the oxidation of catechins to reactive quinones catalyzed by polyphenol oxidase. Polyphenol oxidase can use any of the catechins as a substrate to form the complex polyphenolic constituents found in oolong and black teas. The major condensation compounds are theaflavins and thearubigins. The possible oxidation pathways of tea catechins during fermentation can be divided into (a)

pyrogallol-catechol condensation (Figure 3) and (b) pyrogallol-pyrogallol condensation (Figure 4) (3).

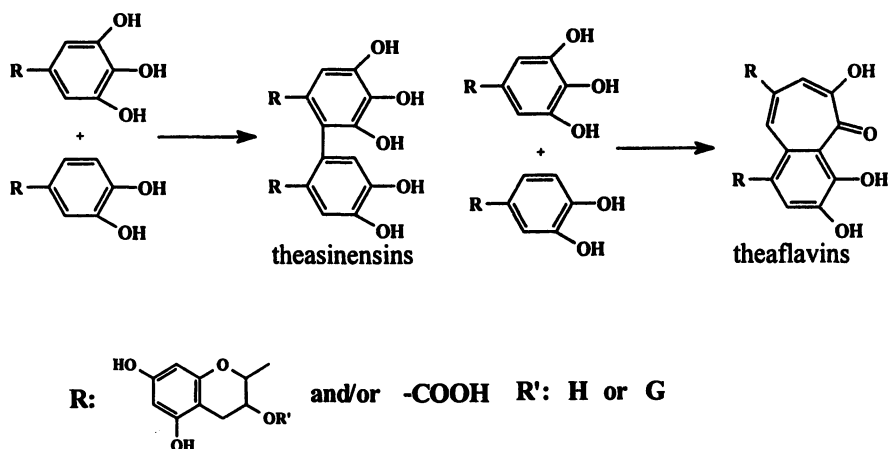
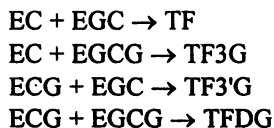


Figure 3. Possible pyrogallol-catechol condensation pathway of tea catechins during fermentation.

Formation of Theaflavins

Theaflavins, which give the characteristic bright orange-red color of black tea, account for 1-2% dry weight of the water extractable fraction. Theaflavins consist of four major components (Figure 5): theaflavin (TF), theaflavin-3-gallate (TF3G), theaflavin-3'-gallate (TF3'G) and theaflavin-3,3'-digallate (TFDG), which are formed by the pair oxidation of catechins as follows (4):



This series of reactions has been established by the use of model tea fermentation systems (5). Total theaflavin content has been shown to have a correlation with the quality of black tea (4).

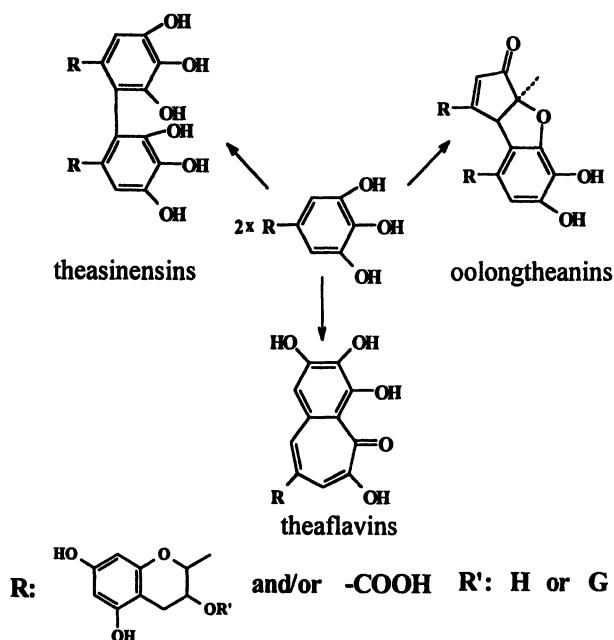
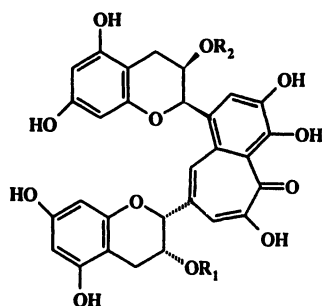


Figure 4. Possible pyrogallol-pyrogallol condensation pathway of tea catechins during fermentation.



		R ₁	R ₂
Theaflavin	TF	H	H
Theaflavin 3-gallate	TF3G	Gallate	H
Theaflavin 3'-gallate	TF3'G	H	Gallate
Theaflavin 3,3'-gallate	TFDG	Gallate	Gallate

Figure 5. Structures of theaflavins.

Formation of Thearubigins

Thearubigins are by far the major components of black tea extract. They constitute as much as 10-20% of the dry weight of black tea. They are the major oxidation product of catechins during fermentation, however, due to the difficulty encountered in their separation, thearubigin chemistry is poorly characterized

Free Radical-Initiated and Chemical Oxidation of Catechins

The first chemical analysis of the products formed from the free radical-initiated oxidation of catechin was reported by Hirose et al. (6). They isolated two products shown in Figure 6 when an ethyl acetate solution of (+)-catechin was irradiated under a fluorescent lamp in the presence of 2,2'-azobis(2-methylpropanenitrile) as a radical initiator. The major step in the formation of products is the radical-initiated oxidative cleavage of the bond between C-3' and C-4' of the B-ring. Figure 7 shows the mechanism for the formation of the product due to intramolecular transformation of the oxidized intermediate.

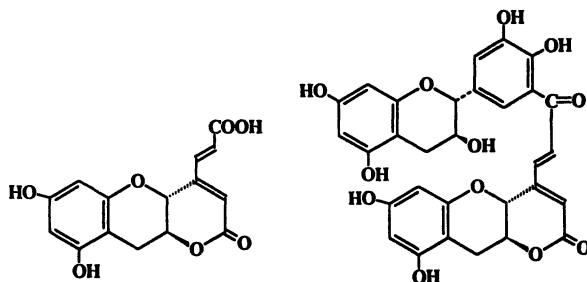


Figure 6. Two compounds identified from peroxy radical-initiated oxidation of (+)-catechin.

Later, when studying the chemical oxidation of ECG with potassium ferricyanide, Wan et al. (7) isolated and elucidated a new type of tea pigment termed theaflavate A (structure shown in Figure 8). This compound was found to have a novel benzotropolone skeleton formed between the B-ring of one ECG molecule and the galloyl ester group of another.

Most recently, the free radical-initiated oxidation of EGCG has been reported (8). Two reaction products (structure shown in Figure 9) of EGCG derived from its reaction with peroxy radicals generated by thermolysis of the initiator 2,2'-azobis(2,4-dimethylvaleronitrile). The products include a seven-membered B-ring anhydride and a novel dimer. Figure 10 shows the probable mechanism for the formation of the seven-membered B-ring anhydride.

All reaction reported so far suggested that the most likely site of oxidation for catechins occurs at the B-ring or the gallate ester moiety.

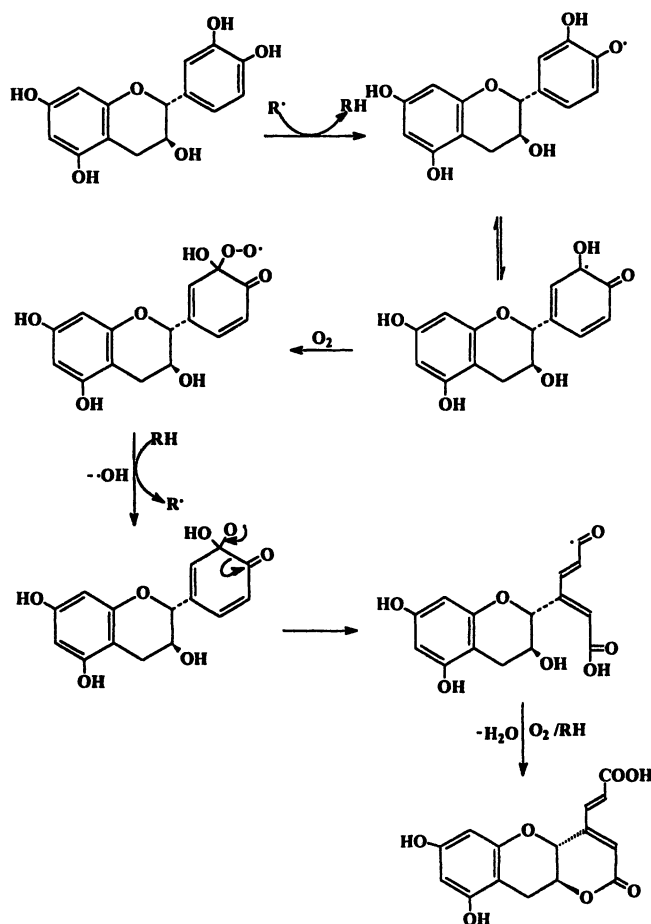


Figure 7. Proposed mechanism for peroxy radical-initiated oxidation of (+)-catechin.

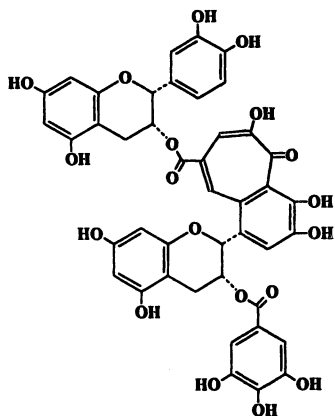


Figure 8. Theaflavate A identified from potassium ferricyanide oxidation of epigallocatechin.

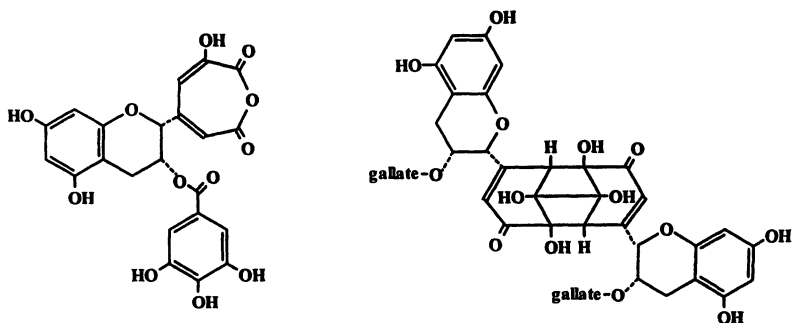


Figure 9. Two compounds identified from peroxy radical-initiated oxidation of epigallocatechin gallate.

Oxidation of EGCG and EGC with H₂O₂

Experimental

200 mg EGCG or EGC and 5 mL water were added to 1 mL H₂O₂ (50%). The reaction mixture was kept at room temperature for 48 hours until no EGCG (EGC) was present as monitored by thin layer chromatography (TLC).

The crude EGCG reaction mixture was loaded directly onto a Sephadex LH-20 column, then the column was eluted with 95% aqueous ethanol and monitored by TLC. Five fractions were collected and evaporated to dryness *in vacuo*. The major products were present in fraction 4. Fraction 4 was purified on a silica gel column using a mixture of ethyl acetate, methanol and water (7:1:1) as eluent. After repeated chromatography, 24 mg of compound 1 and 16 mg of 2 were collected.

Following the same procedure as above, the crude EGC reaction mixture was separated into four fractions. Then fraction 3 was further purified by repeated silica gel chromatography, using ethyl acetate-methanol-water (6.5:1:1) as eluent. After removal of solvent, the combined fractions gave 30 mg of compound 3.

Oxidation products of the reaction of EGCG and EGC with H₂O₂

Compound 1 was isolated as a colorless, amorphous solid. The FAB-MS of 1 showed the molecular ion [M+H]⁺ at m/z 479. Combined with the ¹³C NMR spectral data 1 has a molecular formula of C₂₁H₁₈O₁₃.

The ¹H and ¹³C NMR spectra of 1 were similar to those of EGCG (Valcic et al., 1999) except for those of the A-ring. The two signals at δ 6.47 (2H, s) and δ 7.00 (2H, s) were assigned to H-2', H-6' of ring-B and H-2'', H-6'' of the galloyl moiety. The two broad singlets at δ 5.06 and 5.50, together with the signal δ 2.66 (1H, brd, J=17.6 Hz) and δ 2.82 (1H, dd, J=4.0, 17.6 Hz), were very close to protons H-2, H-3, H-4a and H-4b, respectively of ring C of EGCG (8). Supported by HMQC, HMBC, ¹H-¹H COSY and NOESY, correlations were observed and this data proves that ring-B, ring-C and the galloyl moiety of 1 are intact and the changes in the molecule had only occurred in ring-A of EGCG.

For the modified A-ring, the ¹H NMR spectrum exhibited two signals at δ 3.64 (1H, d, J=16.0 Hz) and δ 3.86 (1H, d, J=16.0 Hz), which had HMQC correlations with C-8 at δ 41.2. In addition, the ¹³C NMR spectrum indicates two carbonyl carbons (δ 171.9 and 175.0). The chemical shifts of two carbons suggests the presence of two acid groups, which were proved by the FAB-MS data. More over, HMBC correlations were observed between H-8 with C-5, C-7, C-9 and H-4 with C-6, thus we assigned the structure of 1 as shown in Figure 11.

Compound 2 was isolated as a colorless amorphous substance. As another oxidized product of EGCG, 2 was found to have a molecular weight of 464 (FAB-MS: m/z 465 [M+H]⁺). This, together with the ¹³C NMR spectrum of 2, led to a

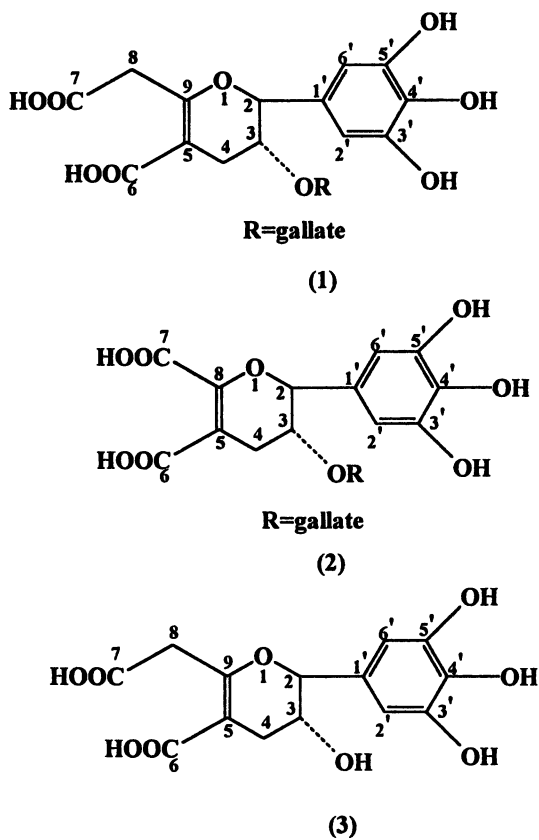


Figure 11. Three novel compounds identified from the H₂O₂ oxidation of epigallocatechin gallate and epigallocatechin

formula of $C_{20}H_{16}O_{13}$. Compared with the 1H and ^{13}C NMR spectra of **1**, the only significant difference is the disappearance of H-8 and C-8 of **1**. In addition, the ^{13}C NMR shift of C-7 was decreased to δ 169.8 because of conjugation with the double bond. Apparently, the methylene group was lost due to oxidation. Therefore, the structure of **2** was elucidated as shown in Figure 11.

Compound **3** was isolated as a colorless amorphous substance with the formula of $C_{14}H_{14}O_9$. The NMR and FAB-MS data are in good agreement with those of **1** except for the galloyl moiety. It is apparent that the difference between **1** and **3** is the disappearance of the galloyl moiety. Because of this, some small change occurs at the chemical shifts of H-2, H-3 and H-4 or C-2, C-3 and C-4. Thus, the structure of **3** was identified as shown in Figure 11.

The isolation and identification of products **1**, **2** and **3** are of great interest. It was previously considered that ring-A is very insensitive to oxidation and, therefore, unlikely to participate directly in the antioxidant reaction. It has been reported (9) that the phenoxyl radical of EGC exhibits a one-electron reduction potential of 0.43 V, whereas that of methyl gallate exhibits a one-electron reduction potential of 0.56 V. The work of Valcic et al. (8) confirmed that the B ring rather than the galloyl moiety, is the principal site of antioxidant in EGCG. In addition, Nanjo et al. (10) and Wan et al. (7) suggested that the galloyl moiety of EGCG and ECG were involved in oxidative reactions. However, there are no reports on the reactions of A-ring. Although further work is needed to understand the mechanism of this oxidation process, the observation that ring-A can be oxidized to form acid provides an unambiguous proof that oxidation can occur at A-ring.

References

1. Forrest, D. *The World Trade: A Survey of the Production, Distribution and Consumption of Tea*; Woodhead-faulkner, Ltd.: Cambridge, UK, 1985.
2. Balentine, D. A. In *Caffeine*; Spiller, G. A., Ed.; CRC Press: Boca Raton, FL, 1998; pp. 35-72.
3. Hashimoto, F.; Nonaka, G.; Nishioka, I. *Chem. Pharm. Bull.* **1988**, *36*, 1676-1684.
4. Yamanishi, T. *Food Rev. Internat.* **1995**, *11*, 457-471.
5. Co, H.; Sanderson, G. W. *J. Food Sci.* **1970**, *35*, 160-164.
6. Hirose, Y.; Yamaoka, H.; Nakayama, M. *J. Amer. Oil Chem. Soc.* **1991**, *68*, 131-135.
7. Wan, X.; Nursten, H. E.; Cai Y.; Davis, A. L.; Wilkins, J. P. G.; Davies, A. P. *J. Sci. Food Agric.* **1997**, *74*, 401-408.
8. Valcic, S.; Muders, A.; Jacobsen, N. E.; Liebler, D. C.; Timmermann, B. N. *Chem. Res. Toxicology.* **1999**, *12*, 382-386.
9. Jovanovic, S. V.; Steenken, S.; Tomic, M.; Marjanovic, B.; Simic, M. G. *J. Am. Chem. Soc.* **1994**, *116*, 4846-4851.
10. Nanjo, F.; Goto, K.; Seto, R.; Suzuki, M.; Hara, Y. *Free Radical Biol. Med.* **1996**, *21*, 895-902.

Chapter 8

Green Pigment Formed by the Reaction of Chlorogenic Acid (or Caffeic Acid Esters) with a Primary Amino Compound during Food Processing

Mitsuo Namiki^{1,3}, Goro Yabuta², and Yukimichi Koizumi²

¹Nagoya University, Nagoya 464-8601, Japan

²Department of Fermentation Science, Tokyo University of Agriculture, Setagayaku, Tokyo 156-8502, Japan

A marked greening observed in some foods, including sweet potato and burdock, during food processing was shown to be due to green pigment formation by the condensation reaction of two molecules of chlorogenic acid or caffeic acid ester with one molecule of a primary amino compound in air and alkali. The reduced and acetylated product of the green pigment was identified as a novel triphenol benzacridine derivative, and the yellowish ethanol solution of this product immediately turned green upon addition of butylamine or diluted alkali. Therefore, the green pigment was assumed to be a oxidized quinone type product of triphenol benzacridine. The structure was supported by comparison of the measured absorption spectra with those calculated theoretically. ESR studies indicated the presence of different types of free radical products in the green reaction mixture; one was determined to be a free radical product of the caffeate, and the others were assumed to be those of further oxidized green products. The formation mechanism of the benzacridine and oxidation products are proposed.

A marked greening is observed in some vegetables, such as sweet potato, burdock and others, during some types of food processing and cooking, e.g., steamed bread containing small cubes of sweet potato which turned bluish-green after

³Current address: Meitoku Yashirodai 2-175, Nagoya 465-0092, Japan.

standing overnight. This greening was shown to be prominent in the case of damaged or infected sweet potato, suggesting that it was enhanced by the oxidation of a polyphenol component such as chlorogenic acid by induced polyphenol oxidase activity. Greening was also prominent under alkaline conditions and in the presence of an amino acid (1,2). Greening of burdock during deep fat frying to make tempura is also attributed to oxidation of its polyphenol component, chlorogenic acid (3,4). Greening is sometimes observed during alkali extraction of protein from sunflower meal and again shown to be due to chlorogenic acid oxidation (5,6). Chlorogenic acid occurs widely in fruit, leaves and other tissues of dicotyledonous plants, such as coffee bean and potato. Browning and sometimes bluish-greening caused by chlorogenic acid oxidation have long been noted, and its name originates in the fact that this component turned green when plant tissue was treated with ammonia (7-9).

This greening is very interesting because the color green is rare in natural food systems, except for chlorophyll and its derivatives. Moreover, the fact that the greening developed very easily in air at room temperature is considered to be due to some oxidation-reduction reaction involving a phenol compound and active oxygen, probably related to the antioxidative and other physiological effects of polyphenols. There have been several studies on the conditions under which this greening occurred (10-14) but the chemical structure of the green pigment is not yet known.

This study was undertaken to elucidate the chemical properties and structure of this green pigment and related products.

Reaction Conditions of Greening

From studies on the greening of sweet potato and burdock, a major contribution of chlorogenic acid was demonstrated, but oxidation of chlorogenic acid alone in alkali produced only browning, and greening developed only when a similar reaction was performed with the addition of amino acid such as glycine and alanine. Thus, the effects of various phenolic compounds and amino compounds on the development of greening were examined. The necessary structures of the reactants for the greening reaction are as follows.

Polyphenol

Chlorogenic acid is the quinic acid ester of caffeic acid, and similar greening was also produced by caffeic acid esters such as methyl, ethyl, and *n*-butyl esters, but isopropyl ester gave a somewhat bluish-green. Caffeic acid amide also produced greening (2). However, free caffeic acid produced no greening. Ferulic acid, isoferulic acid and *p*-coumaric acid and their esters gave no greening. Dehydrocaffeic acid ester and protocatechuic acid ester also proved negative for greening.

It was then demonstrated that an *ortho* phenol, like caffeic acid, with a double bond in the side chain and a carbonyl group in carboxylic acid ester, are necessary for the greening.

Amino compound

A primary amino group such as an amino acid or an alkyl amine is needed, while secondary and tertiary amines and ammonia were negative for greening and mostly showed only browning. However, even among the α -amino acids, those containing a β -hydroxyl group, i.e., serine and threonine, were negative for greening, although the reason for this is not yet known. Proline, cyclic amino acids and cysteine were also negative for greening. The green color showed a somewhat different hue depending on the structure of the amino compound and also on the ester of caffeic acid, varying from green to deep bluish-green or pale green. Figure 1 shows the visible absorption spectra of different amino compound reaction systems. The green color intensity followed the order *n*-butylamine > Gly, Ala > His > Phe >> Glu. λ_{\max} (nm) at pH 9.5; His (695), Phe (692), α -Ala (682), Gly (678), *n*-Butylamine (673).

Other reaction conditions of greening

Usually, the reaction was performed in aqueous or water-ethanol solution with 10 or 20 mM each of two reactants under continuous air bubbling, because the reaction requires oxygen or air. As shown in Figure 2, the greening occurred very slowly at pH 7.0 but, at alkaline pH, it developed immediately after aeration was started and increased with reaction time to a maximum at about 2-3 h. The optimum pH of greening was pH 9.0-9.5. At higher pH, such as 10.5, the reaction occurred more rapidly, but did not increase in intensity and the resulting color was blue-green. The greening reaction occurred even at room temperature with the optimum being around 50°C.

Some Properties of the Green Pigment

The green reaction mixture contained various products other than the green pigment, so isolation and purification of the green pigment was undertaken to investigate its chemical properties. The green pigment that developed in the food system usually formed from chlorogenic acid with an amino acid such as α -alanine; it was water soluble and not extractable with ordinary hydrophobic organic solvents, but the majority of the pigment formed in systems, such as those containing isopropyl caffeate and *n*-butyl-amine, could be extracted with solvents such as ethyl acetate, or chloroform. However, in these cases, the green color was not such a definite green as when chlorogenic acid and amino acid were used, but a pale blue-

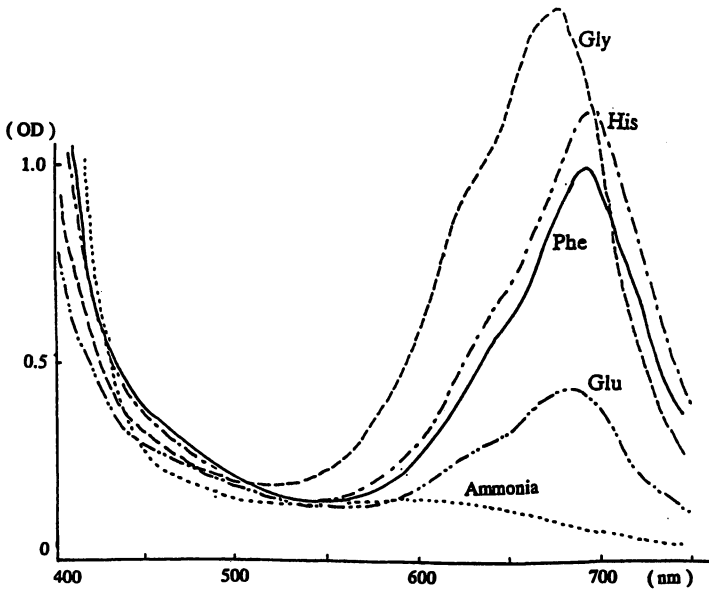


Figure 1. Visible spectra of various reaction mixtures *Et-caffeate* + amino acid (10 mM each), at pH 9.5, 50, 2 hr. (diluted 0.3 ml/4.0 ml dist. water).

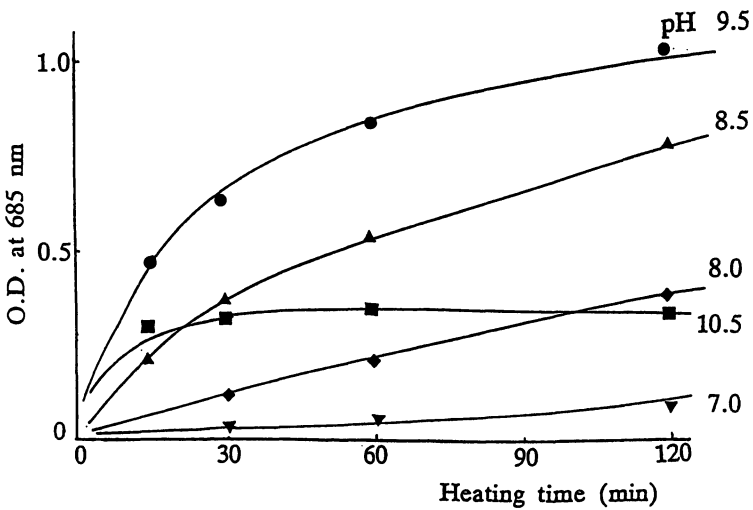


Figure 2. Effect of pH on formation of greening (*Et-caffeate* + α -alanine, 10 mM each, at 50°C).

green. Moreover, these pale blue-green extracts were not so well suited to further purification.

The green pigment appeared to be a kind of amphoteric compound and precipitated at about pH 4.0, in the case of the ethyl caffeate-*n*-butylamine system, but the color of the mixture turned from green to blue-green in the precipitate. The precipitate was insoluble in ether but soluble in ethanol, so precipitation is useful to remove unreacted materials and serve as a first-step treatment for purification of the green pigment.

Isolation and purification of the green pigment were tried by various chromatographic methods. However, the green pigment is not very stable and therefore isolation as the green pigment itself is not easy. For example, the green pigment precipitate obtained at pH 4 usually gave a bluish spot with tailing by silica gel TLC, even upon re-chromatography, and sometimes seemed to separate into blue and yellowish bands on column chromatography with silica gel. On column chromatography with Sephadex XAD-7, the green reaction mixture of ethyl caffeate with alanine first gave brown elutes with 1 % ammonia-water, so it probably contained oxidized phenolic products and unreacted materials. The second fraction, with ammonia-water: methanol (8:2), had a marked green color with λ_{\max} 685 nm, and the third fraction, with methanol alone, showed a definite blue color with λ_{\max} 613 nm.

As shown in Figure 3, the green color fraction of the reaction mixture varied with the pH of the mixture. It turned red violet at acidic pH below 3.0 (λ_{\max} at about 520 nm); this changed to yellow after about 30 min. This yellow solution reverted to the original green when the acidified solution was immediately returned to an alkaline pH of around 9.0. However, the green color was not restored but turned blue (λ_{\max} 596 nm) after standing over 2 h at pH 1-2. This indicates that some irreversible changes in the molecular structure of the green pigment occurred at acidic pH.

Reduction Product of the Green Pigment

The green mixture could be reduced to a yellow mixture by ascorbic acid or NaBH_4 , and most of the reduced products could be extracted by ether. Thus, we tried to isolate the reduction product of the green pigment in order to determine its structure employing the following method. The green reaction mixture prepared from ethyl caffeate and *n*-butylamine at pH 9.5 was adjusted to pH 4.0 with dilute HCl, and the separated green precipitate was washed with ether and dissolved in methanol-dilute HCl (pH 1.0). The wine-red solution was immediately reduced by addition of ascorbic acid until a yellow solution was obtained. Ether extracts of the reduced yellow solution gave several bands on silica gel TLC with ether. Among these, one yellow band (R_f 0.7) giving yellow fluorescence on viewing while under UV light (254 nm), readily turned green when the TLC plate was exposed to air. This color change occurred more rapidly on spraying with diluted benzoquinone solution, whereupon the yellow color turned green, then blue. The color changed back to green then yellow on spraying with ascorbic acid solution. These

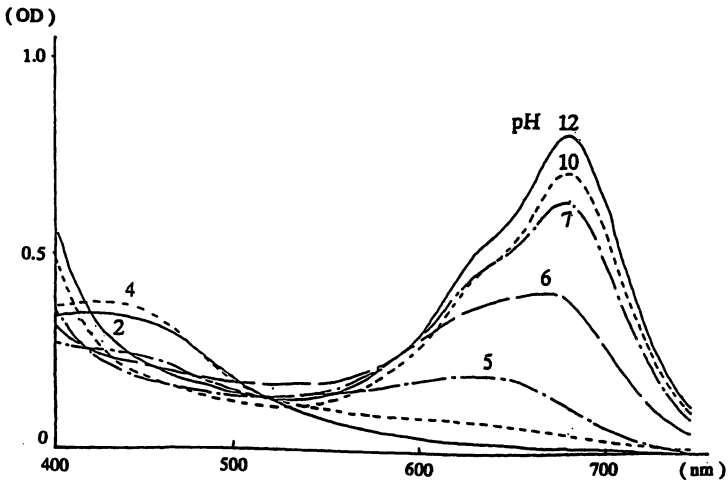


Figure 3. Visible spectra of green reaction mixture at different pH (after 30 min) (Et-caffeate + α -alanine).

observations indicate that the fluorescent yellow reduction product is derived from the green pigment in the green reaction mixture, and that it may be a type of polyphenol product that is very easily oxidized in air to give the original green pigment. However, the reduction product was so easily oxidized that it was necessary to protect it against oxidation by the presence of ascorbic acid in solution. It was difficult to employ conventional chromatography for further purification.

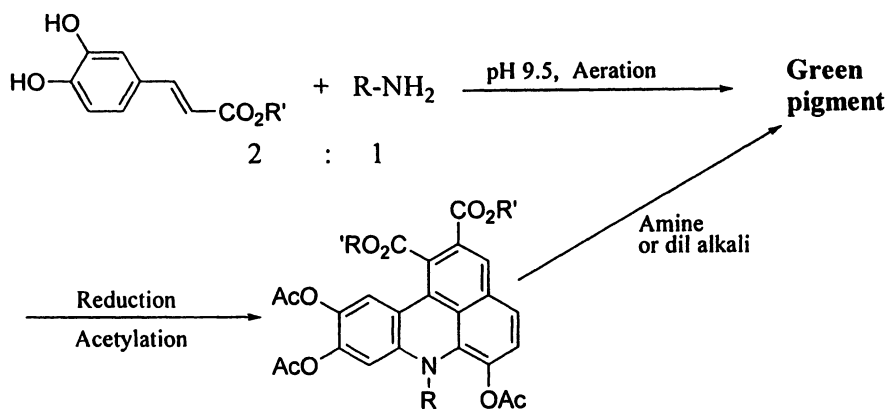
Isolation and Identification of the Reduced and Acetylated Green Pigment

Further purification of the pigment was performed using a more stable acetyl derivative of the reduction product of the green pigment according to the following procedure. The ether extract of the reduced yellow solution was dried and treated with acetic anhydride and triethylamine overnight at room temperature. The crude yellowish products thus obtained were chromatographed on Lichro Prep RP-18 column eluted with ethanol-water (6:4 to 9:1). The crystalline products obtained in the earlier fractions of the chromatography gave white plates (m.pt. 77-8°C) on recrystallization from ethanol-water, and this product was identified as the acetate of the caffeate starting material from the physicochemical data. The other crystalline products from the later fractions gave yellow needles, m.pt. 188°C, on recrystallization with ethanol-water.

Chemical Properties of the Reduced and Acetylated Green Pigment

The yellow needles obtained from the reduced and acetylated product of the reaction mixture of ethyl caffeate and *n*-butylamine provided the following analytical data:

Yellow needles, m.pt. 188°C, λ_{\max} (EtOH) 406, 323, 245 nm. MS (JEOL, AX-505HA). *m/z* at 591 (M^+ , $C_{32}H_{33}O_{10}N$), 549(M-42), 507(M-84), 450(M-142), 408(M-183), NMR (JEOL, α -400 δ ($CDCl_3$, TMS) at 0.76(3H, t, $J=7.3$), 1.15(2H, m), 1.34(3H, t, $J=7.1$), 1.41(3H, t, $J=7.1$), 1.58(2H, m), 2.28, 2.30, 2.38(Ac x3), 3.94(2H, $J=7.2$), 4.40(4H, q, $J=7.1$), 7.05(1H, d, $J=7.2$), 7.47(1H, s), 8.11(1H, s), 8.7(1H, d, $J=7.2$) (15). These data indicate the presence of three acetyl groups, two ethyl esters, one *n*-butyl group, vicinal aromatic hydrogens and three aromatic hydrogens, suggesting that the product is a benzacridine structure having three acetoxy groups. For determination of its structure by X-ray crystallographic analysis, the crystalline products isolated from the reaction of ethyl caffeate and *n*-butylamine resulted in needles that were too small for the analysis, while those from methyl caffeate and *n*-butylamine gave sufficiently large orange yellow plates, m.pt. 170°C, though the yield was less than that in the ethyl caffeate system. The results obtained with these plates indicated that the structure was dimethyl-7-butyl-6,9,10-triacetoxylbenz[k,l]acridine-1,2-dicarboxylate, as shown in Figure 4 (15).



Dialkyl-7-alkyl-6,9,10-triacetoxybenz[k,l]acridine-1,2-dicarboxylate

Figure 4. Formation of reduced and acetylated green pigment from caffeic acid ester and a primary amino compound.

Silica gel TLC of the reduced and acetylated crystalline products gave one spot having a characteristic yellow fluorescence under radiation at 254 nm, and this spot turned green after standing overnight in air. The ethanol solution of the yellow crystalline product also turned green upon the addition of amines, such as *n*-butylamine and triethylamine, and dilute alkali such as dilute NaOH and Na₂CO₃/NaHCO₃ buffer. These observations indicate that the yellow crystalline product was easily deacetylated by amine or weak alkali, and the phenolic product thus obtained was readily oxidized to the green pigment.

Thus, it was demonstrated that the condensation reaction of two molecules of the caffeate and one molecule of an amino compound produced the green pigment, and its reduced and acetylated product was identified as a novel benzacridine derivative (Figure 4). Except for some pyrolytic products (16,17), very few benzacridine derivatives are known. The derivative in the present study is the first one known to be formed from common plant components under common food processing conditions, e.g., baking and deep fat frying

The Blue Pigment of the Reaction Mixture

As mentioned above, chromatography of the green reaction mixture of ethyl caffeate and alanine gave a blue fraction, showing an absorption maximum at around 613 nm. The presence of such a blue fraction, though minor, was also observed in other reaction systems. The blue color turned yellow in acidic solution, and it reverted to its original blue color when the pH was returned to alkaline after it was left to stand overnight. The blue product was also observed on TLC of the reduced yellow product mentioned above. The yellow spot, due to the reduced product, turned green and then blue after standing in air or on spraying with benzoquinone solution. The color changed back to green and then to yellow upon spraying with ascorbic acid solution. Moreover, it was noted that when the green solution was acidified and stood for several hours to give a yellow solution, and then returned to alkaline pH, the color changed to blue instead of the original green.

The blue products thus observed under different conditions were not necessarily the same compound; their chemical structures have not yet been identified. However, there is certainly a reversible oxidation-reduction relationship between yellow, green and blue products of the identified benzacridine derivative.

Possible Oxidation Steps of the Reduced Product of the Green Pigment

Based on the above results, it is proposed that the structures of the green pigment and its related products are oxidized derivatives of the identified reduced benzacridine product. The yellow reduction product has three phenolic hydroxy groups and

dissociates in alkaline solution; this form will easily be oxidized stepwise in air to give free radical and quinone-type products.

Figure 5 shows the three-step oxidation pathway of the reduction product of the green compound. The most probable structures among several possible alternatives, are given at each oxidation step. The first oxidation step gives one electron-oxidized free radical forms such as **Ia-Ic**. These may be readily oxidized to give two-electron-oxidized quinone type products, **IIa** and **IIb**, which may be the green pigment (see following section). The oxidized forms **IIIa** and **IIIb** produced in the third step, may correspond to the blue pigment.

Absorption Spectra of the Benzacridine Compounds Calculated by the PPP Method

Visible absorption spectra and color of the probable structures of oxidized products, including their anionized and cationized forms, were calculated by the PPP method, an advanced molecular orbital method proposed by Pariser, Parr and Pople (18). The results are summarized in Figure 6. The numbers under the structure indicate calculated main absorption peaks and their oscillator strength, and the colors in parentheses indicate those assumed from the calculated values (19).

It was estimated that **IIa'**, the dissociated form of the two-step oxidized compound (**IIa** in Figure 5) showed absorption at 669.9/ 0.462 (nm/f), which means that this molecule showed a blue-green to green color and corresponded well to the measured λ_{max} of the reaction mixture of ethyl caffeate and amine. The calculated value for **IIIb**, the three-step oxidization product, was 666.4/0.102, suggesting a greenish-blue color, corresponding to the blue product in the reaction mixture. As has been described, the green pigment gave a wine-red or pink color at *ca.* pH 1-2, coinciding with the magenta color estimated from the calculated value for structure **IIb+**. The yellow color of the reduction product of the green pigment also corresponded well to the value for the structure of RG. These data strongly support the possible structures of the green pigment, blue pigment, and yellow reduction product.

Possibility of a Quinhydrone-Type Charge Transfer Complex

As noted above, isolation of the green pigment seemed difficult since it sometimes separated into blue and yellow bands on TLC and column chromatography, suggesting that it might exist as a complex compound. The formation of a charge transfer complex, i.e., quinhydrone, between hydroquinone (HQ) and benzoquinone (BQ), brought about a marked bathochromic shift, to give a reddish-brown color, from either of the two colorless solutions. For the formation of

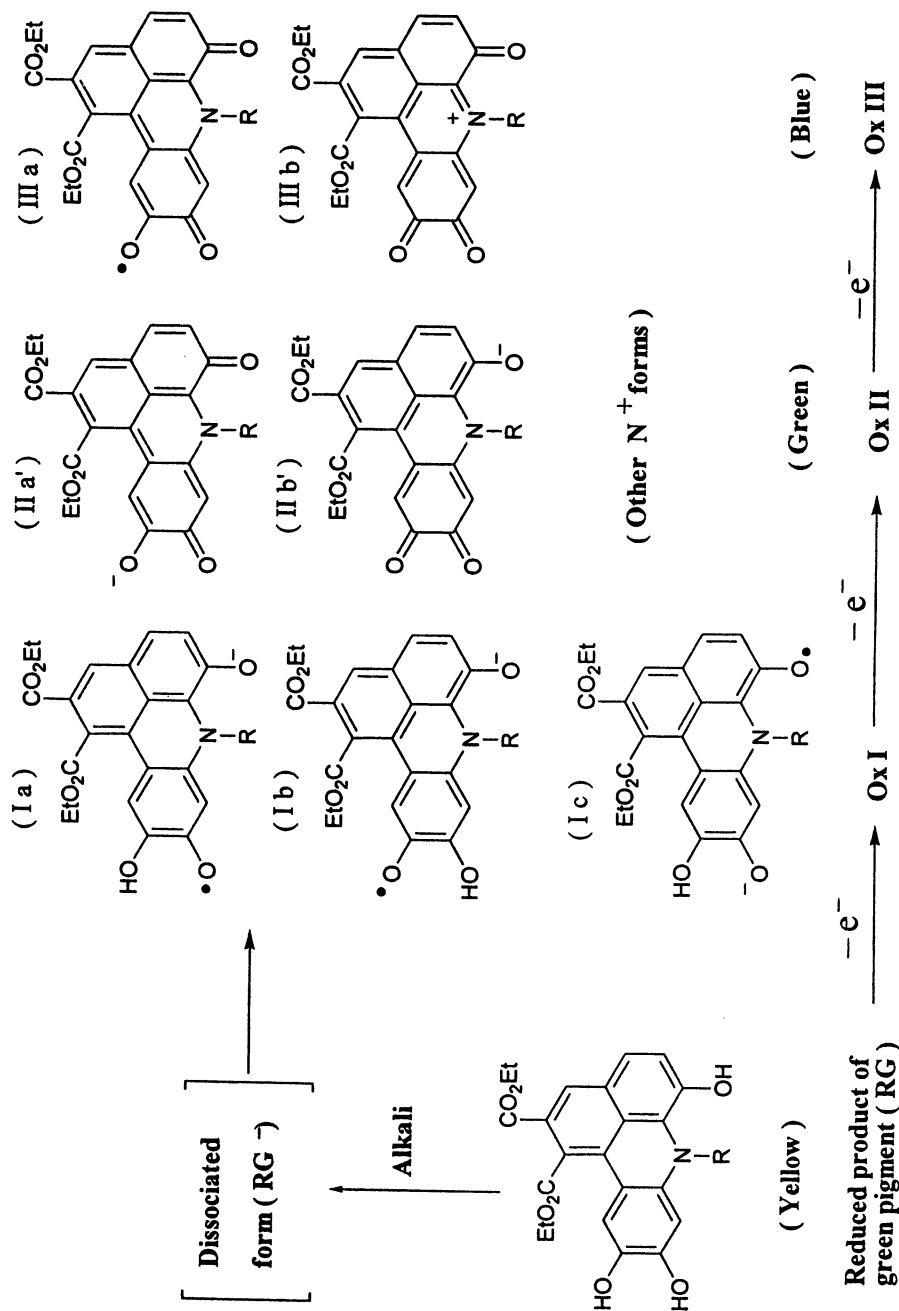
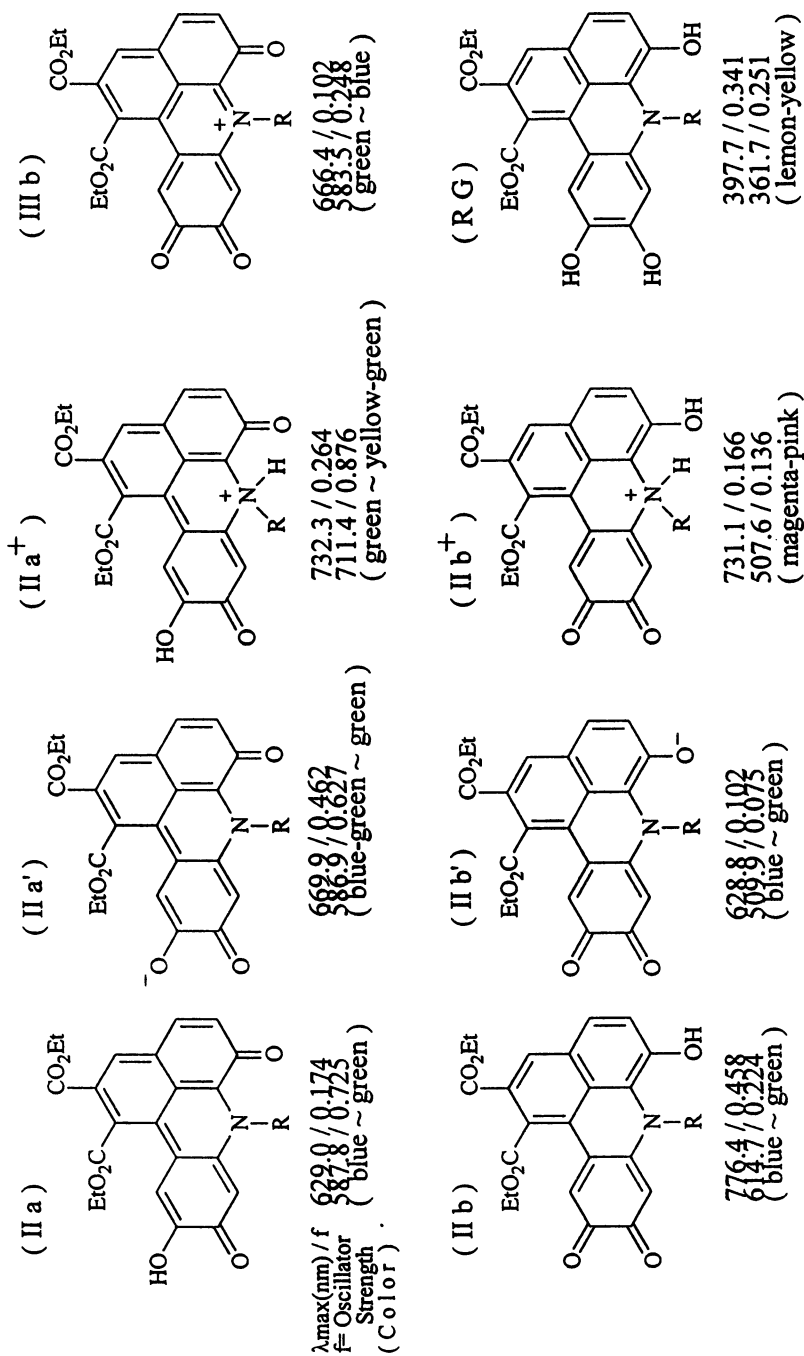


Figure 5. Possible oxidation steps of the reduced product of the green pigment.



Observed spectra (λ_{max} , nm)
 Ethyl caffeate + [Butyl amine (673); Gly (678); Ala (682); Phe (692)]
Figure 6. Visible absorption spectra calculated by PPP method.

such a quinhydrone type complex, the charge transfer energy (the difference between the ionization potential of the donor molecule and the electron affinity of the acceptor molecule) must be *ca.* 2.0 eV or less. We next examined the possibility of the formation of such a quinhydrone-type complex between two of the molecular structures among those listed in Figure 5, based on the charge transfer energy calculated by the molecular orbital method (19).

As shown in Table 1, five pairs of molecular structures can produce a quinhydrone type complex. Therefore, it seems possible that the green pigment in the reaction mixture may exist as any one of these quinhydrone-type complexes.

Table I. Possible Quinhydrone Type Charge Transfer Complexes

<i>Ionic potential of Electron donor -ε(D) homo / eV</i>	<i>Electron affinity of electron acceptor -ε(A) lumo / eV</i>	<i>ΔεCT / eV</i>
hydroquinone [HQ] 7.49	<i>p</i> -benzoquinone [Q] 5.40	2.09
[RG] 7.54	[III b] 5.77	1.77
[II a] 6.87	[III b] 5.77	1.10
[RG] 7.54	[II a] 6.87	0.67
[II a'] 6.78	[III b] 5.77	1.01
[II b'] 7.52	[III b] 5.77	1.75



Structure of each [] symbol : see Figure 5.

ESR Studies on the Greening Reaction Pathways

The formation of the green pigment is essentially oxidation of a polyphenol compound followed by condensation with an amino compound. Therefore, it is reasonable to assume the existence of free radical intermediates in the reaction mixture. We tried to measure ESR spectra directly on the reaction mixture of ethyl caffeate with various amines at room temperature using a JEOL, JES-FA200 ESR

spectrometer. An ESR spectrum was detected early in the greening reaction in most of the systems. It possessed a clear hyperfine pattern split into seven peaks. It could be interpreted as shown in Figure 7(A) and it indicated four protons. This fairly stable ESR spectrum observed from very early on in the reaction process was determined to be due to the oxidized free radical product of ethyl caffeate in alkaline solution using an authentic sample of the caffeate.

We were also able to detect another type of hyperfine ESR spectrum later in the reaction, which was clearly different from that of the phenolic starting material and varied according to the amine used. For example, for *n*-butylamine, we observed a spectrum split into 12 peaks. Although sometimes the spectrum was contaminated by that of ethyl caffeate. To measure the ESR spectrum of the free radicals related to the green pigment more accurately, we examined the fraction of the reduced green products isolated by chromatography (as described above from the reaction systems of ethyl caffeate with various amino compounds).

The reduced and fractionated yellow pigment showed no ESR signal. It easily turned green when left standing in air and at that stage there was no clear signal, but when a small amount of alkali was added, a characteristic hyperfine ESR spectrum was observed for each reaction system. The spectra, in the case of ethyl caffeate and α -alanine, and analysis of its hyperfine structure based on the assumed free radical structure are, shown in Figure 7(B). The radical products detected in the green-blue solution were assumed to be the three-step oxidized form, IIIa in Figure 5.

Formation Mechanism of the Green Pigment and Related Products

The fact that the green pigment, a novel benzacridine derivative, formed so easily from Et-caffeate and amine under aeration is interesting, not only from the viewpoint of food chemistry, but also from that of organic synthesis. Based on various data on the greening reaction conditions, properties of green, blue and yellow pigments, and visible and ESR spectra, we speculated on the formation mechanism of the green pigment. Among various possible pathways considered for the formation process, Figure 8 shows the scheme proposed taking into account the important role of the free radical intermediate. The fairly stable free radicals of caffeate demonstrated by ESR may dimerize to form polymerized brown products if they exist alone, but the presence of an amino compound led to the formation of a novel benzacridine ring structure, and then the green pigment. Figure 9 shows one other pathway, where the *ortho*-quinoid product of caffeate reacts first with an amino compound to give the Schiff base product which undergoes condensation with another quinoid product. This is followed by an intramolecular Diels-Alder type cyclization to give the benzacridine ring structure.

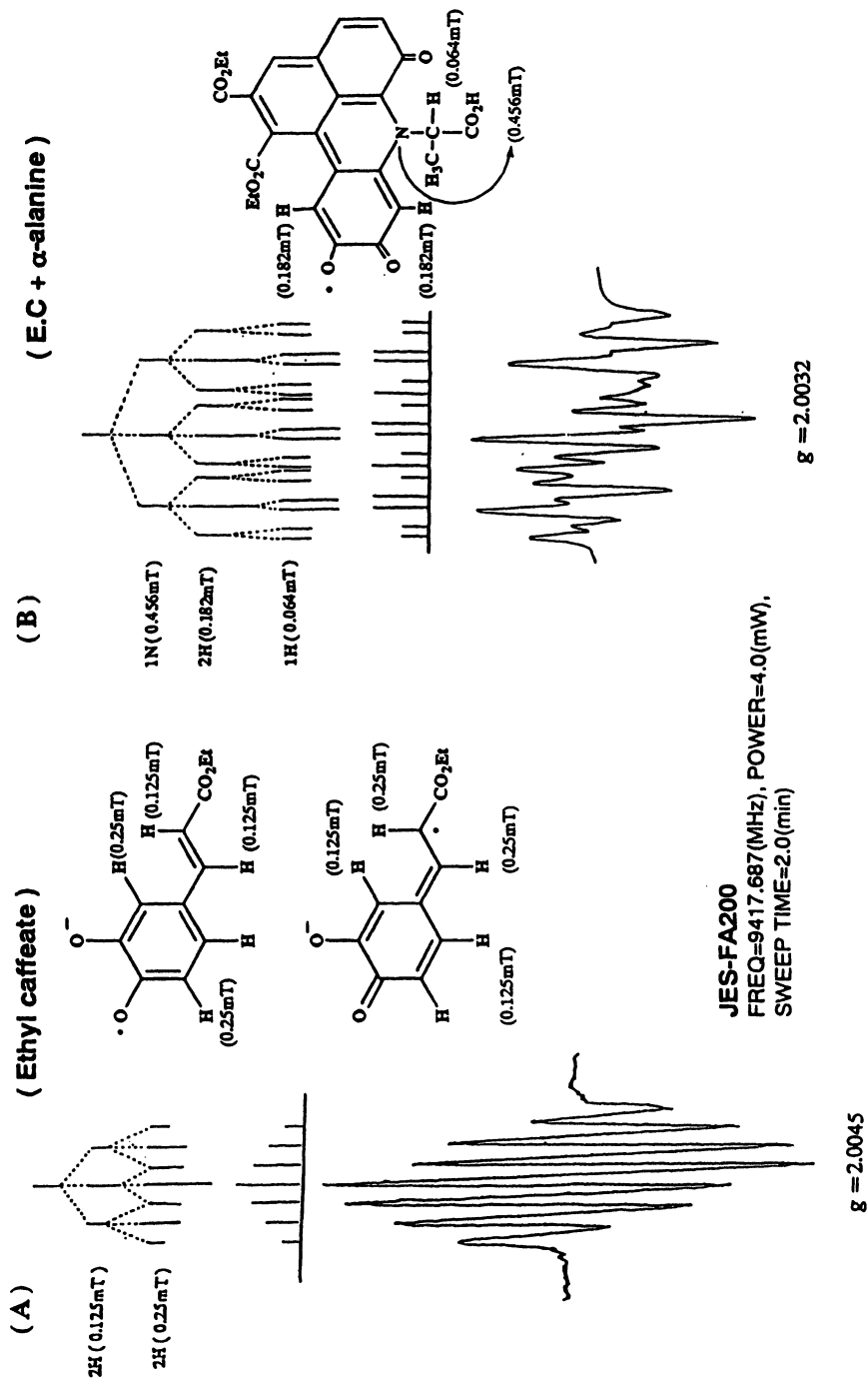


Figure 7. ESR spectra of ethyl caffeate (A) and ethyl caffeate + α -alanine (B) in alkaline solution with aeration.

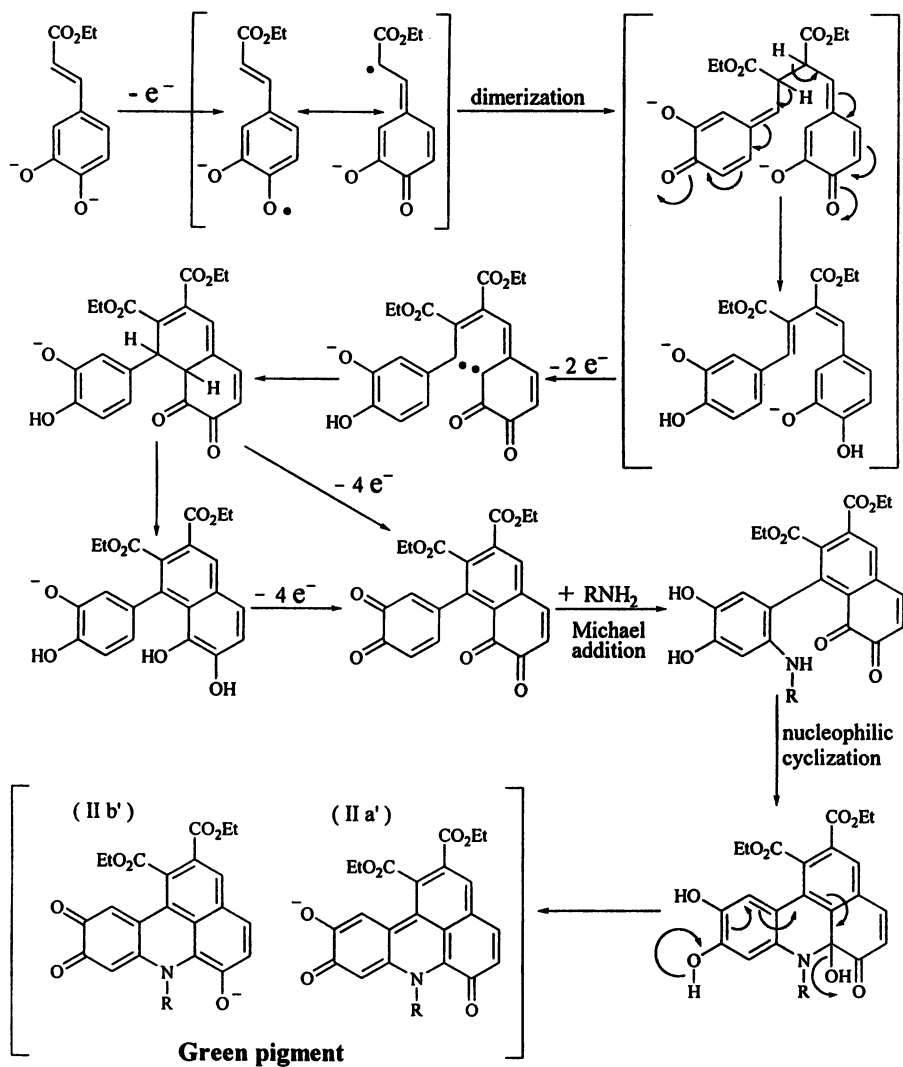


Figure 8. Mechanism of green pigment formation from Et-caffeate and amino compound (Scheme A).

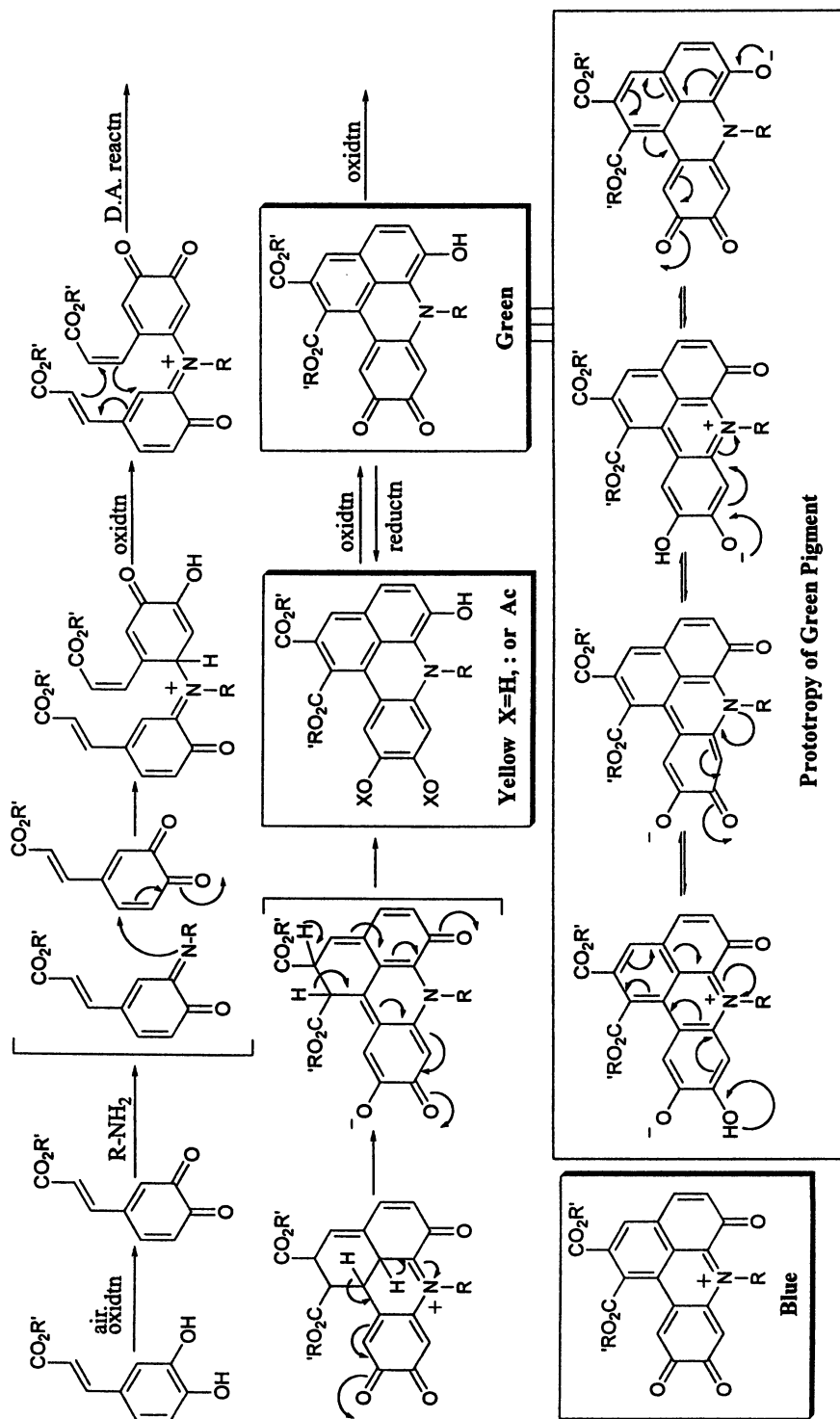


Figure 9. Mechanism of green pigment formation from *Et*-caffeate and amino compound (Scheme B).

Discussion and Conclusion

Browning, and sometimes bluish-greening, of plant food materials caused by chlorogenic acid, particularly a marked greening in the presence of amino acid and alkali, such as sweet potato in steamed bread, have been noted and many studies to elucidate the chemical properties of the green pigment have been undertaken. Up to now, no study has defined the chemical structure of this compound because of the difficulty in isolating it in its purified form.

In this study, it was demonstrated that the green pigment is an oxidized form of a newly discovered benzacridine derivative, formed by the condensation reaction of two molecules of oxidized chlorogenic acid or caffeic acid ester with one molecule of a primary amino compound under aeration in alkaline conditions.

This is very interesting from the viewpoint that green color is rare in food systems and also because benzacridine structures are rare in natural products. This green color is fairly stable in the reaction mixture, but there are still some problems in isolating the purified material. Therefore, the possibility of its use as a food colorant remains to be examined. The green pigment showed no mutagenicity in the Ames test.

Structural features of caffeate (*o*-phenol with a double bond and a carbonyl group in the side chain) play a very important role in the formation of the benzacridine structure. It may provide favorable properties for easy oxidation under alkaline atmospheric conditions by oxygen to give a fairly stable free radical product as shown by ESR, and the *o*-quinone product. On their own, such reactive caffeate derivatives can lead to the formation of polymerized brown products. However, addition of an amino compound brought about significant changes in the reaction system, i.e., the combination of a nucleophilic primary amino compound with the oxidized caffeate molecules resulted in the formation of more stable heterocyclic compound, a benzacridine phenol derivative. Involvement of nitrogen in the ring structure causes a bathochromic effect to give green color due to the merocyanine structure, and an alkyl group on the nitrogen may enhance the electron-donating activity of the nitrogen atom.

The identified compound has three phenol groups in the benzacridine structure, which will easily give a highly conjugated quinone structure by oxidation. This reduction compound is readily oxidized by atmospheric oxygen to give a free radical intermediate, leading to the oxidized form with a green color. This phenol derivative of benzacridine has very interesting properties. The reduction product which is yellow is very easily oxidized by air to give a green and then a blue product. This blue product is easily reduced by ascorbic acid to give the green and then the yellow compound. This oxidation-reduction reaction between a phenol compound and oxygen gives a free radical product and an active oxygen species, such as a superoxide anion radical, that was detected by ESR. These characteristic properties of the green pigment and its derivatives may provide various important physiological functions which remain to be elucidated.

Acknowledgments

We are grateful to Dr. Mitsuhiro Hida, Professor Emeritus of Tokyo Metropolitan University, for valuable suggestions regarding the chemistry and color science of the green pigment. Thanks are also due to Drs. T. Hayashi, M. Isobe, T. Kondo, I. Uritani, K. Namiki, E. Niki and M. Yano for their useful advice and help, and to JEOL for the ESR measurements.

Literature Cited

1. Uritani, I. *Nippon Nogei Kagaku Kaishi (in Japanese)* **1953**, *27*, 781-785.
2. Uritani, I.; Hoshiya, I.; Takita, S. *Nippon Nogei Kagaku Kaishi (in Japanese)* **1953**, *27*, 785-789.
3. Mano, Y.; Kuratomi, M.; Ouchi, K.; Takiguchi, M. *Eiyo to Shokuryo (in Japanese)* **1963**, *16*, 78.
4. Mano, Y. *Eiyo to Shokuryo (in Japanese)* **1964**, *17*, 85.
5. Sabir, M. A.; Sosulski, F. W.; Finlayson, A. *J. Agric. Food Chem.* **1974**, *22*, 575-578.
6. Nakabayashi, T. *J. Food Sci. Technol. Jpn. (in Japanese)* **1984**, *31*, 4508.
7. Payen *Ann.* **1849**, *26*, 108.
8. Gorter, K. *Ann.* **1908**, *354*, 329.
9. Politir *J. Praktika* **1932**, *7*, 249.
10. Horikawa, H., Okayasu, M., Wada, A., Kusama, M., *J. Food Sci. Technol. Jpn. (in Japanese)* **1971**, *18*, 115-118.
11. Nakatani, C.; Karasawa, I. *J. Jpn. Soc. Food Nur. (in Japanese)* **1979**, *32*, 42-53.
12. Matsui, T. *J. Nutr. Sci Vitaminol*, **1981**, *27*, 573-582.
13. Horikawa, H.; Furuya, E. *J. Jpn. Soc. Food Nur. (in Japanese)* **1988**, *41*, 299.
14. Watanabe, S.; Ushizawa, Y.; Kusama, M. *J. Jpn. Soc. Food Sci. Tech. (in Japanese)* **1996**, *43*, 1-6.
15. Yabuta, G.; Koizumi, Y.; Namiki, K.; Kawai, T.; Hayashi, T.; Namiki, M. *Biosci. Biotech. Biochem.* **1996**, *60*, 1701-1702.
16. Sieper, H. *Chem. Ber.* **1967**, *100*, 1646-1654.
17. De jongh, D.C.; Evenson, G.N. *J. Org. Chem.* **1972**, *37*, 2152-2154.
18. Hida, M. *Science of Color; (in Japanese)* Maruzen Co. **1998**, 126.
19. Hida, M. *Dyes and Pigments*, **1995**, *28*, 217.

Chapter 9

Structure, Color, and Formation of Low- and High-Molecular Weight Products Formed by Food-Related Maillard-Type Reactions

T. Hofmann

Deutsche Forschungsanstalt für Lebensmittelchemie,
Lichtenbergstrasse 4, D-85748 Garching, Germany

The Maillard reaction between carbohydrates and amino acids or proteins leads to the formation of a multiplicity of low and high molecular browning substances. To resolve some important reactions of the puzzling network of non-enzymatic browning, key colorants have been identified and their precursors and formation pathways clarified by means of quantitative experiments in combination with synthetic studies and/or by [¹³C]-labelling experiments. This paper gives a survey of important reaction routes leading to key chromophores which, by application of the Color Activity Concept, have been identified in the last years by our group.

The Maillard reaction between reducing carbohydrates and amino acids as well as proteins is chiefly responsible for the development of desirable browning occurring, e.g., during roasting of meat or baking of bread, as well as of undesirable color formation, e.g., during preparation of condensed milk or drying of fruit products. To further improve the quality of foods, e.g., by controlling the non-enzymatic browning reaction more efficiently, a better understanding of the chromophore formation from carbohydrates is required.

As outlined in Figure 1, in the reaction of carbohydrates (I; pentoses: R=H; hexoses: R=CH₂OH) with amino acids, glycosylamines (II) are known to be formed as the first reaction products, which are then easily transformed into deoxyglycosyl amino acids (III) via the so-called Amadori rearrangement (1). These intermediates are not stable and are easily further degraded by loss of the amino acid to form 1-deoxy-2,3-diuloses (1a: R=H; 1b: R=CH₂OH) and 3-deoxy-2-osuloses (2a: R=H; 2b: R=CH₂OH). Due to their α-dicarbonyl functionality, these deoxyosones are very reactive and can either be further degraded by cyclization, resulting in products with intact carbon chain such as furan-2-aldehydes (3a: R=H; 3b: R=CH₂OH) and 2H-furan-3-ones (4a: R=H; 4b:

R=CH₂OH), or by fragmentation reactions, leading to C₂-, C₃- and C₄-carbonyl compounds such as glyoxal (**5**), methylglyoxal (**6**), hydroxyacetaldehyde (**7a**: R=H) and hydroxy-2-propanone (**7b**: R=CH₃). These so called advanced Maillard reaction products are discussed as important intermediates in chromophore formation (2).

Very recently, a novel analytical technique, the so called Color Activity Concept, has been developed offering the possibility of characterizing the key chromophores formed in non-enzymatic browning reactions and of evaluating the color impact of these compounds by calculating their color activity values as the ratio of their concentrations to their color detection thresholds (3,4).

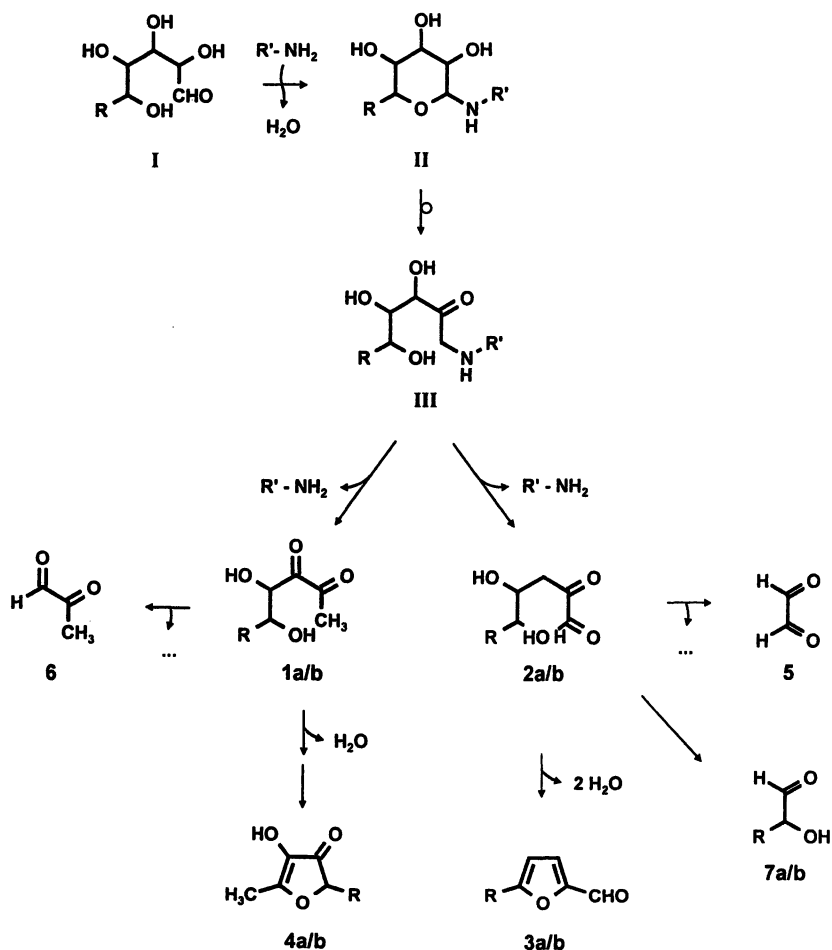


Figure 1. Amino acid catalyzed degradation of carbohydrates via 1-deoxy-2,3-diuloses (**1a**: R=H; **1b**: R=CH₂OH) and 3-deoxy-2-osuloses (**2a**: R=H; **2b**: R=CH₂OH) as the key intermediates. "..." symbolizes by-products formed by fragmentation of deoxyosones.

Besides the knowledge on the chemical structure of these key chromophores, it is a necessary prerequisite to clarify the precursors, and to elucidate their formation pathways in order to gain a better understanding for the puzzling browning mechanisms. Such information on how the carbohydrate is converted into the colored compounds upon thermal food processing will enable the construction of a route map of chromogenic reactions helping to disentangle the complex network of non-enzymatic browning.

The purpose of the present paper is, therefore, to demonstrate how color precursors and formation pathways can be clarified by using quantitative as well as synthetic studies and/or ^{13}C -labelling experiments. This concept will be demonstrated using as an example a novel pyrano[2,3-*b*]pyranone chromophore formed from pentoses. Based on this strategy, an attempt is made to survey some important chromogenic pathways leading to low and high molecular weight colored compounds in the Maillard reaction studied by our group in recent years.

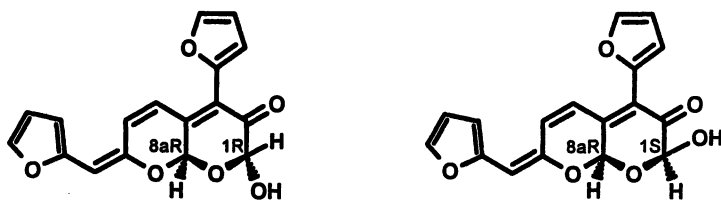
Analytical Strategy for Clarification of Reaction Routes

In order to locate the precursors of Maillard-generated chromophores, the following 2-step concept was developed:

- First, precursor compounds are identified by reacting synthetic carbohydrate-derived intermediates, which are most likely involved in colorant formation, with each other and by determining their effectiveness at generating the target chromophore by means of quantitative measurements.
- In order to clarify the mechanisms of conversion of these precursors to the chromophores, labeling experiments with ^{13}C -labeled carbohydrates or degradation products, were then performed. After isolation of the target compound, the site-specific ^{13}C -enrichment was located by means of ^{13}C -NMR spectroscopy so that the location of certain atoms in the chromophore under investigation could be unequivocally determined.

In the following section, this analytical concept is exemplified using the orange colored (1*R*,8*aR*)- and (1*S*,8*aR*)-4-(2-furyl)-7-[(2-furyl)methylidene]-2-hydroxy-2*H*,7*H*,8*aH*-pyrano[2,3-*b*]pyran-3-ones (**8** in Figure 2), which was recently identified amongst the key chromophores in a xylose/L-alanine/furan-2-aldehyde Maillard mixture by application of the Color Activity Concept (4,5).

It was speculated from its structure that the furan rings of compound **8** correspond to two molecules of furan-2-aldehyde and that, besides the five carbon motive of the intact pentose skeleton, two further carbon atoms were incorporated



8

Figure 2. Structure of orange colored (1*R*,8*aR*)- and (1*S*,8*aR*)-4-(2-furyl)-7-[(2-furyl)methylidene]-2-hydroxy-2*H*,7*H*,8*aH*-pyrano[2,3-*b*]pyran-3-one (**8**)

in the colorant. This encouraged us to study which carbohydrate degradation product with a C-2 skeleton is involved in chromophore formation. The Maillard mixture was, therefore, thermally treated in the presence of either acetaldehyde, hydroxyacetaldehyde or glyoxal, and the amounts of **8** formed were compared with those generated in a control experiment, in which the mixture was heated without addition of a C-2 compound. The results (Table I) showed that, in comparison to the control experiment, 11-fold higher amounts of **8** were produced in the Maillard mixtures containing hydroxyacetaldehyde (**6**). Glyoxal was somewhat less effective, whereas acetaldehyde did not show any significant precursor activity. The favored production of **8** in the presence of hydroxyacetaldehyde clearly pointed out that this C-2 compound is a penultimate precursor in the formation of the chromophore.

Table I. Influence of C-2 carbohydrate fragments on the formation of colorant **8**

<i>C</i> -2 compound	Amount of 8	
	[mg]	[%]
(no additive)	0.5	0.01
Acetaldehyde	0.7	0.01
Glyoxal	3.1	0.06
Hydroxyacetaldehyde	5.6	0.11

^a A mixture of xylose (16.5 mmol) and L-alanine (4.0 mmol) was heated in phosphate buffer (20 mL; 1 mmol/L, pH 7.0) under reflux for 10 min, then, the C-2 compound (0.75 mmol) and furan-2-aldehyde (25 mmol) were added and heating was continued for another 60 min (**6**).

Besides furan-2-aldehyde and hydroxyacetaldehyde, the intact carbon skeleton of the pentose was assumed to be involved in the formation of **8**. In order to study whether the pentose skeleton is incorporated via the 3-deoxypentos-2-

ulose pathway (2a in Figure 1) or the 1-deoxy-2,3-pentodiulose route (1a in Figure 1), the xylose in the Maillard mixture was substituted by the corresponding Amadori rearrangement product N-(1-deoxy-D-xylulos-1-yl)-L-alanine and synthetically prepared 3-deoxypentos-2-ulose, respectively, and the amounts of 8 generated were determined. The results (Table II) showed that the formation of 8 was significantly favored from the 3-deoxypentos-2-ulose, e.g., 3-fold higher amounts of 8 were generated compared to the xylose-containing reaction mixture. These quantitative data indicated the incorporation of the pentose skeleton into 8 via the 3-deoxypentos-2-ulose (2a) as the key intermediate.

To gain further insights into the pathway, concerning the incorporation of 3-deoxypentos-2-ulose into 8, the Maillard reaction was performed with [^{13}C]-labelled xylose in order to follow the fate of the anomeric carbon atom of the pentose during its incorporation into the colorant by ^{13}C NMR spectroscopy. Comparison of its ^{13}C NMR spectrum with the spectroscopic data of the natural ^{13}C -abundant chromophore indicated the site-specific [^{13}C]-enrichment in the carbon atom C(8) marked with a dot in Figure 3.

Table II. Influence of the C-5 moiety of the pentose skeleton on the formation of colorant 8

<i>Precursors [mmol]</i>	<i>Amount of 8</i>	
	<i>[mg]</i>	<i>[%]</i>
Xylose (16.5) / L-alanine (4.0)	5.6	0.11
N-(1-deoxy-D-xylulos-1-yl)-L-alanine (16.5)	7.1	0.14
3-Deoxypentosulose (16.5)	14.8	0.29

The precursor mixtures were heated in phosphate buffer (20 mL; 1 mmol/L, pH 7.0) under reflux for 10 min, then, a mixture of hydroxyacetaldehyde (0.75 mmol) and furan-2-aldehyde (25 mmol) was added and heating was continued for another 60 min (6).

Taking all these data into account, the pentose degradation products furan-2-aldehyde (3a), 3-deoxy-2-pentosulose (2a) and hydroxyacetaldehyde (7a) were proposed to react following the pattern displayed in Figure 3.

Low Molecular Weight Colored Compounds

Application of the Color Dilution Analysis on molecular weight fractions of aqueous carbohydrate/amino acid solutions, which were thermally treated under food-related conditions, revealed that the browning developed mainly corresponds to colored compounds with molecular weights below 1000 Da (7). Chromophores with molecular weights above 3000 Da could be observed only in trace amounts (7). In the following, a survey is given of reaction routes leading to

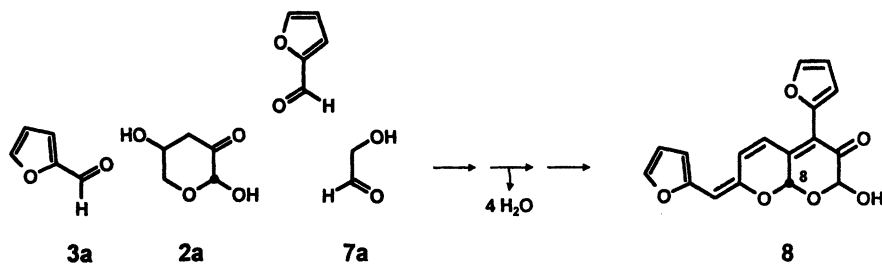


Figure 3. Formation of pyranopyranone 8 from the carbohydrate-derived reaction intermediates 2a, 3a and 7a.

those low molecular weight compounds, which were identified as key chromophores in browned carbohydrate/amino acid mixtures by application of the Color Activity Concept.

Chromogenic Pathways of Pentoses

The pyrano[2,3-*b*]pyran-3-one, 8, was found amongst the most intense colorants formed during pentose degradation. On the basis of quantitative studies and [¹³C]-labeling experiments, which elucidate furan-2-aldehyde, hydroxyacetaldehyde and the 3-deoxy-2-pentosulose as the penultimate precursors of the chromophore (Figure 3), the reaction pathway displayed in Figure 4 was proposed for the formation of 8. To follow the fate of the [¹³C] label of the pentose throughout its incorporation into the colorant, the [¹³C]-enriched atom is denoted as a dot in the structures (Figure 4). Condensation between the methylene-active hydroxyacetaldehyde (7a) and furan-2-aldehyde (3a) yields the 2-(2-furyl) methylidene-2-hydroxyacetaldehyde (I in Figure 4), which could be identified by mass spectrometry. This intermediate reacts with the 3-deoxypentos-2-ulose (2a), formed by dehydration of the pentose at the 3-position (Figure 1), upon condensation at the carbonyl group, followed by subsequent cyclic hemiacetal formation giving rise to the 2,5,6,7,8a-pentahydropyrano[2,3-*b*]pyran-3-one (II). Water elimination leads to the methylene-active intermediate III, which, upon condensation with an additional molecule of furan-2-aldehyde, gives rise to chromophore 8.

In addition, γ -alkylidene- β -pyranones (9a/9b), stabilized as acetals, were identified as pentose-typical chromophores (Figure 4). Although these compounds were reported earlier in the literature (8,9), we now successfully clarified their formation by using [¹³C₁]-labeled xylose. Water elimination from the 3-deoxy-2-pentosulose (2a) yields the 3,4-dideoxy-2-pentosulose (IV), which, after enolization, undergoes condensation with carbonyl compounds at the 4-position giving rise to chromophores 9a/9b.

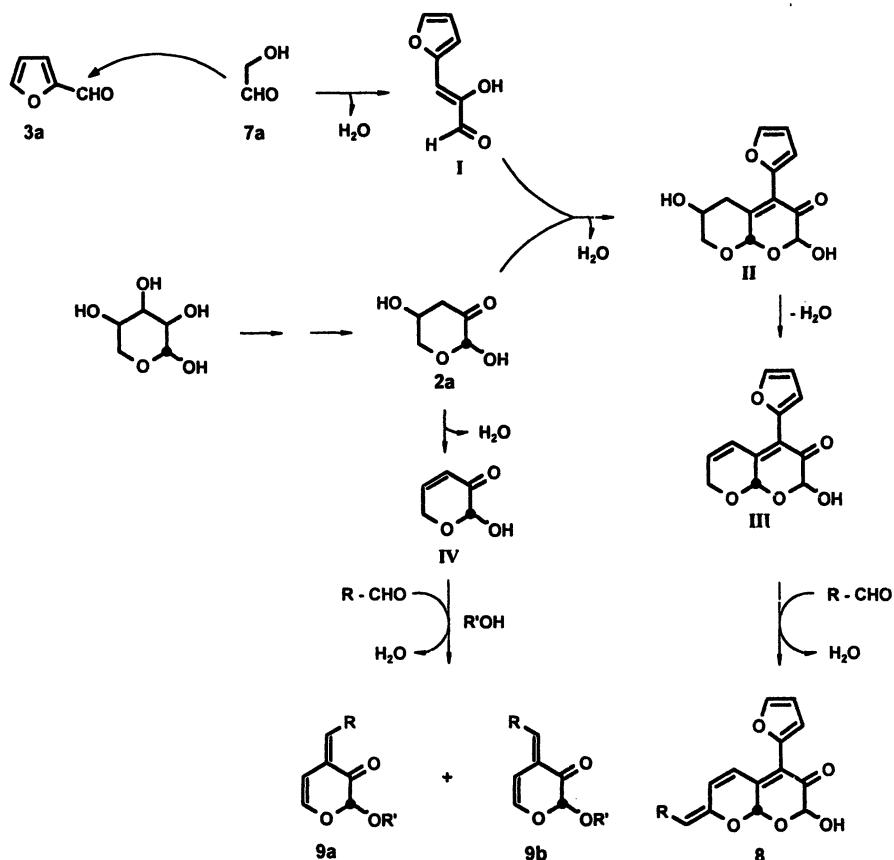


Figure 4. Reaction pathways leading to the formation of colored pyranof[2,3-b]pyranone **8** and γ -alkylidene- β -pyranones **9a** and **9b** via the 3-deoxy-2-pentosulose (**2a**) as the key intermediate.

Besides the nitrogen-free pyranone chromophores **8** and **9a/b**, the amino acid can also be involved in the formation of 3-deoxyosone-derived chromophores. To follow the fate of the label of the pentose throughout its incorporation into the colorants, the ^{13}C -enriched atoms are denoted as dots in the structures in Figure 5. Formation of the five-membered furanoid form (I) via the open-chain form of the 3-deoxy-2-pentosulose (**2a**) and reaction with primary amino acids such as, e.g., L-alanine, leads to the (S)-N-(1'-carboxyethyl)-2-formylpyrrole (II). Reaction with methylene-active carbohydrate intermediates such as 4-hydroxy-5-methyl-2H-furan-3-one (norfuranol, **4a**) gives rise to yellow colored condensation products of type **10** (**10**). If the 3-deoxy-2-pentosulose (**2a**) first reacts with aldehydes, then the condensation product (III), formed, rapidly undergoes cyclization and dehydration in the presence of primary amino acids. The 2H-pyrrolin-3-one (IV) formed exhibits two methylene-active

functions and, therefore, rapidly forms red chromophores of the 3(2*H*)-pyrrolinone-type (11a and 11b) upon condensation with carbonyls such as, e.g., furan-2-aldehyde (10). Besides the incorporation of the intact amino acid moiety, it is also possible that the nitrogen atom is exclusively incorporated into chromophores. E.g., reductive amination of the 3,4-dideoxyosone (V) in course of a Strecker-type reaction forms the aminoketone (VI), which upon subsequent cyclization by an intramolecular Michael addition gives rise to a 3-oxo-pyrrolidine intermediate (VII). Condensation with two molecules of aldehydes leads to the red chromophore (VIII), rapidly stabilizing as the corresponding tetrahydrooxazolidine (12) by reaction with an additional aldehyde (10).

Further experiments also revealed the 1-deoxy-2,3-pentosulose (1a, Figure 1) as an effective progenitor of chromophores, e.g., via its degradation product norfuranol (4a). Reaction with carbonyls rapidly forms yellow monocondensation products of type 13 (5,9) which are, however, not stable end-products of Maillard reactions, but can easily undergo further reactions (Figure 6), e.g., condensation with an additional carbonyl compound leads to higher substituted chromophores of type 14 (5,9). The fate of the carbonyl function of e.g., [¹³C₁]-labeled furan-2-aldehyde (11) throughout its incorporation into the colorants can be followed by a dot. In the presence of primary amino acids, monocondensation products of type 13 can, however, also be rearranged into 3-hydroxy-3-cyclopentene-1,2-diones, 15 (Figure 6). This rearrangement might be induced by a nucleophilic addition and ring-opening of compound 13, yielding the open-chain intermediate I (Figure 6), which undergoes an intramolecular condensation reaction to form the vinylogous hemiaminal, II. Subsequent elimination of the amino acid reflects the catalytic role of the amino acid and forms the 3-hydroxy-3-cyclopentene-1,2-dione (15). In synthetic experiments (12) it could be shown that this CH-acidic compound rapidly undergoes condensation in the presence of aldehydes such as, e.g., furan-2-aldehyde, to give a red colored chromophore of type 16 (Figure 6). These data clearly show that amino acids can not only catalyze the Amadori rearrangement of glycosylamines (Figure 1), but also the conversion of one chromophore into another.

Chromogenic Pathways of Hexoses

Application of the Color Activity Concept recently revealed that the pyrano[2,3-*b*]pyranone 8, identified for the first time in pentose-containing systems (5), also belongs to the key contributors of the overall color of hexose/amino acid mixtures (13). Precursor studies led to the identification of 3-deoxy-2-hexosulose (2b), hydroxyacetaldehyde (7a) and furan-2-aldehyde (3a) as key intermediates in the formation of 8 from hexoses (13). Based on the knowledge of the chromophore formation from pentoses, it was assumed that the hexose backbone is cleaved between C-5 and C-6 to form 8 from hexoses. This hypothesis could be unequivocally confirmed by a labeling experiment using glucose-6-[¹³C₁] (13). The spectroscopic data of the colorant isolated from this labeling experiment were identical with those found for the colorant produced from natural [¹³C]-abundant glucose. On the basis of these results, clearly

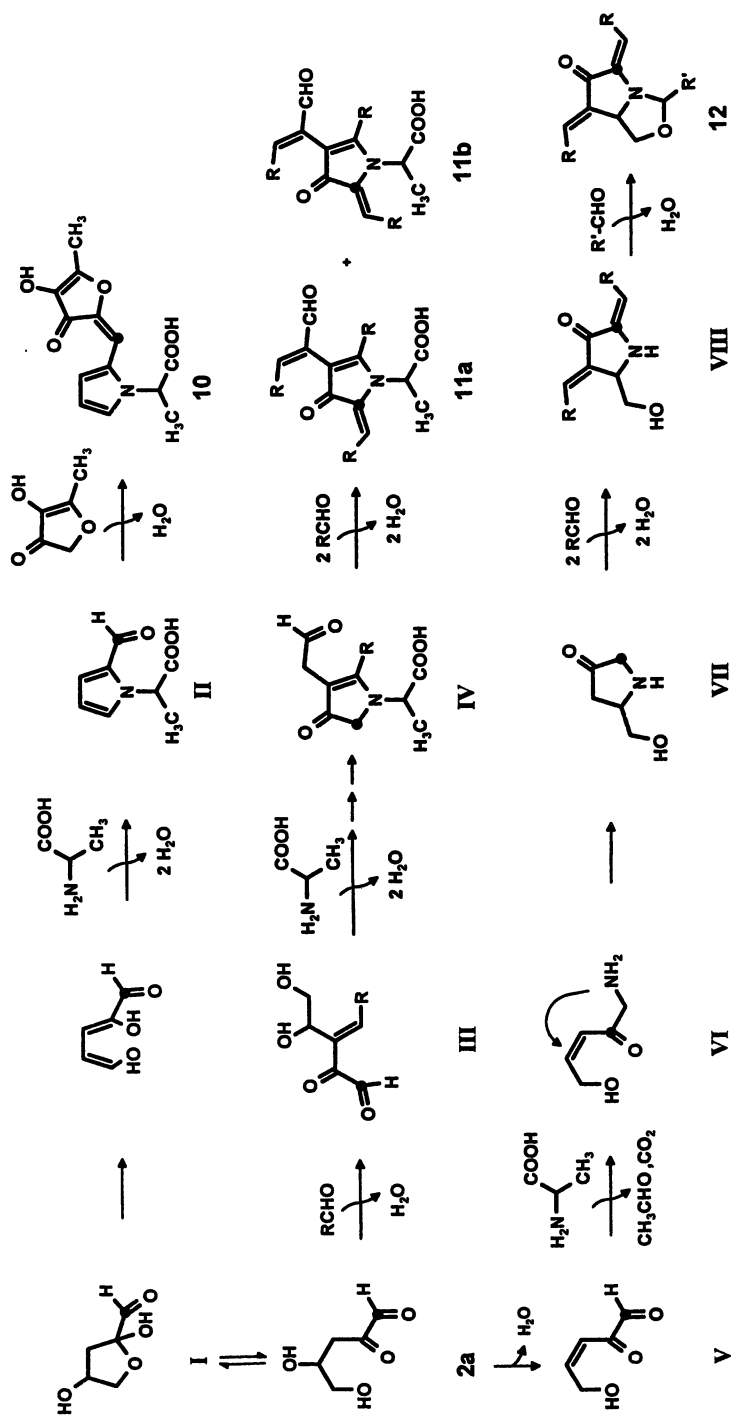


Figure 5. Reaction pathways leading to the formation of nitrogen-containing chromophores 10, 11a/b and 12 via the 3-deoxy-2-pentulose 2a as the key intermediate.

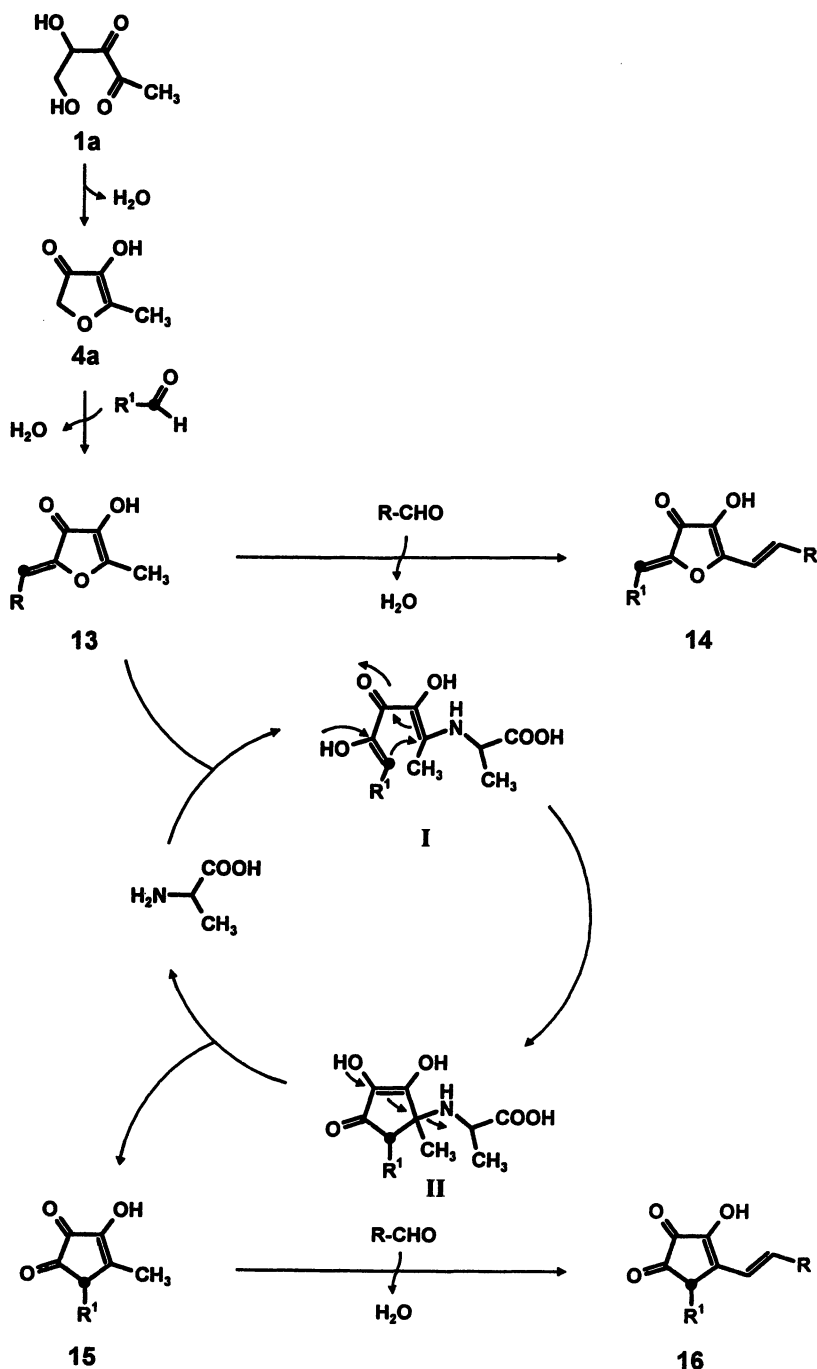


Figure 6. Reaction pathways leading to the formation of colored 2H-furan-3-ones (**13**, **14**) and 3-hydroxy-3-cyclopentene-1,2-diones of type **16** via the 1-deoxy-2,3-pentodiulose (**1a**) as the key intermediate.

demonstrating that the carbon atom C-6 is split off from the hexose skeleton, the following reaction pathway was proposed for the formation of **8** from hexoses (Figure 7).

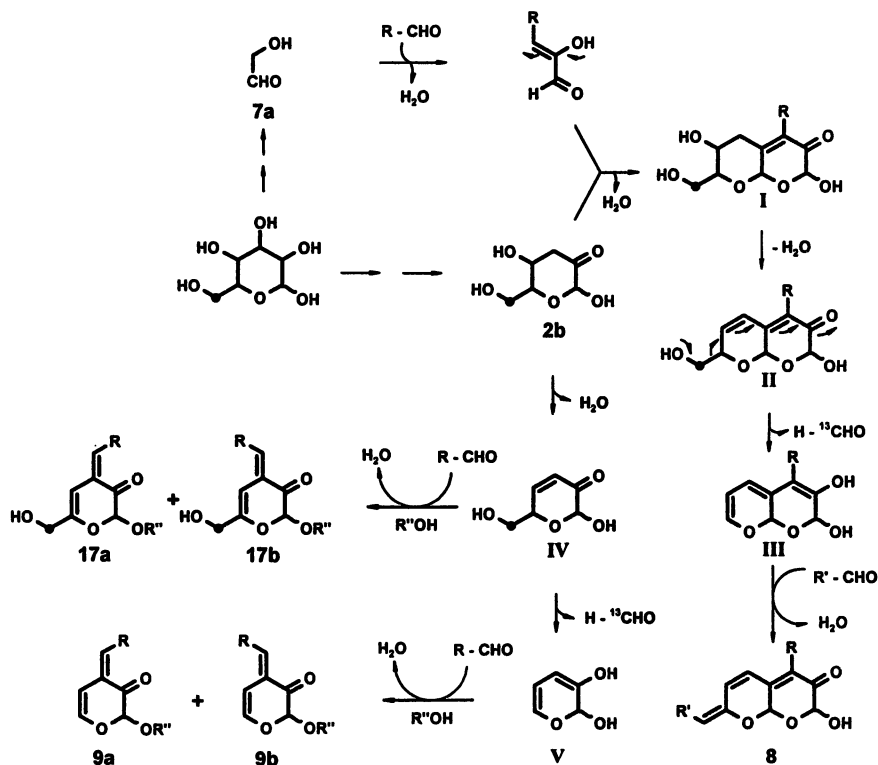


Figure 7. Reaction pathways leading to the formation of pyrano[2,3-*b*]pyranone **8** and β -pyranones **9a/b** and **17a/b** via the 3-deoxy-2-hexosulose (**2b**) as the key intermediate.

As already shown for pentoses, condensation of hydroxyacetaldehyde (**7a**) with an aldehyde and further reaction with the 3-deoxy-2-hexosulose (**2b**) upon ring-closure leads to the intermediate (I). After elimination of an additional molecule of water, the hydroxymethyl group is split off upon a retro-Michael cleavage of formaldehyde (II) giving rise to the methylene-active intermediate III. Condensation with carbonyl compounds finally yields colored pyrano[2,3-*b*]pyranones of type **8** (13).

In hexose-containing Maillard mixtures yellow colored γ -alkylidene- β -pyranones of type **17a/b** (Figure 7) are formed (13). The formation of these pyranones runs via the 3-deoxy-2-hexosulose (**2b**) as the key intermediate (Figure 7). Water elimination at the 4-position gives rise to the 3,4-dideoxyhexosulose (IV), which, upon condensation with an aldehyde at the γ -position, results in the colored γ -alkylidene- ε -hydroxymethyl- β -pyranones **17a** and **17b** (8,13).

However, retro-Michael cleavage of formaldehyde from intermediate IV breaks down the C6-skeleton to the C5- β -pyranone, V, giving rise to the pentose-typical chromophores of type 9a/b (Figure 7). Due to the instability of the β -pyranones 9a/b and 17 a/b, these have been trapped as their stable acetals prior to isolation (8,13). This instability is reflected, e.g., in the rearrangement of the hemiacetal of 17b ($R''=H$; Figure 7) into the yellow colored furanone 18 (Figure 8), when heated in aqueous solution in the presence of carbonyls. Although chromophore 18 was reported earlier (8), we could recently confirm these experiments. The formation of this type of chromophore seems to be a general reaction principle, because the analogous pyrrolinone 11b (Figure 8) could be isolated in a pentose/alanine mixture showing the same carbon backbone with one carbon atom less. Contrary to 18, a third condensation had taken place to form 11b from pentoses (Figure 5).

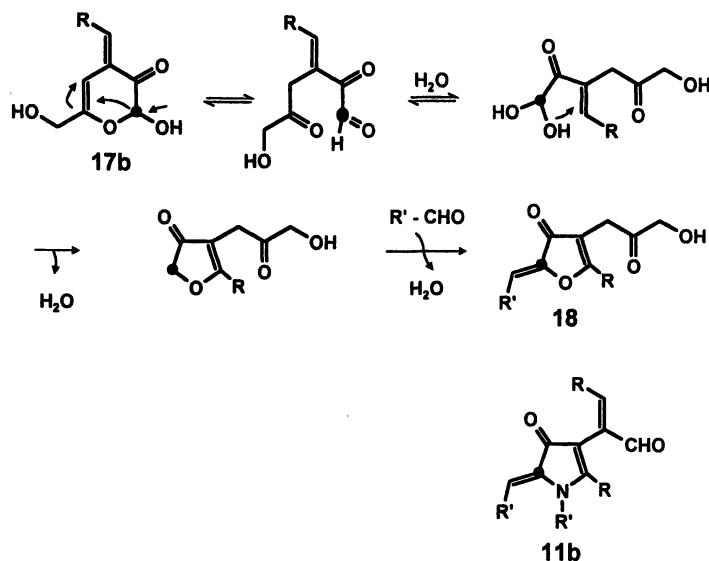


Figure 8: Rearrangement of hemiacetal 17b into furanone chromophore 18.

However, the 1-deoxyhexosones (1b) are also effective color precursors. Via a cyclic β -pyranone intermediate, the 2,3-dihydro-3,5-dihydroxy-6-methyl-4H-pyran-4-one (19) is formed upon water elimination (Figure 9). Due to its acidic methyl group, it undergoes condensation with aldehydes to form yellow chromophores of type 20 (9,13). Via a 5-membered cyclization product, the 4-hydroxy-2-(hydroxymethyl)-5-methyl-2H-furan-3-one (21, Figure 9) arises upon water elimination (12, 14). This compound was found to easily liberate 4-hydroxy-5-methyl-2H-furan-3-one (4a) upon retro-Michael reaction (12, 14). Also in this case the C-6 of the hexose is split off. The cleavage of C_1 -fragments, from hexoses seems to be an important general reaction in non-enzymatic browning. As already shown, compound 4a opens the way to typical pentose reactions, such as the formation of colored 2-alkylidene-4-hydroxy-5-methyl-2H-

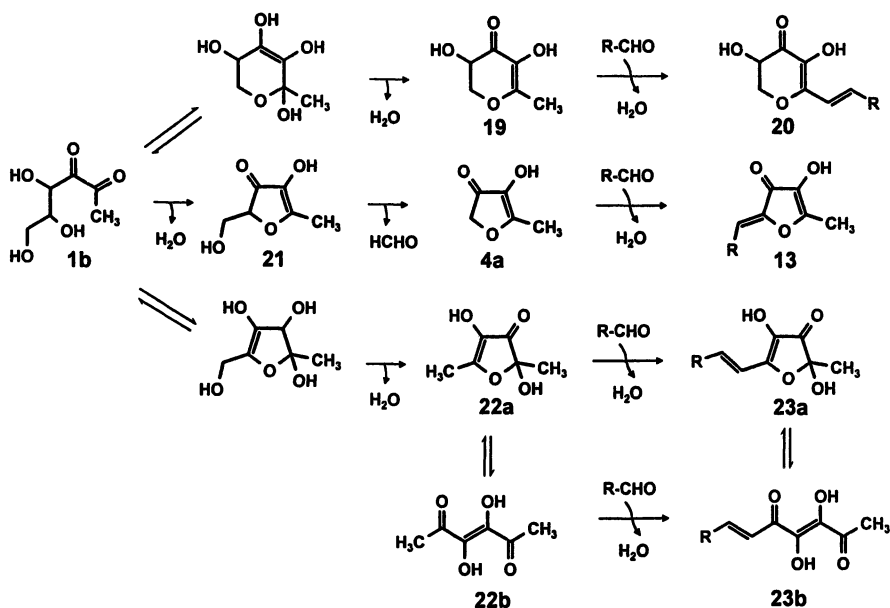


Figure 9. Reaction pathways leading to chromophores of type 20, 13, 23a and 23b via 1-deoxy-2,3-hexodiulose (1b) as the key precursor.

furan-3-ones (13, Figure 9). Cyclization of 1b and water elimination at the 6-position forms the so called acetylformoin consisting of a mixture of 2,4-dihydroxy-2,5-dimethyl-3(2H)-furanone (22a) and 3,4-dihydroxy-3-hexene-2,5-dione (22b). Condensation with aldehydes (15) gives rise to the yellow chromophores 2,4-dihydroxy-2-methyl-5-[(E)-2-alkylidene]methyl-2H-furan-3-one (23a) and 3,4-dihydroxy-6-[(E)-2-alkylidene]-3-hexene-2,5-dione (23b).

However, in the presence of a primary amino acid such as, e.g., glycine, the acetylformoin (22a/b) rapidly forms the 2,4-dihydroxy-2,5-dimethyl-1-carboxymethyl-3-oxo-2H-pyrrole (24), as outlined in Figure 10. As shown for the acetylformoin, this pyrrolinone reductone (24) also forms intensely colored condensation products of type 25 in the reaction with aldehydes (15).

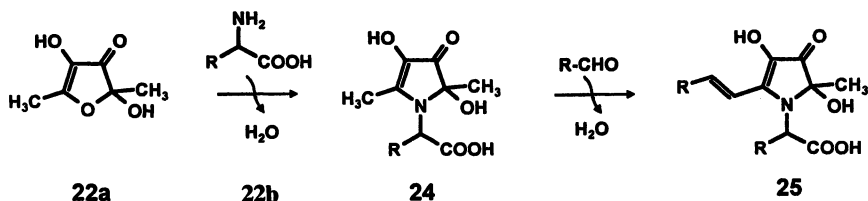


Figure 10. Formation of pyrrolinone reductones (24) and pyrrolinone chromophores of type 25 from acetylformoin (22a/b) and primary amino acids.

Influence of a 1,4-Glycosidic Link in Di- and Polysaccharides on Colorant Formation

Browning measurements on thermally treated solutions of mono- as well as disaccharides revealed pentoses and hexoses as effective browning precursors (16). Independent of the reaction time, disaccharides such as, e.g., maltose, or polysaccharides such as, e.g., starch, did not reach the color intensity of pentose- or hexose- containing solutions (16). Recent investigations provided evidence that the 1,4-glycosidic linkage of di- and polysaccharides is responsible for their lower effectiveness in browning development. This is demonstrated in the following example involving the formation of 3-hydroxy-3-cyclopenten-1,2-dione chromophores. As outlined in Figure 11, the formation of 3-hydroxy-3-cyclopentene-1,2-dione chromophores from pentoses runs via norfuranol (4a) as the key intermediate. Condensation with carbonyls forms chromophore 13, which is then rearranged into the CH-acidic intermediate 15 by amino acid catalysis as detailed in Figure 6. Additional condensation with aldehydes then gives rise to the chromophore 16 (Figure 11).

The same type of chromophore can be formed from hexoses via the key intermediate acetylformoin (22a). Reaction with pyrrolidine, liberated upon thermal degradation of proline, yields the N-(1-methyl-1,2,3-trihydroxy-2-cyclopentene-4-ylidene)-pyrrolidinium betaine (pyrrolidinohexose reductone; 26, Figure 11) as a conversion product (15). This compound is, however, not a stable end product of the Maillard reaction and forms the methylene reductinic acid (27) upon hydrolysis (15). Condensation with aldehydes then results in the formation of the intense red colored chromophore 28, differing from 16 only in the lack of group R (15).

Also, the disaccharide is able to form an aminohexose reductone (29, Figure 11), but in the glycosylated form instead, because the maltose is connected by a 1,4-glucosidic link. The corresponding piperidine derivative was earlier identified by Ledl and his group (17). Because the glucose is a weak leaving group, this N-[1-methyl-1,2-dihydroxy-3-(glyoxyloxy)-2-cyclopentene-4-ylidene]pyrrolidinium betaine (29, Figure 11) cannot liberate the color precursor methylene reductinic acid (27), thus, preventing chromophore formation (12). In model experiments, we could show that this glycoside can be hydrolyzed by α -glucosidase to yield the corresponding pyrrolidinonehexose reductone 26, thereby inducing the monosaccharide-specific reaction pathways (12). Polysaccharides that are connected by a 1,4-glycosidic link such as, e.g., starch or dextrans, can be expected to react in the same way as shown for disaccharides.

High Molecular Weight Colored Compounds (Melanoidins)

Besides the amino acids which lead preferentially to low molecular weight colored compounds in the presence of carbohydrates, proteins are predominating ingredients in most foods. We have recently shown that heating food proteins in the presence of carbohydrates leads to the formation of protein oligomers exhibiting molecular weights of more than 100 000 Da (7). The observed cross-linking of the protein was found to run in parallel with the color intensity of the

products formed, indicating that chromophoric substructures, derived from carbohydrates, are incorporated into these oligomers (7). These brown colored protein-oligomerization products showed spectroscopical characteristics typical for food melanoidins indicating that melanoidins generated during cooking of foods might be generated by a cross-linking reaction between low-molecular weight Maillard reaction products and high-molecular non-colored proteins (7).

To gain insights into the chemical structures of the chromophores attached to the protein, aqueous solutions of proteins, carbohydrates and/or carbohydrate degradation products were reacted. Melanoproteins (MW > 10000 Da) were isolated by ultracentrifugation and, after enzymatic digestion of the protein backbone, the hydrolysate was analysed by HPLC. By comparison of retention times, UV/VIS and LC/MS spectra with those of the synthetic reference compounds, several colored lysine-modifications could be identified (Figure 12). E.g., the (*S*)-*N*-(5-amino-5-carboxy-1-pentyl)-2-(*E*)-(2-furyl-methylene)-4-(*E*)-(1-formyl-2-furyl-1-ethenyl)-5-(2-furyl)-3(2*H*)-pyrrolinone (**30**) was formed from the reaction of 3-deoxy-2-pentosulose (**2a**) and furan-2-aldehyde (**3a**) with food proteins (**18**), the lysyl-pyrrolinone reductone **31** was generated when proteins were reacted in the presence of the carbohydrate degradation products acetylformoine (**22a/b**) and furan-2-aldehyde (**3a**) and the pyrrolinone-derived chromophore **32** was successfully identified in a mixture of proteins, glucose and norfuranol (**4a**).

Besides lysine residues, arginine moieties are also involved in melanoidin formation, e.g., in a reaction involving the carbohydrate degradation products glyoxal (**5**) and furan-2-aldehyde (**3a**) the red colored previously unknown (*S,S*)-1-(4-amino-4-carboxy-1-butyl)-2-imino-4-[(*Z*)-(2-furyl)methylidene]-5-{2-[1-(4-amino-4-carboxy-1-butyl)-4-[(*E*)-(2-furyl)methylidene]-5-oxo-1,3-imidazol-2-yl]}aza-methylidene-1,3-imidazolidine (**33**, Figure 12) was formed (**19**).

These novel colored structures **30-33** demonstrate for the first time how melanoidin-type colorants might be formed by cross-linking and chromophore-generating reactions between carbohydrate-derived intermediates and reactive side chains of a non-colored protein backbone (Figure 12). Obviously, lysine and arginine residues of proteins act as chemical anchors fixing carbohydrate degradation product to the protein backbone and generating the chromophoric substructures of melanoidins. These data confirm the idea that low molecular weight colored compounds might represent some of the substructures incorporated into melanoidins. The proteins might act as the non-colored skeleton of food melanoidins, to which a variety of chromophoric substructures might be covalently bound via reactive side chains.

Due to the high protein content of most foods, e.g., 20-25 % in beef meat, and the ability of proteins to generate high-molecular weight colored compounds, it is very likely that carbohydrate-induced oligomerization and browning of proteins is involved in the formation of food melanoidins.

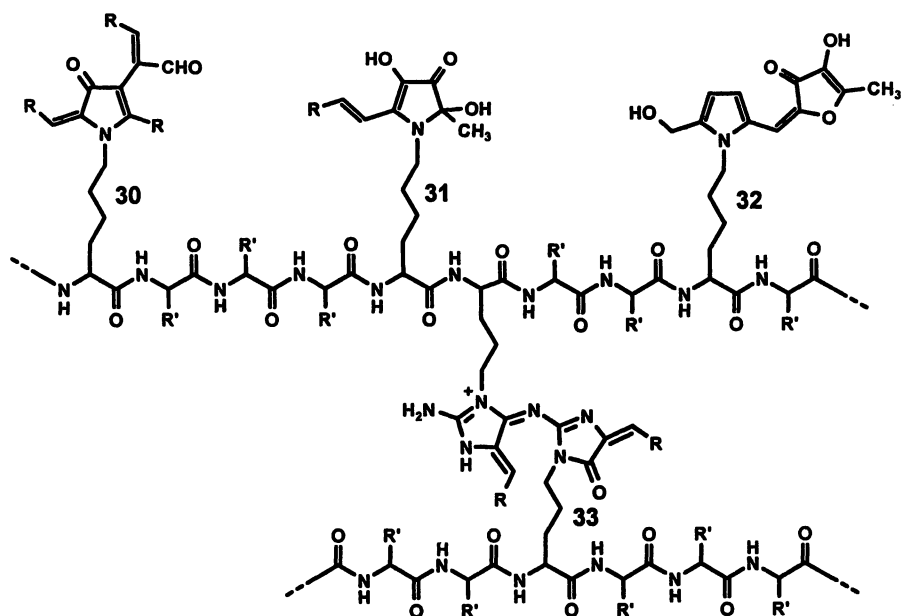


Figure 12. Chromophoric substructures involved in melanoidin formation.

Acknowledgments

The Deutsche Forschungsgemeinschaft, Bonn, is thanked for partly funding the research. We are grateful to Mr. J. Stein for his excellent technical assistance.

Conclusions

These data demonstrate that the identification of precursors by synthetic and quantitative studies, followed by the elucidation of reaction pathways using [^{13}C] labeling experiments, is a suitable strategy to unravel the puzzling network of non-enzymatic browning reactions. Details, obtained thereof, will help to construct a route map of chromogenic reactions, on the basis of which the non-enzymatic browning might be controlled more efficiently.

Literature Cited

1. Kuhn, R.; Weygand, F. *Ber. Dtsch. Chem. Ges.* **1937**, *370*, 769-772.
2. Hofmann, T. *Eur. Food Res. Technol.* **1999**, *209*, 113-121.
3. Hofmann, T. *J. Agric. Food Chem.* **1998**, *46*, 3912-3917.
4. Hofmann, T.; Frank, O.; Heuberger, S. (2000) this book

5. Hofmann, T. *Carbohydr. Res.* **1998**, *313*, 203-213.
6. Hofmann, T. *Carbohydr. Res.* **1998**, *313*, 215-224.
7. Hofmann, T. *J. Agric. Food Chem.* **1998**, *46*, 3891-3895.
8. Ledl, F.; Hiebl, J.; Severin, Th. *Z. Lebensm. Unters. Forsch.* **1983**, *177*, 353-355.
9. Ledl, F.; Schleicher, E. *Angew. Chem.* **1990**, *102*, 587-734.
10. Hofmann, T. *J. Agric. Food Chem.* **1998**, *46*, 3902-3911.
11. Hofmann, T. *J. Agric. Food Chem.* **1998**, *46*, 941-945
12. Hofmann, T. *J. Agric. Food Chem.* **1999**, in prep.
13. Hofmann, T.; Heuberger, S. *Z. Lebensm. Unters. Forsch.*, **1999**, *208*, 17-26.
14. Hiebl, J.; Ledl, F.; Severin, Th. *J. Agric. Food Chem.* **1987**, *35*, 990-993.
15. Hofmann, T. *J. Agric. Food Chem.* **1998**, *46*, 3918-3928.
16. Heuberger, S. Diploma thesis, TU Munich, Munich, Germany, 1998.
17. Papst, H. M. E.; Ledl, F.; Belitz, H.-D. *Z. Lebensm. Unters. Forsch.* **1985**, *181*, 386-390.
18. Hofmann, T. *Z. Lebensm. Unters. Forsch.* **1998**, *206*, 251-258.
19. Hofmann, T. *J. Agric. Food Chem.* **1998**, *46*, 3896-3901.

Chapter 10

Chemistry and Possible Physiological Function of Selected Components of a Glucose–Lysine Model System

Jennifer M. Ames, Glenn R. Gibson, Richard G. Bailey,
and Anthony Wynne

Department of Food Science and Technology, The University of Reading,
Whiteknights, Reading RG6 6AP, United Kingdom

Aqueous solutions of glucose and lysine were heated at pH 3–7 at different temperature/time combinations and at different pH values. Reversed phase HPLC separated several components as sharp peaks superimposed on a broad band of unresolved, colored material (melanoidins). Five reaction products were identified as 2,3-dihydro-3,5-dihydroxy-6-methyl-(4*H*)-pyranone (compound 2), 4-hydroxy-2-(hydroxymethyl)-5-methyl-3(2*H*)-furanone (compound 4), 2-amino-6-(2-formyl-5-hydroxymethyl-1-pyrrolyl)-hexenoic acid (pyrraline, compound 5), the new compound 1-(carboxy-5-aminopentyl)-2-formyl-3-(1,2,3-trihydroxypropyl)-pyrrole (compound 1) and 5-hydroxymethylfurfural (HMF). The %peak area values varied greatly with both temperature/time combination and pH. E.g., compound 1 predominated at 55 °C and relative amounts decreased with increasing temperature while compound 4 predominated under reflux with relative amounts decreasing with decreasing temperature between reflux and 55 °C. HMF accounted for *ca.* 90% of the total peak area at pH 3 while compounds 2 and 4 each accounted for *ca.* 50% of the total peak area at pH 7. The behavior of the melanoidins in the human gut was studied using anaerobic *in vitro* batch culture of fecal bacteria. No evidence could be found for the degradation of melanoidins in simulated peptic or pancreatic digestions but melanoidins were well fermented by gut bacteria.

The Maillard reaction takes place during most food processing operations (1). Food manufacturers depend on it for the formation of desirable flavors and colors in commodities such as coffee, beer, bread, cookies, flour confectionery, meat and breakfast cereals. Due largely to the availability of gas chromatography-mass spectrometry, considerable progress has been made in

understanding the chemical pathways leading to the formation of volatile flavor compounds as a result of the Maillard reaction. By comparison, study of the colored Maillard reaction products has been largely neglected. These colorants may be divided into low molecular mass components (less than about 1000 daltons), and higher molecular mass melanoidins which are macromolecular materials of undetermined structures and functions (other than color).

It has been established that food processing variables, including temperature and time of heating, pH and moisture content, as well as variations in raw materials, affect the profiles of Maillard reaction products, including the colorants (2,3). The ability to control and optimize properties of products, including color, is of great value to the industry and an understanding of the chemical pathways involved is helpful to achieve this goal.

Due to the wide distribution of Maillard reaction products in a typical Western diet, quantities of these materials enter the gut each day and the available data on the fate of melanoidins has been reviewed (4). Most studies concerning melanoidins have used rats and it has been demonstrated that the vast majority of melanoidins prepared from glucose heated with either glycine or lysine was excreted in the feces and not absorbed (5-9). The human colon contains a total of *ca.* 10^{14} prokaryotic cells, and this represents more than 90% of all cells in the body (10). Moreover, it is now accepted that the flora of the large intestine play an important role in human health (10) but there is very little information concerning the effect of melanoidins on human colonic bacteria (11).

This study used an aqueous glucose-lysine model system and the objectives were two-fold. The effects of temperature/time combinations and of pH on the profiles of reaction products were investigated and some of the compounds were identified. Secondly, the effects of digestion on melanoidins were studied using *in vitro* stomach, small intestine and large intestine fermenters.

Experimental

Model systems were prepared by dissolving glucose (0.1 mol) and lysine monohydrochloride (0.1 mol) in water (100 ml). The pH was adjusted to the predetermined value (3, 4, 5, 6, 7) before heating using 3M hydrochloric acid or 3M sodium hydroxide solution. During heating (at 35, 55, 70, 80 °C and under reflux), pH control was achieved by intermittent addition of 3M sodium hydroxide solution. Systems were heated for up to 10 weeks (35 °C), 4 days (55 °C), 6 h (70 °C) and 2 h (under reflux). Further details are given by Bailey et al. (12).

Following cooling, model systems were analyzed by HPLC using a reversed phase column, a water-methanol gradient and detection at 280 and 460 nm (12). Selected peaks were isolated by solvent extraction, preparative HPLC and freeze-drying (13). Identifications were achieved by ^1H and ^{13}C nuclear magnetic resonance spectroscopy (NMR), including DEPT and COSY experiments, and electrospray mass spectrometry (ES-MS) (13).

Melanoidins samples (M) were prepared from the model system heated under reflux for 2 h at pH 5. Ultrafiltration was performed using a 3000 dalton

nominal molecular mass cut-off membrane (11). Elemental analysis was performed on the melanoidins.

Sample M was incubated at pH 2 with pepsin, to simulate digestion in the stomach. The resulting material (MP) was adjusted to pH 7 and incubated with bile and pancreatin to simulate digestion in the small intestine, to give MPB (11,14). MP and MPB were each subject to ultrafiltration and the ultrafiltrates were analyzed by HPLC to monitor for melanoidin degradation products. Digestion in the large intestine was simulated using anaerobic batch culture fermenters containing a basal growth medium and either sample M or sample MPB as the sole carbohydrate source. Fermenters were inoculated with feces to give a final concentration of 10 gL^{-1} (11). After 0, 6 and 24 h, samples were removed from the fermenter and enumerated following (a) plating out on to culture media designed to recover predominant gut bacterial groups and (b) using 16S rRNA probes in combination with a fluorescence *in situ* hybridization technique (FISH). Further details are given by Ames et al. (11). Samples were also removed for ultrafiltration and the ultrafiltrates were analyzed by HPLC.

Results and Discussion

HPLC Profiles of Colored Reaction Products

Profiling Maillard model systems using a technique such as HPLC permits the rapid comparison of the components of each system reacted under different sets of conditions. As well as indicating which peaks may be worthy of isolation and subsequent structural analysis, HPLC chromatograms can be used to compare the relative amounts of reaction products.

The chromatographic behavior of reaction products formed in aqueous sugar-amino acid model systems has previously been divided into four types (12) namely, unretained peaks, resolved peaks, a tailing broad band and a convex broad band. The convex broad band is due to high molecular mass material (melanoidins) (15). All four types of behavior are evident in Figure 1a which shows the 460 nm chromatogram obtained for the system heated under reflux for 2 h with the pH controlled at 5. Figure 1 also illustrates an example of the effect of heating conditions on the reaction product profile. Heating at $80 \text{ }^\circ\text{C}$ for 6 h (Figure 1b) resulted in a weaker chromatogram, fewer resolved peaks and a very much reduced convex broad band, compared to heating under reflux for 2 h (Figure 1a).

Compound Identification

The compounds responsible for five of the resolved peaks detected on the 280 nm chromatogram (see Figure 2) obtained for the systems heated for 6 h at $80 \text{ }^\circ\text{C}$ and pH 5 were isolated. Analysis by NMR and MS resulted in identifications for four of them (see Table I). All these compounds, except 1-

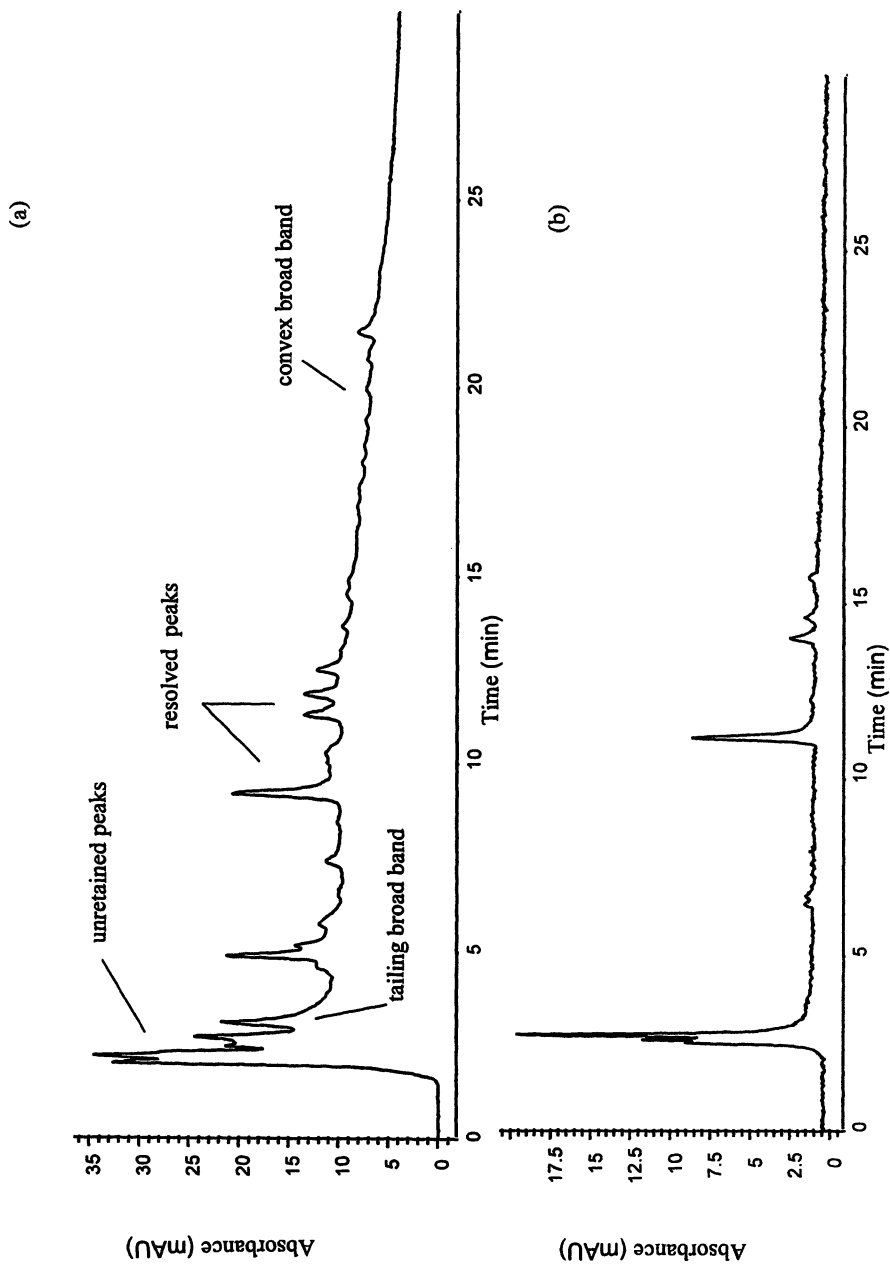


Figure 1: G/L at pH 5 (460 nm traces). Comparison of (a) reflux for 2 h with (b) 80 °C for 6 h.

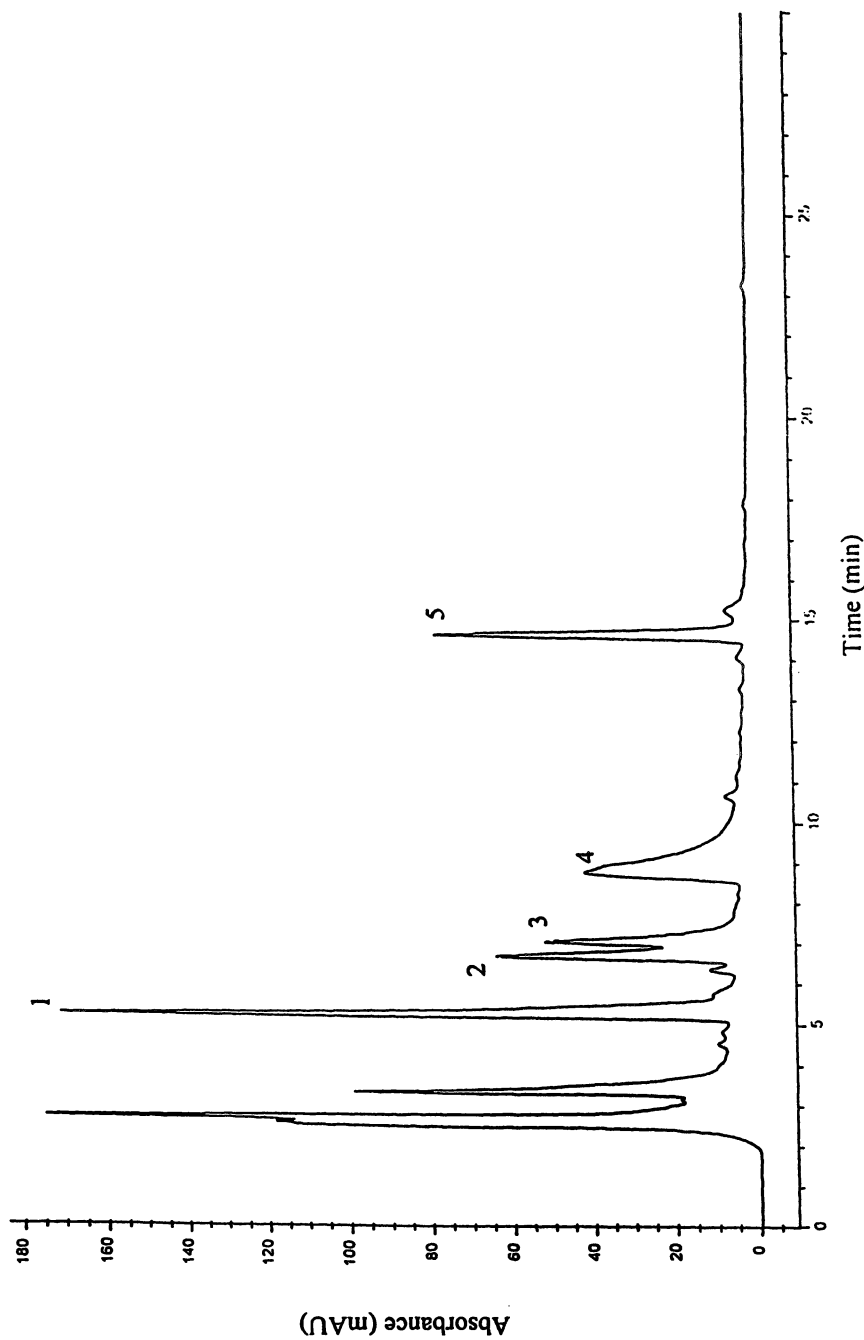


Figure 2. G/L at pH5 (280 nm trace).

Table I Compounds isolated from G/L heated at 80 °C for 6 h.

<i>Com- pound</i>	<i>Name</i>	<i>Structure</i>
1	1-(Carboxy-5-aminopentyl)-2-formyl-3-(1,2,3-trihydroxypropyl)-pyrrole	
2	2,3-Dihydro-3,5-dihydroxy-6-methyl-(4<i>H</i>)-pyranone	
3	(not identified)	
4	4-Hydroxy-2-(hydroxymethyl)-5-methyl-3(2<i>H</i>)-furanone	
5	2-Amino-6-(2-formyl-5-hydroxymethyl-1-pyrrolyl)-hexenoic acid (pyrraline)	

(carboxy-5-aminopentyl)-2-formyl-3-(1,2,3-trihydroxypropyl)-pyrrole, compound 1) are known Maillard reaction products. Compounds 1-5 are all colorless but they possess reactive groups and would be expected to participate in further reactions, including those leading to colored components. Compounds 2 and 4 are well known for their abilities to participate in further reactions. For example, compound 5 was first reported from glucose-lysine (16) and has subsequently been identified in enzymatic hydrolyzates of milk powders and bakery products (17). The epsilon amino group of lysine residues of proteins can react to give protein-bound pyralline. The closely related compound 1 would also be expected among the hydrolysis products of protein heated with carbonyl compounds, but it remains to be reported in such systems.

Effect of Heating Conditions on Reaction Products

Effect of Temperature/Time Combinations

Levels of compounds 1-5 formed at different temperature/time combinations are summarized in Figure 3. Figure 3a shows that the peak area for every compound decreases with temperature (although the heating time was increased as the temperature was decreased). Figure 3b is a plot of the %peak area for each compound at each temperature. This shows that compound 1 gives the largest peak at 55 and 35 °C and the relative amount of compound 1 increases as the temperature decreases from reflux to 55 °C. In contrast, under reflux, compound 4 gives by far the largest peak area and the relative amount decreases with decreasing temperature between reflux and 55 °C. Compound 2 was only detected at 80 °C and under reflux and accounted for less than 15% of the total peak area. Differences in the peak area and relative amount of each reaction product may be attributed to various factors including the activation energy of each component and the ease with which it can undergo subsequent reactions.

Effect of pH

In general, levels of most of the compounds increased with pH on heating at 80 °C for 6 h (Figure 4a). However, 5-hydroxymethylfurfural (HMF) gave lower peak areas at pH 4 than at pH 3 and was not detected at the higher pH values. Also, compound 3 was not detected above pH 5 and compounds 1 and 5 were not detected at pH 7. Figure 4b, which depicts the %peak area for each compound at each pH, shows this effect more clearly. HMF is favored by pH 3 and 4, compounds 2 and 4 dominate at pH 6 and 7 and compounds 1, 3 and 5 have the greatest %peak areas at pH 4-5.

The data presented in Figures 3 and 4 serve to illustrate how susceptible even a model Maillard system can be to variations in temperature/time combinations and pH. In real food systems, even more variables come into play, such as water activity, oxygen content, presence of metal ions and other reactive food components. In order to understand more fully the effects of several variables, careful experimental design coupled with statistical analysis of the data, e.g., using response surface regression analysis is required (3).

Possible Physiological Function of Melanoidins

The yield of melanoidins (based on the combined masses of glucose and lysine used) was *ca.* 0.5%. Elemental analysis gave 44.34% carbon, 7.31% hydrogen, 6.95% nitrogen and (by difference) 41.04% oxygen. This corresponded to an empirical formula of $C_{7.44}H_{14.62}NO_{5.22}$. Since the carbon:hydrogen ratio is about 1:2, this formula suggests little unsaturation or aromaticity.

HPLC analysis of the ultrafiltrates of the melanoidins after simulated stomach or small intestine digestion, i.e., the ultrafiltrates of samples MP and MPB, resulted in no melanoidin degradation products being detected. Therefore, work on simulated digestion in the large intestine focused on sample M, the melanoidin sample that had not been treated with pepsin, pancreatin or bile.

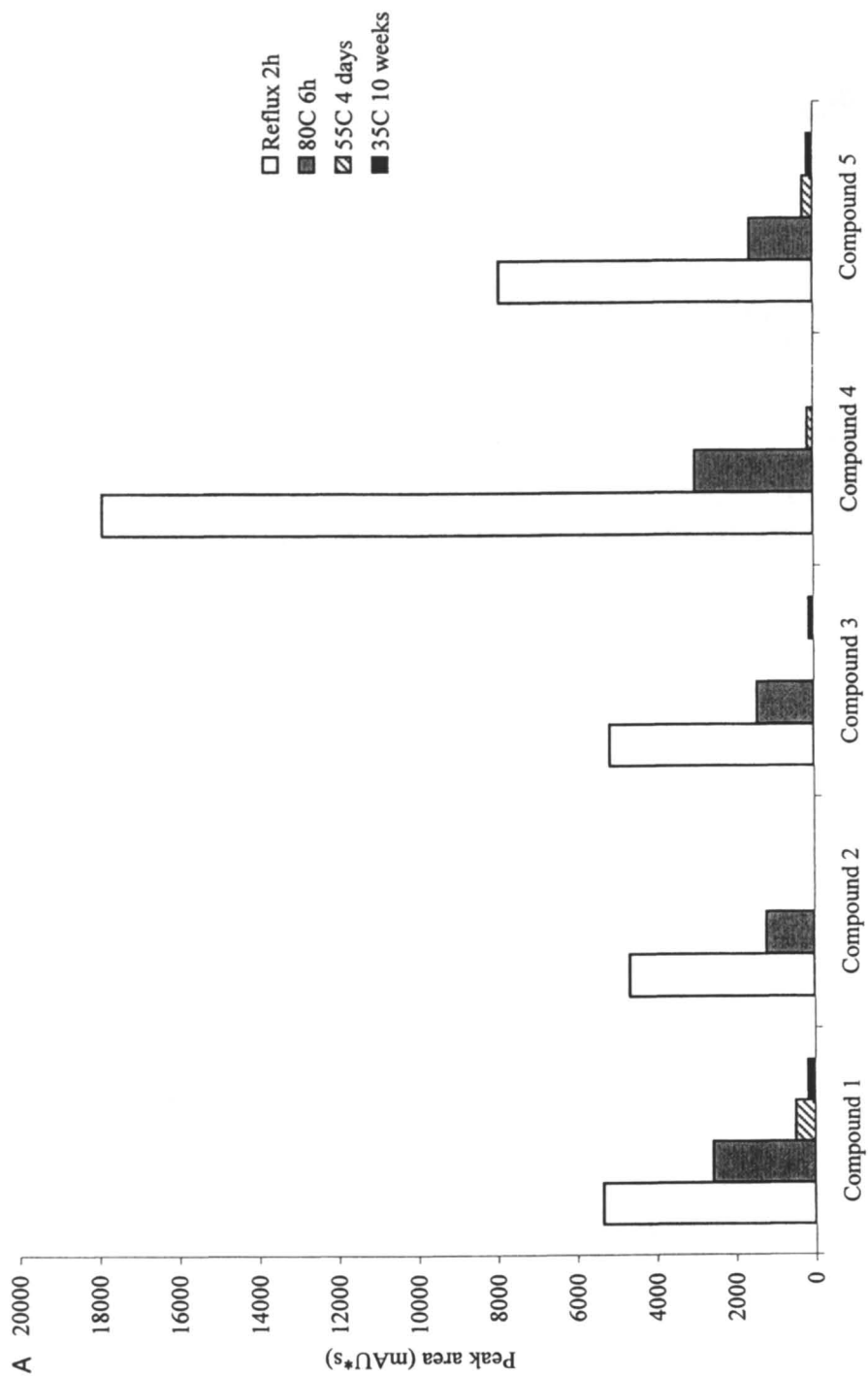
Two different methods, culturing on agar plates and the FISH probing technique, were used to enumerate bacteria from the batch fermenters. These two techniques provide complementary information. The cultural approach (agar plates) permits the growth of colonies of bacteria that are able to grow on the chosen media and these are counted after incubation. Thus, non-viable bacteria are not enumerated but the media are not completely selective, leading to errors. In contrast, the FISH technique, which is based on the principles of molecular biology, can be more specific than agar plates, but non-cultural organisms are also enumerated. The results from both procedures are illustrated in Figure 5 and it is immediately apparent that the FISH technique gave higher counts for every bacterial group at time zero, compared to agar plates.

Figure 5a shows a significant ($p < 0.05$) increase in numbers of total anaerobes, bacteroides and clostridia after 6 h incubation (compared to time zero), while bifidobacteria increased significantly ($p < 0.05$) after 24 h. In contrast, the FISH technique gave no significant differences in numbers of bacteria between 0 and 6 h, but bacteroides, clostridia and lactobacilli all increased significantly ($p < 0.05$) after 24 h (Figure 5b). However, the observed increase in lactobacilli using the FISH technique may be at least partially accounted for by the probe also responding to enterococci.

Therefore, fecal bacteria do respond to the presence of melanoidins prepared from glucose and lysine in an *in vitro* system. No convincing evidence could be found by HPLC for the presence of melanoidin degradation products, including bacterial metabolites of melanoidins, in the ultrafiltrates of the fermenter broth. Further work is needed using analytical conditions better suited to the analysis of components, including short chain fatty acids and free lysine.

Previous studies, using *in vitro* pure cultures systems (18) and rats (19), have demonstrated the ability of Maillard reaction products to increase lactobacilli. Horikoshi et al. (18) were also able to show no effect of total (low and high molecular mass) Maillard reaction products on enterococci, coliforms or clostridia.

There is almost no information available concerning the degradation of melanoidins by gut bacteria. It has been shown that various organisms unrelated to digestion in humans (*Coriulus versicolor* IFO 30340, and *Streptomyces werraensis* TT14) can decolorise model melanoidin prepared from xylose and glycine or from glucose and lysine while *Paecilomyces canadensis* NC-1 can decolorise xylose-glycine melanoidin only (20). However, melanoidin degradation products were not investigated.



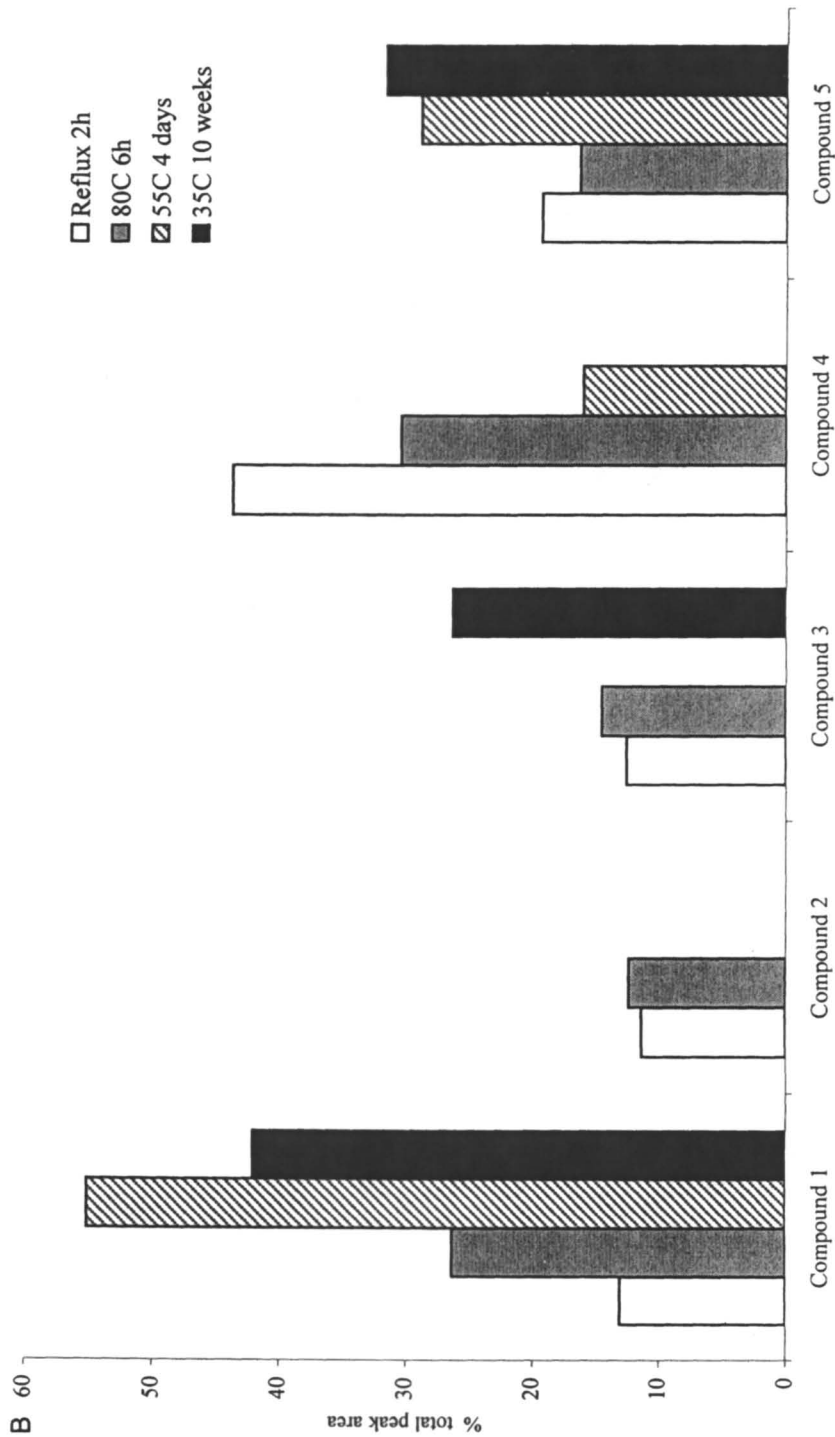
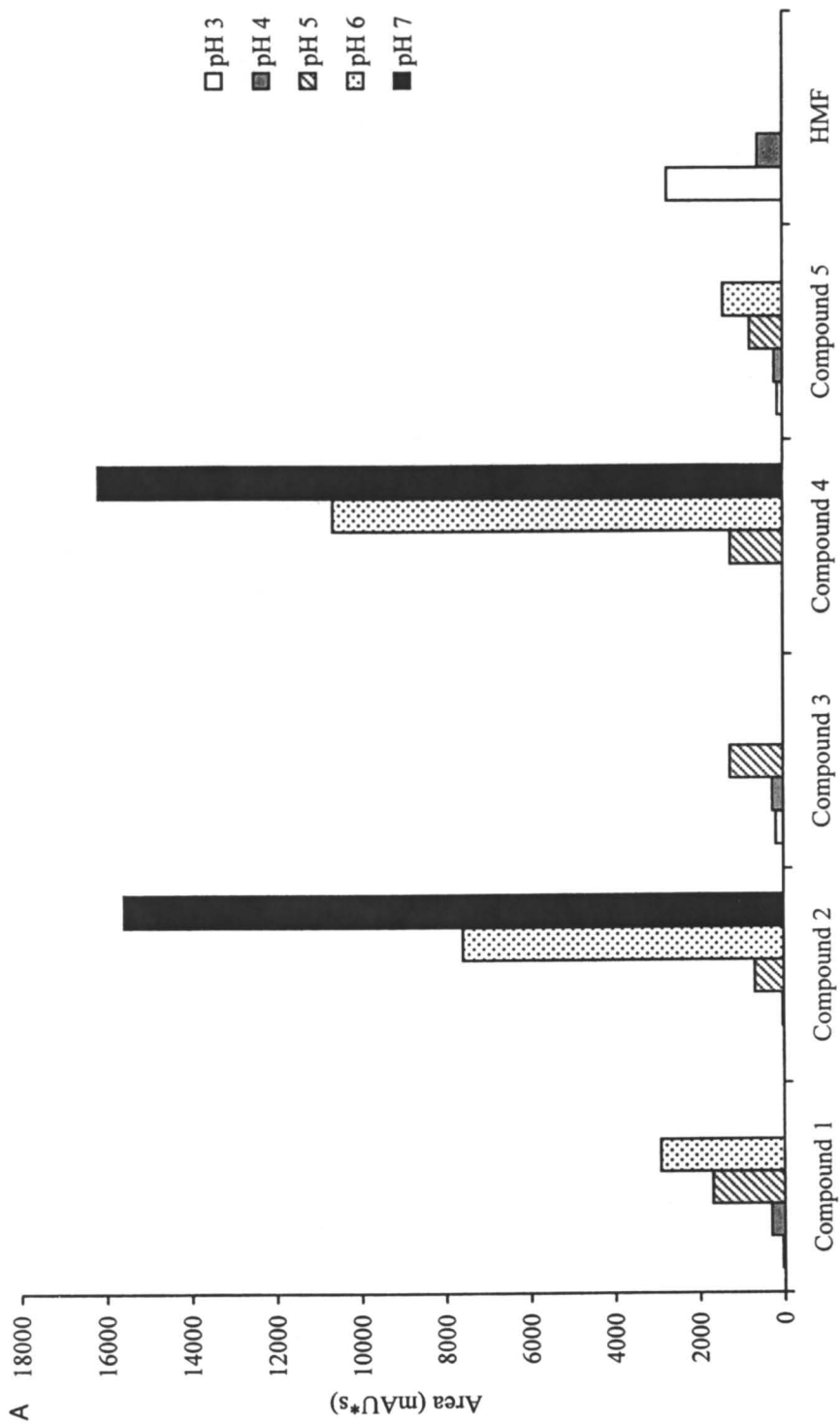


Figure 3. Variation in peak area with temperature/time (pH 5). (a) All 4 temperatures. (b) Area of each peak as a % of the total at each temperature/time.



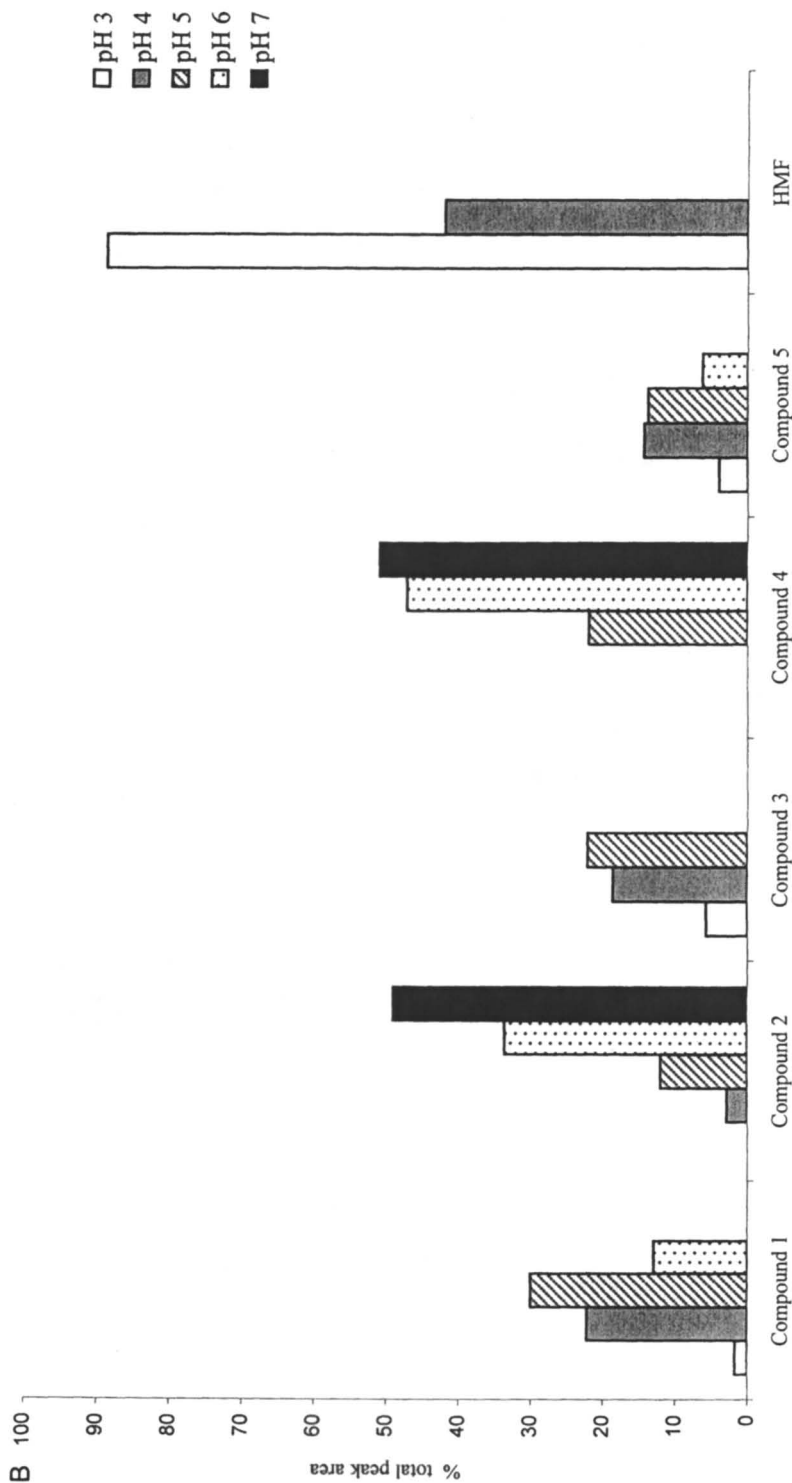
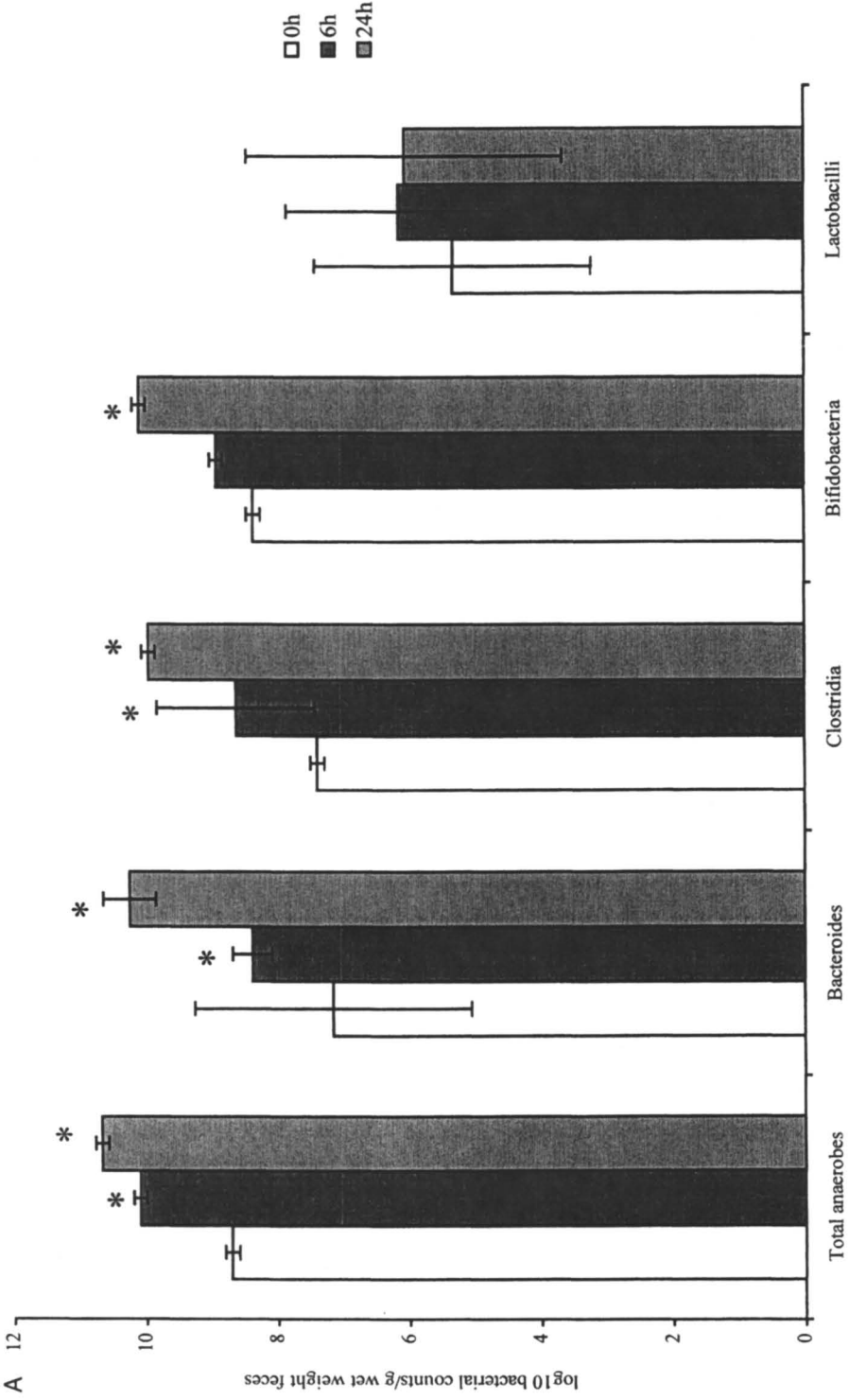


Figure 4. Variation in peak area with pH (80 °C for 6 h). (a) All 5 pH values. (b) Area of each peak as a % of the total at each pH.



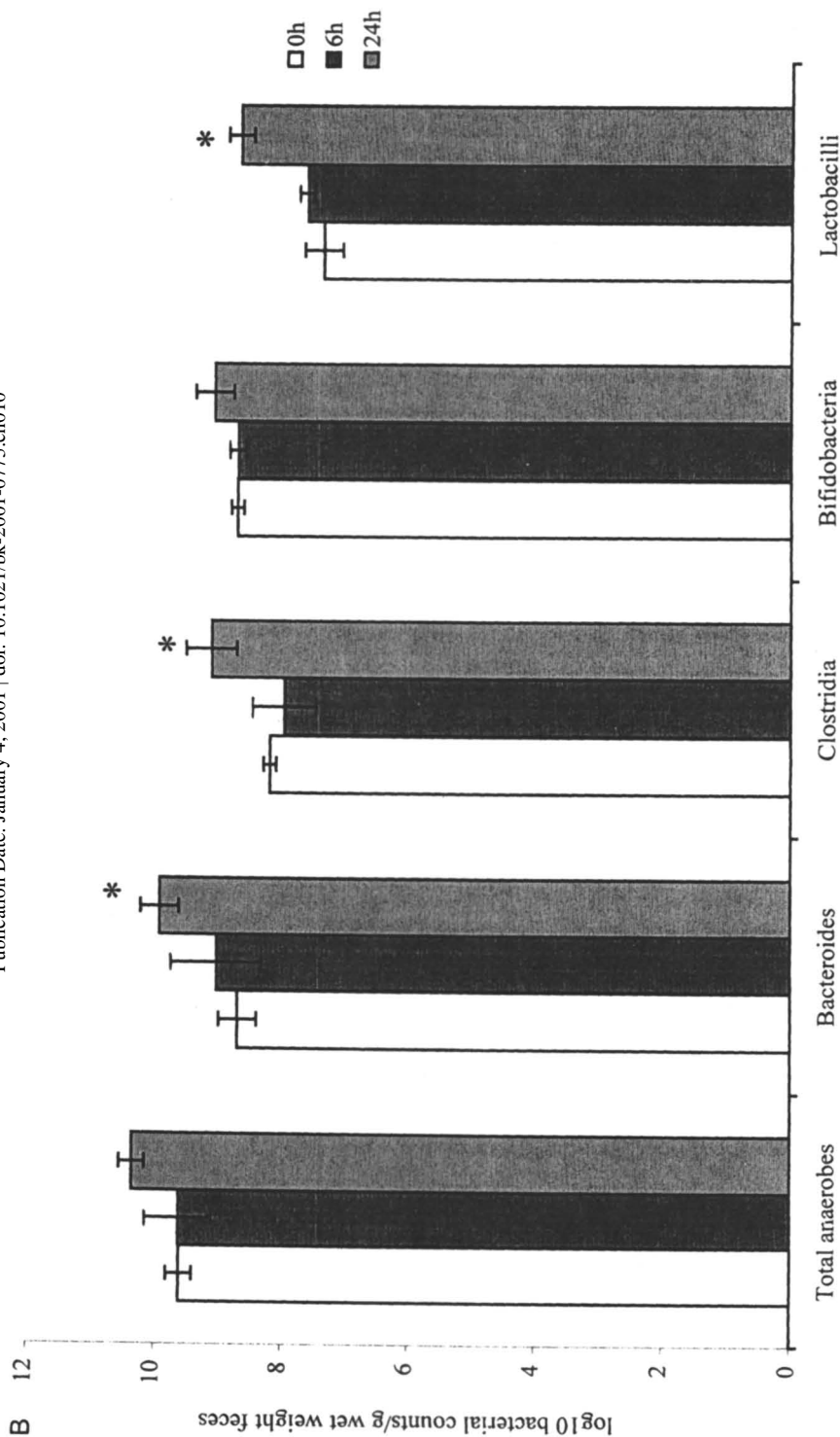


Figure 5. Effects of the fermentation of melanoidins (sample M) in batch culture fermenters on fecal bacteria after incubation for 0, 6 and 24 h, as evidenced by enumeration on (a) agar plates and (b) FISH probes. (11). Values are the means of triplicate experiments. *, $p < 0.05$.

Conclusion

A new Maillard reaction product is reported from a glucose-lysine model system. The relative amounts of Maillard reaction products are affected by both temperature/time and the pH conditions applied. Further work is needed to understand the affects of different processing parameters on levels of Maillard reaction products and, ultimately, to apply the results of such findings in the food industry.

Melanoidins prepared from glucose and lysine allow the growth of certain human gut bacteria. If the bacteria are able to use melanoidins as a source of carbohydrate, the resulting degradation may also result in the release or binding of other components in the gut, such as metal ions.

Acknowledgments

Saskia Plos and Andrea Hofmann (University of Münster, Germany) are thanked for expert technical assistance, and The University of Reading is thanked for a travel grant. The work was partly funded by the European Union (grant CT1080).

References

1. Ames, J.M. *Food Chem.* **1998**, *62*, 431-439.
2. Ames, J.M. *Trends in Food Science and Technology* **1990**, *1*, 150-154.
3. Bates, L.; Ames, J.M.; MacDougall, D.B.; Taylor, P. *J. Food Sci.* **1998**, *63*, 991-996.
4. O'Brien, J.; Morrissey, P.A. *Crit. Revs. Food Sci. Nutr.* **1989**, *28*, 211-248.
5. Finot, P.A.; Magnenat, E. In *Maillard Reactions in Food*; Eriksson, C., Ed.; Pergamon Press: Oxford, UK, 1981, pp. 193-207.
6. Homma, S.; Fujimaki, M. In *Maillard Reactions in Food*; Eriksson, C., Ed.; Pergamon Press: Oxford, UK, 1981, pp. 209-216.
7. Nair, B.M.; Oste, R.; Asp, N.G.; Pernemalm, P.-A. In *Maillard Reactions in Food*; Eriksson, C., Ed.; Pergamon Press: Oxford, UK, 1981, pp. 217-222.
8. Finot, P.A. (1990) In *The Maillard Reaction in Food Processing, Human Nutrition and Physiology*; Finot, P.A.; Aeschbacher, H.U.; Hurrell, R.F.; Liardon, R., Eds.; Birkhäuser: Basel, Switzerland, 1990, pp. 259-271.
9. Lee, I.E.; van Chuyen, N.; Hayase, F.; Kato, F. *Bioscience, Biotechnology and Biochemistry* **1992**, *56*, 21-23.
10. Gibson, G.R.; Wynne, A.; Bird, A. In *Encyclopedia of Human Nutrition*; Sadler, M.J.; Strain, J.J.; Caballero, B., Eds.; Academic Press: London, UK, 1999, pp. 1282-1289.
11. Ames, J.M.; Wynne, A.; Hofmann, A.; Plos, S.; Gibson, G.R. *British Journal of Nutrition* **1999**, *82*, 489-495.
12. Bailey, R.G.; Ames, J.M.; Monti, S.M. *J. Sci. Food Agric.* **1996**, *72*, 97-103.

13. Bailey, R.G., Ames J.M. and Mann, J. unpublished.
14. Minihane, A.-M.; Fox, T.E.; Fairweather-Tait, S.J. *Bioavailability* **1993**, *93*, 175-179.
15. Royle, L.; Bailey, R.G.; Ames, J.M. *Food Chem.* **1998**, *62*, 425-430.
16. Nakayama, T.; Hayase, F.; Kato, H. *Agric. Biol. Chem.* **1980**, *44*, 1201-1202.
17. Henle, T.; Schwarzenbolz, U.; Walter, A.W.; Klostermeyer, H. In *The Maillard Reaction in Foods and Medicine*; O'Brien, J.; Nursten, H.E.; Crabbe, M.J.C.; Ames, J.M., Eds.; Royal Society of Chemistry: Cambridge, UK, 1998, pp 178-183.
18. Jemmali, M. *Journal of Applied Bacteriology* **1969**, *32*, 151-155.
19. Horikoshi, M.; Ohmura, M.; Gomyo, T.; Kuwabara, Y.; Ueda, S. In *Maillard Reactions in Food*; Eriksson, C., Ed.; Pergamon Press: Oxford, UK, 1981, pp. 223-228.
20. Terasawa, N.; Murata, M.; Homma, S. *J. Food Sci.* **1996**, *61*, 669-672.

Chapter 11

The Color Activity Concept: An Emerging Technique to Characterize Key Chromophores Formed by Non-Enzymatic Browning Reactions

T. Hofmann, O. Frank, and S. Heuberger

Deutsche Forschungsanstalt für Lebensmittelchemie,
Lichtenbergstrasse 4, D-85748 Garching, Germany

It is well accepted that the non-enzymatic browning of thermally processed foods originates mainly from the Maillard reaction between reducing carbohydrates and amino compounds. To evaluate the key chromophores amongst the multiplicity of reaction products formed, a screening method was developed which is based on the determination of the visual threshold of colored fractions obtained after HPLC separation. This so called Color Dilution Analysis (CDA) is exemplified in the following paper which describes a browned aqueous xylose/furan-2-aldehyde/L-alanine solution. Twenty colored fractions were obtained, amongst which five fractions were evaluated with by far the highest color impacts. The identification experiments were, therefore, focused on the compounds evoking the intense color of these fractions. They revealed two 3(2*H*)-furanones (I, II), a 3(2*H*)-pyrrolinone (III), a pyrano[2,3-*b*]pyranone (IV) and a dione (V) as the key chromophores. In order to evaluate the color impact of these color-active compounds more exactly, their absolute color contribution was measured by calculating their color activity values as the ratio of their concentrations to their color detection thresholds. By application of this novel analytical strategy, which we call the color activity concept, 13.5 % of the overall color of the reaction mixture was shown to be accounted for five colorants of known structures.

Besides the unique aroma, brown color is a key factor in consumer acceptance of thermally processed foods such as, e.g. roasted coffee, bread crust or roasted meat. This non-enzymatic browning mainly originates from interactions between reducing carbohydrates and amino compounds, known as the Maillard reaction. In spite of the long-standing interest in Maillard-derived

food coloring materials, surprisingly little is known about the chromophores responsible for the typical brown color.

Due to the complexity and multiplicity of the non-volatile Maillard reaction products (1), several model studies have been conducted in order to provide more information on the structures of the colored compounds formed. However, most reactions have been carried out in organic solvents, rather than in aqueous solution, and using synthetically related amines instead of amino acids (2,3). Because these amines do, however, not occur in foods, it is questionable, whether the results of such studies can be extrapolated to the situation in real food systems. Very recently, systematic studies indicated condensation reactions between methylene-active intermediates and carbonyl compounds, both derived from carbohydrate degradation, as a general key reaction type in non-enzymatic browning (4-6).

It is well accepted in the literature that the amino acid-catalyzed conversion of reducing carbohydrates during the Maillard reaction results in a tremendous variety of reactive carbonyl compounds as well as methylene-active compounds (4,7). The reaction of a certain methylene-active compound such as, e.g., 4-hydroxy-5-methyl-3(2H)-furanone (norfuranol), with different carbonyls such as, e.g., furan-2-aldehyde, pyrrolaldehydes, acetaldehyde, acetone or 2-oxopropanal (Figure 1), was found to generate the same type of chromophore varying only in their substituents (2,8). In order to reduce the multiplicity of derivatives of one type of chromophore to one key colorant representing that class of chromophore, we forced all methylene-active intermediates to react with the same carbonyl compound by heating carbohydrate/amino acid mixtures in the presence of an excess amount of a major carbohydrate derived carbonyl such as furan-2-aldehyde (5).

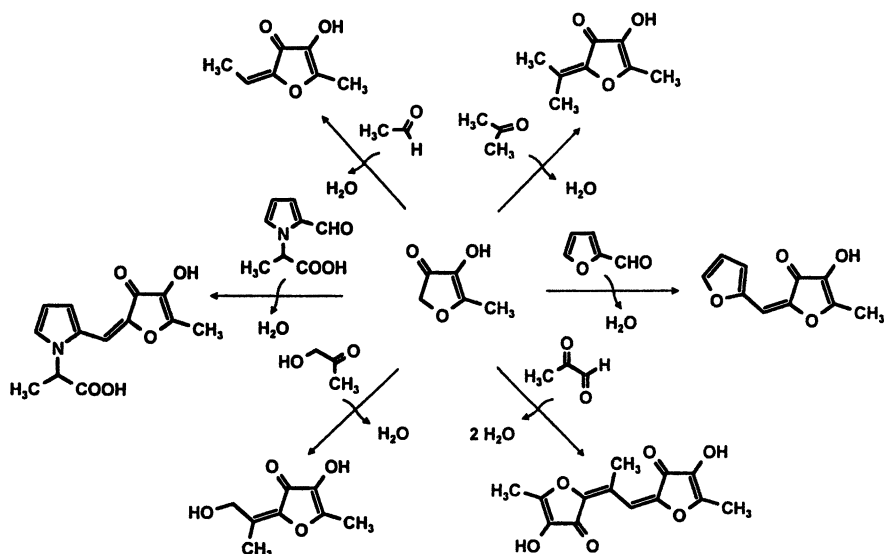


Figure 1. Formation of colored condensation products from carbohydrate-derived carbonyls and 4-hydroxy-5-methyl-3(2H)-furanone (norfuranol).

Besides the lack in information on the structures of Maillard-type chromophores, it is unclear to what extent these chromophores really contribute to the overall color of non-enzymatically browned Maillard mixtures. In the last 15 years, the identification of odor-active compounds by aroma extract dilution analyses and the calculation of so called odor activity values as the ratio of concentration to odor threshold of individual odorants has been successfully used to elucidate the contribution of single odor-active compounds to the overall aroma of processed flavors generated by thermal treatment of carbohydrate/amino acid mixtures (9-11) as well as of foods such as, e.g., wheat and rye bread crust (12) or fresh strawberry juice (13). The same analytical strategy might be promising to establish the contribution of key chromophores in evoking the overall color of browned carbohydrate/amino acid mixtures.

The aim of the following study was, therefore, (i) to develop an analytical strategy offering the possibility of characterizing the key chromophores formed in Maillard reactions and (ii) to rank them according to their color activities. This concept will be demonstrated using an aqueous xylose/L-alanine solution heated in the presence of the pentose degradation product, furan-2-aldehyde.

Experimental

The following reference compounds were prepared as recently reported in the literature: 2-[(Z)-(2-furyl)methylidene]-4-hydroxy-5-methyl-2H-furan-3-one, I (14); 2-[(Z)-(2-furyl)methylidene]-4-hydroxy-5-[(E)-(2-furyl)methylidene]-methyl-2H-furan-3-one, II (14); 2-[(E)-(2-furyl)methylidene]- and 2-[(Z)-(2-furyl)methylidene]-(S)-4-[(E)-1-formyl-2-(2-furyl)ethenyl]-5-(2-furyl)-2,3-dihydro- α -amino-3-oxo-1H-pyrrole-1-acetic acid, III (15,16); (1R,8aR)- and (1S,8aR)-4-(2-furyl)-7-[(2-furyl)methylidene]-2-hydroxy-2H,7H,8aH-pyrano[2,3-b]pyran-3-one, IV (14); (E)- and (Z)-1-furyl-1-[(2-furyl)methylidene]butane-2,3-dione, V (8); (2R)-4-oxo-3,5-bis[(2-furyl)methylidene] tetrahydropyrrolo-[1,2-c]-5-(S/R)-(2-furyl)oxazolidine, VI (5).

Maillard Reaction Mixture

A solution of D-xylose (66 mmol) and L-alanine (16 mmol) in phosphate buffer (90 mL; 1 mmol/L, pH 7.0) was refluxed for 15 min, then, furan-2-aldehyde (100 mmol) was added and heating was continued for another 60 min. After cooling, the pH was adjusted to 3.0 and the aqueous mixture was extracted with ethyl acetate. The combined organic layers were dried over Na₂SO₄, the volatiles were removed in high vacuo and the colored residue was dissolved in ethyl acetate.

Color Dilution Analysis

An aliquot of the solvent extractable non-volatile fraction of the Maillard reaction mixture was analyzed by HPLC/DAD. The effluents of peaks exhibiting absorption maxima above 320 nm were separately collected and were diluted with water to exactly 1 mL. The colored fractions were then diluted stepwise, 1:1, with water and each dilution was visually judged until a color difference between

the diluted fraction in a glass vial (10 mm i.d.) and two blanks (tap water) could just be detected visually. This dilution was defined as the Color Dilution (CD)-factor (14).

Quantification

The solvent-extractable fraction of the reaction mixture was first pre-separated by column chromatography using silica gel. After membrane filtration, the sub-fractions were analyzed by RP-HPLC and the colorants detected were quantified by comparing the peak areas obtained at the absorption maximum of each colorant with those of defined standard solutions of each reference compound in acetonitrile (17).

Results and Discussion

Thermal treatment of an aqueous solution of xylose and L-alanine in the presence of furan-2-aldehyde led to a rapid colorization of the reaction mixture. Colored reaction products were registered after separation of the non-volatile fraction by RP-HPLC using a diode array detector monitoring in the wavelength range between 220 and 500 nm. To characterize the key chromophores, i.e., those mainly evoking the color of the mixture, we developed the so called Color Activity Concept (17), consisting of the following five analytical steps:

- Screening of the most intense colored reaction products by application of the Color Dilution Analysis
- Identification of the compounds evaluated with the highest color impacts
- Quantification of the most color-active compounds
- Calculation of color activity values on the basis of a dose/activity relationship
- Estimation of the percent contribution of each chromophore to the overall color of the Maillard mixture.

Screening for Intense Colored Compounds by Color Dilution Analysis

The browned solution consisted of a tremendous variety of different reaction products, of which only a limited number of key chromophores were expected to contribute significantly to the overall color of the Maillard mixture. Since the aim was to locate these key colorants in the complex reaction mixture, we recently developed a screening technique, which we call Color Dilution Analysis (CDA), offering the possibility of ranking the colored compounds according to their relative color impact (14). Thus, an aliquot of the reaction mixture was separated by RP-HPLC (Figure 2, left side), and the effluents of peaks were separately collected in one HPLC run. Twenty colored fractions were obtained, which were then ranked in order of color intensity. To achieve this, these fractions were diluted with water to the same volume. Each fraction was then diluted stepwise (1:1) with water and each dilution was judged visually by color using a triangle test until the detection threshold was reached. The dilution, at which a color

difference between the diluted fraction and two blanks (tap water) could just be visually detected, was defined as the Color Dilution (CD)-factor (14). As the CD factor obtained for each compound is proportional to its color activity in water, it allows the ranking of the 20 fractions according to their relative color intensity, which is outlined in Figure 2 (right side). On the basis of their high CD factors the yellow colored fraction no. 7 and the red colored fraction no. 17 possessed the highest color impacts, followed by the red and orange colored fractions no. 9 and no. 12, respectively, showing somewhat lower color activities (Figure 2). Fractions no. 1, 4, 6, 10, 13-15, 18 and 20 showed significantly lower CD factors and are, therefore, only of minor importance to the color of the reaction mixture.

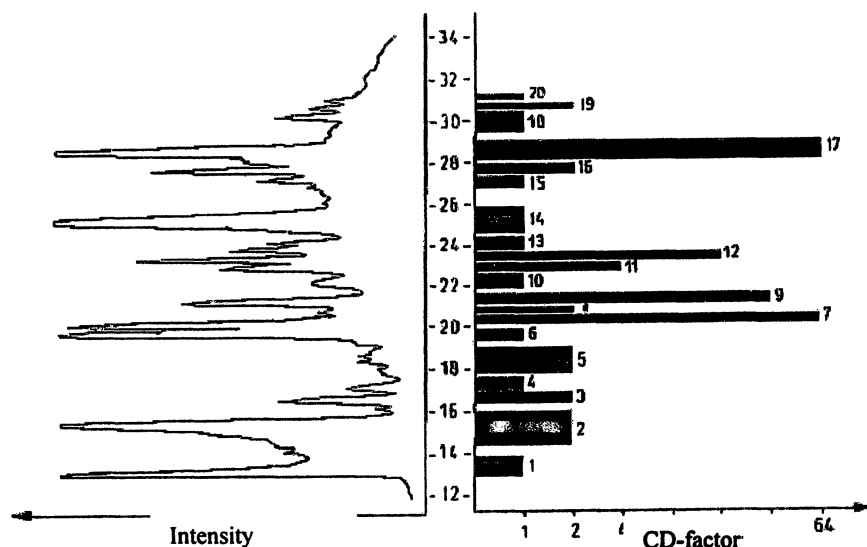


Figure 2. RP-HPLC chromatogram ($\lambda = 320 \text{ nm}$; left side) and Color Dilution (CD) chromatogram (right side) of the solvent-extractable fraction of the reaction mixture.

The striking advantage of this screening procedure is that the key chromophores can be located in complex Maillard mixtures without knowledge of their structures. The identification experiments were then focused on the compounds evoking the color of the fractions 7, 9, 12 and 17 and, in consequence, contributing mainly to the color of the heated Maillard mixture. In addition, the chromophores in fractions no. 16 and 19, which possessed somewhat lower CD-factors, were included in the identification experiments.

Identification of the Most Intense Colored Reaction Products

For the identification of the key colorants in fractions no. 7 and no. 17, exhibiting absorption maxima at 360 and 426 nm, respectively, the colored fractions were separated by flash chromatography on silica gel as well as RP-18 material. On the basis of NMR, LC/MS, and UV/VIS spectroscopical measurements their structures were proposed as 2-[(Z)-(2-furyl)methylidene]-4-

hydroxy-5-methyl-2*H*-furan-3-one (**I**, Figure 3) and 2-[(*Z*)-(2-furyl)methylidene]-4-hydroxy-5-[(*E*)-(2-furyl)methylidene]-methyl-2*H*-furan-3-one (**II**, Figure 3). These structures could be confirmed by synthesis from 4-hydroxy-5-methyl-2*H*-furan-3-one and furan-2-aldehyde (*14*). Both colorants were described earlier in the literature (*4*), however, their importance in evoking the color of a Maillard mixture has not previously been documented.

In fraction no. 9, which was evaluated with a CD factor of 32, an intense red colored compound was detected exhibiting absorption maxima at 330, 414 and 480 nm. On the basis of identical chromatographic and spectroscopic data obtained for a red colored compound synthesized recently from furan-2-aldehyde and L-alanine (*15,16*), this compound could be unequivocally identified as a mixture of 2-[(*E*)-(2-furyl)methylidene]- and 2-[(*Z*)-(2-furyl)methylidene]-(*S*)-4-[(*E*)-1-formyl-2-(2-furyl)ethenyl]-5-(2-furyl)-2,3-dihydro- α -amino-3-oxo-1*H*-pyrrole-1-acetic acid (**III**, Figure 3) existing in a ratio of 15:1.

After chromatographic separation of the colored fraction no. 12, an intense orange colored compound could be isolated showing an absorption maximum at 460 nm. The determination of its chemical structure was performed by several one- and two-dimensional NMR techniques, and, in addition, by LC/MS and UV/VIS spectroscopy. The spectroscopic data were consistent with the structure of 4-(2-furyl)-7-[(2-furyl)methylidene]-2-hydroxy-2*H*,7*H*,8*aH*-pyrano[2,3-*b*]pyran-3-one (**IV**, Figure 3) existing as a mixture of the (1*R*,8*aR*)- and the (1*S*,8*aR*)-diastereomers (*14*). The proposed hemiacetal structure was further confirmed by formation of the corresponding 2-ethoxy derivatives upon heating an ethanolic solution of **IV** in the presence of trace amounts of hydrochloric acid (*14*). To our knowledge, this intense orange colored compound **IV** showing an extinction coefficient of $1.0 \times 10^4 \text{ l mol}^{-1} \text{ cm}^{-1}$ (in water, pH 7.0) has not been previously described in the literature.

From fraction 16, evaluated with a somewhat lower color impact, an intense yellow colored compound (**V**) was isolated by flash-chromatography, showing an absorption maximum of 320 nm and a shoulder at 340 nm. NMR studies and mass spectroscopic measurements suggested the structure of **V** to be a 3:2-mixture of (*E*)- and (*Z*)-1-furyl-1-[(2-furyl)methylidene]butane-2,3-dione (**V**, Figure 3). The proposed structure could be confirmed by synthesis from furan-2-aldehyde and hydroxy-2-propanone, as reported in the literature (*18*).

Although judged with a somewhat lower CD factor, an additional red colored compound could be successfully isolated from fraction no. 19, showing an extinction coefficient of $1.0 \times 10^4 \text{ l mol}^{-1} \text{ cm}^{-1}$ at 456 nm (in water, pH 7.0). On the basis of one and two-dimensional NMR experiments and LC/MS, as well as UV/VIS spectroscopy, the structure of compound **VI** was assumed to be a mixture of (2*R*)-4-oxo-3,5-bis-[(2-furyl)methylidene]tetrahydropyrrolo-[1,2-*c*]-5(*S*)-(2-furyl)-oxazolidine and its 5(*R*)-(2-furyl)-oxazolidine diastereomer (Figure 3). Very recently (unpublished results), the proposed structure of **VI** was confirmed following the synthetic sequence outlined in Figure 4. Starting with 4-hydroxyproline methylester (**1**), the amino- and the hydroxy-function was first BOC-protected (**2**), and the ester function was then reduced to the primary alcohol (**3**). Deprotection upon exposure of trifluoroacetic acid (**4**), followed by reaction with furan-2-aldehyde yielded the oxazolidine system (**5**). Using pyridinium chlorochromate, **5** was mildly oxidized to the corresponding

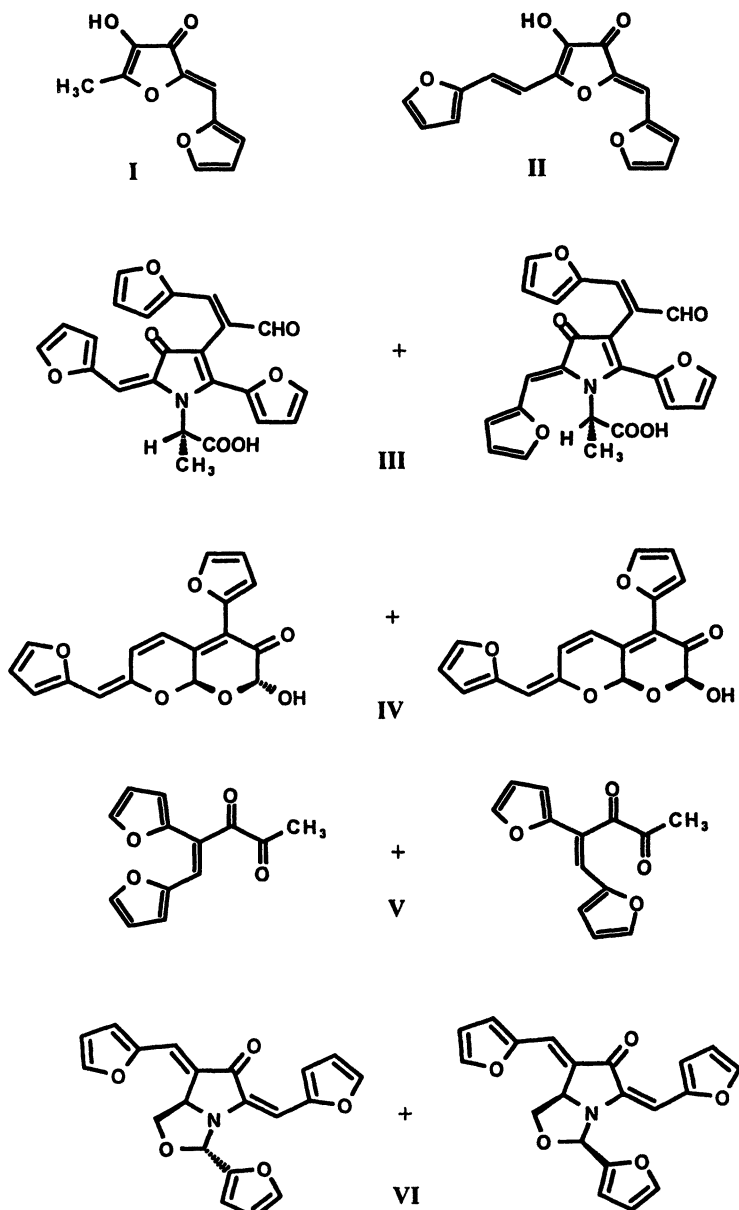


Figure 3. Structures of the key colorants identified: 2-[(Z)-(2-furyl)methylidene]-4-hydroxy-5-methyl-2H-furan-3-one (**I**), 2-[(Z)-(2-furyl)methylidene]-4-hydroxy-5-[(E)-(2-furyl)methylidene]-methyl-2H-furan-3-one (**II**), 2-[(E)-(2-furyl)methylidene]- and 2-[(Z)-(2-furyl)methylidene]-(S)-4-[(E)-1-formyl-2-(2-furyl)ethenyl]-5-(2-furyl)-2,3-dihydro- α -amino-3-oxo-1H-pyrrole-1-acetic acid (**III**), (1R,8aR)- and (1S,8aR)-4-(2-furyl)-7-[(2-furyl)methylidene]-2-hydroxy-2H,7H,8aH-pyran[2,3-b]pyran-3-one (**IV**), (E)- and (Z)-1-furyl-1-[(2-furyl)methylidene]butane-2,3-dione (**V**), (2R)-4-oxo-3,5-bis[(2-furyl)methylidene]tetrahydropyrrolo-[1,2-c]-5(S/R)-(2-furyl)oxazolidine (**VI**).

pyrroline-3-one (**6**), which was subsequently condensed with furan-2-aldehyde, yielding the colored target compound **7**, which showed identical spectroscopic data to compound VI, isolated from the Maillard mixture. To our knowledge, this red colored compound has not previously been reported in the literature.

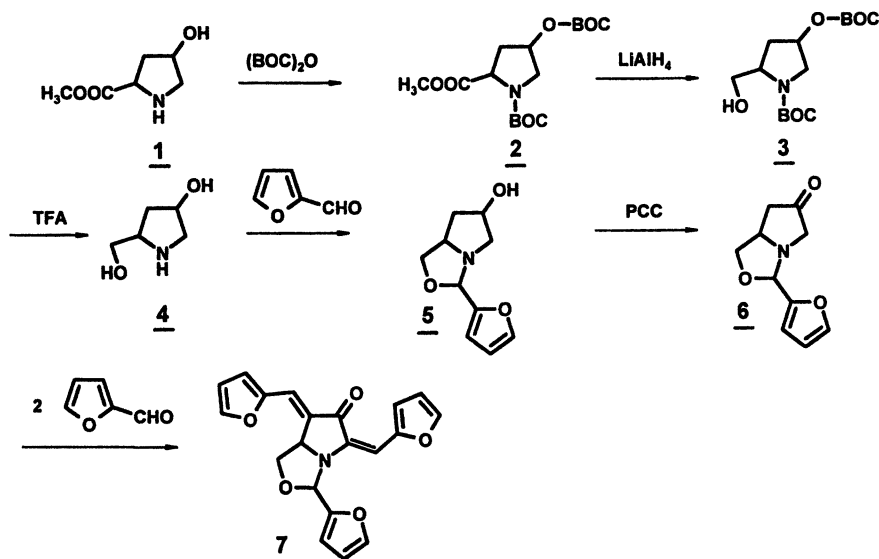


Figure 4. Synthetic sequence used for the preparation of (2*R*)-4-oxo-3,5-bis[(2-furyl)methylidene] tetrahydropyrrolo-[1,2-*c*]-5(*S/R*)-(2-furyl)oxazolidine (VI).

Although the most intense colored compounds in fraction nos. 7, 9, 12, 16, 17 and 19 of the color dilution analysis have been identified, it is possible that additional colorants of unknown structure co-eluted in the effluents of these fractions. This would result in an overestimation of the CD-factor and, consequently, also in the color contribution of the compounds I-VI. To determine the contribution of the colorants more accurately, the amounts of compounds I-VI were quantified in the browned reaction mixture.

Quantification of Selected Key Colorants

The browned Maillard mixture was separated by HPLC and colorants I-VI were quantified by means of diode array detection using the pure reference compounds as external standards (Table I).

The data, given in Table I, showed that the 3(2*H*)-furanone chromophores I and II were formed at levels of 142.5 and 163.8 mg per kg of the Maillard reaction mixture, respectively, which represented by far the highest concentrations of colorants. The pyrano[2,3-*b*]pyranone IV and the 3(2*H*)-pyrrolinone III, respectively, were present in somewhat lower amounts, i.e., 4.2 and 6.9-fold lower concentrations of IV and III, respectively, were determined compared to II. The yellow colorant V was found only in trace amounts.

Table I. Concentrations of selected colored compounds Formed in the Maillard reaction mixture (MRM)

<i>Colorant^a</i>	<i>Concentration [mg/kg of MRM]</i>
I	142.5
II	163.8
III	23.8
IV	38.8
V	0.6
VI	5.0

^a The structures of the colorants are displayed in Figure 3.

Calculation of Color Activity Values

However, the quantitative data alone do not allow an estimation of the importance of these colorants in evoking the overall color of the browned solution. In order to gain insights into their color contribution, the actual amount of each colorant in the Maillard mixture was correlated with its visual detection threshold by combining chemical and instrumental techniques with visual (sensory) analysis. To determine the color impact of a single colored reaction product, we recently defined the Color Activity Value (CAV) of a colorant, *x*, as the ratio of its concentration to its detection threshold, as follows (17):

$$CAV_x = \frac{\text{concentration}_x (\mu\text{g/kg})}{\text{detection threshold}_x (\mu\text{g/kg})}$$

Colorants, the actual concentrations of which in a solution are at or above their detection threshold, show, by definition, CAVs ≥ 1 and, consequently, contribute to the overall color of the solution.

To calculate the CAVs of colorants I-VI, first, the detection threshold of each compound was determined in water (Table II). Aqueous solutions containing known amounts of each colorant were diluted step by step with water until no color difference between the diluted sample and two blanks containing tap water could be detected visually using a triangle test (17). As given in Table II, the lowest threshold of 0.6 mg/kg (water) was found for colorant V, followed by the pyrrolinone III with 1.0 mg/kg. In comparison, colorant VI showed a 11-fold higher detection threshold concentration compared to compound V.

Using the color activity concept, the colorants I-VI were then ranked according to their color activities as given in Table II. The highest color activity of 95 was found for I, followed by II showing a 1.5-fold lower CAV (17). Also, colorant III showed a high color activity, because its concentration was 24-fold above its detection threshold. Despite the higher concentration of colorant IV in

Table II. Detection thresholds and color activity values (CAV) of selected colored compounds in the Maillard mixture

<i>colorant^a</i>	<i>Detection threshold^b</i> <i>[mg/kg water]</i>	<i>CAV^c</i>
I	1.5	95
II	2.5	66
III	1.0	24
IV	4.1	10
V	0.6	1
VI	6.2	<1

^a The structures of the colorants are displayed in Figure 3.

^b The detection threshold was determined in water using a triangle test.

^c Color Activity Value (CAV) is calculated from the ratio of the concentration to the visual threshold (in water).

comparison to **III**, this colorant contributed less than **III** to the overall color, because its detection threshold was more than 4-fold higher. These data demonstrate that, after identification and quantification of the colorants, the calculation of CAVs is necessary to rank colorants based on their color contribution. Since it possesses a $CAV < 1$, colorant **VI** is not involved in the overall color of the reaction mixture; its concentration of 5 mg/kg in the Maillard mixture was below its detection threshold concentration.

Estimation of the Color Contribution of Key Chromophores

The calculated CAVs rank the colorants based on their relative effectiveness in generating the overall color of the browned Maillard mixtures. To evaluate the percent color contribution of a chromophore, the measurement of the overall color intensity of the browned Maillard solution is a necessary prerequisite. To achieve this, the color dilution factor of the complete reaction mixture, the CD_{total} -factor, was determined. The complete Maillard solution was diluted step by step with water until no color difference between a diluted aliquot and two blanks containing tap water could be detected visually using a triangle test. A CD_{total} -factor of 1450 was found for the browned aqueous mixture, indicating that the color of the undiluted, original reaction mixture was 1450-fold above its detection threshold. Also, the CAV of a distinct colorant corresponds, by definition, to the factor to which the actual concentration is above the detection threshold. The percent color contribution of a single colorant, x , could, therefore, be calculated from the color activity value of the colorant (CAV_x) and the CD_{total} factor of the complete Maillard mixture, which was defined as possessing a color activity of 100 %, as follows (17):

$$\text{color contribution of compound } x \text{ [\%]} = \frac{\text{CAV}_x}{\text{CD}_{\text{total}}} \times 100$$

Using this equation, the percent contributions of compounds I-VI were calculated and are listed in Table III. As an example, the CAV of 95 for I means that the actual concentration of I is 95-fold above its detection threshold (Table III). Since the complete Maillard mixture, accounting for 100 % of the overall browning, is 1450-fold above its detection threshold, it can be estimated that about 6.4 % of the overall color is caused by compound I. The data given in Table III showed that colorants I and II contributed 6.4 and 4.6 %, respectively, at most, to the total color of the reaction mixture (17). Also, compounds III, IV and V contribute significantly to the color of the browned Maillard mixture, because the color contribution was estimated to be 1.7, 0.7 or 0.1 %, respectively. Taking all these data into account, it can be estimated that about 13.5 % of the overall color of the aqueous Maillard mixture is accounted for by only five types of key chromophores.

Table III. Contribution of selected colored compounds to the overall color of the browned Maillard mixture

<i>Colorant^a</i>	<i>Color effectivity^b</i>	<i>Contribution to total color [%]</i>
I	95	6.4
II	66	4.6
III	24	1.7
IV	10	0.7
V	1	0.1
VI	<1	0.0
$\sum (\text{CAV}_{\text{I-VI}})$:	198	13.5
$\text{CD}_{\text{total}}\text{-factor}^{\text{c}}$:	1450	100.0

^a The structure of the colorant is displayed in Figure 3.

^b The color effectivity of the colorants I-VI were calculated as their CAVs.

^c The color effectivity of the Maillard mixture was determined by measuring the color dilution factor.

Conclusions

The data presented demonstrate that CDA is a suitable screening technique to locate intensely colored compounds in complex Maillard reaction mixtures. The

color activity concept, correlating quantitative data with the color detection threshold of a compound, then allows the determination of the color impact of these key colorants and measurement of their contribution to the total color of heated Maillard mixtures. The fact that only five key colorants account for 13.5 % of the overall color of the aqueous reaction mixture, indicates that the structural variety of key chromophores might be limited in the Maillard reaction. The characterization of additional colorants and the determination of their color activities are, however, necessary to gain a complete insight into the complex network of non-enzymatic browning reactions involving carbohydrates and amino acids.

Acknowledgments

The Deutsche Forschungsgemeinschaft, Bonn, is thanked for funding the research. We are grateful to Mr. J. Stein for his excellent technical assistance.

Literature Cited

1. Ames, J. M. In *Progress in Food-Proteins - Biochemistry*; Hudson, B.J.F., Ed.; Elsevier Applied Science, London, 1992, pp 99-153.
2. Ledl, F.; Severin, Th. *Z. Lebensm. Unters. Forsch.* **1978**, *167*, 410-413.
3. Ledl, F.; Hiebl, J.; Severin, Th. *Z. Lebensm. Unters. Forsch.* **1983**, *177*, 352-255.
4. Ledl, F.; Schleicher, E. *Angew. Chem.* **1990**, *102*, 597-734.
5. Hofmann, T. *J. Agric. Food Chem.* **1998**, *46*, 3902-3911.
6. Hofmann, T. *J. Agric. Food Chem.* **1998**, *46*, 3918-3928.
7. Hofmann, T. *Eur. Food Res. Technol.* **1999**, *209*, 113-121.
8. Hofmann, T. unpublished.
9. Schieberle, P.; Hofmann, T. *Lebensmittelchemie*, **1996**, *50*, 105-108.
10. Schieberle, P.; Hofmann, T. In *Chemical Reactions in Foods III*; Velisek, J.; Davidek, J.; Eds.; Proceedings of the 3rd Symposium on the Chemical Reactions in Food, Prague, Czech Republic, 1996, pp 89-93.
11. Schieberle, P.; Hofmann, T. In *Flavour science - recent developments*; Taylor, A.J., Mottram, D.S., Eds.; Proceedings of the 8th Weurman Flavour Research Symposium, Reading, UK, Royal Society of Chemistry, Cambridge, 1996, pp 175-181.
12. Schieberle, P.; Grosch, W. *Z. Lebensm. Unters. Forsch.* **1994**, *198*, 292-296.
13. Schieberle, P.; Hofmann, T. *J. Agric. Food Chem.* **1997**, *45*, 227-232.
14. Hofmann, T. *Carbohydr. Res.* **1998**, *313*, 203-213.
15. Hofmann, T. *Helv. Chim. Acta.* **1997**, *80*, 1843-1856.
16. Hofmann, T. *J. Agric. Food Chem.* **1998**, *46*, 932-940.
17. Hofmann, T. *J. Agric. Food Chem.* **1998**, *46*, 3912-3917.
18. Ledl, F. *Z. Lebensm. Unters. Forsch.* **1982**, *175*, 203-207.

Chapter 12

Maillard Modifications in Beer

M. A. Glomb¹, D. Rösch¹, and R. H. Nagaraj²

¹Institute of Food Chemistry, Technical University of Berlin, T1B 4/3–1,
Gustav-Meyer-Allee 25, 13355 Berlin, Germany

²Center of Vision Research, Department of Ophthalmology, University
Hospitals of Cleveland, Cleveland, OH 44106

For the first time, an arginine Maillard reaction product, *N*^δ-(5-hydroxy-4,6-dimethylpyrimidine-2-yl)-L-ornithine (Argpyrimidine), was identified in beer. Two mechanisms of formation could be verified, the major route *via* methylglyoxal, the minor *via* 5-deoxypentoses. Quantification of Argpyrimidine in beer revealed positive correlation with wort content and beer color.

The non-enzymatic browning or Maillard reaction has a direct impact on the final quality of beer. This beverage is traditionally made from water, barley, hops and yeast. During manufacture, enzymatic activity results in the breakdown of proteins to smaller peptides and amino acids, and of starch to oligosaccharides, maltose and glucose. Favored by the high temperatures during kilning, mashing and wort boiling, the reducing sugars react with amino compounds in complex cascades, leading from an initially formed aminoketose or Amadori product *via* highly reactive intermediates to more stable products (2). In this way, the Maillard reaction directly influences beer color and significantly contributes to aroma and taste.

Only recently, a method was developed to isolate and quantify the colored polymer fraction of beer (3). By combining several chromatographic steps, the amount of these melanoidins could be determined to be *ca.* 7% in pale beers. An attempt was made to further characterize the material by IR and elemental analysis. The molecular weight appeared to be rather uniform, as the majority of the material eluted within 2.3 – 2.6 times the void volume of a Sephadex G-50 column.

In contrast, the flavor contribution of the Maillard reaction has been studied extensively (4). Major structural classes found in beer include furans, pyrroles, thiophenes, pyrones, aldehydes and pyrazines.

Efforts to elucidate amino acid modifications have so far focused solely on proline, as it represents by far the quantitatively most important amino acid in malt and also in beer (up to *ca.* 500 ppm). Although endless structures have been isolated

from reaction mixtures of proline with mainly monosaccharides, only the few structures depicted in Figure 1 have been identified in malt, wort and beer (5-10). In all cases, the carboxylic function of proline has been lost, while the original pyrrolidine ring is still present in many cases. The relatively unpolar properties of the pyrrolizines and the pyridines result in their contribution to beer aroma with cookie, bready and smoky, roasty odors, respectively. The azepine and oxazine are reported to possess bitter taste qualities.

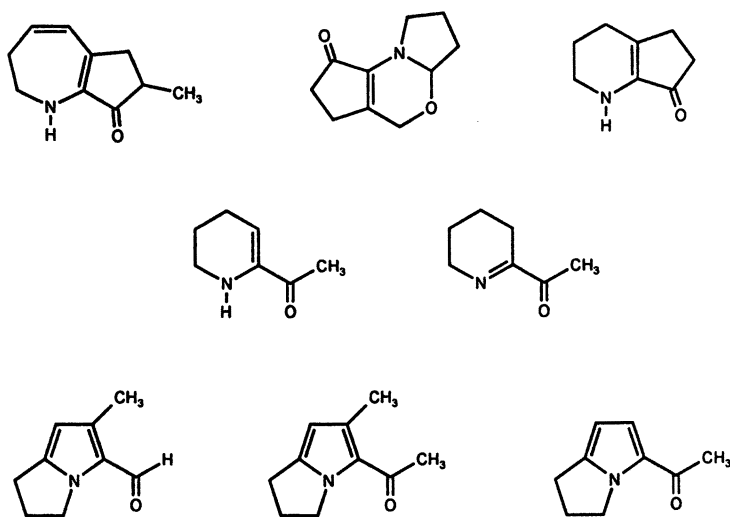


Figure 1. Proline-derived Maillard products in beer.

Compounds incorporating the intact amino acid backbone have not been identified in beer so far. Based on these considerations, we started to investigate the chemistry of methylglyoxal, a known Maillard reaction intermediate of maltose (Figure 2). Furthermore, methylglyoxal has been found in beer at concentrations of 0.08-0.2 ppm. The ϵ -amino function of lysine reacts with methylglyoxal to form carboxyethyllysine and a imidazolium crosslink structure called imidazolysine or MOLD (11,12). Both compounds have been isolated from model systems incorporating proteins and *in vivo* samples, but not from foods. The guanidino group of arginine reacts with methylglyoxal to form an imidazolinone, the formation of which has been established in pretzel crusts and various other snacks (13). MODIC (Figure 2) basically represents the same structure, crosslinking arginine with lysine residues (14). So far, it has only been identified in protein-methylglyoxal incubations. Recently, we identified Argpyrimidine as a novel fluorescent pyrimidine derivative from reaction mixtures of N^2 -t-BOC-arginine and methylglyoxal (15). Its structure was confirmed by $^1\text{H}/^{13}\text{C}$ -NMR, high resolution FAB/MS and independent synthesis from 3-O-acetyl-2,4-pentandione 1 (Figure 3). In this context, it was proposed that the formation of an imidazolone occurred on slow oxidation of the imidazolinone (Figure

2) (16). This molecule showed the same fluorescent properties as Argpyrimidine. Latest investigations have shown the structure to be a misinterpretation of spectroscopic data and the material to be identical to Argpyrimidine (16-18).

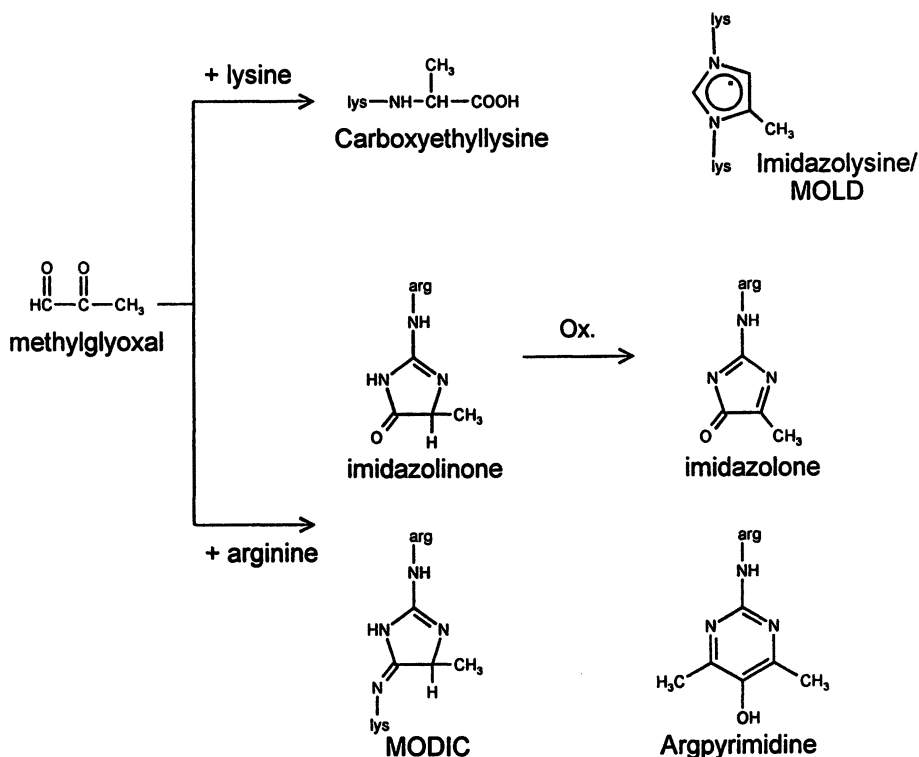


Figure 2. Amino acid modifications by methylglyoxal.

Formation and Quantification of Argpyrimidine in Beer

We propose that two molecules of methylglyoxal react *via* an intermolecular Cannizzaro reaction to the intermediate reductone 3-hydroxy-2,4-pentanedione 2, which will subsequently condense with the guanidino group of arginine to give Argpyrimidine (Figure 3). In the course of this reaction formic acid will be generated. Reductones are extremely sensitive to oxidation and fragmentation reactions. Therefore, in order to support the hypothesized reaction mechanism, we synthesized 3-hydroxy-2,4-diethoxypentane-1,4-diene 3 as a stable derivative from methylformiate and ethoxyvinylolithium. The vinyl ether-protected carbonyl functions can be set free under mild acid conditions. Incubations of the reductone 2 yielded 8 times more

Argpyrimidine than when incubations used the same amounts of methylglyoxal, as the starting material.

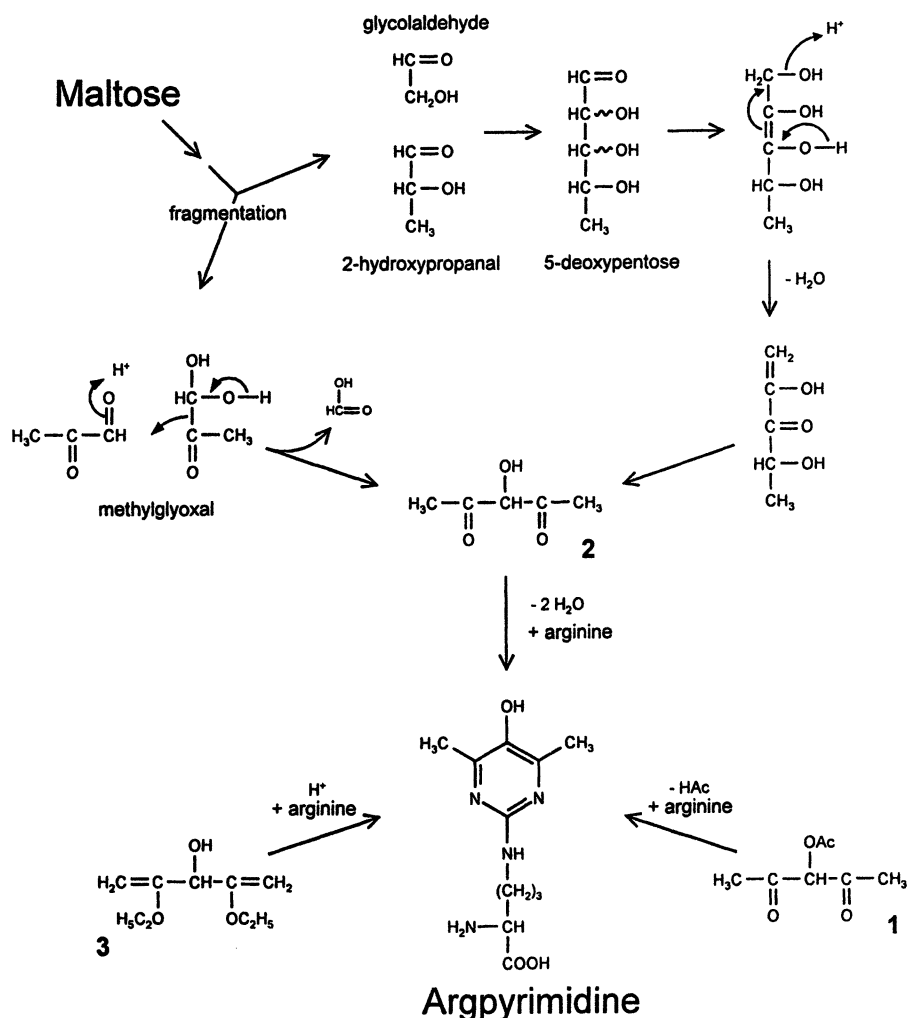


Figure 3. Mechanism of Argpyrimidine formation.

Alternatively, Argpyrimidine could be formed from maltose via the known sugar fragmentation products glycolaldehyde and 2-hydroxypropanal. Aldol condensation leads to 5-deoxypentoses which, after enolisation and cleavage of water, result in reductone 2 which gives Argpyrimidine. As a probe for this reaction pathway, 5-deoxyribose was synthesized in a five-step sequence. Reaction mixtures with N^{α} -t-BOC-arginine indeed showed the formation of Argpyrimidine but, compared to

methylglyoxal, yields are very low (Table I). Thus, methylglyoxal is by far the better precursor within the reaction scheme shown. This also means that, starting from 5-deoxyribose, both possible pathways for Argpyrimidine formation need to be considered.

Table I. Incubation of *N*^ε-t-BOC-Arginine with Sugars

<i>Incubation Time (d)</i>	<i>5-Deoxy-D-ribose</i>	<i>D-Ribose</i>	<i>D-Glucose</i>	<i>D-Maltose</i>	<i>Methylglyoxal</i>
Argpyrimidine (μmol/mol Arginine)					
1	26	9	n.n.	n.n.	33100
2	44	29	n.n.	n.n.	42800
3	116	52	n.n.	n.n.	47500
4	116	73	n.n.	n.n.	54200
7	214 (2.27)	94 (1)	17	12	49800
Methylglyoxal (μmol/mol Arginine)					
7	1330 (1.16)	1150 (1)			

NOTE: Both reactants 50mM at 55°C in 0.1M phosphate buffer, pH 7.4.
Methylglyoxal was quantified as the corresponding quinoxaline derivative.

To differentiate the two pathways, formation of Argpyrimidine and methylglyoxal in reaction mixtures with 5-deoxyribose and ribose were compared (Table I). Ribose is an ideal substrate in this respect because, as a C5-aldose, it should show the same reactivity concerning methylglyoxal synthesis, but formation of 5-deoxypentoses should be negligible. The incubations show that 5-deoxyribose leads to 2.27 times more Argpyrimidine than ribose, while only 1.16 times more methylglyoxal is produced.

Thus, only half of the Argpyrimidine synthesized in 5-deoxyribose mixtures can be explained *via* methylglyoxal, the other half must proceed through the alternative mechanism. 5-Deoxyribose was indeed identified as a novel intermediate in glycolaldehyde/hydroxyacetone-, as well as in maltose/lysine-reaction mixtures by GC/MS.

Due to its fluorescence at 320nm (ex.)/398nm (em.), Argpyrimidine can be quantified by HPLC at extremely low levels. However, protein incubations first need to be enzymatically hydrolysed, as the molecule is not stable under the conditions of classic protein hydrolysis. As beer contains significant amounts of free amino acids, we developed an assay for free pentosidine. To remove carbohydrates, beer is passed through a protonated cation exchanger. After washing with water, amines are eluted with diluted ammonia, solvents are evaporated and the residue is subjected to HPLC on a reversed phase column with a MeOH/water-eluent and heptafluorobutyric acid as the ion pair reagent (Figure 4, A). Eluent with material having the same retention as authentic Argpyrimidine was collected, solvents were evaporated and subjected

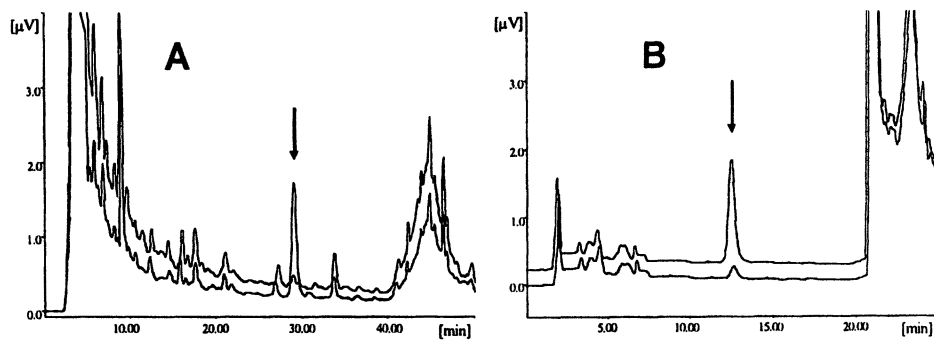


Figure 4. Detection of Argpyrimidine in Beer by a 2 stage HPLC-system. Additions of standard are marked with an arrow.

again to HPLC with a propanol/water-eluent and sodium dodecylsulfate as the ion pair reagent (Figure 4, B). The lower trace in the chromatogram B shows a baseline separated signal corresponding to 450 fmol of Argpyrimidine, which clearly increases after addition of the authentic compound. In selected cases, the identity of the material quantified was confirmed by GC/MS after derivatization to the N^{α} -trifluoroacetyl- N^{δ} -(5-methoxy-4,6-dimethylpyrimidine-2-yl)-L-ornithinemethylester. Analysis of 35 different lager-type beer varieties revealed a positive correlation between Argpyrimidine concentration and wort and beer color, respectively (Figure 5).

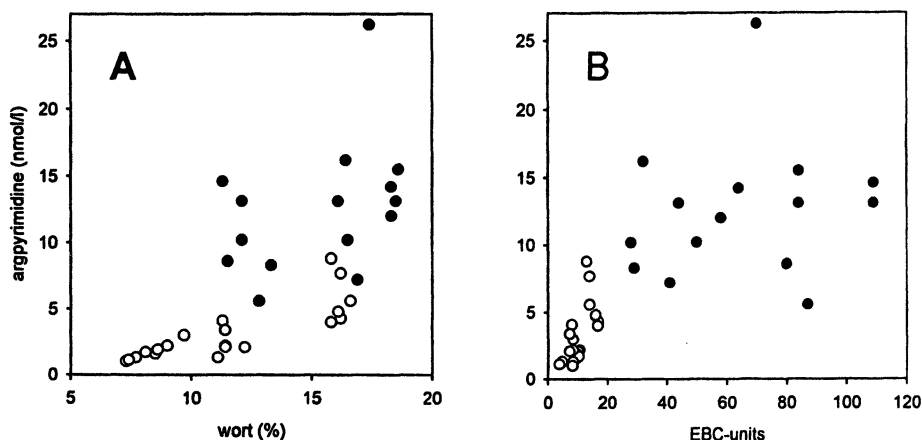


Figure 5. Correlation of Argpyrimidine concentration with wort content (A) and beer color expressed as EBC-units (B). Closed symbols indicate beer varieties with EBC-units of more than 28.

Literature Cited

1. Glomb, M. A.; Rösch, D.; Nagaraj, R. H. *J. Agric. Food Chem.* 2000 (unpublished).
2. Ledl, F.; Schleicher, E. *Angew. Chem.* 1990, 102, 597-626.
3. Kuntcheva, M. J.; Obretenov, T. D. *Z. Lebensm. Unters. Forsch.* 1996, 202, 238-243.
4. Tressl, R. *Brauwelt* 1976, 116, 1252-1257.
5. Tressl, R.; Grünewald, K. G.; Helak, B. *In Flavor 81*; Schreier, P., Ed.; Walter de Gruyter: Berlin, New York, 1981; pp 397-416.
6. Tressl, R.; Grünewald, K. G.; Silwar, R.; Helak, B. *Proceedings of the 18th EBC Congress*; Copenhagen, p 391.
7. Tressl, R.; Helak, B. *Helv. Chim. Acta* 1982, 65, 483-489.
8. Helak, B.; Spengler, K.; Tressl, R.; Rewicki, D. *J. Agric. Food Chem.* 1989, 37, 400-404.
9. Pabst, H. M. E.; Ledl, F.; Belitz H.-D. *Z. Lebensm. Unters. Forsch.* 1985, 181, 386-390.
10. Tressl, R.; Helak, B.; Köppler, H.; Rewicki, D. *J. Agric. Food Chem.* 1985, 33, 1132-1137.
11. Ahmed, M. V.; Brinkmann Frye E.; Degenhardt, T.P.; Thorpe, S. R.; Baynes, J. W. *Biochem. J.* 1997, 324, 565-570.
12. Nagaraj, R. H.; Shipanova, N.; Faust, F. M. *J. Biol. Chem.* 1996, 271, 19338-19345.
13. Henle T.; Walter, A. W.; Walter, H.; Klostermeier, H. *Z. Lebensm. Unters. Forsch.* 1994, 199, 55-58.
14. Lederer, M. O.; Gerum, F.; Severin, T. *Bioorg. Med. Chem.* 1998, 6, 993-1002.
15. Shipanova, I.; Glomb, M. A.; Nagaraj, R. H. *Arch. Biochem. Biophys.* 1997, 344, 29-36.
16. Lo, T. W. C.; Westwood, M. E.; McLellan, A. C.; Selwood, T.; Thornalley, P. J. *J. Biol. Chem.* 1994, 269, 32299-32305.
17. Oya, T.; Hattori, N.; Mizuno, Y.; Miyata, S.; Maeda, S.; Osawa, T.; Uchida, K. *J. Biol. Chem.* 1999, 274, 18492-18502.
18. Glomb, M. A.; Nagaraj, R. H. *unpublished*.

Chapter 13

Peanut Roast Color and Sensory Attribute Relationships

H. E. Pattee¹, T. H. Sanders¹, T. G. Isleib², and F. G. Giesbrecht³

¹Market Quality Research and Handling, Agricultural Research Service, U.S. Department of Agriculture, Campus Box 7625, North Carolina State University, Raleigh, NC 27695

²Department of Crop Science, Campus Box 7620, North Carolina State University, Raleigh, NC 27695

³Department of Statistics, Campus Box 8203, North Carolina State University, Raleigh, NC 27695

Peanut roasting develops not only a pleasing sensory flavor but also a pleasing color. In studying the genetic relationships between sensory attributes and peanut genotypes, roast color of the peanut paste test sample is an important source of variability that must be considered. Intensity of the roasted peanut sensory attribute has a quadratic relationship to CIELAB L^* with an optimum for roast color at 58.7. Changes in roasted peanut, sweet, bitter, and astringent sensory attributes as roasting progresses are discussed as are the effects of peanut market-type on the intensity and rate of change in the sensory attributes. Differences in the roasted peanut quality of the peanut market-types point to the importance of cooperative efforts between plant breeders and food scientists to ensure that when new varieties are released they not only have superior agronomic characteristics but also maintain or improve upon the flavor quality characteristics.

Baking, cooking and roasting are all thermal processes used in many commodities (e.g., breads, cereals, coffee and cocoa beans, meats, nuts such as peanuts, vegetables, etc.) to generate both sensory and taste stimuli important to overall flavor (1,2). One important sensory stimulus produced is color. It serves as a cue to food doneness and is correlated with changes in aroma and flavor. The initial quality of a product often is judged by color and appearance. Lawless and Heymann (3) have reviewed the impact of color and appearance attributes on sensory evaluation and indicated that sensory color measurements are frequently neglected. In this chapter we will discuss the importance of controlling peanut roast color and discuss the relationship of peanut roast color to selected sensory responses and some factors which influence roast color optimization.

Peanut roasting develops not only a pleasing color but also a pleasant flavor. Thus roasting has important implications for peanut quality. There is considerable literature available on the effect of peanut roasting on volatile and sensory intensities (4-8; for review see 9,10). The literature on the effect of roasting on color is less extensive (11-15). The source of color generation during peanut roasting has been reviewed by Ahmed and Young (16). Color generation is due primarily to the sugar-amino acid reactions with the subsequent production of melanoidins (17). Caramelization of sugars may contribute to the brown coloration; however, Mason *et al.* (18) found sugar degradation products in much smaller quantities compared to sugar-amine reaction products.

Enhancement of roasted peanut flavor has been a long-standing objective of the peanut industry. However, subjective evaluation is necessary in studying roasted peanut quality. In a complex sensory profile, such as that for roasted peanuts, many factors interact to influence the perceived intensity of the attribute of interest. An understanding of the basic physiological and psychological factors that may influence sensory perception enables one to minimize variability and bias (19). Identification of interactions among roasted peanut, overroast, underroast and fruity enabled Pattee and coworkers (13,20) to reduce appreciably the unexplained variability occurring in the roasted peanut attribute (21) and to determine broad-sense heritability estimates of the roasted peanut, sweet, bitter and astringent attributes (20,22). In such applications of sensory data it is important that attribute scores not be compromised by non-genetic factors resulting from suboptimal roasting and environmental effects. Peanut samples, which have not been roasted to their optimum state as indicated by CIELAB L^* color values for roasted peanut paste of <56 or >62 , produce undesirable levels of overroast or underroast attributes (13). These observations on roasted peanut attribute response in relation to roast color have been confirmed by Crippen *et al.* (14).

There are four market-types of peanuts in the U.S., and each has a distinct primary usage. The runner market-type is used in the manufacture of peanut butter, the large-seeded Virginia market-type for ballpark and grocery in-shell, the Spanish market-type for confections and the Valencia market-type for grocery in-shell. These market-types are genetically diverse in parentage. The runner and Virginia market-types have an alternate branching pattern typical of subspecies *hypogaea* and pod characteristics typical of botanical variety *hypogaea*. Their genetic base is predominantly the *hypogaea* botanical variety, but current cultivars and breeding lines have at least some ancestry from subspecies *fastigata*. The Spanish and Valencia market-types are entirely from the subspecies *fastigata* Waldron, the Spanish lines from botanical variety *vulgaris* Harz and the Valencia lines from botanical variety *fastigata*. Because the Virginia and runner market-types come from a distinctly different genetic background than the *fastigata* types, it is conceivable and perhaps likely that these differences can be important in roast color and sensory attribute relationships. The market-types Spanish and Valencia have been combined in the data set because of an insufficient number of Valencia entries to properly represent the group.

The relationships between roast color and sensory attributes and the influences of market-type on these relationships will be discussed as well as peanut seed maturity effects on roast color.

Materials and Methods

The data used for this study were gathered over an 11-year span and include four peanut market-types, 343 different genotypes and 53 environments (year-by-location combinations). In the data set there are 1822 observations on roasted peanut attribute, 1779 on sweet and bitter attributes, and 1460 on the astringent attribute.

Plant Materials. Samples were obtained from various production regions throughout the U.S. All samples were obtained from plants grown and harvested under standard recommended procedures for the specific location.

Sample Handling. Across years samples were shipped to Raleigh, NC in February following harvest and placed in controlled storage at 5° C and 60% RH until analyzed.

Sample Roasting and Preparation. The peanut samples were roasted using a Blue M "Power-O-Matic 60" laboratory oven at 165° C. They were then air-cooled, hand-blanching, and ground into a paste using an Olde Tyme peanut butter mill (Olde Tyme Food Products, 143 Shaker Road, E. Long Meadow MA 01028). Random subsamples of the peanut paste were placed into Falcon 1007, 60 x 15 mm, disposable petri dishes. The remainder of each ground peanut paste sample was placed into a glass jar, sealed, and stored at -10 to -20° C until sensory evaluation.

Color Measurement. CIELAB $L^*a^*b^*$ values were obtained with a Minolta Chroma Meter II CR-300 system (Minolta Camera Co., Ltd., Osaka, Japan). The illumination was supplied by a D6500 K light source, and the spectra responses approximate the CIE colorimetric standard observer. Measurements were taken at three different locations for each subsample.

Sensory Evaluation. A long-standing six to eight-member highly-trained roasted peanut profile panel at the Food Science Department, North Carolina State University, Raleigh, NC, evaluated all peanut-paste samples using a 14-point intensity scale. Panel orientation, sensory attributes, and reference control were as described by Pattee and Giesbrecht (20) and Pattee *et al.* (23,24). Two sessions were conducted each week on nonconsecutive days.

Statistical Analysis. PROC CORR, PROC GLM and PROC GPLOT in SAS (25) were used to perform the statistical analyses in this chapter.

Results and Discussion

Optimal Roast Color for Maximal Roasted Peanut Attribute Response. When conducting flavor studies on genetic resources, the sources of variability in the sensory attribute of interest should be identified. Overroasting, as indicated by the sensory attribute overroast, underroasting, as indicated by the sensory attribute underroast, and an off-flavor, indicated by the sensory attribute fruity, are factors that contribute to variability in the attribute roasted peanut (13,20). Pattee and Giesbrecht (21) have proposed appropriate covariance adjustments. They suggested that unadjusted roasted peanut sensory data be statistically examined for the effects of these relationships before proceeding with additional statistical analyses, especially

when the maximum response value is desired. They showed by plotting the roasted peanut intensity against underroast attribute, overroast attribute and CIELAB L^* values, that effects of both under- and overroast could be mitigated by adjusting roasted peanut intensity for a quadratic relationship with color values. The relationship between roasted peanut intensity and roast color is illustrated in Figure 1. Improperly roasted peanut samples, i.e., those which produce undesirable values for underroast and overroast, had roasted peanut paste (CIELAB L^*) color values <56 or >62 . Plausible explanations for this relationship are that these samples (a) either have not generated the full intensity of volatiles responsible for the roasted peanut response, (b) have begun to generate volatile products which mask the roasted peanut attribute response, or (c) are breaking down the volatiles responsible for the roasted peanut response into other products. Both over- and underroasting cause a lowering of the roasted peanut attribute values. Determination of the maximum point in the quadratic equation indicates that the optimal roasted peanut sensory attribute scores, in the 11-year data set, are obtained with a CIELAB L^* value of 58.7 (Figure 1).

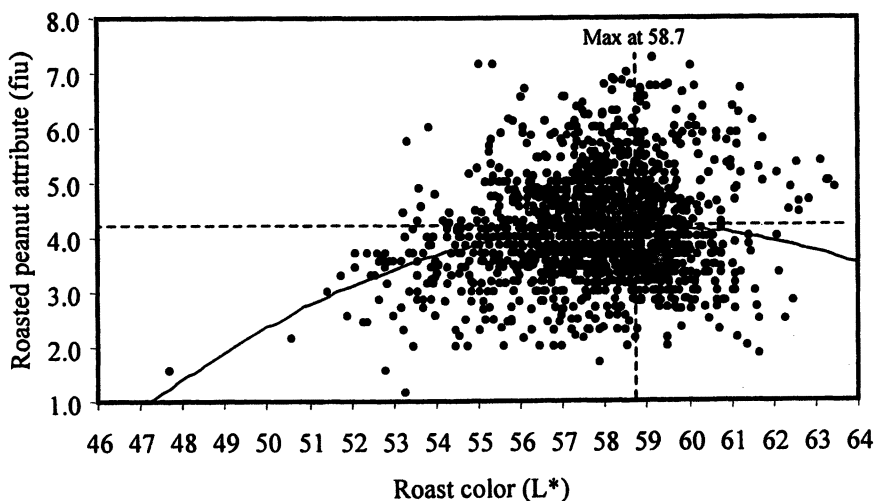


Figure 1. Overall relationship between roasted peanut attribute and roast color.

The consistency of the optimum roast color value across years is shown in Table I. The variation is generally within a narrow range of 57.1 to 59.5. It is noted that only in 1990 and 1994 did the optimum roast color vary substantially from a CIELAB L^* of 58. In these years the individual CIELAB L^* sample values varied in a very narrow range (1990) or had a number of outlier values (1994) that produced uncharacteristic curves.

The consistency of the optimum roast color value across market types can be judged by comparing Figure 1 and Figure 2. Figure 1 represents a single second order curve fitting roasted peanut attribute intensities on CIELAB L^* values for all samples. Figure 2 shows the separate second order regression curves of roasted peanut attribute

Table I. Roast color values associated with maximal roasted peanut attribute values across years.

Year	Optimum Roast Color
	L* Value
1997	57.2
1996	57.8
1995	58.3
1994	54.1
1993	58.6
1992	57.1
1991	57.9
1990	61.2
1988	58.6
1987	59.5
1986	58.7

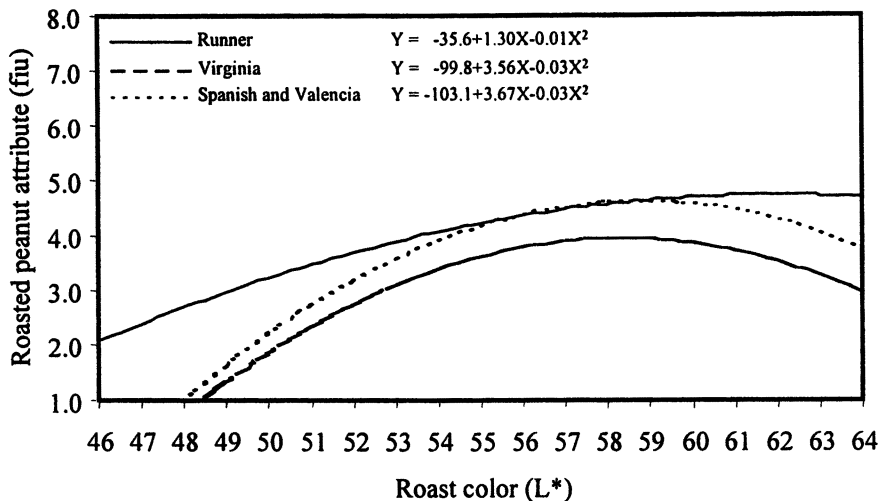


Figure 2. Influence of market-type on the relationship between roasted peanut attribute and roast color.

on CIELAB L^* values on runner-type peanuts, Virginia-type peanuts and combined Spanish-Valencia-type peanuts. The Virginia and Spanish-Valencia market-types have similar regression curves with the optimum roast color for Virginia and Spanish-Valencia being 58.3 and 58.8, respectively. The regression curve for the runner market-type suggests a much broader optimum range for roast color. The calculated roast color optimum point is 61.9 which further emphasizes the broadness of the

relationship. Some of the reasons for this broadness will become evident as the relationships between roast color and other sensory attributes are presented and the interactive relationships between sensory attributes are discussed.

Although the curves relating roasted peanut attribute on CIELAB L^* values for Virginia and the combined Spanish-Valencia market-types have similar shapes, we note that the maximum intensity of roasted peanut attribute for Spanish-Valencia peanuts is much higher than for Virginia-type peanuts. The maximum intensity of the roasted peanut attribute of the runner and Spanish-Valencia market-types are similar. Interactive relationships with the intensity of other sensory attributes (sweet, bitter and astringent), which will be discussed latter, may contribute to these observed differences in maximum intensity of roasted peanut between Virginia and the other market-types.

To evaluate closeness of the relationship between roasted peanut attribute and the L^* values we defined a new variable: $dV_Color = (Roast\ Color - 58)^2$. This new variable enables us to calculate the correlation value of the quadratic relationship. The correlation value was determined to be $r = -0.19$. This means the dV_Color variable is accounting for 4% of the variation in the 1822 obs. The minus sign indicates that roasted peanut attribute intensity is decreasing on either side of the 58 value. From these results we can conclude that the objective of roasting to an L^* value of 58 for maximizing roasted peanut attribute sensory response is appropriate. It has become our standard statistical practice to use the quadratic adjustment for color proposed by Pattee and Giesbrecht (21).

Relationship of sweet attribute to roast color. It is well documented that carbohydrate components are involved as substrates during the peanut roasting process for the formation of the roasted color and roasted peanut volatile components (9,16). Thus it might be expected that intensity of the sweet attribute would diminish with roast color. Regression analysis of the data indicates that sweet intensity, in the general population of peanut lines, increases slightly with increase in roast color, i.e., decrease in L^* value (Figure 3). This is in contrast to the results of Smyth *et al.* (10) which indicated that sweet attribute intensity decreased with roast time. Several things need to be considered before drawing a conclusion about this difference. Smyth *et al.* (10) used oil roasting (152, 163, 174° C) and only a single seed group (extra large Virginia) versus dry roasting (165° C) and a mixed size group (sound mature kernels) in this data set. It is unknown whether the two roasting procedures differ in their process of color generation (caramelization vs Maillard reaction) and volatile production. Kroh (26) discussed some of the differences between caramelization and the Maillard reaction and the carbohydrate polymerization reactions that occur during caramelization. Mason *et al.* (4) showed that phenylacetaldehyde was one of the main contributors to the sweet aroma of roasted peanuts and removal of this component from the volatile profile resulted in loss of the sweet background of the roasted peanut aroma. Peanut market-type may also contribute to these differences. Pattee *et al.* (27) reported a positive correlation between total sugars and sweetness, but the expected generalized relationship of total sugars or sucrose to sweetness could not be established because the relationship was not the same across all market-types. They

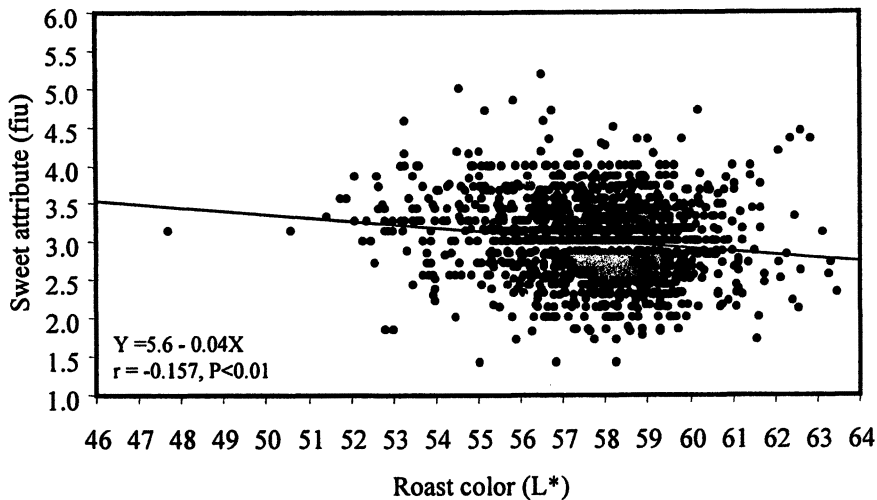


Figure 3. Overall relationship between sweet attribute and roast color.

suggested that there may be a bitter principle, particularly in the Virginia market-type, which modifies the sweet response and interferes with the sensory perception of sweetness. The relationships between roast color and sweet attribute response are different between peanut market-types (Figure 4). The combined Spanish and Valencia market-types showed the largest increase in sweet intensity with increasing

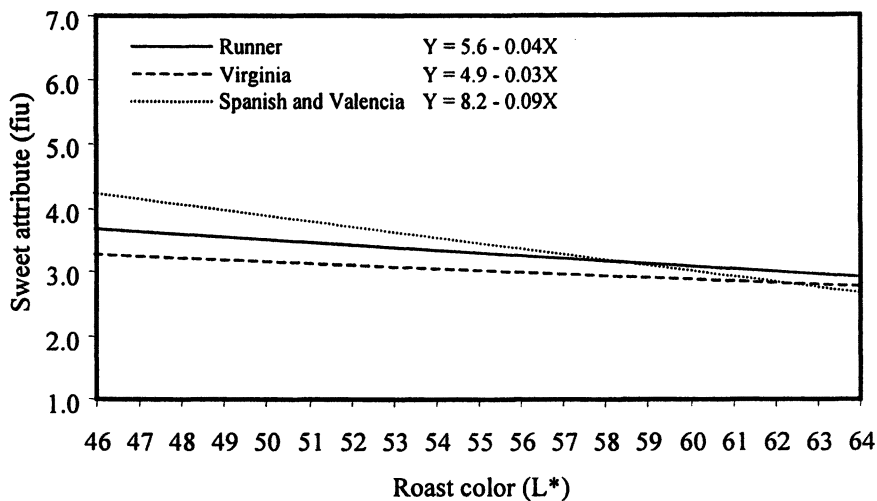


Figure 4. Influence of market-type on the relationship between sweet attribute and roast color.

roast color, i.e., decreasing L^* value (Sweet=8.2-0.09 L^*) and lowest impact in the Virginia market-type (Sweet=4.9-0.03 L^*). Pattee *et al.* (27) also found the strongest correlations ($r=0.917$, $P<0.05$) between sweetness and total sugars in the Spanish-Valencia market-types and the lowest correlation in the Virginia market-types. The results of Smyth *et al.* (10) taken in concert with these results would thus seem to confirm that in Virginia market-type peanuts there are constituents that have a negative impact on the sweet response in roasted peanuts. The impact of the oil roasting procedure may well be to accentuate the bitter attribute contributors. Such speculation deserves further investigation.

Relationship of bitter attribute to roast color. Bitterness as an attribute component in roasted peanuts has not been studied in detail although it is always a component of any sensory lexicon for roasted peanuts. Understanding the relationship of bitterness to the peanut roasting process is important for several reasons: (a) the interrelationships known to exist between the sensory attributes roasted peanut, sweet and bitter (22); (b) bitter attribute, as a heritable trait in peanuts, must be considered in the quality evaluation of new peanut varieties (28,29); (c) the interactive sensory impact of bitter and sweet attributes (30,31). Roasting of peanuts intensifies the bitter attribute (Figure. 5) (10). The correlation of bitter attribute to roast color ($r=-0.36$) is highly significant and the linear equation indicates that bitter intensity increases at a rate of 0.22 flavor intensity units (fiu) per L^* unit decrease. Such a rate of increase emphasizes the importance of optimizing roast color for the attribute of interest.

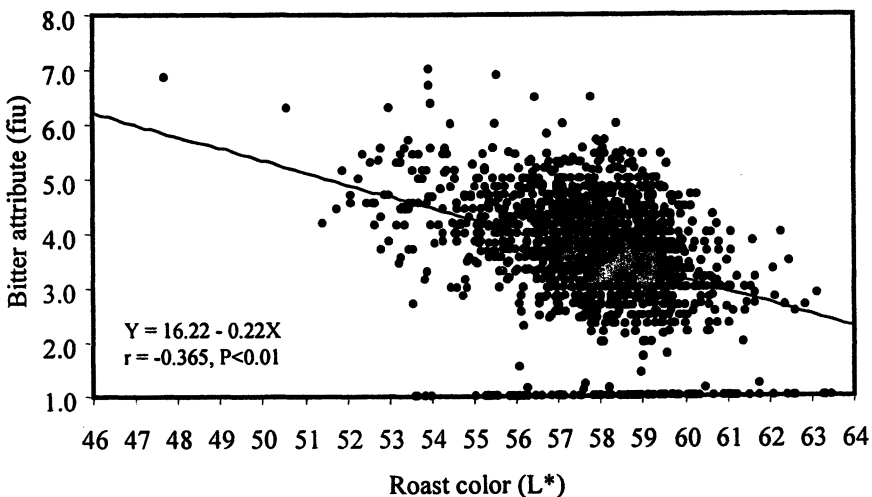


Figure 5. Overall relationship between bitter attribute and roast color.

Pattee *et al.* (22) found the correlation of bitter to roasted peanut intensity ($r = -0.59$, $P<0.01$) to be very strong and bitter attribute intensity to impact the roasted peanut intensity -0.41 fiu per bitter fiu. They reported the correlation of bitter to

sweet attribute to be $r = -0.80$ ($P > 0.01$) and the bitter attribute intensity to impact the sweet intensity -0.95 flu per bitter flu. The negative impact that the bitter attribute has on the roasted peanut and sweet attributes as roasting progresses and the concurrent decrease in flavor quality indicates the awareness one must have of the bitter intensity within the total sensory profile.

A difference in bitter intensity development was observed between peanut market-types (Figure 6). In the raw state the Virginia market-type typically has the lowest bitter intensity. As the roasting process progresses, indicated by decreasing L^* values, bitter intensity in the Virginia market-type increases at a faster rate (0.26 flu per L^* unit) than in the runner or Spanish-Valencia market-types and reaches a higher intensity level (4.1 for Virginia vs 3.8 and 3.4 for runner and Spanish-Valencia, respectively at $L^* = 56$, the minimum acceptable roast color). The runner and Spanish-Valencia market-type have almost parallel responses. Little is known about the precursors to, or the components which produce, the bitter response.

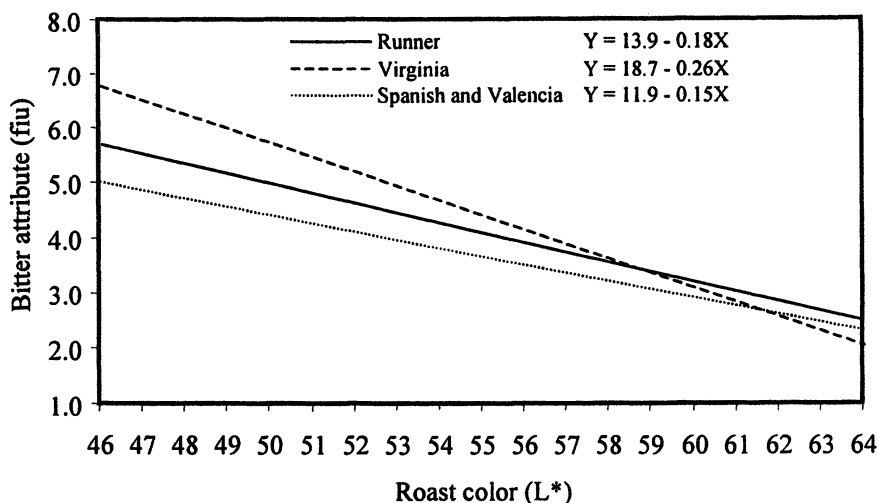


Figure 6. Influence of market-type on the relationship between bitter attribute and roast color.

Relationship of astringent attribute to roast color. The astringent sensory attribute in roasted peanuts, like the bitter attribute, has not been studied in detail. Pattee and Giesbrecht (20) reported astringency to have a heritability factor in peanuts at about the same level as the bitter attribute (0.06). The relationship of astringency to the peanut roasting process (roast color) has not been reported previously. As with the bitter attribute, the astringent attribute intensifies as the roasting process proceeds (roast color decreases) (Figure 7). The correlation of astringent attribute to roast color is $r = -0.35$ ($P < 0.01$) and the linear equation indicates that astringent intensity increases at a rate of 0.12 flavor flu per L^* unit, about half the rate of the bitter attribute increase. The increasing of astringency with degree of roasting raises some

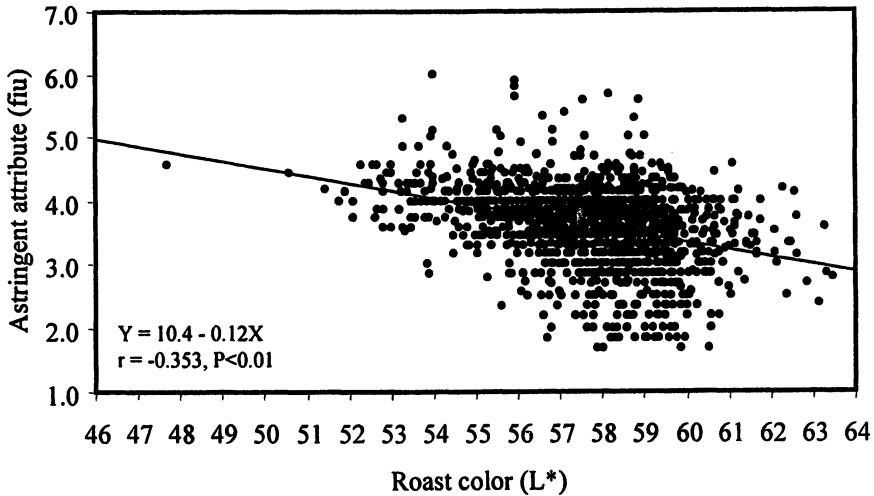


Figure 7. Overall relationship between astringent attribute and roast color.

interesting questions about the components responsible for this complex sensation. Astringency is generally thought to be produced by tannins, alums, and acids in foods (32). Tannins, in peanuts, are predominantly confined to the hull and testa of the fruit with only negligible amounts in the cotyledons (33). It was suggested that the amount present in the cotyledons may have been due to contact with the testa. This brings up an interesting possibility. Because peanuts are roasted with the testa still intact, is there a diffusion of components responsible for the astringency response from the testa into the cotyledons during the roasting process? Although they did not specify the specific flavors, Newell *et al.* (34) indicated threonine, tyrosine, lysine and an unknown acid were considered precursors of atypical flavor.

Changes in astringency during the roasting process in the Virginia market-type are much the same as observed with the bitter attribute (Figure 8). The Virginia market-type was lowest in the astringent attribute in the raw state, increased in astringency intensity at the fastest rate (0.14 fiu per L^* unit) as roasting progressed, and reached the highest level in the overroast state ($L^* = 46$). Changes in astringency during roasting in the runner and Spanish-Valencia market-types were not as dynamic as the bitter changes. Although astringency at the initial levels of roasting in the Spanish-Valencia market-type was highest among the market-types, the slow rate of change (0.03 fiu per L^*) placed it nearly a full flavor intensity unit below the Virginia market-type in the overroasted condition ($L^* = 46$). The runner market-type was intermediate to the Virginia and Spanish-Valencia market-types. It is of interest that the intensity level of astringency at the optimum roast color value is nearly equal in all market types.

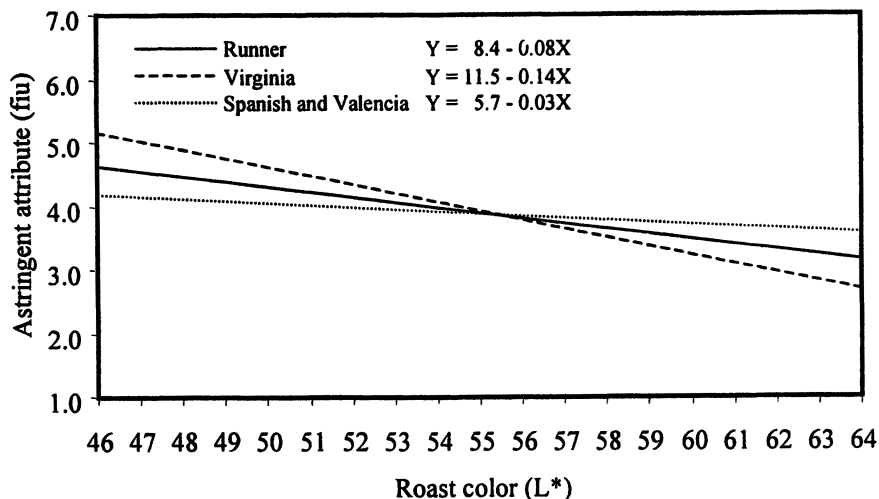


Figure 8. Influence of market-type on the relationship between astringent attribute and roast color.

Roast Color - Peanut Seed Maturity Relationships. One of the significant factors affecting roast color of peanuts is maturity (35). Peanut maturity as discussed progression of physiological maturity from Yellow to Black. Peanuts (seed) from the maturity classes (Table II) were sized over slotted screens to eliminate the effect of seed size on degree of roast. Roast color (L^*) increased as maturity of peanuts increased when peanuts of different maturity of the same commercial size were roasted for the same time. The degree to which this phenomenon occurs is easily verified by examination of commercially available roasted whole peanuts, wherein a range of colors may commonly be seen. Previous studies have demonstrated that free sugars and free amino acids are found in higher concentration in immature peanuts and contribute to the reactant pool for the Maillard reaction responsible for color development. The pattern of dark to light roast color is consistent from year to year but the absolute difference among classes and the range from least to most mature is variable in different crop years and for different harvest dates (36).

Roast Color - Single Seed, Lot, and Paste Color Relationships. Single seed roast color distribution, mean roast color and paste color of peanuts from sequential weekly harvest dates obtained using the same roast protocol are shown in Figure 9. With progressive harvest dates, higher percentages of mature seed are found in the sized class and the shift to a higher percentage of lighter roasted seed is evident in the distributions. The paste color resulting from the different harvest dates is a function of the distribution of roast colors in the lot. Paste color becomes consistently lighter with progressive harvest dates as a result of the increase in lighter roast (mature) peanuts. Christie and Sanders (37) reported that single seed roast color distribution, average

Table II. Influence of pod maturity on roast color of medium grade kernels roasted 21 min at 165°C.

<i>Maturity class</i>	<i>Roast color</i>
Mesocarp color	L* Value
Yellow (immature)	56.2
Orange A	57.2
Orange B	59.1
Brown	60.0
Black (Mature)	60.2

seed roast color and paste color were very highly correlated, allowing for conversion between systems using experimental equations. Although the mean of single seed roast color was a strong predictor of paste color, average color (one measurement on a collective sample) currently remains a more efficient predictor of paste color. All three color measurements can be used to illustrate changes in roasted peanut flavor intensity within a grade size over a variety of roast conditions.

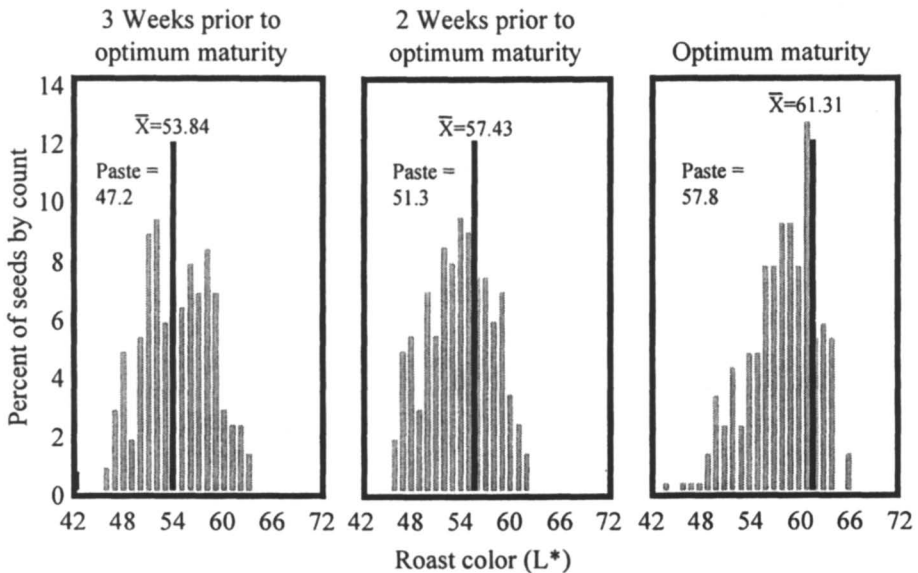


Figure 9. Distribution of roast color of individual seeds and the paste made from them as a function of average maturity.

Conclusion

The generalized responses of the sensory attributes roasted peanut, sweet, bitter, and astringent with progression of the roasting process (decrease in L*) were as

anticipated except for the slight increase in sweetness as roasting progressed. Separating out the influence of the three market-type components, Virginia, runner, and Spanish-Valencia on the sensory attributes begins to expose the similarities and dissimilarities of the flavor qualities for these market types. The Virginia market-type was shown to have the lowest roasted peanut response levels among the three market-types (Figure 2). Insight into some of the possible causes of this low sensory response are found in the responses of the other attributes during the roasting process. The sweet attribute showed relatively little change as roasting progressed, while the bitter attribute increased at a rate 1.5 to 2 times that found for the other market-types. Although the astringent attribute increased at rates nearly 2 to 5 times faster than that for runner or Spanish-Valencia, intersection of the equations near the minimum for optimum roast color ($L^*=56$) would suggest that astringency contributed little to the roasted peanut quality differences. Because little is known about the substrates and components that contribute to the bitter attribute in roasted peanuts further research in this area could help to explain these observations.

The observations on differences in the roasted peanut quality of the peanut market-types also point to the importance of cooperative efforts between plant breeders and food scientists to ensure that when new varieties are released that they not only have superior agronomic characteristics but also maintain or improve upon the flavor quality characteristics.

Literature Cited

1. *Volatile Compounds in Foods and Beverages*; Maarse, H., Ed.; Marcel Dekker: New York, 1991.
2. O'Brien, J.; Morrissey, P. A. *Crit. Rev. Food Sci. Nutr.* **1989**, *28*, 211-248.
3. Lawless, H. T.; Heymann, H. *Sensory Evaluation of Food: Principles and Practices*, Chapman & Hall, New York, 1998; pp 406-429.
4. Mason, M. E.; Johnson, B. R.; Hamming, M. C. *J. Agric. Food Chem.* **1967**, *15*, 66-73.
5. Mason, M. E.; Newell, J. A., Johnson, B. R.; Koehler, P. E.; Waller, G. R. *J. Agric. Food Chem.* **1969**, *17*, 728-731.
6. Koehler, P. E.; Mason, M. E.; Odell, G. V. *J. Food Sci.* **1971**, *36*, 816-818.
7. Buckholz, L. L.; Daun, H.; Stier, E.; Trout, R. *J. Food Sci.* **1980**, *45*, 547-554.
8. Bett, K. L.; Boylston, T. D. In *Lipid Oxidation in Food*; St. Angelo, A. J., Ed.; ACS Symposium Series 500, American Chemical Society, Washington, DC, 1992; pp. 322-343.
9. Sanders, T. H.; Pattee, H. E.; Vercellotti, J. R.; Bett, K. L. In *Advances in Peanut Science*; Pattee, H. E., Stalker, H. T., Eds.; American Peanut Research and Education Society, Stillwater, OK, 1995; pp. 528-553.
10. Smyth, D. A.; Macku, C.; Holloway, O. E., Deming, D. M.; Slade, L.; Levine, H. *Peanut Sci.* **1998**, *25*, 70-76.
11. Moss, J. R.; Otten, L. *Can. Inst. Food Sci. Technol. J.* **1989**, *22*, 34-39.

12. Chiou, R. Y.-Y. Chang, Y.-S.; Tsai, T.-T.; Ho, S. *J. Agric. Food Chem.* **1991**, *39*, 115-1158.
13. Pattee, H. E.; Giesbrecht, F. G.; Young, C. T. *J. Agric. Food Chem.* **1991**, *39*, 519-523.
14. Crippen, K. L.; Vercellotti, J. R.; Lovegren, N. V.; Sanders, T. H. In *Food Science and Human Nutrition*, Charalambous, G., Elsevier Publishing Co., Amsterdam, The Netherlands, 1992; pp. 211-227.
15. Vercellotti, J. R.; Crippen, K. L.; Lovegren, N. V.; Sanders, T. H. In *Food Science and Human Nutrition*, 29, Ed.; G. Charalambous. Elsevier Publishing Co., Amsterdam, The Netherlands, 1992; pp. 183-209.
16. Ahmed, E. M.; Young, C. T. In *Peanut Science and Technology*, Pattee, H. E.; Young, C. T., Eds.; Amer. Peanut Res. Educ. Soc: Stillwater, OK, 1982; pp 655-688.
17. Hodge, J. E. *J. Agric. Food Chem.* **1953**, *1*, 928-943.
18. Mason, M. E.; Johnson, B. R.; Hamming, M. C. *J. Agric. Food Chem.* **1966**, *14*, 454-460.
19. Meilgaard, M.; Civille, G. V.; Carr, B. T. *Sensory Evaluation Techniques*, 2nd Ed., CRC Press, Boca Raton, FL, 1991; pp. 38-39.
20. Pattee, H. E.; Giesbrecht, F. G. *Peanut Sci.* **1990**, *17*, 109-112.
21. Pattee, H. E.; Giesbrecht, F. G. *J. Sensory Studies* **1994**, *9*, 353-363.
22. Pattee, H. E.; Isleib, T. G.; Giesbrecht, F. G. *Peanut Sci.* **1998**, *25*, 63-69.
23. Pattee, H. E.; Giesbrecht, F. G.; Mazingo, R. W. *Peanut Sci.* **1993**, *20*, 24-26.
24. Pattee, H. E.; Williams, D. E.; Sanchez-Dominguez, S.; Giesbrecht, F. G. *Peanut Sci.* **1995**, *22*, 18-22.
25. SAS Institute Inc. *SAS/STAT Software: Changes and enhancements through release 6.12*, SAS Inst., Inc, Cary, NC, 1997.
26. Kroh, L. W. *Food Chem.* **1994**, *51*, 373-379.
27. Pattee, H. E.; Isleib, T. G.; Giesbrecht, F. G.; McFeeters, R. F. *J. Agric. Food Chem.* **2000**, In Press.
28. Pattee, H. E.; Isleib, T. G.; Giesbrecht, F. G. *Peanut Sci.* **1994**, *21*, 94-99.
29. Pattee, H. E.; Isleib, T. G.; Giesbrecht, F. G. *Peanut Sci.* **1997**, *24*, 117-123.
30. Lawless, H. T. *J. Sensory Studies*. **1986**, *1*, 259-274.
31. Walters, D. E; Roy, G. In *Flavor-Food Interactions*; McGorin, R. J., Leland, J. V., Eds.; ACS Symposium Series 633, American Chemical Society, Washington, DC, 1996; pp. 130-142.
32. Lawless, H. T.; Heymann, H. *Sensory Evaluation of Food: Principles and Practices*, Chapman & Hall, New York, 1998; pp 66-67.
33. Sanders, T. H. *Peanut Sci.* **1977**, *4*, 51-53.
34. Newell, J. A.; Mason, M. E.; Matlock, R. S. *J. Agric. Food Chem.* **1967**, *15*, 767-772.
35. Sanders, T. H.; Vercellotti, J. R.; Crippen, K. L.; Civille, G. V. *J. Food Sci.* **1989**, *54*, 475-477.
36. Sanders, T. H.; Bett, K. L. *Peanut Sci.* **1995**, *22*, 124-129.
37. Christie, L. R.; Sanders, T. H. *Proc. Amer. Peanut Res. and Educ. Soc.* **1998**, *30*, 31. (Abstract).

Chapter 14

Contribution of Pyrrole Formation and Polymerization to Non-Enzymatic Browning during Chicken Roasting

Francisco J. Hidalgo, Manuel Alaiz, and Rosario Zamora

Instituto de la Grasa, Avenida Padre Garcia Tejero 4, 41012 Sevilla, Spain

Protein pyrrolization produced during chicken roasting was studied to better understand the molecular mechanisms involved in the resulting browning. Chicken legs were roasted at 200 °C for different periods of time and their colors determined using a chromameter. In addition, the skins of roasted legs were homogenized in sodium phosphate buffer and studied for browning, fluorescence, lipid oxidation, protein pyrrolization, and amino acid losses. Chicken roasting resulted in both peroxidation of lipids and losses of some of the amino acid residues of skin proteins, including lysine. In addition, there was a very good correlation between these two measurements, suggesting that the formation of oxidized lipid/amino acid products was occurring and pyrrole formation was a consequence of these reactions. Furthermore, there were very good correlations among browning, fluorescence and pyrrolization produced during chicken roasting, which suggested, in accordance with previous studies, that pyrrole formation and polymerization were contributing to the formation of both browning and fluorescence in this system.

The processing of foods for consumption often causes changes in their functional properties, nutritive value, flavor and color. The magnitude of these changes is related to both the kind of food and the type of processing. Food roasting has been used by man from ancient times to alter sensory properties of foods, to improve palatability and to extend the range of tastes, aromas and textures in the diet. In addition, it destroys enzymes and micro-organisms and lowers the water activity of the food to some extent, thereby increasing its shelf-life (1). When meats are roasted, the production of aromas is observed in addition to the characteristic golden brown color.

This color is believed to be a consequence of the Maillard reaction, the caramelization of sugars and dextrans (either present in the food or produced by hydrolysis of starches) to furfural and hydroxymethyl furfural, and the carbonization of sugars, fats and proteins (1). However, the molecular mechanisms by which this color is produced are mostly unknown at present, and most investigations have been carried out using model systems.

In an attempt to investigate browning reaction mechanisms in real food systems, the present study was undertaken to analyze the production of brown color in chicken skins during roasting. Chicken skins were selected because they are mostly composed of lipids and proteins, and carbohydrates are almost absent. In fact, the proximate composition described for chicken skins, which is related to the diet and the age of the birds, is 47.9-52.6 % moisture, 37-45 % lipid, 7-9 % protein, and 0.4-0.5 % ash (2-3). In addition, poultry lipids generally exhibit a higher degree of unsaturation compared to red meats, thus being more prone to oxidation (4). Therefore, in this system oxidation of lipids is likely to occur, and the formed lipid oxidation products may react with the reactive amino acid residues of proteins to produce oxidized lipids/amino acid reaction products (OLAARPs).

Previous research from this laboratory has shown that, in model systems, OLAARPs are able to contribute to the browning and fluorescence produced in lipid/protein systems by a mechanism which implies the formation and polymerization of pyrrole derivatives at the ϵ -amino group of lysine residues (5). The key intermediates in these reactions seem to be the *N*-substituted 2-(1-hydroxyalkyl)pyrroles produced by reaction of epoxyalkenals and the ϵ -amino group of lysine residues. A general scheme for the reactions produced between epoxyalkenals and other products of lipid peroxidation, including oxidized fatty acids with the structure of 4,5-epoxy-1-oxo-2-pentene, with protein reactive groups is shown in Figure 1. This mechanism not only produces color and fluorescence but it has also been related to the production of volatile heterocyclic compounds in oxidized lipid/protein mixtures (6) and short chain aldehydes (7).

The production of *N*-substituted 2-(1-hydroxyalkyl)pyrroles is always accompanied by formation of *N*-substituted pyrroles, which are much more stable and have been found in more than twenty fresh food products, including meats, fishes, vegetables and nuts (8). However, the spontaneous polymerization of the *N*-substituted 2-(1-hydroxyalkyl)pyrroles, which may take place both intra- and intermolecularly with one or several molecules of protein implicated, produces sequentially dimers, trimers, tetramers, as well as melanoidin-like polypyrroles (9-10). Due to the instability of hydroxyalkylpyrroles, their determination in food systems is very difficult. Nevertheless, recent studies have shown that when pyrrole formation and polymerization contribute to non-enzymatic browning, a high correlation among browning, fluorescence and pyrrolization measurements is observed (Zamora *et al.*, unpublished results). Therefore, the present investigation was undertaken with two objectives. First, to study the pyrrolization of chicken leg skin proteins as a consequence of roasting, and then to investigate possible correlations among protein pyrrolization, browning and fluorescence production in this food system.

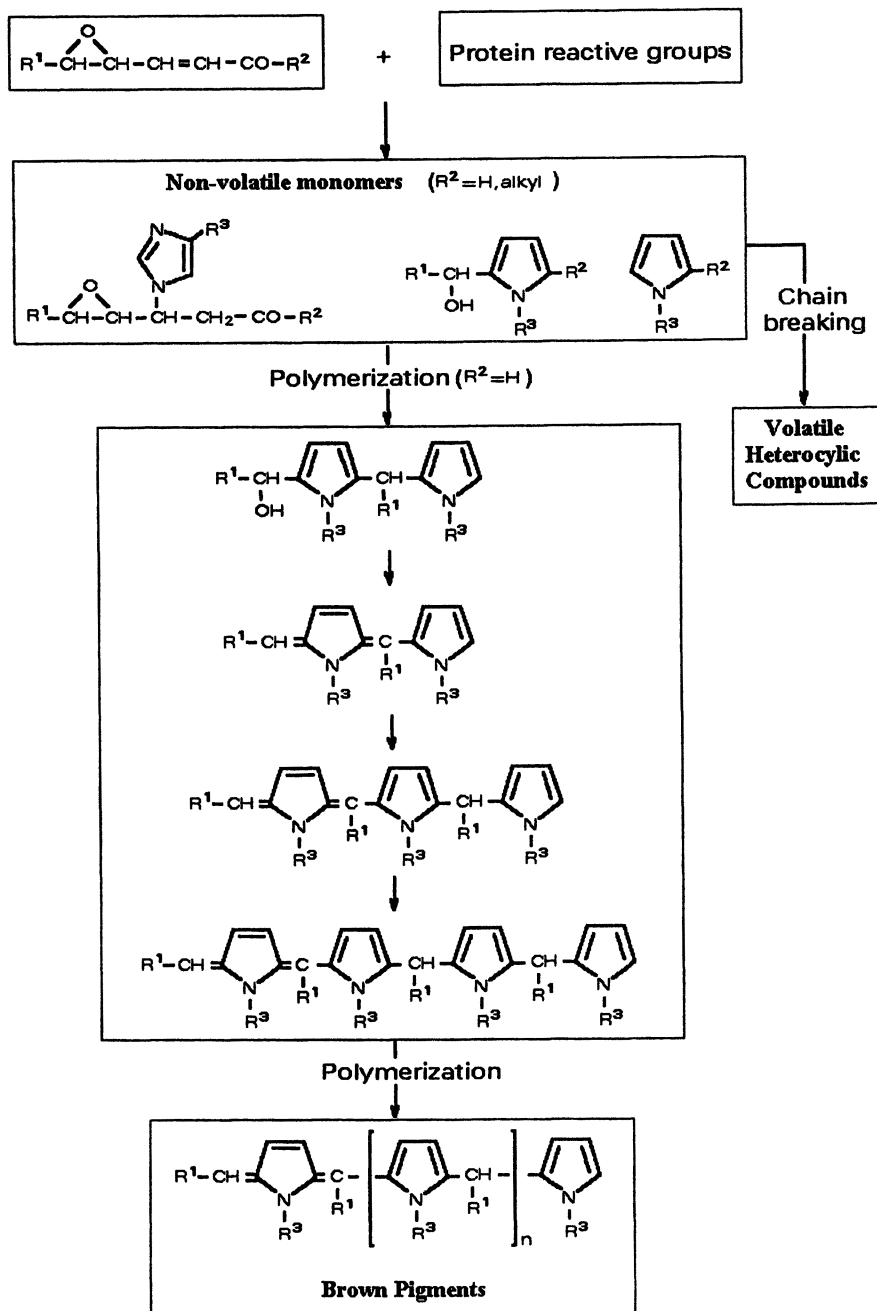


Figure 1. Reaction mechanisms of epoxyalkenals and epoxyketopentene fatty acids with amines, amino acids, and proteins. (Reproduced with permission from reference 10).

Materials and Methods

Chicken Leg Roasting

Fresh legs from six to eight week old broilers, weighing 120-130 g, were purchased in local markets and roasted, uncovered, on aluminum cooking pans in a Panasonic Dimension 4 convection oven (Matsushita Electric Industrial Co., Osaka, Japan). The oven was always preheated to 200 °C and, after introducing the samples, these were heated for 15, 30, or 45 min at the same temperature. All samples were allowed to cool at room temperature and their colors determined using a Minolta CR200 chromameter (Minolta Camera Co., Osaka, Japan). The difference in color (ΔE) between incubated and initial samples was determined using the following equation (11):

$$\Delta E = [(\Delta a^*)^2 + (\Delta b^*)^2 + (\Delta L^*)^2]^{1/2}$$

Roasted leg skins (2.5 g) were then collected and homogenized in 15 mL of 50 mM sodium phosphate buffer, pH 7.4. Analytical determinations were carried out using this homogenate.

Analytical Determinations

For analytical determinations, the homogenate was treated in two different ways. In the first method, the homogenate (1 mL) was treated with 334 μ L of trichloroacetic acid (TCA) solution (30 %) at 0 °C for 15 min and centrifuged at 20000 g for 10 min. The supernatant was separated (SP fraction) and the precipitate was resuspended in 1 mL of 50 mM sodium phosphate buffer, pH 7.4, and stirred. The solids were separated by centrifugation at 20000 g for 10 min, and the solution used for determinations (PT fraction). In the second procedure, the homogenate (2 mL) was extracted three times with 3 mL of chloroform-methanol (2:1) and each time the sample was centrifuged at 700 g. The organic and aqueous phases were collected (OR and AQ fractions, respectively) and used for determinations.

Fat content was determined by weighting the residue obtained after evaporation of the solvent in the OR fraction.

Color was determined in the SP, PT, and AQ fractions using the weighted-ordinate method (11), as described previously (12).

Fluorescence spectra were recorded on a Perkin-Elmer LS-5 fluorescence spectrometer using 150 μ L of SP, PT, and AQ samples diluted with 2.5 mL of 50 mM sodium phosphate buffer, pH 7.4. A slit width of 5 nm was used, and the instrument was standardized with quinine sulfate (0.1 μ M in 0.1 N H₂SO₄) to give a fluorescence intensity of 100 at 450 nm, when excitation was at 350 nm.

Protein pyrrolization was determined in the SP and PT fractions by treating with Ehrlich's reagent prior to the precipitation with TCA. The homogenate (800 μ L) was treated with 128 μ L of Ehrlich's reagent (13) and incubated at 45 °C for 30 min. Then, 310 μ L of TCA solution was added and the samples were incubated at 0 °C for 15 min. The supernatant obtained after centrifugation was measured directly and the precipitate was resuspended in 1 mL of 6 M guanidine.HCl with 20 mM potassium phosphate:trifluoroacetic acid, pH 2.3, for dissolution. The controls were prepared in the same way but without *p*-(dimethylamino)benzaldehyde.

Lipid peroxidation was determined in the OR fraction by using the thiobarbituric acid reactive substances (TBARS) test as described previously (14).

Amino acid analysis was carried out in the SP and PT fractions (after acid hydrolysis) by both HPLC and GC following previously described procedures (15-16). The protein content in the different fractions was calculated by using the data obtained in the amino acid analyses.

Results

Roasting the chicken legs resulted in weight loss and the appearance of the characteristic golden brown color. The loss of weight was a consequence of the loss of both moisture and fat. Figure 2 shows the decrease of both the weight of the chicken leg and the fat content of its skin, as a function of roasting time.

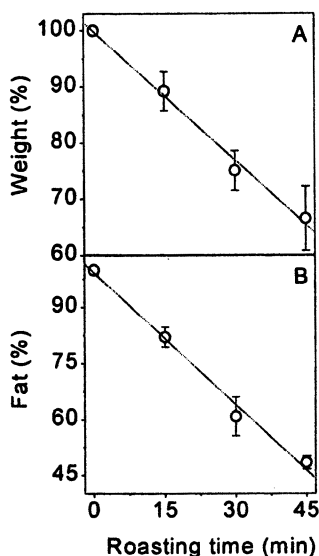


Figure 2. Time-course of: A, weight; and B, fat content of the skin, of chicken legs during roasting.

The loss of weight was linear as a function of the roasting time ($r = -0.996$, $p = 0.004$), and an analogous behavior was observed in the fat content determined in the skin after extraction with $\text{CHCl}_3/\text{MeOH}$ (2:1) ($r = -0.995$, $p = 0.005$). In fact, there was a good correlation between both measurements ($r = 0.9996$, $p = 4.088 \cdot 10^{-4}$).

Browning of the chicken legs paralleled weight loss. When this color change was measured directly on the surface of the chicken leg using a chromameter, a linear increase in the color difference was observed as a function of the roasting time ($r = 0.991$, $p = 0.0016$).

Although an important contribution to these color changes has often been assumed to be a consequence of the Maillard reaction, the almost absence of carbohydrates in the chicken skin suggested that other carbonyl–amine reactions might be implicated. Thus, when the chicken skin was studied for production of lipid peroxidation, a linear increase of TBARS was observed as a function of the roasting time ($r = 0.980$, $p = 0.02$) (Figure 3).

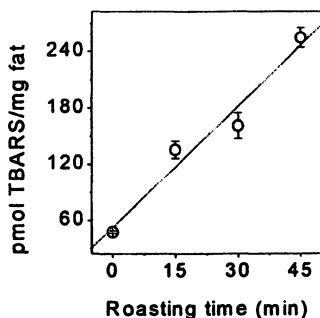


Figure 3. Time-course of lipid peroxidation in chicken leg skins during roasting.

A decrease in some of the amino acids recovered after acid hydrolysis was also observed in parallel with lipid peroxidation. Figure 4 shows the results obtained for lysine. This amino acid decreased linearly as a function of the roasting time ($r = -0.993$, $p = 0.007$). In addition, this decrease paralleled to the increase observed in the lipid peroxidation, and both measurements were correlated ($r = -0.997$, $p = 0.0034$). The results shown in Figure 4 are for the PT fraction. Analogous results were obtained for the SP fraction (data not shown).

The correlation observed between lipid peroxidation and lysine loss suggested that these consequences of roasting might be related, and that lysine losses might result, at least partially, as a consequence of the reaction of this amino acid with the lipid peroxidation products.

Previous research from this laboratory has shown that one of the consequences of oxidized lipid/protein reactions is protein pyrrolization (12). Therefore, the determination of pyrrolized proteins in the roasted chicken leg skins was the first objective of the present investigation to confirm that oxidized lipid/protein reactions were being produced.

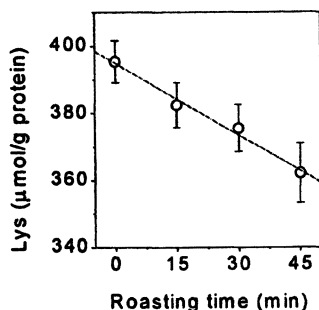


Figure 4. Lysine recovered after acid hydrolysis from chicken leg skins as a function of roasting time.

The presence of pyrrole rings in proteins can be easily detected and quantified by Ehrlich's reagent using a previously described procedure (13). When roasted chicken leg skins were treated with *p*-(dimethylamino)benzaldehyde, the formation of Ehrlich's adducts was observed in both SP and PT fractions. Figure 5 shows the absorbance spectra obtained for the PT fractions of samples roasted for 0, 15, 30 and 45 min at 200 °C. The figure also includes the spectra obtained for the controls. Spectra obtained for the SP fractions were the same.

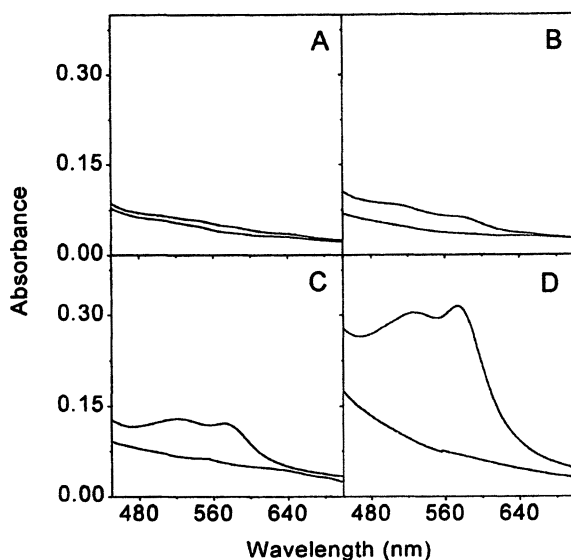


Figure 5. Absorbance spectra of Ehrlich's adducts produced in the proteins of chicken leg skins roasted for: A, 0; B, 15; C, 30, and D, 45 min at 200 °C. All graphs include control spectra for comparison (see Materials and Methods section).

In addition to pyrrolization of the proteins, the appearance of browning and fluorescence was observed in the roasted skins. Figure 6 shows the fluorescence spectra exhibited by the AQ fractions obtained from the chicken leg skins roasted at 200 °C for 0, 15, 30, and 45 min. During the first fifteen minutes no significant fluorescence was observed, however, at longer roasting times the appearance of fluorescence was observed and it increased with roasting time. The wavelengths of maximum fluorescence intensity obtained at the different times were always similar, and all of them were analogous to those described for melanoidins obtained from sugar-amino acid model systems (17) and for lipofuscins (18), and also to the previously described melanoidin-like and lipofuscin-like polypyrroles (9). Analogous results, with respect to both the wavelength and the intensity of maximum fluorescence, were also obtained for the PT and SP fractions.

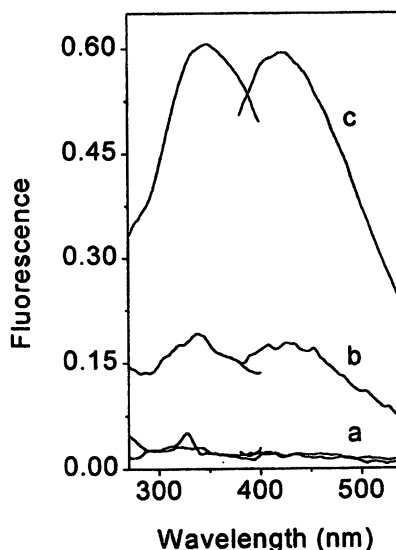


Figure 6. Fluorescence spectra of AQ fractions obtained from chicken leg skins roasted for: a, 0 and 15 min; b, 30 min; and c, 45 min.

When the formation of browning, fluorescence and pyrrolization were studied comparatively, very similar kinetics for the three processes were observed in both SP and PT fractions. Figure 7 shows the kinetics obtained for these fractions. The three measurements increased with incubation time. During the first fifteen minutes there was an induction period with very small changes in browning, fluorescence and pyrrolization. Then, a significant increase was observed during the second fifteen minutes and, finally, the highest increases were observed during the last heating period. As for previous studies carried out using 4,5(*E*)-epoxy-2(*E*)-heptenal/lysine and linolenic acid/lysine model systems (Zamora et al., unpublished results) these measurements could be adjusted using the Boltzman equation (Microcal™ Origin™, v. 4.10, Microcal Software, Northampton, MA):

$$y = [(A_1 - A_2)/(1 + (e^{(x-x_0)/dx})] + A_2$$

where A_1 is the initial Y value, A_2 is the final Y value, x_0 is the x value at Y50, and dx is the width of the curve obtained. Also, in agreement with the model reactions, the width of the adjusted curves was slightly lower for pyrrolization than for the color difference (8.43 and 6.98 min for browning and pyrrolization, respectively, in the PT fraction, and 7.98 and 5.46 min for browning and pyrrolization, respectively, in the SP fraction), suggesting that pyrrolization was produced slightly faster than browning in accordance with the described mechanism. However, the widths of the curves, adjusted for the formation of fluorescence, were smaller than the widths of the curves adjusted for either browning or pyrrolization, in contrast to previous studies carried out in model systems. This suggested that, in chicken leg skins, other mechanisms, in addition to pyrrole polymerization, might also be contributing to the formation of fluorescence.

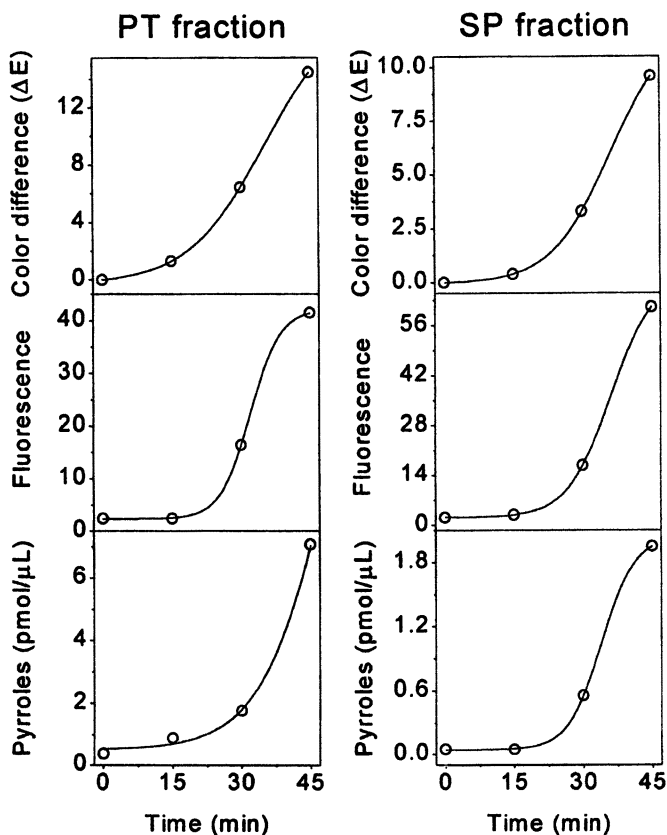


Figure 7. Color, fluorescence and pyrrolization produced in PT and SP fractions obtained from chicken leg skins as a function of roasting time.

When the correlations among browning, fluorescence, and pyrrolization were studied for both PT and SP fractions, a high correlation was always obtained. These correlations are shown in Table I and were better for the SP fraction than for the PT fraction. This is likely to be a consequence of the incomplete solubilization of the PT fraction (Table I).

Table I. Correlations Among Browning, Fluorescence, and Pyrrolization

<i>Correlations</i>	<i>PT Fraction</i>	<i>SP Fraction</i>
Browning/Fluorescence	$r = 0.995$ $p = 0.005$	$r = 0.996$ $p = 0.004$
Browning/Pyrrolization	$r = 0.968$ $p = 0.032$	$r = 0.997$ $p = 0.003$
Fluorescence/Pyrrolization	$r = 0.980$ $p = 0.020$	$r = 0.9996$ $p = 0.00038$

Discussion

Although almost 90 years have passed since the first research on the Maillard reaction and more than 150 years since the first observation of lipofuscins, it is still not possible to present a complete reaction scheme of these and other similar reactions (18-19). However, the research carried out over the years has pointed to the thermodynamically favored, time-dependent, carbonyl-protein crosslinking reactions as the most likely mechanism, at least as an initial step. This mechanism, which produces pyrroles among many other products, may be followed by a polymerization of these compounds to produce melanoidin-like and lipofuscin-like polypyrroles, as has been determined for both oxidized lipid/protein reactions and the Maillard reaction (9,20,21).

Until very recently, it has not been possible to study easily either protein pyrrolization in food systems or the contribution of these produced pyrroles to non-enzymatic browning. However, recent studies from this laboratory have proposed a method to determine the pyrrole content of food proteins that is based on the reaction of food proteins with *p*-(dimethylamino)benzaldehyde (13). When this method was applied to the study of roast chicken leg skins, pyrrolization of skin proteins was observed and it increased with roasting time. This protein pyrrolization seemed to be essentially a consequence of oxidized lipid/protein reactions since there was a very low concentration of sugars in chicken leg skins, and due to the production of lipid peroxidation and the decrease of the lysine recovered after acid hydrolysis. There was also a good correlation between these last two measurements.

This pyrrolization of chicken leg skins proteins seemed to be only the first step in a polymerization process that contributes to browning and fluorescence in this system. This was suggested by previous research that indicated that if non-enzymatic browning and fluorescence were produced by oxidized lipid-protein reactions, good correlations among browning, fluorescence, and pyrrolization should be expected.

All these results suggest that the pyrrole formation and polymerization in chicken leg skins are a consequence of roasting and contribute to the production of both browning and fluorescence in this system. Additional studies are needed to reveal if this is a general mechanism that takes place in all food systems and to apply the methods used in this work to much more complex food systems where other mechanisms (like caramelization or enzymatic browning) might also be occurring.

Acknowledgments

This study was supported in part by the Comisión Interministerial de Ciencia y Tecnología of Spain (Project ALI97-0358) and the Junta de Andalucía (Project AGR 0135). We are indebted to Mr. J. L. Navarro for technical assistance.

Literature Cited

1. Fellows, P. *Food Processing Technology. Principles and Practice*; VCH: Weinheim, Germany, 1988.
2. Bonifer, L. B.; Froning, G. W. *J. Food Sci.* **1996**, *61*, 895-898.
3. Swatland, H. J.; Barbut, S. *Int. J. Food Sci. Technol.* **1991**, *26*, 373-380.
4. Pikul, J.; Kummerow, F. A. *J. Food Sci.* **1990**, *55*, 30-37.
5. Hidalgo, F. J.; Zamora, R. *J. Agric. Food Chem.* **1995**, *43*, 1023-1028.
6. Zamora, R., Ríos, J. J., Hidalgo, F. J. *J. Sci. Food Agric.* **1994**, *66*, 543-546.
7. Zamora, R., Hidalgo, F. J. *Biochim. Biophys. Acta* **1995**, *1258*, 319-327.
8. Zamora, R.; Alaiz, M.; Hidalgo, F. J. *J. Agric. Food Chem.* **1999**, *47*, 1942-1947.
9. Hidalgo, F. J.; Zamora, R. *J. Biol. Chem.* **1993**, *268*, 16190-16197.
10. Hidalgo, F. J.; Zamora, R. *Grasas Aceites* **2000**, *51*, in press.
11. Hunter, R. S. *The Measurement of Appearance*; Hunter Associates Laboratory: Fairfax, VA, 1973.
12. Hidalgo, F. J.; Alaiz, M.; Zamora, R. *J. Agric. Food Chem.* **1999**, *47*, 742-747.
13. Hidalgo, F. J.; Alaiz, M.; Zamora, R. *Anal. Biochem.* **1998**, *262*, 129-136.
14. Zamora, R.; Alaiz, M.; Hidalgo, F. J. *Biochemistry* **1997**, *36*, 15765-15771.
15. Alaiz, M.; Navarro, J. L.; Girón, J.; Vioque, E. *J. Chromatogr.* **1992**, *591*, 181-186.
16. Chen, Z.; Landman, P.; Colmer, T. D.; Adams, M. A. *Anal. Biochem.* **1998**, *259*, 203-211.
17. Nursten, H. E.; O'Reilly, R. *Dev. Food Sci.* **1986**, *13*, 17-28.
18. Yin, D. *Free Radical Biol. Med.* **1996**, *21*, 871-888.
19. Ledl, F.; Schleicher, E. *Angew. Chem. Int. Ed. Engl.* **1990**, *29*, 565-706.
20. Friedman, M. *J. Agric. Food Chem.* **1996**, *44*, 631-653.
21. Tressl, R.; Wondrak, G. T.; Krüger, R.-P.; Rewicki, D. *J. Agric. Food Chem.* **1998**, *46*, 104-110.

Author Index

- Alaiz, Manuel, 199
Ames, Jennifer, M., 1, 150
Bailey, Richard G., 150
Degenhardt, Andreas, 22
Durst, Robert W., 64
Frank, O., 166
Garcia-Viguera, Cristina, 54
Gibson, Glenn R., 150
Giesbrecht, F. G., 185
Giusti, M. Monica, 64
Glomb, M. A., 178
Heuberger, S., 166
Hidalgo, Franciso, J., 199
Ho, Chi-Tang, 100
Hofmann, T., 1, 132, 166
Huang, Tzou-Chi, 100
Isleib, T. G., 185
Joshi, P., 42
Knapp, Holger, 22
Koizumi, Yukimichi, 111
Mercadante, Adrianna Zerlotti, 90
Nagaraj, R. H., 178
Namiki, Mitsuo, 111
Pattee, H. E., 185
Rodriguez-Saona, Luis, E., 64
Rosch, D., 178
Sanders, T. H., 185
Winterhalter, Peter, 22
Wrolstad, Ronald E., 64
Wynne, Anthony, 150
Yabuta, Goro, 111
Zafrilla, Pilar, 54
Zamora, Rosario, 199
Zhu, Nanqun, 100

Subject Index

A

- Absorption, color generation, 44–45
- Amadori rearrangement, 134
- Amino compounds
 - reaction conditions of greening, 115, 116f
 - See also Green pigment
- Annatto
 - analysis methods of preparations, 94
 - carotenoid in *Bixa orellana* seed coat, 93, 95f
 - commercial annatto preparations, 93
 - competition with other colors, 93
 - diapocarotenoids with ester, ketone, or aldehyde groups, 96, 97f
 - earliest recorded case of use, 93
 - future work, 100
 - HPLC of commercial preparation for coloring cheese, 96, 99f, 100
 - isolation method of new minor carotenoids from seeds, 94
 - methyl esters of apocarotenoids (C₃₀ and C₃₂), 95f
 - minor apo and diapocarotenoids, natural metabolites of C₄₀-carotenes, 96
 - newly discovered minor carotenoids, 94, 96
 - oil-soluble samples with bixin as major carotenoid with small amounts of isomers and norbixin, 98f
 - production and use of colorants, 92–93
 - temporary acceptable daily intake, 93
 - water-soluble samples with norbixin as major carotenoid with small amounts of isomers, 98f
- Anthocyanidins
 - biosynthesis, 9f
 - effect of pH on structure and color, 11f
 - structure and biosynthesis, 8
 - structures of anthocyanidin–sulfite reaction products, 10, 11f

Anthocyanins

- antioxidant capacity values, 41t
- biological activity, 40
- biosynthesis of anthocyanidins, 9f
- black currant, 34–35
- comparing separations of black currant, using countercurrent chromatography (CCC) methods, 35f
- comparison of radish and red-fleshed potato anthocyanin extracts, 85–86
- effect of pH on structure and color of anthocyanidins, 11f
- extraction method from red wine, 24
- high speed countercurrent chromatography (HSCCC) separation of red cabbage, 38f, 39t
- HPLC with diode array detection (HPLC–DAD) method, 26
- HSCCC separation of roselle, 37f
- HSCCC separation of *Tradescantia pallida*, 39f
- isolation method from *T. pallida*, 25
- naturally occurring pigments, 1
- occurrence in selected fruits, 8t
- pH dependence of color, 30, 34
- physiological properties, 10
- red cabbage, 37–38
- red wine, 36
- reproducibility of anthocyanin separation from black currant by HSCCC, 35
- roselle, 37
- search for novel stable, 34
- separation of red wine anthocyanins by HSCCC, 36f
- stability and effects of food processing, 8, 10
- structure and biosynthesis, 8
- structures of anthocyanidin–sulfite reaction products, 11f
- structures of selected, 7t
- Tradescantia pallida*, 38
- See also Natural colorants in foods and beverages; Radish anthocyanin

extract; Red-fleshed potato extract;
Separation of natural food colorants

Anthocyanins, changes during food processing

- ascorbic acid addition, 63
- benzoate addition, 62
- CIEL*a*b* values for jellies with pomegranate juice of pH 4, pH 3.5, and pH 3, 64f
- CIEL*a*b* values for pomegranate juice with and without ascorbic acid, 63f
- CIEL*a*b* values for pomegranate juice with benzoate addition, 63f
- concentration of Chandler (Ch), Tudla (Td), and Oso Grande (OG) strawberries, 58f
- concentration of fresh raspberry fruit (FF), frozen (FzF), and jams prepared with fresh (FJ) or frozen (FzJ) fruit, 58f
- influence of freezing fruit, 58–59
- influence of fruit variety, 57–58
- influence of light during storage, 61
- influence of processing conditions, 59–61
- influence of storage conditions, 61
- materials and methods, 57
- percentage anthocyanin and color degradation in strawberry jams after storage at 5°C, 20°C, and 37°C, 62f
- percentage retention in strawberries after 1 year at -20°C, 59f
- percentage strawberry anthocyanin loss during jam preparation under different conditions, 60f
- pH modification on novel pomegranate jelly product, 64
- relationship between concentration and color, 60

Antioxidant effects

- antioxidant capacity values, 41t
- food components, 2
- melanoidins, 18

Appearance

- consumer perception of espresso coffee, 48, 49f
- every-day color physics, 48–49
- gloss, 48
- influence of shape in absorption efficiency, 47f
- Kubelka–Munk theory, 49
- light reflected from matt, semi-matt, and high gloss surfaces, 48f

physical aspects, 46, 48

reflectance spectra for milks of varying fat content, 47f

Argpyrimidine. *See* Beer

Ascorbic acid, influence on anthocyanins and color in pomegranate products, 63

Astringent attribute

relationship to roast color of peanuts, 195–196

See also Peanut roasting

B

Beer

amino acid modifications by methylglyoxal, 182f

Argpyrimidine (N^ε-(5-hydroxy-4,6-dimethylpyrimidine-2-yl)-L-ornithine) formation from maltose, 183–184

comparing formation of Argpyrimidine and methylglyoxal in reaction mixtures with 5-deoxyribose and ribose, 184

correlation of Argpyrimidine concentration with wort content and beer color, 185f

detection of Argpyrimidine by 2-stage HPLC system, 185f

formation and quantification of Argpyrimidine in beer, 182–185

identification of Argpyrimidine, 181–182

incubation of N^ε-t-BOC-arginine with sugars, 184t

investigating chemistry of methylglyoxal, 181–182

Maillard reaction influencing color, aroma, and taste, 180

mechanism of Argpyrimidine formation, 183f

method to isolate and quantify colored polymer fraction, 180

non-enzymatic browning, 180

proline-derived Maillard products, 181f

proposing Cannizzaro reaction and subsequent condensation, 182–183

structures from reaction mixtures of proline with monosaccharides, 180–181

Beer–Bouger–Lambert law, color, 49–50

Benzacridine derivative

oxidized form of green pigment, 130

See also Green pigment

- Benzoate**
 antimicrobial properties, 62
 influence on anthocyanins and color in pomegranate products, 62, 63*f*
- Beverages.** *See* Natural colorants in foods and beverages
- Biological activity, plant-derived food colorants,** 40
- Bitter attribute**
 relationship to roast color of peanuts, 194–195
See also Peanut roasting
- Bixa orellana* L..** *See* Annatto
- Black currant**
 anthocyanins, 34–35
 clean-up method of pigments from, 24–25
 comparing anthocyanins separation using countercurrent chromatography (CCC) methods, 35*f*
 reproducibility of anthocyanins separation using high speed CCC, 35*f*
- Black tea**
 extraction method of flavonol glycosides, 24
 main stages of manufacture, 15
 outline of conversion of flavanols to theaflavic acids, theaflavins, and thearubigins during black tea manufacture, 14*f*
 popular in North America and Europe, 102
 range of antioxidant capacity and phenolic content, 16*t*
See also Enzymatic browning; Green tea; Tea
- Browning, enzymatic and non-enzymatic.** *See* Natural colorants in foods and beverages
- Browning, non-enzymatic.** *See* Chicken roasting; Maillard reaction
- C**
- Caffeic acid esters.** *See* Greening; Green pigment
- Caramelization reaction, outline of formation of colored compounds,** 17*f*
- Carotenoids**
 annual production in nature, 3
 biosynthesis via deoxy-D-xylulose 5-phosphate pathway, 4*f*
 concentration in selected foods, 3*t*
 extraction method of water-soluble, from saffron, 24
Gardenia jasminoides, 29
 levels of selected individual, as % total carotenoids in some foods, 3*t*
 naturally occurring pigments, 1 non-polar, 27
 physiological properties, 6, 8
 possible degradation pathways for *b*-carotene, 7*f*
 role in human diet, 40
 saffron, 27–28
 stability and effects of food processing, 6
 structure and biosynthesis, 2–3
 structures of selected, 5*f*
 water-soluble, 27–29
See also Annatto; Natural colorants in foods and beverages
- Carotenoids, water-soluble, HPLC with diode array detection (HPLC–DAD) method,** 26
- Catechins, antioxidant activity,** 15
- Cheese, HPLC of commercial preparation for coloring cheese,** 96, 99*f*, 100
- Chicken roasting**
 absorbance spectra of Ehrlich's adducts produced in proteins of chicken leg skins roasted at 200°C, 207*f*
 analytical determinations, 204–205
 chicken leg roasting method, 204
 color, fluorescence, and pyrrolization produced in fractions from chicken leg skins as function of roasting time, 209*f*
 contribution of oxidized lipids/amino acid reaction products (OLAARPs) to browning, 202
 correlation between lipid peroxidation and lysine loss, 206
 correlations among browning, fluorescence, and pyrrolization, 210*t*
 detecting and quantifying pyrrole rings in proteins, 207
 fluorescence spectra of aqueous fractions from roasted chicken leg skins, 208*f*
 general scheme for reaction between epoxyalkenals and epoxyketopentene fatty acids with amines, amino acids, and proteins, 203*f*
 lysine recovered after acid hydrolysis from chicken leg skins as function of roasting time, 207*f*

- mechanism for melanoidin-like and lipofuscin-like polypyrroles, 210
- pyrrole formation and polymerization contributing to non-enzymatic browning, 202, 210–211
- skin composition, 202
- studying formation of browning, fluorescence, and pyrrolization, 208–209
- time-course of lipid peroxidation in chicken leg skins during roasting, 206*f*
- time-course of weight and fat content of skin of chicken legs during roasting, 205*f*
- weight loss and appearance, 205–206
- Chlorogenic acid**
- contribution to greening reaction, 114–115
- greening in presence of amino acid and alkali, 130
- See also* Green pigment
- Chromophores.** *See* Color Activity Concept
- Coffee**, visual impression of espresso, 48, 49*f*
- Color**
- advances in measurement, 51
- Beer–Bouguer–Lambert law, 49–50
- challenge of foods, 51
- CIE (Commission Internationale de l'Éclairage) parameters, 51–52
- CIEL*a*b* system, 52
- color circle, 45*f*
- consumer perception of espresso coffee, 48, 49*f*
- every-day physics, 48–49
- generation in absence of colorants, 46
- how we see, 44–46
- influence of storage conditions of strawberry jam, 61, 62*f*
- initial quality of product, 187
- light interaction with colored samples, 50*f*
- light source, 44
- measurement in specular component included mode (SCI) and specular component excluded mode (SCE), 50–51
- measurement instruments, 50
- object, 44–45
- observer, 45–46
- physical aspects of appearance, 46, 48
- quantifying, 49–51
- relationship to anthocyanin concentration, 60–61
- schematic of spectrophotometer and colorimeter, 51*f*
- understanding colored food system, 52–53
- visual aspects of food, 43
- See also* Anthocyanins, changes during food processing; Appearance
- Color Activity Concept**
- analytical steps, 171
- analytical technique characterizing key chromophores in non-enzymatic browning reactions, 135
- application leading to low molecular weight chromophores for browning, 138–139
- calculating percent color contribution of single colorant, 177–178
- calculation of color activity values, 176–177
- chemical structure determination of intense orange colored compound (IV), 173
- chromophore identification in xylose/L-alanine/furan-2-aldehyde Maillard mixture, 136
- Color Activity Value (CAV) equation**, 176
- color dilution analysis (CDA) method, 170–171
- concentrations of selected colored compounds formed in Maillard reaction mixture, 176*t*
- contribution of selected colorant compounds to overall color of browned Maillard mixture, 178*t*
- detection thresholds and CAV of selected colored compounds in Maillard mixture, 177*t*
- estimation of color contribution of key chromophores, 177–178
- identification of most intense colored reaction products, 172–175
- Maillard reaction mixture, 170
- quantification method, 171
- quantification of selected key colorants, 175
- reference compounds preparation, 170
- reverse phase HPLC (RP–HPLC) chromatogram and color dilution (CD) chromatogram of solvent-extractable fraction of reaction mixture, 172*f*
- screening for intense colored compounds by CDA, 171–172

- strategy characterizing key chromophores, 170
- structures of key colorants identified, 174f
- synthetic sequence for preparation of intense orange colored compound (IV), 175f
- See also* Maillard reaction
- Color and sensory attribute relationships. *See* Peanut roasting
- Color dilution analysis (CDA)
- screening technique for locating intensely colored compounds, 178–179
- See also* Color Activity Concept
- Colorants
- HPLC analytical method of choice, 27
- naturally occurring and formation during food processing, 1
- See also* Annatto; Natural colorants in foods and beverages
- Colorants, separation. *See* High speed countercurrent chromatography (HSCCC)
- Colorimeter, color measurement, 50, 51f
- Commission Internationale de l'Eclairage (CIE) parameters, 51–52
- Countercurrent chromatography (CCC)
- all-liquid technique, 23
- general procedure for CCC separations, 25–26
- method, 25–26
- superior for preparative separations, 23
- techniques, 22–23
- See also* Separation of natural food colorants

D

- Diapocarotenoids. *See* Annatto
- Dietary components, physiological effect, 1–2
- Digestion
- melanoidins, 159
- method simulating digestion of melanoidins, 154
- See also* Glucose-lysine model system
- dV_Color variable
- evaluating closeness of relationship between roasted peanut attribute and L* values, 192
- See also* Peanut roasting

E

- Enzymatic browning
- biosynthesis and structure of products of, 12
- effects of food processing, 12, 15
- formation of color, 1
- outline of biochemical steps, 13f
- outline of conversion of flavanols to epitheflavic acids, theaflavins, and thearubigins during black tea manufacture, 14f
- physiological properties of theaflavins and thearubigins, 15–16
- See also* Black tea; Natural colorants in foods and beverages
- Epigallocatechin (EGC)
- oxidation with H₂O₂, 110–112
- structure, 103f
- theaflavate A from potassium ferricyanide oxidation, 108f
- See also* Tea catechins
- Epigallocatechin gallate (EGCG)
- oxidation with H₂O₂, 110–112
- proposed mechanism for peroxy radical-initiated oxidation, 109f
- structure, 103f
- two compounds from peroxy radical-initiated oxidation of EGCG, 108f
- See also* Tea catechins
- Espresso coffee, consumer perception, 48, 49f

F

- Fat, scattering incident light in milk, 48
- Fermentation, black tea manufacture, 15
- Firing, black tea manufacture, 15
- Flavonoids
- antioxidant activity, 15
- basic structure in tea, 103f
- biological activity, 40
- See also* Tea catechins
- Flavonol glycosides
- extraction method from black tea, 24
- HPLC with diode array detection (HPLC–DAD) method, 26
- separation from tea leaves, 30
- varying polarity of solvent for separation, 30, 31f, 32f, 33f
- See also* Separation of natural food colorants
- Food colorants
- biological activity of plant-derived, 40

- categories, 2
- non-nutritive effects, 2
- See also* Natural colorants in foods and beverages
- Food components, antioxidant effects, 2
- Food processing
 - anthocyanins, 8, 10
 - carotenoids, 6
 - formation of desirable flavors and colors, 152–153
 - influence of freezing on anthocyanin concentration in raspberry products, 58–59
 - influence on anthocyanin concentration in strawberry products, 59–61
 - products of enzymatic browning, 12, 15
 - products of non-enzymatic browning, 16, 18
 - See also* Anthocyanins, changes during food processing; Glucose-lysine model system; Maillard reaction
- Food roasting
 - purpose, 201
 - See also* Chicken roasting
- Foods
 - challenge to color physics, 51
 - color, 43–44
 - visual aspects, 43
- Freezing, influence on anthocyanin concentration in raspberry products, 58–59
- French paradox, potential health effects of red wine, 40
- Fruit
 - influence of variety on anthocyanin concentration, 57–58
 - level of individual anthocyanins as % of total in, 10*t*
 - occurrence of total anthocyanins, 8*t*
 - See also* Anthocyanins

G

- Gardenia jasminoides*
 - biological activity, 40
 - water-soluble carotenoids, 29
 - See also* Separation of natural food colorants
- Gloss, surface property, 48
- Glucose-lysine model system
 - compound identification, 154, 158
 - compound identification for four of five peaks, 157*t*

- culturing on agar plates and FISH
 - probing technique for enumerating bacteria from batch fermenters, 159
- digestion simulation method, 154
- effect of heating conditions on reaction product profile, 155*f*
- effect of heating conditions on reaction products, 158
- effect of pH, 158
- effect of temperature/time combinations, 158
- effects of fermentation of melanoidins in batch culture fermenters on fecal bacteria after incubation for 0, 6, and 24 h, 164*f*, 165*f*
- experimental, 153–154
- fecal bacteria responding to melanoidins, 159
- HPLC profiles of colored reaction products, 154, 155*f*
- melanoidins samples preparation, 153–154
- model systems analysis methods, 153
- model systems preparation method, 153
- possible physiological function of melanoidins, 159
- resolved peaks for system at 80°C for 6 h and pH 5 on 280 nm chromatograph, 156*f*
- variation in peak area with pH (80°C for 6 h), 162*f*, 163*f*
- variation in peak area with temperature/time (pH 5), 160*f*, 161*f*
- Glycosylamines
 - first reaction products in Maillard reaction, 134, 135*f*
 - See also* Maillard reaction
- Greening
 - addition of amino compound, 115
 - color rare in natural food systems, 114
 - effect of pH on formation of greening (Et-caffeate + α -alanine), 116*f*
 - electron spin resonance (ESR) studies on reaction pathways, 125–126
 - ESR spectra of ethyl caffeate and ethyl caffeate + α -alanine, 127*f*
 - occurrence, 113–114
 - oxidation of chlorogenic acid, 114
 - polyphenol necessary for, 114–115
 - reaction conditions, 114–115
 - visible spectra of various reaction mixtures of Et-caffeate + amino acid, 116*f*

Green pigment

absorption spectra of benzacridine compounds calculated by Pariser, Parr, and Pople (PPP) method, 122, 124f

blue pigment of reaction mixture, 121
chemical properties of reduced and acetylated, 119, 121

formation mechanism of, and related products, 126

formation of reduced and acetylated, from caffeic acid ester and primary amino compound, 120f

green color fraction varying with pH of mixture, 117, 118f

isolation and identification of reduced and acetylated, 119

isolation and purification, 117

mechanism of formation from Et-caffeate and amino compound, 128f, 129f

possessing three phenol groups in benzacridine structure, 130

possibility of quinhydrone-type charge transfer complex, 122, 125

possible oxidation steps of reduced product, 121–122, 123f

properties, 115, 117

reduction product, 117, 119

role of structural features of caffeate, 130

silica gel thin-layer chromatography of reduced and acetylated crystalline products, 121

See also Greening

Green tea

popular in Asian countries, 102

range of antioxidant capacity and phenolic content, 16t

See also Black tea; Tea

H**Hexoses**

chromogenic pathways to low molecular weight compounds, 141, 144–146

See also Maillard reaction

High speed countercurrent chromatography (HSCCC)

hydrodynamic equilibrium, 23

separating column, 22–23

See also Separation of natural food colorants

J

Juice model systems, pigment and color stabilities of radish and red-fleshed potato anthocyanins, 85–86

K**Kaempferol-rutinoside**

flavonol glycoside from tea leaves, 30
structure, 32f

Kubelka–Munk theory, advantages of additivity, 49

L

Light, interaction with colored samples, 50f

Light source, component of color perception, 44–45

M**Maillard reaction**

γ -alkylidene- β -pyranoses (9a/9b) as pentose-typical chromophores, 139

Amadori rearrangement, 134

amino acid-catalyzed conversion of reducing carbohydrates, 169

amino acid-catalyzed degradation of carbohydrates via 1-deoxy-2,3-dioloses and 3-deoxy-2-oxuloses as key intermediates, 135f

amino acid involvement in formation of 3-deoxyosone-derived chromophores, 140–141

analytical strategy for clarification of reaction routes, 136–138

¹³C-labelled xylose for insights into pentose skeleton incorporation into 8, 138

chromogenic pathways of hexoses, 141, 144–146

chromogenic pathways to pentoses, 139–141

chromophore formation, 135

chromophoric substructures for melanoidin formation, 150f

Color Activity Concept, 135

1-deoxy-2,3-pentosulose effective progenitor of chromophores, 141

1-deoxyhexosones effective color precursors, 145

- disaccharide forming aminohexose reductone, 147, 148f
- food processing applications, 152–153
- food processing variables affecting product profiles, 153
- formation of colored condensation products from carbohydrate-derived carbonyls and 4-hydroxy-5-methyl-3(2H)-furanone, 169f
- formation of pyranopyranone 8 from carbohydrate-derived intermediates, 139f
- formation of pyrrolinone reductones and pyrrolinone chromophores from acetylformoin and primary amino acids, 146f
- glycosylamines as first reaction product, 134
- high molecular weight colored compounds (melanoidins), 147, 149
- influence of 1,4-glycosidic link in di- and polysaccharides on colorant formation, 147
- influence of C-2 carbohydrate fragments on formation of colorant 8, 137t
- influence of C-5 moiety of pentose skeleton on formation of colorant 8, 138t
- influence of carbohydrate moiety on formation of 3-hydroxy-3-cyclopenten-1,2-dione chromophores, 148f
- intense colorant pyrano[2,3-b]pyran-3-one (8) from pentose degradation, 139
- lacking information on structures of chromophores, 170
- low molecular weight colored compounds, 138–147
- melanoidin formation, 149
- outline of formation of colored compounds, 17f
- physiological properties of foods having undergone, 18
- previous model studies, 169
- proposed reaction pathway for formation of 8, 140f
- pyranones from hexose-containing Maillard mixtures, 144–145
- reaction pathways leading to colored 2H-furan-3-ones and 3-hydroxy-cyclopentene-1,2-diones via 1-deoxy-2,3-pentodiulose as key intermediate, 143f
- reaction pathways leading to formation of colored pyrano[2,3-b]pyranone (8) and γ -alkylidene- β -pyranoses (9a and 9b) via 3-deoxy-2-pentosulose as intermediate, 140f
- reaction pathways leading to nitrogen-containing chromophores via 3-deoxy-2-pentosulose as key intermediate, 142f
- reaction pathways leading to pyrano[2,3-b]pyranone and β -pyranones via 3-deoxy-2-hexosulose as key intermediate, 144f
- reaction pathways to chromophores via 1-deoxy-2,3-hexodiulose key precursor, 146f
- rearrangement of hemiacetal into furanone chromophore, 145f
- reducing carbohydrates and amino acids/proteins, 134
- structure of orange colored (1R,8aR)- and (1S,8aR)-4-(2-furyl)-7-[(2-furyl)methylidene-2-hydroxy-2H,7H,8aH-pyranol[2, 3-b]pyran-3-one (8), 136, 137f
- studying pentose skeleton incorporation, 137-138
- wide distribution of products in Western diet, 153
- See also* Beer; Glucose-lysine model system
- Maraschino cherry
founder, 66–67
- practical issues and current status of colorant, 79
- radish anthocyanin extract as colorant, 67–68
- See also* Radish anthocyanin extract
- Meat roasting
browning by Maillard reaction, 201–202
- See also* Chicken roasting
- Melanoidins
antioxidant activity, 18
- chromophoric substructures in formation of, 150f
- digestion, 159
- effects of fermentation of melanoidins in batch culture fermenters on fecal bacteria after incubation for 0, 6, and 24 h, 164f, 165f
- fecal bacteria responding to presence of, 159
- formation, 147, 149
- high molecular weight colored, 147, 149

method simulating digestion of, 154
 possible physiological features, 159
 sample preparation, 153–154
See also Glucose-lysine model system;
 Maillard reaction

Milk

fat scattering incident light, 48
 reflectance spectra with varying fat
 content, 47*f*

Modeling. *See* Glucose-lysine model
 system

Multilayer coil countercurrent chroma-
 tography (MLCCC)
 separation column, 22–23
See also High speed countercurrent
 chromatography (HSCCC)

N

Natural colorants, separation. *See* High
 speed countercurrent chromatography
 (HSCCC)

Natural colorants in foods and beverages
 annual carotenoid production in natu-
 ral, 3

anthocyanins, 8–10

biosynthesis and structure of enzy-
 matic browning substrates, 12

biosynthesis of anthocyanidins, 9*f*

biosynthesis of carotenoids via deoxy-
 D-xylulose 5-phosphate pathway, 4*f*

carotenoids, 2–8

concentration of total carotenoids in
 selected foods, 3*t*

effect of pH on structure and color of
 anthocyanidins, 11*f*

effects of food processing on enzy-
 matic browning, 12, 15

effects of food processing on non-enzy-
 matic browning, 16, 18

levels of selected anthocyanins as % to-
 tal anthocyanins in some fruits, 10*t*

levels of selected individual carot-
 enoids as % of total carotenoids in
 some foods, 3*t*

occurrence of total anthocyanins in se-
 lected fruits, 8*t*

outline of biochemical steps for enzy-
 matic browning, 13*f*

outline of conversion of flavanols to
 epitheflavic acids, theaflavins, and
 thearubigins during black tea manu-
 facture, 14*f*

outline of formation of colored com-
 pounds formed during carameliza-
 tion and Maillard reaction, 17*f*

physiological properties of anthocya-
 nins and other flavonoids, 10

physiological properties of carot-
 enoids, 6, 8

physiological properties of foods hav-
 ing undergone Maillard reaction, 18

physiological properties of theaflavins
 and thearubigins, 15–16

possible degradation pathways for β -
 carotene, 7*f*

products of enzymatic browning,
 12–16

products of non-enzymatic browning,
 16–18

range of antioxidant capacity and phe-
 nolic content of commercial green
 and black teas, 16*t*

stability and effects of food processing
 on anthocyanins, 8, 10

stability and effects of food processing
 on carotenoids, 6

structure and biosynthesis of anthocya-
 nins, 8

structure and biosynthesis of carot-
 enoids, 2–3

structures of anthocyanidin–sulfite re-
 action products, 11*f*

structures of selected carotenoids, 5*f*

Non-enzymatic browning

effects of food processing, 16, 18

melanoidins, 18

outline of formation of colored com-
 pounds formed during carameliza-
 tion and Maillard reaction, 17*f*

physiological properties of foods hav-
 ing undergone Maillard reaction, 18

See also Beer; Chicken roasting; Color
 Activity Concept; Maillard reaction;
 Natural colorants in foods and bev-
 erages

O

Object, component of color perception,
 44–45

Observer, component of color percep-
 tion, 45–46

Oolong tea, variant between black and
 green, 102

Oxidative transformation. *See* Tea cate-
 chins

P

Peanut roasting

changes in astringency during roasting, 196

color measurement by CIELAB
L*a*b* values, 189

consistency of optimum roast color
across market types, 190–191

consistency of optimum roast color
value across years, 191f

distribution of roast color of individual
seeds and paste made from
them as function of average maturity,
198f

dV_Color variable to evaluate closeness
of relationship between roasted
peanut attribute and L* values, 192

factors contributing to variability in
attribute roasted peanut, 189–190

influence of market-type on relationship
between astringent attribute
and roast color, 197f

influence of market-type on relationship
between bitter attribute and
roast color, 195f

influence of market-type on relationship
between roasted peanut attribute
and roast color, 191f

influence of market-type on relationship
between sweet attribute and
roast color, 193f

influence of pod maturity on roast
color of medium grade kernels
roasted 21 min at 165°C, 198f

literature on effect of roasting on
color, 188

market-types of peanuts in United
States and primary usage, 188

materials and methods, 189
objective of enhancement of roasted
peanut flavor, 188

optimal roast color for maximal
roasted peanut attribute response,
189–192

overall relationship between astringent
attribute and roast color, 196f

overall relationship between bitter
attribute to roast color, 194f

overall relationship between roasted
peanut attribute and roast color,
190f

overall relationship between sweet
attribute and roast color, 193f

plant materials, 189

relationship of astringent attribute to
roast color, 195–196

relationship of bitter attribute to roast
color, 194–195

relationship of sweet attribute to roast
color, 192–194

roast color-peanut seed maturity relationships,
197

roast color-single seed, lot, and paste
color relationships, 197–198

runner market-type, 188

sample handling methods, 189

sample roasting and preparation, 189

sensory evaluation, 189

Spanish market-type, 188

statistical analyses methods, 189

Valencia market-type, 188

Virginia market-type, 188

Pentoses

chromogenic pathways to low molecular
weight compounds, 139–141

See also Maillard reaction

pH

effect on glucose-lysine reaction products,
158

influence on anthocyanins and color in
pomegranate products, 64

variation in peak area for glucose-lysine
reaction with pH, 162f, 163f

Physiological effect, dietary components,
1–2

Pigments

clean-up method from black currant
and red cabbage, 24–25

extraction method from roselle, 24

Polyphenol

reaction conditions of greening,
114–115

See also Greening

Pomegranate products

ascorbic acid addition, 63

benzoate addition, 62

influence of pH on color and anthocyanin
concentration, 64

Potato. *See* Red-fleshed potato extract

Pyrrole formation and polymerization.

See Chicken roasting

Q

Quercetin-rutinoside

flavonol glycoside from tea leaves, 30

structure, 32f

R

- Radish anthocyanin extract**
 agronomic factors, 78–79
 changes in L*, chroma, and hue angle of model juices colored with potato and radish anthocyanins during storage, 88f
 changes in L*, chroma, and hue angle of syrup samples with time, 71f, 72f, 73f
 changes in monomeric anthocyanin content and polymeric color of syrup samples with time, 69f, 70f
 chemical structure of radish pelargonidin derivatives, 77f
 colorant for maraschino cherries, 67–68
 color similarities and differences with red-fleshed potato, 85
 commercial status, 79
 comparison to red-fleshed potato anthocyanin extract, 85–86
 electrospray mass spectroscopy (ESMS) of radish anthocyanins, 75f
 HPLC separation of red radish anthocyanins, 74f
 monomeric anthocyanin degradation and polymeric color formation in model juices, 87f
 MS–MS fragmentation pattern of peak 4 pg-3-(feruloyl-soph)-5-(malonyl-glu), 76f
 pigment and color stabilities in juice model system of radish and red-fleshed potato, 85–86
 practical issues and current status, 79
 preparation, 67
 structure of pigments, 68, 78
 total monomeric anthocyanin pigment content for winter and spring cultivars, 78
See also Anthocyanins
- Raspberry products**
 factors affecting loss of red color, 56
 influence of freezing on anthocyanin concentration, 58–59
 influence of variety on anthocyanin concentration, 58
- Red cabbage**
 anthocyanins, 37–38
 anthocyanins separation by high speed countercurrent chromatography (HSCCC), 38f, 39f
 clean-up method of pigments from, 24–25
- Red color, factors affecting loss, 56**
- Red-fleshed potato extract**
 anthocyanins, 80
 changes in L*, chroma, and hue angle of model juices colored with potato and radish anthocyanins during storage, 88f
 color similarities and differences with radish, 85
 comparison to radish anthocyanin extract, 85–86
 electrospray mass spectroscopy (ESMS) of potato pigment isolate, 84f
 HPLC separation of anthocyanins, 81f
 HPLC separation of saponified potato anthocyanins and their acylating groups, 82f
 monomeric anthocyanin degradation and polymeric color formation in model juices, 87f
 pigment and color stabilities in juice model system of radish and red-fleshed potato, 85–86
 spectral characteristics of potato anthocyanins indicating glycosylation and acylation patterns, 83f
See also Anthocyanins
- Red wine**
 anthocyanins, 36
 anthocyanins separation by high speed countercurrent chromatography (HSCCC), 36f
 extraction method of anthocyanins, 24
 potential health effects, 40
- Reflection**
 color generation, 44–45
 reflectance spectra for milks with varying fat content, 47f
- Roasting. *See* Chicken roasting; Peanut roasting**
- Roselle**
 anthocyanins, 37
 anthocyanins separation by high speed countercurrent chromatography (HSCCC), 37f
 extraction method of pigments, 24
- Runner market-type**
 peanuts, 188
See also Peanut roasting

S

Saffron

- biological activity, 40
 - extraction method of water-soluble carotenoids, 24
 - high speed countercurrent chromatography (HSCCC) separation of water-soluble carotenoids from, 28f
 - structures of isolated carotenoids, 28f
 - water-soluble carotenoids, 27–28
- See also* Separation of natural food colorants

Scattering

- color generation, 44–45
- incident light by fat in milk, 48
- Sensory attribute and color relationships. *See* Peanut roasting

Separation of natural food colorants

- anthocyanins, 30, 34–39
- anthocyanins from black currant, 34–35
- anthocyanins from red cabbage, 37–38
- anthocyanins from red wine, 36
- anthocyanins from roselle, 37
- anthocyanins from *Tradescantia pallida*, 38, 39f
- clean-up of pigments from black currant and red cabbage, 24–25
- comparing separation of black currant anthocyanins using multilayer coil countercurrent chromatography (MLCCC) and HSCCC, 35f
- countercurrent chromatography (CCC) method, 25–26
- electrospray ionization ion trap multiple mass spectrometry (ESI–MS/MS) method, 26–27
- experimental materials, 23–24
- extraction method of flavonol glycosides from black tea, 24
- extraction method of pigments from roselle, 24
- extraction method of water-soluble carotenoids from saffron, 24
- flavonol glycosides from tea leaves, 30
- Gardenia jasminoides*, 29
- general procedure for CCC separations, 25–26
- HPLC with diode array detection (HPLC–DAD) method, 26
- HSCCC separation of methanolic extract from *G. jasminoides*, 29f

HSCCC separation of water-soluble carotenoids from saffron, 28f

isolation method of anthocyanin from *T. pallida*, 25

isolation method of anthocyanins from red wine, 24

non-polar (apo-) carotenoids, 27

proton magnetic resonance spectroscopy (¹H NMR) method, 26

purification of four major pigments from red cabbage, 38f, 39t

reproducibility of black currant anthocyanin separation, 35

resolution equation, 34

saffron, 27–28

search for novel stable anthocyanins, 34

structures of isolated carotenoids from saffron, 28f

structures of kaempferol 3-O-rutinoside and quercetin 3-O-rutinoside, 32f

varying polarity of solvent system for separating flavonol glycosides from black tea, 30, 31f, 32f, 33f

water-soluble carotenoids, 27–29

See also High speed countercurrent chromatography (HSCCC)

Spanish market-type

peanuts, 188

See also Peanut roasting

Spectrophotometer, color measurement, 50, 51f

Specular component excluded mode (SCE), color measurement, 50–51

Specular component included mode (SCI), color measurement, 50–51

Storage conditions, influence on anthocyanin concentration in strawberry jams, 61, 62f

Strawberry products

factors affecting loss of red color, 56

influence of processing conditions on anthocyanin concentration, 59–60

influence of storage conditions on anthocyanins, 61, 62f

influence of variety on anthocyanin concentration, 57, 58f

relationship between anthocyanin concentration and color, 60–61

Sweet attribute

relationship to roast color of peanuts, 192–194

See also Peanut roasting

T

Tea

- analysis of flavonol glycosides by high speed countercurrent chromatography (HSCCC), 31*f*, 32*f*, 33*f*
- black and green, 102
- Camellia sinensis*, 102
- effects of components on grown of human cancer cell lines, 16
- major chemical changes during processing, 103–106
- outline of conversion of flavanols to epitheafavic acids, theaflavins, and thearubigins during black tea manufacture, 14*f*
- possible protective effects, 15
- separation of flavonol glycosides, 30
- See also* Black tea; Green tea; Separation of natural food colorants; Tea catechins
- Tea catechins
 - basic flavonoid structure, 103*f*
 - experimental procedures for oxidation with H₂O₂, 110
 - formation of theaflavins, 104
 - formation of thearubigins, 106
 - free radical-initiated and chemical oxidation of catechins, 106–107
 - major catechins in tea, 103*f*
 - oxidation of epigallocatechin gallate (EGCG) and epigallocatechin (EGC) with H₂O₂, 110–112
 - oxidation products of EGCG and EGC with H₂O₂, 110, 112
 - oxidative conversion and polymerization, 103–104
 - possible pyrogallol-catechol condensation pathway during fermentation, 104*f*
 - possible pyrogallol-pyrogallol condensation pathway during fermentation, 105*f*
 - predominant form of flavonoids in fresh tea leaves, 103
 - proposed mechanism for peroxy radical-initiated oxidation of (+)-catechin, 107*f*
 - proposed mechanism for peroxy radical-initiated oxidation of EGCG, 109*f*

- structures of theaflavins, 105*f*
 - theaflavate A from potassium ferricyanide oxidation of EGC, 108*f*
 - three novel compounds from H₂O₂ oxidation of EGCG and EGC, 111*f*
 - two compounds from peroxy radical-initiated oxidation of (+)-catechin, 106*f*
 - two compounds from peroxy radical-initiated oxidation of EGCG, 108*f*
- Temperature/time
- effect on glucose-lysine reaction products, 158
 - variation in peak area for glucose-lysine reaction, 160*f*, 161*f*

Temperature/time

- effect on glucose-lysine reaction products, 158
- variation in peak area for glucose-lysine reaction, 160*f*, 161*f*

Theaflavins

- formation, 104
- physiological properties, 15–16
- structures, 105*f*
- See also* Tea

Thearubigins

- formation, 106
- physiological properties, 15–16
- See also* Tea

Thermal processes. *See* Peanut roasting*Tradescantia pallida*

- anthocyanins, 38
- anthocyanins separation by high speed countercurrent chromatography (HSCCC), 39*f*
- isolation method of anthocyanins, 25
- Trolox equivalent antioxidant capacity (TEAC), anthocyanins and other antioxidants, 41*t*

V

- Valencia market-type
 - peanuts, 188
 - See also* Peanut roasting
- Virginia market-type
 - peanuts, 188
 - See also* Peanut roasting

W

- Withering, black tea manufacture, 15